A new physics-based method for estimating the excess turbulence downstream of a structure

Melvin Koote

4th September 2017

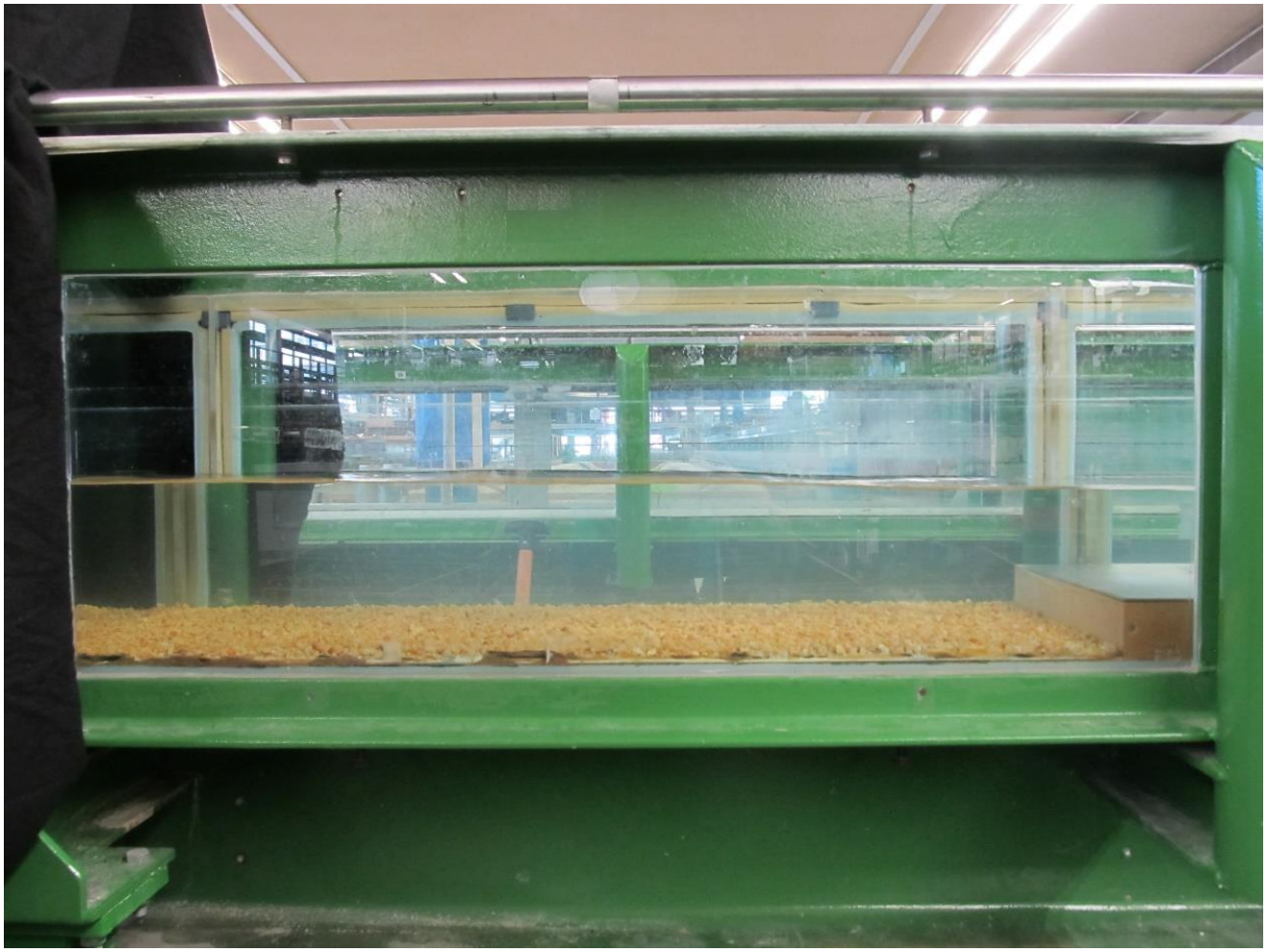

TU Delft ARCADIS

A new physics-based method for estimating the excess turbulence downstream of a structure

Melvin Koote

Master thesis

Hydraulic Engineering

Delft University of Technology

4th September 2017

Graduation committee:

Prof. dr. ir. W. S. J. Uijttewaal	Delft University of Technology
Dr. ir. H. G. Voortman	Arcadis
Dr. ir. B. Hofland	Delft University of Technology
Dr. ir. J. D. Bricker	Delft University of Technology

Voorwoord / Preface

Dit rapport is het resultaat van mijn onderzoek naar de ontwikkeling van turbulente energie benedenstrooms van een waterbouwkundig kunstwerk. Dit onderzoek heb ik gedaan ter afsluiting van mijn MSc studie Hydraulic Engineering aan de TU Delft.
Dit onderzoek is mede tot stand gekomen bij ingenieursbureau Arcadis. Tijdens mijn project daar heb ik veel geleerd over de werkzaamheden van een ingenieursbureau en deze kennis en ervaringen vormen een grote inspiratie voor mijn latere werkzame leven.

Graag zou ik enkele personen willen bedanken voor hun bijdrages aan het tot stand komen van dit rapport:

Allereerst is dit Hessel Voortman, die dit project voorstelde. Daarnaast was hij mijn dagelijks begeleider, wat inhield dat mij op weg hielp, me tips gaf en me opbeurde als ik het even niet meer zag zitten.
Ook wil ik Wim Uijttewaal bedanken voor het voorzitten van mijn afstudeercommissie, zijn grote kennis van turbulentie, zijn kritische blik die me scherp hield en het feit dat ik experimenten mocht uitvoeren in het Waterlab.
Bas Hofland wil ik bedanken voor het delen van zijn kennis over turbulentie en bodembeschermingen en het geven van waardevolle tips over het meetprogramma en de verwerking van de resultaten.
Voor het completeren van mijn afstudeercommissie en zijn tips over het rapport, wil ik graag Jeremy Bricker bedanken.
Henry Tuin is de persoon die me een wat intensievere begeleiding gaf toen ik even in een dipje zat, waar ik mede dankzij hem weer uitkwam. Uiteraard wil k hem daar hartelijk voor bedanken, evenals voor zijn positief-kritische feedback op tussenrapportages en zijn begeleiding met Mathcad.
Zonder de experimenten in Het Waterlab had dit onderzoek niet kunnen bestaan. Daarom wil ik heel graag Sander de Vree en de overige medewerkers bedanken voor het beschikbaar stellen van een stroomgoot in het Waterlab, de planning en opbouw van mijn meetopstelling en het herstellen van de laser-opstelling, wanneer deze niet meer werkte.
Verder wil ik Jos van Kerckhoven bedanken voor de kans die hij me heeft gegeven om mijn afstudeerproject bij Arcadis te doen.
Daarnaast wil ik graag alle secretaresses bedanken voor het plannen van afspraken en ander secretarieel werk. Hierbij is, vanwege hun vele werk, een extra vermelding voor Otti Kievits (TU Delft), Martine Pelgrim (Arcadis) en Chantal Besamusca (Arcadis) op zijn plaats.
Ook wil ik graag alle collega's van Arcadis bedanken voor de gezellige sfeer op de werkvloer en de vele interessante gesprekken. De drie personen die ik hierbij wil uitlichten zijn Matthijs Benits, Jos van der Baan en Kasper Stoeten, voor hun begeleiding met enkele computerprogramma's.
Tot slot wil ik graag mijn ouders en andere familieleden bedanken voor het feit dat ze me een thuis gaven, interesse toonden in mijn werk en altijd in me geloofden.

Ik wens u allen veel leesplezier toe met mijn afstudeerscriptie.

Met vriendelijke groet,

Melvin Koote
4 september 2017

Abstract

Erosion and sedimentation are natural processes that occur in natural flows.
If the erosion is a threat for a structure, a bed protection is necessary to stop this process. A bed protection usually consists of relatively large stones.

For calculating the required dimeter of the stones several formulae are available, of which the formula of Shields is the most well-known. In most of these formulae the required dimeter depends on the maximum flow velocity.

Almost all flows in hydraulic engineering are turbulent. This means that the velocities are not constant in time, but fluctuating. Due to this irregular nature, the flows are described in a statistical way with a mean velocity and a standard deviation. This standard deviation is called turbulence.
In a uniform flow, the amount of turbulent remains constant, but it increases rapidly just behind a hydraulic structure and decreases gradually further downstream. The situation that will be dealt with in this research is that of the Backward Facing Step.
The turbulence is often represented as the amount of turbulent energy.

If the relative turbulence is known, the maximum velocity can be calculated and from that follows the required stone diameter. Knowing the standard deviation of the velocities is therefore very important, since having too small stones can destroy the bed protection and too large stones are more expensive and their placement could lead to practical problems.

Voortman (2013) came up with a new method to predict the turbulent energy, based on the energy cascade. He assumed that the dissipation rate of the turbulent energy depends on the amount of energy itself. Hoeve (2015) concluded, based on earlier experiments, that the method might work for the increase of turbulence, but that not enough data was available for calibrating the method for predicting the decrease of turbulence further downstream.

For this reason, twelve new experiments were done in the Laboratory for Fluid Mechanics of the Delft University of Technology. The experiments consisted of a step and a certain combination of water depth, flow velocity and bed roughness behind the step.

In these experiments, the flow velocities were measured at various locations and levels, so that the mean velocity and standard deviations at various locations are known.
In combination with the measured water depths, the head levels and turbulent energy could be calculated at each location and from that the change in head level and turbulent energy could be calculated.

The measurement data was obtained in both the deceleration zone and behind the reattachment point.
After a careful analysis, it turned out that it is possible to describe the dissipation of the turbulence with an exponential function, as suggested by Voortman (2013).
With the obtained data it should be possible in the near future to find a better link between the generation and dissipation of turbulent energy as well, leading to the creation of a new turbulence method and resulting in better bed protections.

Contents

List of symbols

α	Correction coefficient for kinetic energy	(-)
A	Cross-sectional area of the flow	(m^2)
β	Correction coefficient for momentum	(-)
B	Width of the flow	(m)
c	A certain constant	(-)
d	Depth of the flow	(m)
D	Diameter of the stones	(m)
E	Mean flow energy	(J/m^3)
f	Variable used in the analytical solutions of ATM	(1/m)
ϕ	Dissipation coefficient used in ATM	(-)
Fr	Froude number	(-)
g	Gravitational constant	(m/s^2)
h	Water level	(m)
h_b	Water level with respect to the bed level	(m)
h_{step}	Height of the step in BFS flow	(m)
H	Energy head of the mean flow	(m)
$\widehat{H}$	Energy head of mean flow and turbulence combined	(m)
k	Turbulent kinetic energy	(m^2/s^2)
$\bar{k}$	Depth-averaged turbulent kinetic energy	(m^2/s^2)
L	Length scale	(m)
M	Temporal and depth-averaged momentum	(kg m/s)
μ	Average	(depends on situation)
ν	Kinematic viscosity	(m^2/s)
$\bar{p}$	The root-mean-squared pressure fluctuations	(N/m^2)
$\bar{P}$	The time-averaged pressure fluctuations	(N/m^2)
q	Specific discharge	(m^2/s)
Q	Discharge	(m^3/s)
r	Turbulence intensity	(-)

R	Hydraulic radius	(m)
Re	Reynolds number	(-)
ρ_w	Density of water	(kg/m^3)
ρ_s	Density of stones	(kg/m^3)
σ	Standard deviation	(depends on situation)
t	Time	(s)
u	Velocity in streamwise direction	(m/s)
$\tilde{u}$	Instantaneous velocity	(m/s)
$\bar{u}$	Temporal averaged streamwise velocity	(m/s)
$\bar{\bar{u}}$	Temporal and depth-averaged streamwise velocity	(m/s)
$\acute{u}$	Variation from temporal averaged streamwise velocity	(m/s)
u'	Root-mean-square of velocity fluctuations	(m/s)
v	Velocity in vertical direction	(m/s)
w	Velocity in transverse direction	(m/s)
x	Streamwise coordinate	(m)
y	Vertical coordinate	(m)
y_b	Height of the bed level	(m)
z	Transverse coordinate	(m)

List of figures

List of tables

List of images

Chapter 1

Introduction

1.1 Background information

The Netherlands is a low country with lots of water in and around it. In fact, more than a quarter of The Netherlands is located beneath sea level. (PBL) For this reason, people of The Netherlands have been protecting their country against the water for many centuries, leading to the construction of protections such as dikes, dams and barriers. Because the water was everyone's enemy, all people had to work together to defeat the water. The Dutch word "poldermodel", used in consensus decision-making, has its origin in this practice.

Weirs and sluices were built to control the water level in rivers. Most of these structures are accompanied with locks, to keep the rivers navigable for ships, and fish passages, so that the fishes can swim uninterruptedly in the whole river.

At those structures, often a bed protection is used. Under normal conditions a balance exists between the characteristics of the water and the river bed, but at structures the velocities are usually higher, leading to erosion. Erosion itself is not a problem, but it will be when it undermines the stability (and thus safety) of a structure or adjacent dike. The bed protection is therefore needed to maintain the stability of the structure.

A bed protection usually consists of large rocks that will not be transported by the water and so preventing the smaller stones underneath them from being transported as well.

Over the centuries, the dimensions of these protections have been calculated via multiple different methods. From the twentieth century on, a more scientific approach came into existence, although a lot of formulae still use empirical determined coefficients.

To calculate the size of the required rocks, the velocity of the water needs to be known. Under normal circumstances water in rivers and canals has a chaotic pattern, called turbulence. Because of this the velocity is not constant, which makes the calculation more complicated.
Because the bed protection must remain stable under (almost) all conditions, the maximum hydraulic load needs to be known and therefore the standard deviation of the velocities needs to be available.

1.2 Research motivation

For most practical cases, the real amount of turbulent energy is unknown, because a tool that can calculate that amount in a relatively short time is still unavailable. Therefore, usually a certain value for the turbulence is assumed, based on crude empirical formulae. For safety reasons, this value is usually too big, leading to a possible overestimation of the dimensions of the bed protection, resulting in excessive costs.

Based on the energy balance equation, Voortman (2013) came up with a much faster mathematical solution to predict the amount of turbulent energy after a sudden increase of turbulence, for instance behind a backward facing step. Hoeve (2015) analysed some earlier experiments with this

step to check the validity of this concept and he concluded that this new method could work, but that not enough data were available to come up with a definitive answer.

1.3 Research objectives

The main objective of this research is improving the new method of Voortman, which could lead to a better understanding of the physics behind turbulence. When successful, this method could be used to design a bed protection in a shorter amount of time.

One of the key factors in this method is the rate of dissipation of turbulence.
The dissipation of turbulence itself is difficult to measure, but it can be obtained from the total (turbulent) energy cascade. The second objective is therefore to get good measurements of the amount of turbulent energy at several locations and an understanding of how the amount of turbulent energy changes in stream wise direction.

Since the dissipation of turbulence is the difference between the generation of turbulence and the actual turbulence, the generation rate has to be known as well to calculate the dissipation rate of turbulence. If it is assumed that turbulence is generated from the decrease of mean flow energy, calculating the mean flow energy at various locations will be the third objective.

The fourth objective is again a consequence of the above: to determine the mean flow energy, both the water depths and velocities at certain locations should be known. The last objective is therefore to create new reliable data about the water depth and velocities for different flow scenarios.

1.4 Methodology

The aim of this report is to be complimentary to the existing theories on mean flow characteristics and turbulence. For this reason, these existing theories are described in Chapters 2 and 3.

Since Hoeve found out that not much data was available downstream from the step, a new experiment with a backward facing step was executed during this research. The experiment was executed in a flume and consisted of twelve different flow scenarios in which the water depths and flow velocities were measured at different heights in the water column and at various locations in streamwise direction.
From these measured water depths and velocities both the energy level and the amount of turbulence could be calculated at every location.

With these calculated results, the method of Voortman could be improved, which might result in a better understanding of the physical phenomena responsible for turbulence and leads to a more efficient (process of designing a) bed protection.

Chapter 2

Introduction to stationary turbulent flows and bed protections

2.1 Introduction

In this chapter will be treated what bed protection is and how it can be designed, but before doing so, the processes in the flow will be discussed.
The most important process for this thesis is the occurrence of turbulence. Since the mean flow is the most important source for turbulence (Tennekes & Lumley, 1972), its characteristics will be treated before (the effects of) turbulence will be introduced.

The basic formula for the discharge is $Q = A * u$ (2.1), with A being the cross-sectional area and u being the (temporal and depth-averaged) flow velocity.
Since mass (of water) cannot be generated or destroyed, the discharge remains constant, as long as there is no extra inflow or outflow.

In reality, the flow is 3-Dimensional, which means that fluctuations occur in all directions. In this report, however, only the streamwise direction and the vertical direction are considered, which reduces the flow to a 2-Dimensional situation. Furthermore, it is assumed that the cross-section of the flow is rectangular and that the width is constant, which means that $q = \frac{Q}{B}$ (2.2) is constant as well.
In this report, all flows are assumed to be stationary. This means that the stochastic characteristics of the flow do not change in time at any point in the fluid. In reality, small variations might happen, but when they are small enough and do affect the mean motion, the flow can still be seen as stationary.
A flow is called uniform if the characteristics of the flow do not change in space either (MIT, 2006). In this report, both uniform and non-uniform flows will be treated.

The height of the water layer can be described in three ways: the thickness of the water layer (d), the height of the water layer above a certain reference point (h) or the height of the water layer above the bed (h_b). All three notations play a role in this report and are visualized in Figure 1.

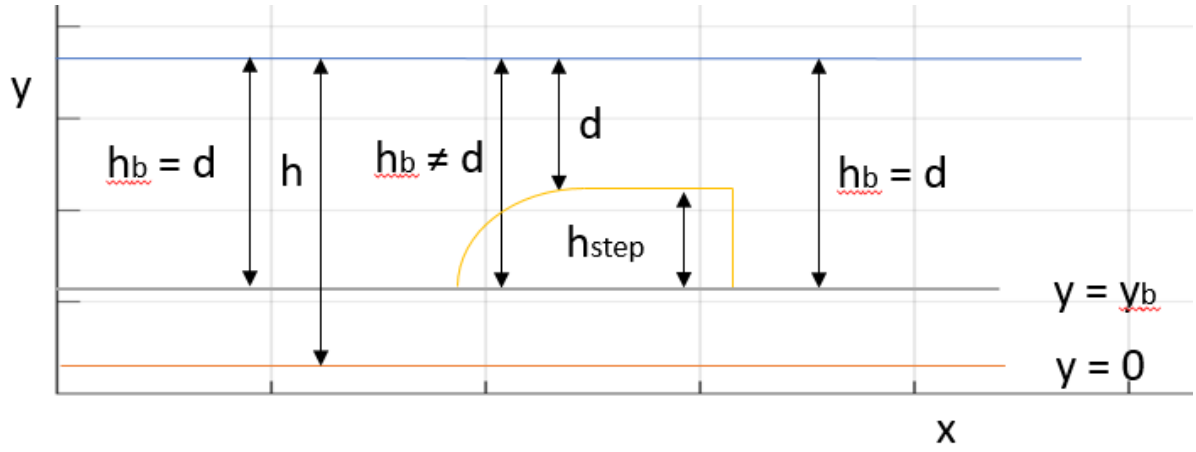

Figure 1: The difference between water depth and water height.

Apart from the height of the water, the bed level (y_b) plays a role. This is the height of the bed relative to a certain reference point. For an (almost) horizontal situation y_b can be seen as constant and is then usually left out of the equation. (Figure 2 and 3). The water level is then defined as:

$$h = y_b + h_b \quad (2.3)$$

This means that h and h_b are identical, if the bed layer lies at y=0.

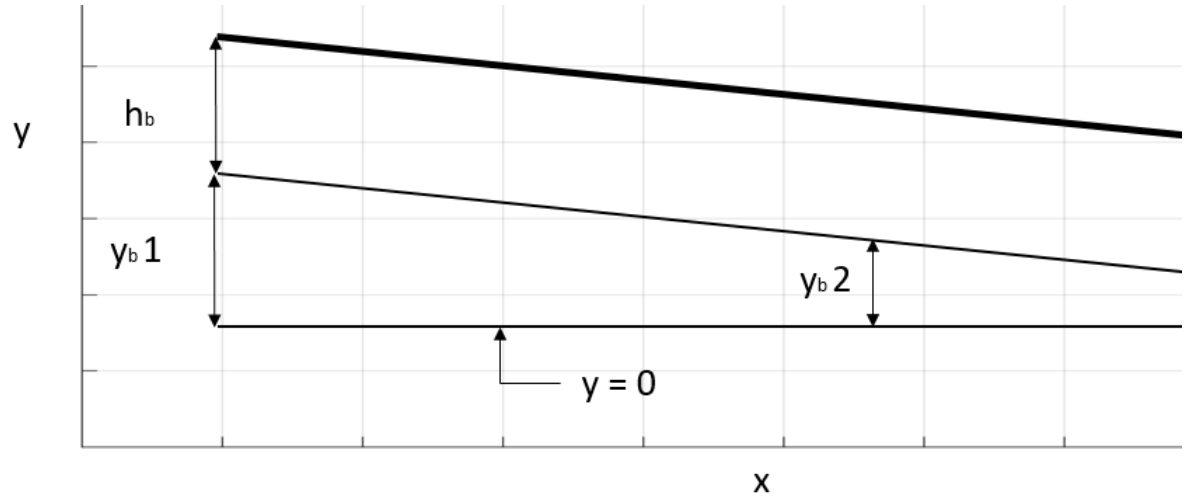

Figure 2: Uniform flow on a sloping bed.

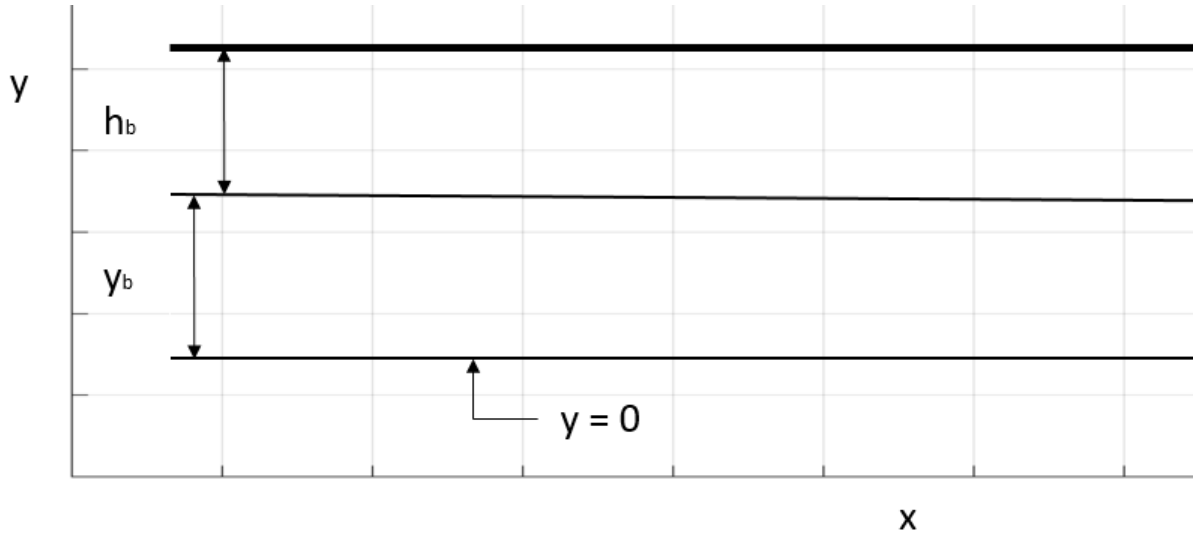

Figure 3: Uniform flow on a horizontal bed (with the bed not at y=0).

2.2 Defining turbulent flows

Most flows in hydraulic engineering are turbulent. These flows do not have such a nice organized structure, but are more chaotic, which means that flow is going in all directions and the flow is not constant in time.
This is in contrast with laminar flows, whose streamlines are parallel.

Because of their irregular behaviour, turbulent flows are usually defined in a statistical way. (MIT, 2016)
Although the flow goes in multiple directions, normally one direction is the dominant one and the characteristics in this direction can often be assumed to be stationary.

This can be done by dividing the flow velocity in a mean and a fluctuating part. This procedure is known as the Reynolds decomposition (as discussed by e.g. Hinze, 1975):

$$\tilde{u} = \bar{u} + \acute{u} \quad (2.4)$$

In this formula is $\tilde{u}$ the instantaneous flow velocity, $\bar{u}$ the average velocity and $\acute{u}$ the variation from the average velocity. By definition $\sum \acute{u} = 0$ and thus the average of the fluctuations is zero.
Since turbulent flows are chaotic and thus not constant in both time and space, the average velocity itself gives little information about the total flow and therefore the standard deviation is calculated as well.
The standard deviation is the root-mean-square of the velocity fluctuations over time and will be called u':

$$u' = \sqrt{\frac{\sum_{i=1}^{T} (\tilde{u_i} - \bar{u})^2}{T}} \quad (2.5)$$

This procedure is applicable for all three directions.

A good indication if the flow is laminar or turbulent, is given by the Reynolds number, which is defined as the ratio between advection term and diffusion terms (or as a ratio between the inertial and viscous forces) in a flow and can be written as (Reynolds 1883):

$$Re = \frac{\bar{\bar{u}} d}{\nu} \quad (2.6)$$

Since the kinematic viscosity (v) is, under normal conditions, constant for a given fluid, the Reynolds number depends mainly on the velocity and the depth of the flow.
Usually it is assumed that for an open channel the flow is turbulent for Re > 2000. (Cruise et al., 2007)

The Froude number is defined as: $Fr = \frac{\bar{\bar{u}}}{\sqrt{gd}}$ (2.7)
This number is used to determine if a flow is subcritical or supercritical. The former is the case when Fr<1 and the latter happens when Fr>1.

2.3 The (turbulent) energy of flowing water

The energy in flowing water can be divided into two parts: potential energy and kinetic energy. The potential energy is a result of gravity and is defined as the height of the water above a certain reference point. The standard formula for potential energy is $E_p = mgh$ (2.8)

The kinetic energy is the result of motion and can be described with $E_k = \frac{1}{2}\, m\, \bar{\bar{u}}^2$ (2.9)

The total energy is then $E_t = E_p + E_k = mgh + \frac{1}{2}\, m\, \bar{\bar{u}}^2$ (2.10)

In hydraulic engineering, this total energy is usually expressed per unit of volume and presented as:

$$E = \rho g h + \frac{1}{2}\, \rho\, \bar{\bar{u}}^2 \quad (2.11)$$

This energy is often divided by the mass density and the gravitational acceleration and called the (energy) head level: $H = h + \frac{1}{2}\frac{\bar{\bar{u}}^2}{g}$ (2.12). This concept is visualized in Figures 4 and 5.

Besides the above mentioned mean flow energy, also turbulent energy plays a minor role in the total energy.

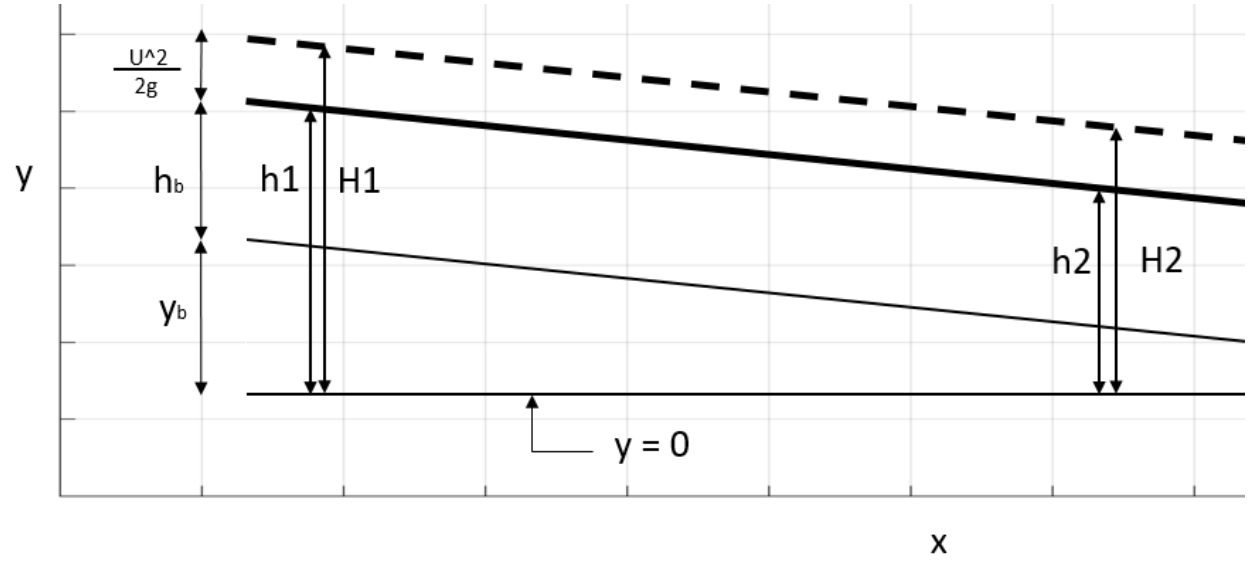

Figure 4: Energy head on a sloping bed.

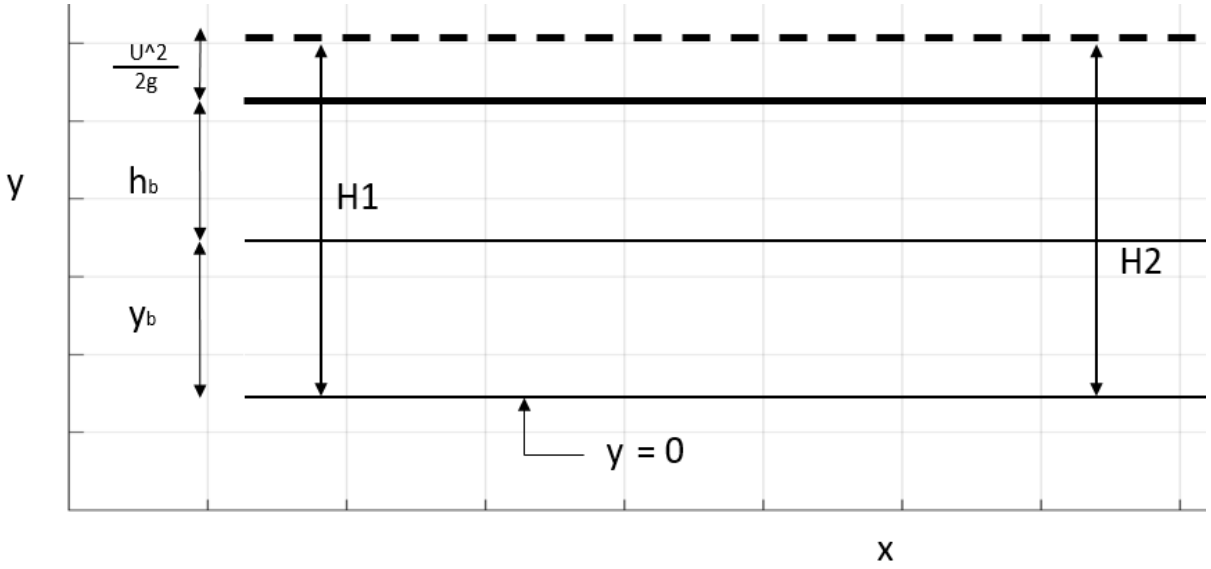

Figure 5: Energy head on a horizontal bed (with the bed not at y=0).

Energy is a preserved property and cannot be created or destroyed, but only converted in another form, like heat.
When the energy head remains constant, the energy is preserved within the flowing water. If the energy head decreases, the energy is converted and it will be called energy loss in this report, since the energy does not contribute to the flow anymore.

The case that the energy head remains constant is better known as Bernoulli's equation and is based on the 1-Dimensional Euler equations, that stated that along a streamline, the energy remains constant.
In Bernoulli's equation, it was assumed that the kinetic energy is evenly distributed over the depth, requiring the same velocity at all heights (at one location). Because of friction near the bottom, the velocity there is lower than in the upper part of the flow. This means that the assumption is not completely true.

The total kinetic energy is the square of the velocity, integrated over depth, which is not the same as the depth-averaged velocity squared.
This means that at every height the velocity should be known, which is quite difficult. It can, however, be described by multiplying the average velocity with a correction factor α that takes the effects of the velocity profile into account (Cruise et al., 2007).

The result of this is:

$$H = y_b + h_b + \alpha \frac{1}{2}\frac{\bar{\bar{u}}^2}{g} \quad (2.13)$$

α can be calculated with the formula from Cruise et al. (2007):

$$\alpha = \frac{1}{A * \bar{\bar{u}}^3} \int \bar{u}^3 \, dA \xleftrightarrow{B=constant} \alpha = \frac{1}{d * \bar{\bar{u}}^3} \int_0^d \bar{u}^3 \, dy \quad (2.14)$$

Because α has a considerable influence on the total energy, calculating the proper values of α is an important aspect in this research that deals mainly with non-uniform flow.

In a uniform flow, the velocity distribution over depth can be described with a logarithmic profile. The consequence is that in these situations α≈which means that the correction factor is usually left out of the equation. In Cruise et al. (2007), more information about the assumptions of Bernoulli's equation can be found.

When formula for the energy head is differentiated in the streamwise direction, it becomes:

$$\frac{dH}{dx} = \frac{dy_b}{dx} + \frac{dh_b}{dx} + \frac{\alpha}{g}\bar{\bar{u}}\frac{d\bar{\bar{u}}}{dx} + \frac{\bar{\bar{u}}^2}{2g}\frac{d\alpha}{dx} \quad (2.15)$$

This is the stationary version of the one-dimensional Saint-Venant equation without a friction term.

For a flow over a slope $\frac{dy_b}{dx} < 0$ which means that the other parts of the equation must change as well so to make sure that $\frac{dH}{dz} = 0$.

In reality, the bottom is never frictionless, which means that also the dissipation of energy, which results from the bottom friction, must be included in the energy equation.

Because the bed of a flow is never completely smooth, small disturbances arise in the flow and if the flow has a Reynolds number above 2000 (Cruise et al., 2007), the flow will be turbulent.
The turbulence itself contains kinetic energy as well.

The turbulence kinetic energy is the sum of the turbulent energy in all three directions, defined as (Schiereck, 2001):

$$k(y) = \frac{1}{2}\left(u'^2 + v'^2 + w'^2\right) \quad (2.16)$$

Since in this study only 2 components have been measured (u and v), an assumption should be made for the fluctuation magnitude in the transverse direction. In Nakagawa & Nezu (1987) was found that $w'^2 \approx \frac{u'^2+v'^2}{2}$ (2.17) in uniform flow. This ratio is not constant for all the locations in the flow, so it can be a source of inaccuracies.

For a 2-Dimensional situation the depth-averaged turbulence is then defined as (Schiereck, 2001):

$$\bar{k} = \frac{1}{d}\int_0^d k(y)\,dy \quad (2.17)$$

In practical situations, often the relative turbulence is used since that term is an indication about the variations in the flow velocity, but independent of the velocity itself. The relative intensity turbulence in the whole water column for a 2-Dimensional situation is defined as (Hoffmans, 1993):

$$r = \frac{u'^2}{\bar{\bar{u}}} \quad (2.18)$$

Hoffmans (1993) found that for uniform flow:

$$\bar{k} \approx (r * \bar{\bar{u}})^2 \quad (2.19)$$

which means that in those cases r can also be calculated via:

$$r = \frac{\sqrt{k}}{\bar{\bar{u}}} \quad (2.20)$$

The complete energy balance equations for both the mean flow and turbulent energy are given by i.a. George (2013).
The most important conclusion for this research is that the turbulent stresses are a dissipation term in the equation for the mean flow energy, while it is the only production term in the equation for the turbulent kinetic energy. (Hoeve, 2015)

From this can be concluded that, under the assumption that the other sink terms in the mean flow energy are negligible, the reduction of the kinetic energy of the mean flow is almost equal to the generation of the turbulent energy. This means that the decay of mean flow energy can be seen as the main source of turbulent energy.

The dissipation of mean flow energy is a result of shear stress. In a uniform flow, this is due to the friction at the bed.
Schiereck (2001) showed that the transition of mean flow energy into heat is negligible compared to the dissipation of turbulent energy.
The reason for this mechanism is that the dissipation of (mean flow) energy takes place via the shear stress:

$$\tau = \rho\nu\frac{d\bar{u}}{dy} \quad (2.21)$$

Except close to the bottom, the value of $\frac{d\bar{u}}{dy}$ is usually very small and thus τ is too small to transform all the energy into heat. (Schiereck, 2001) When turbulence plays a role, the velocity gradient is much higher due to the local velocity differences.

The decrease of the whirls inspired Richardson (1922) to write a poem:

"Big whirls have little whirls that feed on their velocity,

And little whirls have smaller whirls and so on to viscosity"

This means that due to the larger effects of viscosity, the dissipation of turbulent energy takes place on the smallest scales.

2.4 Uniform (turbulent) flows

The term "stationary flow" does not mean that the flow characteristics remain the same at all locations, it just means that at a certain location the characteristics do not change. As a result, accelerations and decelerations in the flow are possible, but they will always be located at the same places.
If the flow does have the same characteristics at all locations in the streamwise direction, it is called uniform flow. (MIT, 2006)

This means that a steady uniform flow does not change in both space and time, while a steady non-uniform flow is only constant in time. The latter one is more common in this research, but to get to a complete solution, the first one has to be treated as well.

Since in uniform flow the characteristics of the flow are constant in x-direction, $\frac{dh}{dx} = \frac{d\bar{\bar{u}}}{dx} = \frac{d\alpha}{dx} = 0$ and the change in energy level reduces to $\frac{dH}{dx} = \frac{dy_b}{dx}$ resulting in a head level change that is equal to the bed slope.

For uniform flow over a rough bottom Chezy came up with a formula that can be found in e.g. Schiereck (2001):

$$\bar{\bar{u}} = C\sqrt{R\left|\frac{dH}{dx}\right|} \quad (2.22)$$

with R being the hydraulic radius, defined as the area divided by the perimeter, and C being the Chezy coefficient, related to the bed friction. Since the energy head is non-increasing, $\frac{dH}{dx}$ is negative or zero, hence the absolute value should be used.

Substituting this formula in the energy equation (2.15) leads to:

$$\frac{dy_b}{dx} = \frac{dH}{dx} = -\frac{\bar{\bar{u}}^2}{C^2 R}$$

Which means that for uniform flow the bed slope and velocity are related.

According to Hoffmans (1993) the amount of turbulent energy is constant in uniform (stationary) flow, which means that the dissipation of turbulence must be equal to its generation. Constant turbulence does not mean that there are no variations in the flow, but it means that the standard deviation of the variations is constant.
The amount of relative turbulence is given by:

$$r_0 = c_0 \frac{\sqrt{g}}{C} \quad (2.23)$$

in which c_0 has a value of 1.21 based on several experiments (Hoffmans, 1993).

2.5 Stationary non-uniform (turbulent) flows

A flow is non-uniform when the properties of the flow do change in space. This happens when the circumstances change, e.g. the widening of the flow or a change in discharge, but it can also happen when the bed slope is zero.
In these cases an acceleration or deceleration takes place which also affects the water depth. When the construction period is just done, the flow will change in time, but after some time the flow will be stationary.

In these situations, the amount of turbulent energy does not have to remain constant either. When the flow accelerates, the amount of turbulent energy will remain almost the same since the flow lines become more closed together so no extra vortices can arise (Schiereck, 2001), but for a deceleration zone this works differently.

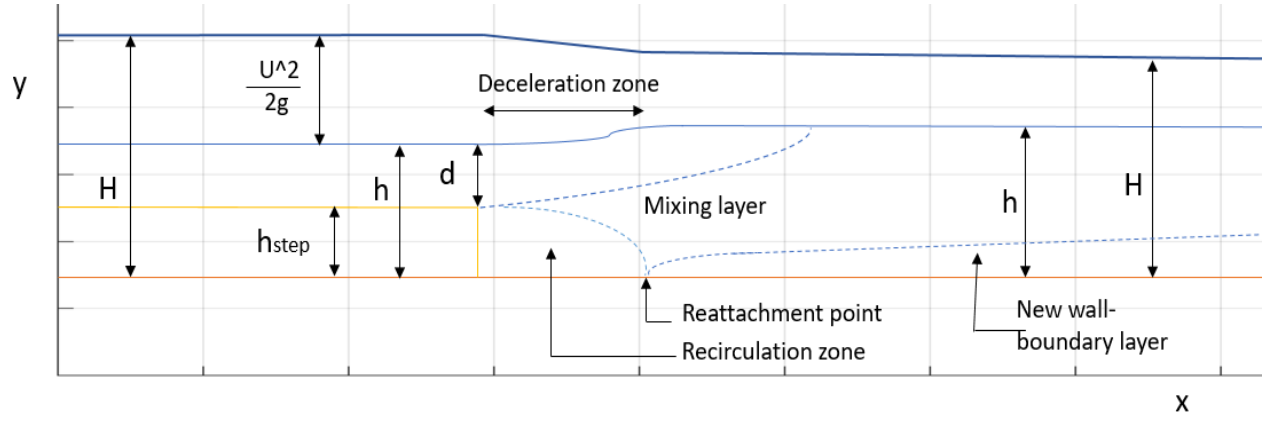

Figure 6: A schematic overview of a BFS situation with both the water and head levels.

The flow situation that will be dealt with in the rest of this research is the so called backward facing step (BFS) flow, which is visible in Figure 6.

In this case water flows over a step which influences the characteristics of the flow. The water depth is then reduced (since the bottom is increased) and the continuity of mass (q = constant) states that the flow velocity increases in that case. Because the head level remains the same (Bernoulli's equation of conservation of energy), this leads to a decrease of the water level.
As long as the bottom friction and wakes on top of the step are very small, the energy losses are negligible. The energy loss that results from flow separation at the beginning of the step is negligible as well, if the slope is smooth enough (Greenblatt & Wygnanski, 2000).
As a result it is assumed that there will be no energy loss until the end of the step.

Behind the step, the water depth becomes larger again and as a result the velocity decreases and the water level rises.
Downstream of the step, three different flow regions can be distinguished: recirculation zone, mixing layer, and new wall-boundary layer (Hoffmans, 1993). In Figure 4 these different regions are visualized with dotted lines.
The formation of a recirculation zone is a result of the fact that just behind the step, the water is mainly stagnant up until the height of the step. Above this height, the water is flowing because of the upstream water that enters this location.
This flowing water then acts a force on the stagnant water, so that the top of this stagnant water also becomes flowing. At the bottom, the water flows in the opposite direction, to balance the amount of water in this region. This results in a recirculation zone in which the vertically averaged velocity is zero.

The length of the recirculation zone is not constant, but seems to depend on the Froude number and the roughness of the bed (Hofland, 2005). The reattachment point lies between 5 till 12 times the step height.

The development of the new boundary layer is described by the formula of Schlichting (1949):

$$\delta(x) = 0.37 * \left(\frac{\nu}{\bar{\bar{u}}}\right)^{\frac{1}{5}} * x^{\frac{4}{5}} \quad (2.24)$$

Although this formula was meant for smooth plates, it is assumed that it can also as a first approximation for rough beds if the stones are not too large.

Due to the deceleration of the flow, the energy is no longer maintained, which makes it difficult to calculate the water levels and velocities behind the step.
In that case, it is more convenient to use the momentum balance at an infinitely small distance from the step.

In this research, the flow situations on top of the step are the ones that are determined beforehand. The momentum balance will then be used to check what the equilibrium water level is and it will give a rough indication about the distance needed to reach the equilibrium water level.
To simplify the problem, the bottom is assumed to be (almost) horizontal, which is not a big mistake compared to a real river, given the small spatial extent.

Hoeve (2015), among others, reasoned that the amount of momentum just behind the step can then be calculated as:

$$M_{upstream} = \frac{1}{2}\,\rho_w\, g\,(d_{on\ the\ step} + h_{step})^2 + \rho_w\, d_{on\ the\ step}\,\overline{\overline{u_{on\ the\ step}}}^2 \quad (2.25)$$

With $M_{upstream} = M_{downstream}$ and $q = d_{on\ the\ step} * u_{on\ the\ step} = h_{downstream} * u_{downstream}$ the water depth (far) downstream of the step can be calculated.

If Fr < 1, the flow is subcritical, which means that the downstream water level determines the upstream water level. This means that with this formula the upstream water level can be calculated if the downstream water level is known. If the water level on top of the step is known, it can be calculated what the water level at the downstream side (and far away from the step) is supposed to be.

This recirculation becomes smaller further from the step, since more stagnant water is brought into motion by the flowing water on top of it. The point where the height of the recirculation zone becomes zero, is called the reattachment point. After this point, a new boundary layer will be formed.

In case of a supercritical flow (Fr > 1), the upstream water level is independent from the downstream water level and the downstream water level can be calculated via the formulae valid for weirs, but that situation will not be further treated in this report.

When the flow decelerates, for instance behind a backward facing step, the opposite is true. Just behind the step the average flow is zero in the region from the bed to the height of the step and non-zero in the region from the step height up until the water level. This leads to friction between the flowing and non-flowing water resulting in circulating patterns in the water, called eddies. Since the flowing water already has fluctuations, also the friction will not be constant and the eddies will fluctuate even more. This leads to higher fluctuations in the flow and hence a higher turbulence.

Research of Mierlo & De Ruijter (1988) has shown that behind a step the turbulence energy k_m in the centre of the mixing layer grows to a maximum at the reattachment point. After this point k_m decreases and it becomes small compared to the turbulence energy k_b that is generated by the bed. Formulae for k_m and k_b as a function of the distance behind the step were given by Hoffmans (1992), but these formulae were primarily meant to be used near scour holes.
That research was done for the flow behind a sand dune shape, which is not exactly the same as the Backward Facing Step flow studied in this report.

Hoffmans (1993) combined these formulae to create one formula for the amount of relative turbulence behind the reattachment point of a short sill:

$$r_0 = \sqrt{\beta_k C_k \left(1 - \frac{h_s}{d}\right)^{-2} \left(\frac{L - 6h_s}{\lambda} + 1\right)^{\alpha_k} + c_0 \frac{g}{C^2}} \quad (2.26)$$

In this formula (for scour holes) L stands for the length of the bed protection, λ is the relaxation length and α_k is a factor that has a value of -1.08. Furthermore, it was assumed that the reattachment point is located at a distance 6 times the step height downstream of the step.

More than 250 experiments were executed to check the validity of this formula, but a good fit to give an accurate value of r_0, could not be found. (Hoffmans, 1993)

In Schiereck (2001) this formula was expanded with the values found by Hoffmans (1993) resulting in:

$$r_0(x) = \sqrt{0.5\, k_0 \left(1 - \frac{h_s}{d}\right)^{-2} \left(\frac{x}{\lambda} + 1\right)^{-1.08} + 1.45 \frac{g}{C^2}} \quad (2.27)$$

with $\lambda \approx 6.67 * d$, $k_0 \approx 0.045$ and x being the distance behind the reattachment point.

Although Hoffmans (1993) initially came up with his formula for a short sill, Schiereck (2001) presents it as universally applicable for turbulence behind a step.
It is uncertain whether this is justified.

The above equations are built on the assumption that behind the reattachment point both the water depth and the amount of mean flow energy do not change anymore and that as a result no more extra turbulence is generated.

At the reattachment point, the flow near the bottom goes from a negative to a positive value and can therefore be assumed to be zero at the reattachment point. Based on this, Hoeve (2015) assumed that the velocity profile can be described as triangular, meaning that $\alpha \approx 2$.
After a certain length, the flow will be uniform again. In that case, it can be described with a logarithmic profile meaning that $\alpha \approx 1$.
Under the assumptions that both the energy and discharge remain constant, combining the two scenarios leads to:

$$h_r + 2\,\frac{\left(\frac{q}{h_r}\right)^2}{2g} = h_u + 1\,\frac{\left(\frac{q}{h_u}\right)^2}{2g} \quad (2.28)$$

in which h_r and h_u are the water depths at the reattachment point and for uniform flow respectively.

If it is true that there will be no head level loss behind the reattachment point, the water depth will increase, since from the above equation follows $h_u > h_r$ for all situations with subcritical flow.
This means that the head level water depth cannot both remain constant.

Hoeve (2015) found in earlier experiments that the water level increase is less than could be expected from the above equation. In combination with a decreasing value of α, this means that the head level is decreasing as well.
A possible explanation for this is the internal friction resulting from the decreasing velocity. This friction then leads to the production of extra turbulence.

Hoeve (2015) thereby suggested the possibility that even after the reattachment point turbulence is produced.

More experiments with measurements (far) behind the reattachment point are required to see if this conclusion is justified.

2.6 The aim of a bed protection

A phenomenon that takes place in most natural flows, is the transportation of sediment.
This process is the result of three different forces, namely drag force, lift force and shear force.
In Schiereck (2001) it is shown that these three forces are all proportional to the water density, the square of the velocity near the stone and the square of the diameter of the stone.
In an equilibrium situation, the lift force is balanced by the submerged weight of the stone, while the other two forces are balanced by either a friction force or the torque around the stone.
This balance can be represented as $\rho_w * u^2 * d^2 \propto (\rho_s - \rho_w) * g * D^3 \quad (2.29)$ (Schiereck, 2001)

When a structure is built the processes of erosion and sedimentation are usually not in balance, because around the structures the flow is not uniform and during and shortly after the construction period, the flow is not stationary either.
Near a structure the flow velocity might be higher, which leads to erosion. This is not necessarily a problem, but when the stability of the structure is at risk, this potential erosion must be opposed.
If that is the case a bed protection is used, whose goal it is to prevent the river bed to erode.

The conclusion of the above is that a bed protection is necessary when erosion of a river bed causes a potential danger for instability of a structure.

2.7 Existing design approaches for a rock bed protection

The biggest demand for a bed protection is that it cannot be damaged by the flowing water.
In this report, the focus lies on the top layer of a bed protection. Other aspects, like filters, are beyond the scope of this report and will not be treated.

The erosion of bed material is related to the bottom shear stress, but since this is difficult to measure, it is most of the time related to the (depth-averaged) flow velocity. Because of this, the most important design parameter is the critical flow velocity, which is the flow velocity at which the bed protection will start to erode.

From equation 2.29 can be concluded that $u_c{}^2 = \mathrm{K}\,\Delta g D \quad (2.30)$, in which u_c is the maximum horizontal velocity near the bed, K is a constant that depends on the given situation and Δ is the relative submerged density.

That means that the required stone diameter can be calculated if K, Δ and u are known for a certain situation.

The value of Δ depends on the used stones and will not be further treated. For the value of K two basic alternatives are available: the methods of Izbash (1935) and Shields (1936) respectively, which are both explained very well in Schiereck (2001).

Izbash (1935) came up with an expression when the (critical) local velocity near the bed is known. The value of K is then approximately 2.88, but the formula is better known in this form:

$$u_c = 1.2\sqrt{2\,\Delta\,\mathrm{g}\,\mathrm{D}} \quad (2.31)$$

The disadvantage of this formula is that the relation with the water depth is not clear (Schiereck, 2001) and that usually the velocity at the bottom is not known.

Shields (1936) introduced another parameter ψ_c, which is a stability parameter that uses a critical value of the (shear) velocity.

It is defined as $\psi_c = \frac{\tau_c}{(\rho_s - \rho_w)\,g\,D} = \frac{{u_{*c}}^2}{\Delta \mathrm{g D}}$ (2.32) (Schiereck, 2001)

Since u_* is related to u via $u_* = \frac{\bar{\bar{u}}*\sqrt{g}}{C}$ (2.33), the required stone diameter can be calculated when an appropriate value of ψ_c is found. The value of ψ_c is related to the particle Reynolds number and both Shields (1936) and Van Rijn (1984) presented a graph from which the value of ψ_c can be read. Van Rijn's graph has the advantage that this value is directly related to the diameter of the stone. The consequence of this is that determining the required stone diameter is an iterative process. For larger stones (diameters larger than 1 cm) the value of ψ_c remains constant at about 0.055.

This Shields equation can be rewritten to come up with one basic stability formula for uniform flow on a horizontal bed (Schiereck, 2001):

$$D_{n50} = \frac{\overline{\overline{u_c}}^2}{\psi_c \Delta C^2} \quad (2.34)$$

Extra parameters have to be added to this equation when the bed is not horizontal or when the flow is non-uniform.

Pilarczyk (1995) combined the formulae of Shields and Izbash and added various coefficients and factors to come to one overall relationship between stone diameter and hydraulic loads. This formula is also given in the Rock Manual (2007):

$$D = \frac{\varphi_{sc}}{\Delta}\,\frac{0.035}{\psi_c}\,k_h {k_{sl}}^{-1} {k_t}^2 \frac{\bar{\bar{u}}^2}{2g} \quad (2.35)$$

On page 551 of the Rock Manual (2007) also correction factors for the average velocity are given, which could be used when the water depth is different.

2.8 The influence of turbulence in the design of a bed protection

In uniform flow, the formula of Shields can be used, but it may lead to wrong conclusions in other situations.

In the above equation for the required stone diameter the depth-averaged velocity is used. The design value is usually defined as the average velocity plus three times the turbulence, so that the real velocity is in 99.87% of the cases lower than this value. This design value is called the peak velocity.

$$u_{peak} = (1 + 3r)\,\bar{\bar{u}} \quad (2.36)$$

In non-uniform flow, a correction factor must be introduced to compensate for the higher local loads. This is because the velocity and turbulence are not constant everywhere, leading to much higher velocities and loads at certain locations.

Schiereck (2001) showed that for an accelerating flow, for instance on top of a sill, the relation between the critical velocity and stone diameter is comparable with that for a uniform flow, so that the use of a correction factor is not necessary.

The opposite is true for decelerating flows. As explained in Chapter 3 the turbulence levels are much higher in this region, resulting in stones moving at a lower critical velocity. To compensate for this, a correction factor must be included in the stone stability formula.

Schiereck (2001) defines this factor as the ratio between the average critical velocity at normal flows and the average critical velocity with increased loads.

$$K_v = \frac{\overline{\overline{u_{cu}}}}{\overline{\overline{u_{cs}}}} \quad (2.37)$$

It can be assumed that for incipient motion the extreme situations of both velocities are the same, leading to $(1 + 3r_{cu}) * \bar{\bar{u}}_{cu} = (1 + 3r_{cs}) * \bar{\bar{u}}_{cs}$

This means that the value of K_v can also be calculated via the ratio of the two different values of the relative turbulence:

$$K_v = \frac{1 + 3r_{cs}}{1 + 3r_{cu}} \quad (2.38)$$

This value of K_v, which is higher when the turbulence intensity is higher, is then included in the formula for stone stability and this results in the required stone diameter for the bed protection.

In the above-mentioned formula of Pilarczyk the factor k_t takes the effects of turbulence into account. The Rock Manual (2007) gives $k_t = \frac{1+3r}{1.3}$ (2.39), in which r is the depth averaged relative turbulence. In the Rock Manual is defined that $k_t^2>2$ for particular cases.

Table 5.55 of the same Rock Manual gives for a few different scenarios some common used values for r that can be used as a good guess. For use in the formula of Escarmeia &May, the Rock Manual (2007) gives a value of r = 0.6 for situations downstream of hydraulic structures, but since the definition of r is the same in both formulae, this value can be used in the formula of Pilarczyk as well. The corresponding value of k_t is then 2.15, which is well over the demanded value.

In Appendix A, an example is given in which the formulae of Pilarczyk and Escarmeia &May are compared. With a few rough estimations, the answers are more or less equivalent. Especially when higher turbulence levels occur, the differences can be large.

For designing purposes this approach is the most used, since it can be executed relatively fast. There is, however, no evident physical basis behind the used values of k_t and the decay of turbulent energy in downstream direction is omitted in this formula (Voortman, 2013). Therefore, it is questionable if this is the best approach for designing a bed protection.
For instance, Hoeve (2015) showed that for cases with low flow velocities the design can be optimized if the real amount of turbulent energy of the hydraulic structure is known. It is uncertain if the same holds for scenarios with higher flow velocities.

For using this theory in practice, two otherer aspects should be taken in mind, namely: r is depth averaged, which means that the relative turbulence near the bed is still unknown and the velocity distribution is not normal distributed, which means that 1+3r is not a perfect prediction for the maximum velocity.
Besides the velocity also other forces influence the stability of the bed protection, but they will not be treated in this report.

Chapter 3

A fast method to model turbulence for practical use

3.1 The basic concept of the Arcadis Turbulence Method

Several methods for modelling the turbulence are currently available (Appendix B), but using them is a very time-consuming task. On the other hand, it was shown in Chapter 4 that correctly predicting the amount of turbulence can be important when designing a bed protection. Using a new method might be able to combine the two demands accuracy and speed.

Based on the energy cascade, Voortman (2013) came up with a new method for turbulence modelling. The aim of this method is to give a faster answer than a computational model, but with a better understanding of the physical processes than is done in the current approach. This method is currently called the Arcadis Turbulence Method (ATM).

The remaining of this section is mainly taken from Voortman (2013).
This method has its basis in an energy balance for the depth-averaged turbulence kinetic energy. Since $\bar{k}$ is a kinetic energy divided by the density, this turbulent energy can be added to the mean flow energy to get the "total" energy:

$$\hat{E} = E + E_t = \left(\rho g y_b + \rho g h_b + \alpha \frac{1}{2} \rho \bar{\bar{u}}^2\right) + \rho \bar{k} \quad (3.1)$$

When this is divided by the density and the gravitational acceleration the "total" energy head level can be defined as:

$$\hat{H} = \frac{\hat{E}}{\rho g} = y_b + h_b + \frac{\alpha}{2g} \bar{\bar{u}}^2 + \frac{\bar{k}}{g} \quad (3.2)$$

Figure 7 gives a schematic view of this concept for a uniform flow.

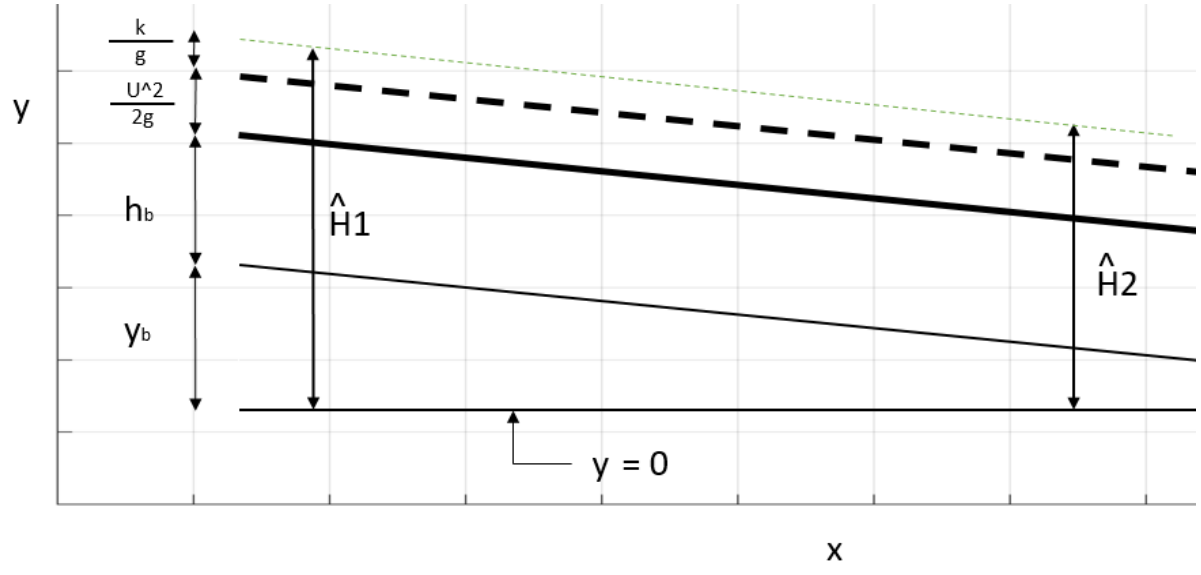

Figure 7: A schematic overview of the "total" energy head (as defined by Voortman (2013)) in a uniform flow situation.

In Figure 8 a BFS situation is shown. The flow is developed when the new wall-boundary layer reaches the water level.

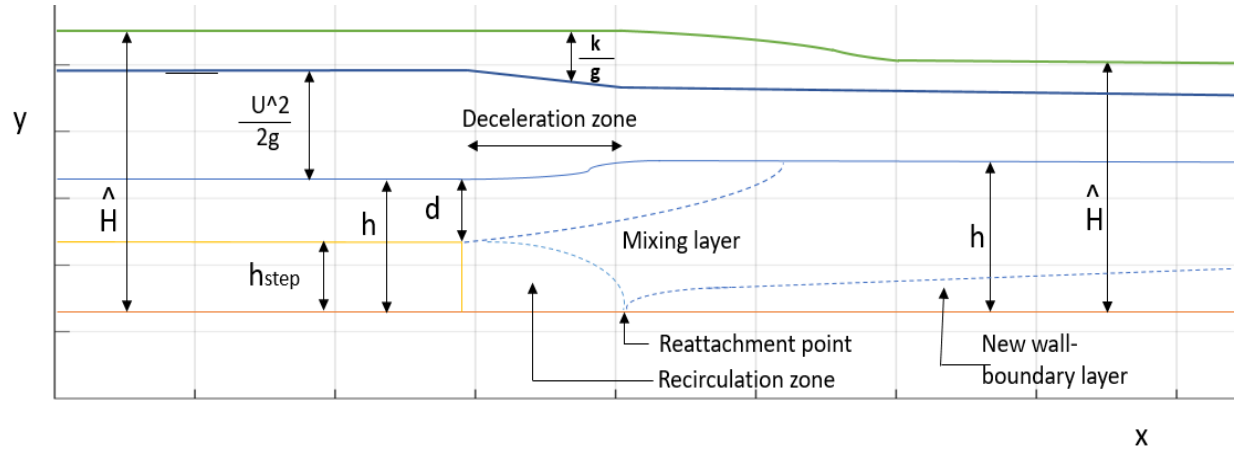

Figure 8: A schematic overview of the "total" energy head in a BFS.

Under the assumption that during the production of turbulence this "total" energy remains constant, the following is true:

$$\frac{d\hat{H}}{dx} = \frac{dy_b}{dx} + \frac{dh_b}{dx} + \frac{\alpha}{g}\bar{\bar{u}}\frac{d\bar{\bar{u}}}{dx} + \frac{\bar{\bar{u}}^2}{2g}\frac{d\alpha}{dx} + \frac{1}{g}\left(\frac{d\bar{k}}{dx}\right)_{prod} = 0 \quad (3.3)$$

For the special case of uniform flow, in which almost all derivatives are zero, this becomes:

$$\frac{d\hat{H}}{dx} = \frac{dy_b}{dx} + \frac{1}{g}\left(\frac{d\bar{k}}{dx}\right) = \frac{dH}{dx}$$

Furthermore, since in uniform flow $\frac{dH}{dx} = \frac{dy_b}{dx}$, it becomes clear that $\frac{d\bar{k}}{dx} = 0$, which is what can be expected in uniform flows.

Rewriting equation (3.3) gives:

$$\left(\frac{d\bar{k}}{dx}\right)_{prod} = -g\left(\frac{dy_b}{dx} + \frac{dh_b}{dx} + \frac{\alpha}{g}\bar{\bar{u}}\frac{d\bar{\bar{u}}}{dx} + \frac{\bar{\bar{u}}^2}{2g}\frac{d\alpha}{dx}\right) = -g\left(\frac{dH}{dx}\right) \quad (3.4)$$

In Chapter 2 Chezy's formula for the dissipation of the head level was introduced, which can be rewritten as:

$$\frac{dH}{dx} = -\frac{\bar{\bar{u}}^2}{C^2 R} \overset{E=\rho g H}{\Longleftrightarrow} \frac{dE}{dx} = -\frac{g}{C^2}\frac{\rho\bar{\bar{u}}^2}{d}$$

In the formula on the right the term $\frac{g}{C^2}$ is a dimensionless constant, which means that the decay of (mean flow) energy is then proportional to the velocity squared multiplied by the density and divided by the hydraulic radius. R is replaced by d, since it is a 2-Dimensional situation.

Since the amount of turbulent energy is the velocity squared, Voortman (2013) suggested that the same strategy can be used for the dissipation of turbulence, leading to:

$$\left(\frac{dE}{dx}\right)_{turb} = \rho\frac{d\bar{k}}{dx} = -\varphi\frac{\rho k}{R} \overset{E=\rho\bar{k}}{\Longleftrightarrow} \left(\frac{d\bar{k}}{dx}\right)_{diss} = -\varphi\frac{\bar{k}}{R} \quad (3.5)$$

in which φ is a yet unknown constant.

The total rate of turbulence can then be written as the sum of the production and dissipation:

$$\frac{d\bar{k}}{dx} = \left(\frac{d\bar{k}}{dx}\right)_{prod} + \left(\frac{d\bar{k}}{dx}\right)_{diss} = -g\frac{dH}{dx} - \varphi\frac{\bar{k}}{R} \quad (3.6)$$

3.2 An updated version of this method.

This section is mainly taken from Voortman (2016).
After observing a landing plane, Voortman (2016) came up with a new suggestion.
Instead of assuming that the dissipation rate *in space* is proportional to the amount of turbulent energy, it was now assumed that the dissipation rate *in time* is proportional to the amount of turbulent energy.

$$\left(\frac{d\bar{k}}{dt}\right)_{diss} \sim -\varphi\,\bar{k} \quad (3.7)$$

Since ATM in the near future will be used for stationary flows, the rate of change in time is less important than the rate of change in space. For this reason, the equation has to be improved to give derivative in x-direction.

When it is assumed that $\frac{dk}{dx} = \frac{dt}{dx}\frac{dk}{dt} = \frac{1}{\bar{\bar{u}}}\frac{dk}{dt}$ this leads to:

$$\left(\frac{d\bar{k}}{dx}\right)_{diss} \sim -\frac{1}{\bar{\bar{u}}}\varphi\,\bar{k} \quad (3.8)$$

From an analysis of the dimensions and the assumption that the flow is completely 2-Dimensional, the equation for the dissipation can be rewritten as:

$$\left(\frac{d\bar{k}}{dx}\right)_{diss} = -\frac{\varphi}{\bar{\bar{u}}}\sqrt{\frac{g}{d}}\,\bar{k} = -\frac{\varphi}{q}\sqrt{gd}\,\bar{k} \quad (3.9)$$

The total equation becomes then:

$$\frac{d\bar{k}}{dx} = \left(\frac{d\bar{k}}{dx}\right)_{prod} + \left(\frac{d\bar{k}}{dx}\right)_{diss} = -g\frac{dH}{dx} - \frac{\varphi}{q}\sqrt{gd}\,\bar{k} \quad (3.10)$$

3.3 Analytical solutions for this method

The production term can be written as:

$$k_{prod}(x) = -g\frac{dH}{dx}x \quad (3.11)$$

If it is assumed that the dissipation of mean flow energy is a linear function, the production of turbulent energy is linear as well.

The dissipation equation is a first-order differential equation. This equation for dissipation can be generalised as:

$$\left(\frac{d\bar{k}}{dx}\right)_{diss} = -f\varphi\,\bar{k} \quad (3.12)$$

in which f is a constant based on the used method, which means that $f = \frac{1}{R}$ for the first idea and $f = \frac{\sqrt{gd}}{q}$ for the second suggestion.

The analytical solution for this differential equation is an exponential function.

$$k_{diss}(x) \sim k_0\, e^{-f\varphi x} \quad (3.13)$$

with k_0 being the maximum amount of turbulent energy.

Since the amount of turbulent energy always reaches an equilibrium (Schiereck, 2001) and it is assumed that the turbulent energy has its maximum near the reattachment point, the above equation has to be expanded to become:

$$k_{diss}(x) = (k_0 - k_{eq}) * \exp(-f\varphi(x - x_{reatt})) + k_{eq} \quad (3.14)$$

3.4 Theoretical validity of this method

The theoretical validity of this method was mainly studied in Hoeve (2015). This section will be a summary of the findings in that report.

For equilibrium flow situations, the amount of turbulence does not change, so $\frac{dk}{dx} = 0$. As described in Chapter 2 the dissipation of mean flow energy is in that case equal to the bottom friction and both are equal to the last term on the right-hand-side of equation: $g\frac{\bar{\bar{u}}^2}{C^2 * R} = -g\frac{dH}{dx} = \varphi\frac{\bar{k}}{R}$, leading to: $\bar{k} = g\frac{\bar{\bar{u}}^2}{C^2 * \varphi}$

Combining this with the formula of Hoffmans (1993) for constant turbulence gives:
$g\frac{\bar{\bar{u}}^2}{C^2 * \varphi} = {c_0}^2\frac{g}{C^2}\bar{\bar{u}}^2$ which results in: $\varphi = \frac{1}{{c_0}^2}$

Hoeve (2015) used the energy cascade and validated the assumption that the increase of turbulence is (almost) the same as the decrease of mean flow energy. The amount of mean flow energy that is directly dissipated is very small and can therefore be neglected, especially in a model that only gives a first estimate about the order of magnitude of the amount of turbulence, which was also already described in Schiereck (2001).

To validate the correctness of the ATM for dissipation Hoeve (2015) used the dissipation ratio described in Chapter 2: $\varepsilon = \frac{{u'}^3}{L}$. This is however the dissipation rate in time instead of space, so it was divided by the average velocity.

Comparing this with the dissipation rate of the ATM leads to

$$\varphi = \frac{u'}{\bar{\bar{u}}}\frac{2R}{L} \quad (3.15)$$

The conclusion from this was that φ can only be constant if $\frac{\overline{u'}}{\bar{\bar{u}}} = constant$, which is almost never the case.

For this reason, from four earlier experiments different experiments the depth-averaged velocity, the mean flow energy and the turbulence were calculated, in order to come up with proper values of φ for different flow scenarios.

3.5 Practical applications of this method

At the end of Chapter 2 it was explained that the amount of turbulence has an influence on the required stones for a bed protection.

The actual amount of turbulence is only determined in unusual cases, since it is very time-consuming and thus costly. Instead a certain value for the turbulence is assumed and that is put into the equation to determine the stone diameter.

The disadvantage of this approach is the possibility of calculating a wrong stone size. If the stones are heavier than necessary, they will be more expensive and if they are too small, they can be transported, which will ruin the bed protection.
Another option is that, based on the assumption of a too high turbulence (and thus the need of a larger-than-necessary stone diameter), the decision is made that a bottom protection should be replaced, while in reality the turbulence is lower than expected and the placed stones have still the right diameter. That means that the whole replacement (and its costs) would have been avoided if the right turbulence levels were known beforehand.

The method described in this report is relatively simple and can be executed in a relatively short amount of time. With this result the order of magnitude of the turbulent energy can be better calculated, from which the standard deviation of the velocity can be calculated, leading to the required stone dimensions. The disadvantage is that the conversion from k to u' might introduce an inaccuracy in the result.

Hoeve (2015) showed that with this method the dimensions of the required stones can be smaller than currently used, according to the current guide lines.

3.6 Introduction to experimental research for improving ATM

Based on the calculated head levels Hoeve (2015) reasoned that in the case of ATM a convex polynomial decay of mean flow head level would give the best fit, because in that case the production of turbulence will become smaller at each location. The amount of turbulence will grow if the dissipation is smaller than the production, which will happen until the maximum is reached, whereafter the dissipation is larger and the amount of turbulence decreases.
For a linear decay of the head levels, the production of turbulence is constant. The amount of turbulence will then grow until the production and dissipation are equal. Since the production does not become smaller and the dissipation cannot become larger as it depends on the amount of turbulence available at that point, the amount of turbulence will remain the same.

Although the polynomial head level input alternative was the most promising one beforehand, it turned out that with this input alternative the calculated peak of the turbulence was in almost all situations found closer to the step than what followed from the measurements.
Hoeve (2015) therefore stated that the linear head level input alternative gave the best results since

it calculated the amount of turbulence quite good up until the reattachment point, where the turbulent energy has its peak. There was however no decrease in turbulence.

An alternative that Hoeve did not consider was an exponential decay of the head level. The results for the turbulent energy will have the same look as for the convex polynomial head level alternative, but this approach might lead to better results.

An important disadvantage of all four experiments used by Hoeve (2015) was that the measurements were only done until shortly behind the reattachment point. It was therefore unclear what happened further downstream when the amount of turbulence was expected to decrease.

The result of this was that Hoeve could use these experiments to prove that this method could work for predicting the production of turbulent energy, but doing research on the dissipation of turbulence was not possible with the results of these experiments, since it is expected that the added turbulence will dissipate behind the reattachment point.

To get an indication of the dissipation of the added turbulence, new experiments were executed in a flume at the Laboratory for Fluid Mechanics of the TU Delft. In these experiments, the measurements were done up to a few metres behind the reattachment point.

These experiments will be treated in the next chapters and by using their results, it can be checked if the dissipation of turbulent energy can be predicted by Voortman's method as well. That will be the main focus for the rest of this research.

Chapter 4

Experimental research

4.1 Measurement goals

The goal of this experiment was to calculate and visualise the development of both the head level and the turbulent energy in downstream direction, especially behind the reattachment point.
For this reason, measurements of velocity and water level had to be done at various locations and at various heights.

With the data from the velocity measurements, the temporal averaged velocity and the standard deviation of the velocity components u and v at each measurement point can be calculated.
From the time-averaged velocities, the depth-averaged velocity and the correction factor α at each measurement location can be calculated. Combining this result with the water level gives the head level at each location.
From the calculated standard deviation, the longitudinal turbulence intensity at each location can be calculated and the order of magnitude of the turbulent energy can be calculated.

With the combination of head level change and turbulent energy change the new method can be improved.

4.2 The experimental set-up

4.2.1 The basic set-up

All experiments were executed in a 0.4 m wide flume and the basic design of the experiments is visualised in Figure 9.

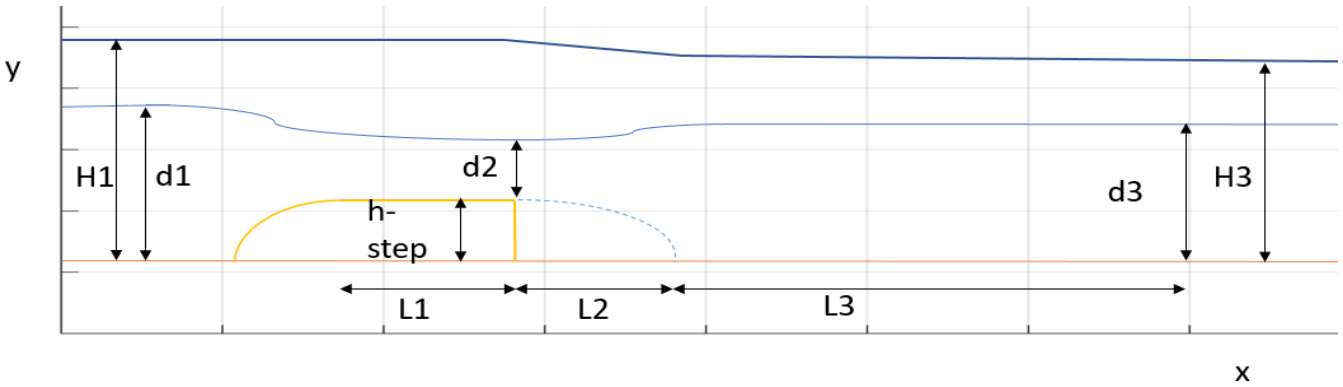

Figure 9: The experimental set-up of the flow

In Figure 9 is L_1 the length of the step, with L_2 being the distance between the step and the reattachment point and L_3 the distance between the reattachment point and the location where the flow is uniform again. As an initial guess, it is assumed that L2 is six times the step height.

For an optimal result the step height was set at 0.05 m, but since the bed protection has a thickness of about 0.003 m, the effective height is 0.047 m. For convenience purposes, it was decided that the step would be fixed and that the other parameters could be changed. This also means that L_2 is 0.30 m for all cases.

4.2.2 Three different parameters

Since the main goal of this research is to predict the generation and dissipation of turbulence under various circumstances, twelve different flow scenarios were used.

Three independent input parameters were used for the flow scenarios: water depth on top of the step, Froude number on top of the step and bottom roughness.

Two values were used for the water depth on top of the step: 0.07 m and 0.10 m. Smaller values would lead to a negligible energy decrease, while larger water depths would lead to high values for L_1 and L_2.

For the Froude numbers on top of the step three values were used: 0.25, 0.50 and 0.75. These values we chosen to get a wide and evenly distributed range of data. A Froude number of 1 was considered, but with that Froude number a lot of irregularities occurred in the fluming, leading to a very impractical situation for measurements.

The equations for the discharge and Froude number can be combined so that the discharge can be calculated as a function of the Froude number and the water depth on top of the step:

$$Q = Fr\sqrt{g}{d_2}^{3/2}B \quad (4.1)$$

For the bed layer, two configurations were used: “rough” and “smooth”. Both configurations consist of plates with a single layer of stones glued on them, to prevent erosion during the experiments. On the “rough” plates the diameter of the used stones was in the order of 1 cm, while on the “smooth” plates this was around 3 mm. The stones were not uniform, so an average was estimated based on a few measurements.
It was assumed initially that all the experiments were performed in a hydraulically rough environment (Appendix D) and it was checked afterwards if this was really the case.

Combining the three parameters leads to twelve distinct flow situations.

4.2.3 The expected length and velocity scales.

The (expected) flow depths and velocities behind the step can be calculated via the momentum balance for a given discharge and upstream water depth.

Since the goal of the experiments was being able to calculate the development of both mean flow and turbulent energy, it was desirable to do measurements up to the location where the flow is fully developed and the step does not affect the flow anymore. Since this happens when the boundary layer covers the entire water depth, the required distance can be calculated by rewriting the formula of Schlichting (1942):

$$L = \left(\frac{d}{0.37}\right)^{1.25} \left(\frac{u}{\nu}\right)^{0.25} \quad (4.2)$$

Since the length of the flume was 14 metres, the length scales of the experiments should be short enough so that the whole research area fits into the flume. On the other hand, the flow depths must not be too small, since then the differences in stream wise direction would be barely noticeable. This means that a balance had to be found between availability and applicability.
With these demands in mind the values for L_1 and L_3 could be calculated, which are given in Table 1.

Case	d_2 *[m]*	Fr *[-]*	Q *[m^3/s]*	u_2 *[m/s]*	L_1 *[m]*	d_3 *[m]*	u_3 *[m/s]*	L_3 *[m]*	L_2+L_3 *[m]*
1	0.07	0.25	0.006	0.207	2.66	0.119	0.122	4.52	4.82
2	0.07	0.50	0.012	0.413	3.15	0.122	0.237	5.50	5.80
3	0.07	0.75	0.017	0.622	3.51	0.128	0.340	6.41	6.71
4	0.10	0.25	0.010	0.247	4.32	0.149	0.165	6.46	6.76
5	0.10	0.50	0.020	0.495	5.16	0.153	0.322	7.93	8.13
6	0.10	0.75	0.030	0.743	5.72	0.162	0.459	9.25	9.55

Table 1: The expected results of the experiments based on the momentum balance

To make sure the flow at the end of the step is almost uniform for most of the cases, the step must be long enough. Based on Table 1 it was decided that the step should have a length of 5 metres, which is sufficient for most cases.

The total length of the flume is 14 m, which means that after the step circa 8.0 m is left, considering the need for some extra space near the entrance and exit of the flume.

The consequence is that in the experiments 5 and 6 both the step and the available length behind the step are too short.
A result of the first shortcoming is that the flow on top of the step might not be completely developed, meaning that in these experiments the correction factor for calculating the energy head cannot be neglected.
The second shortcoming means that in experiments 5 and 6 it is not expected that the boundary layer is fully developed at the end of the flume.

4.2.4 Measurement locations

With a step height of about 5 cm and assuming that the reattachment point lies between 6 to 12 times the step height, the reattachment point is located somewhere between 30 and 60 cm downstream of the step.
Since most of the decay of the mean flow energy is expected to happen before the reattachment

point, more measurements will be executed in this region, at 10, 20, 30, 45 and 60 cm downstream of the step.
After the reattachment point it is expected that the changes will be more gradually. Therefore in this region the distance between the measurement locations will gradually increase, leading to locations at 80, 105, 150, 250, 350 and 500 cm behind the step.
Although it follows from Table 1 that for most cases the flow is not expected to be completely uniform at the last measuring point, the velocity profiles all looked almost uniform at the last location, so for efficiency reasons it was decided that taking measurements further downstream would not be a significant improvement of the results.

The velocity measurements will also take place at different heights in the flow. The lowest measurement will take place near the bottom and the highest measurement takes place as high as possible in the water column. Since the velocity gradient is highest near the bottom, most measurements are executed near the bottom and the distance between two respective measurements will gradually increase to a maximum of 2 cm.

4.3 The measurement devices

4.3.1 Measuring the discharge

The discharge was measured with a Rehbock weir (Appendix E). The discharge could be calculated from the water depth above this weir.

4.3.2 Measuring the water depth

The water depth is measured with a level needle. The needle can be moved in the vertical direction and when the tip of the needle just touches the water the water level can be read.
With the Vernier scale on the needle means the accuracy of the measurement is up to 0.1 mm, and since this needle system could be moved in the x-direction.

Before the measurements started, the bottom of the flume has been measured at multiple locations. The water depth at each located can then be calculated as the difference between the water level and the (average) height of the bed.
It turned out that the average level of the “rough” plates was 1 mm higher than that of the “smooth” plates. To compensate for this effect, it was decided that y=0 should be at the top of the “small” stones, meaning that for the “rough” plates the bottom is at y=0.001 m.
The same procedure was executed for the water depth on top of the step, which was located 4.78 cm higher than the “smooth” bed.
In situations 3 and 6 small oscillations occurred in the flow, leading to a slightly lower accuracy of about 0.5 mm.

4.3.3 Measuring the flow velocity

Several methods for measuring turbulence in flowing water are available, divided in using electrical, optical or acoustic devices.

In order to get a good measurement of the amount of turbulence, a high sampling frequency and high spatial range were required. For this reason, two options remained: PIV and LDA, both using optical devices.

PIV can obtain many velocity measurements simultaneously, but the needed light flash is very intense, which might cause eye damage and makes it necessary to build a good protection around this set-up (De Vree, 2016).
For this reason, LDA was chosen instead.

LDA stands for Laser Doppler Anemometry and it is based on the principle that when a velocity produces a shift in the frequency.
The set-up consists of two monochromatic HeNe-laser beams with the same frequency and wave length, that are oriented in a different direction. (Bernard & Walllace, 2002)
These two beams pass through the water and intersect at a certain point, forming a probing volume where the particles in the flow scatter the light of the laser beams, causing a frequency shift in the scattered beams. The light energy from the scattered beams will then be received by a photodetector, which turns it into an electrical signal. (CIE 5312, 2016)
Since the frequencies are usually outside of the range of the photodetector, only the Doppler signal will be measured. The Doppler frequency is composed of the difference between the frequencies of the two reflected laser beams and can be calculated from the electrical signal. With this Doppler frequency and when the original frequency, the wave length and the angle between the two laser beams are known, the flow velocity can be calculated. (Bernard & Walllace, 2002)

If two or three pairs of these laser beams are used, the velocities in two respectively three directions can be obtained.
The advantages of this method are that it is relatively simple to use and that it gives quite satisfactory results. The disadvantage is that it focusses at one point only, so multiple measurements, at different heights and locations, are necessary.

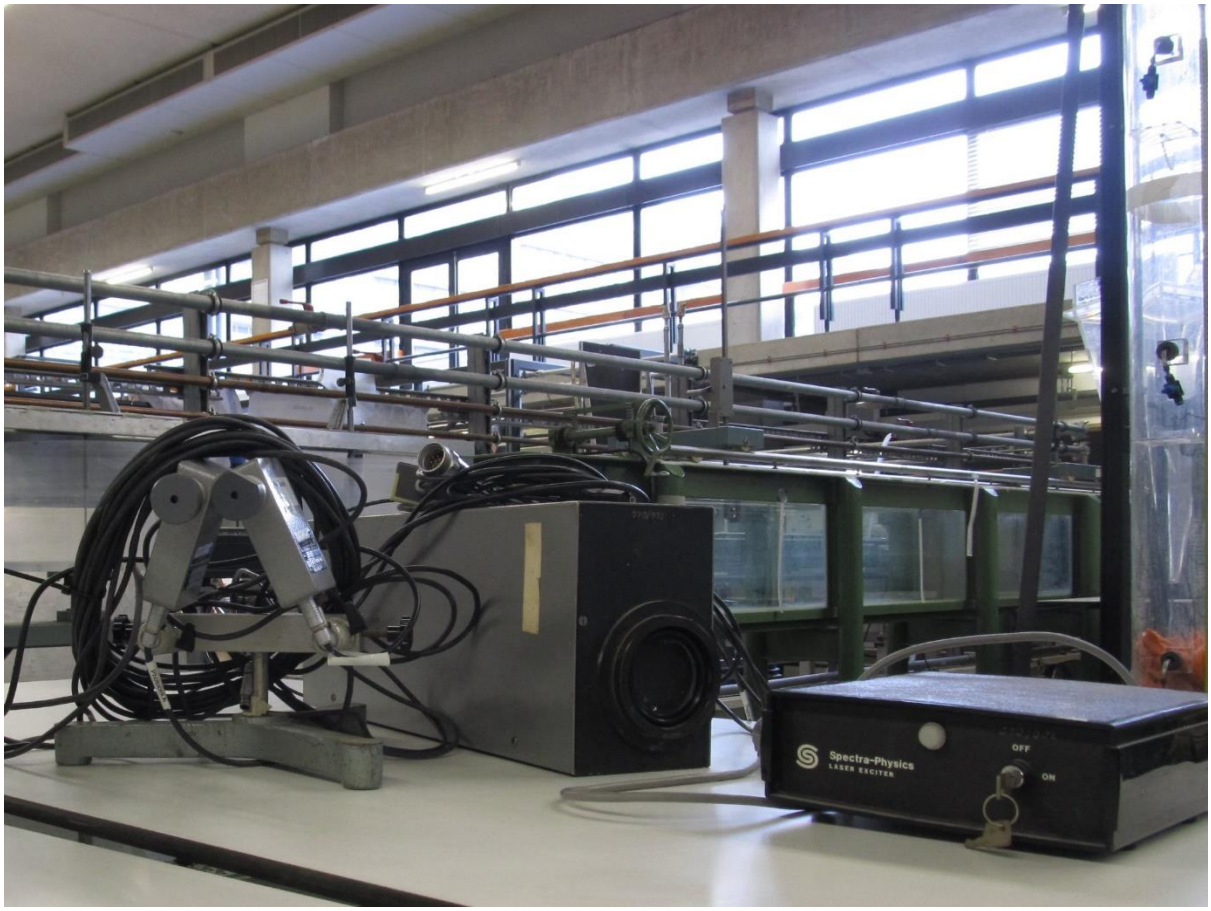

Image 1: The various aspects of the LDA set-up, with on the left the detector and on the right the laser.

In the laboratory, a device was available that allowed velocity measurements in two directions. Since during this research the transverse direction is neglected, it was decided to measure the velocity in stream wise and vertical directions only.
The complete set-up needed for this method is visible in Image 1 and in Image 2 the laser beams can be seen through the flow.

The duration of the measurements was in all cases more than 3 minutes to create a time-series with converged statistics, from which the mean and standard deviation could be computed.
It was established experimentally that the results of measuring durations of 3 and 5 minutes were almost identical, leading to the conclusion that the measuring time should be at least 3 minutes. The sampling frequency was 20000 Hz.

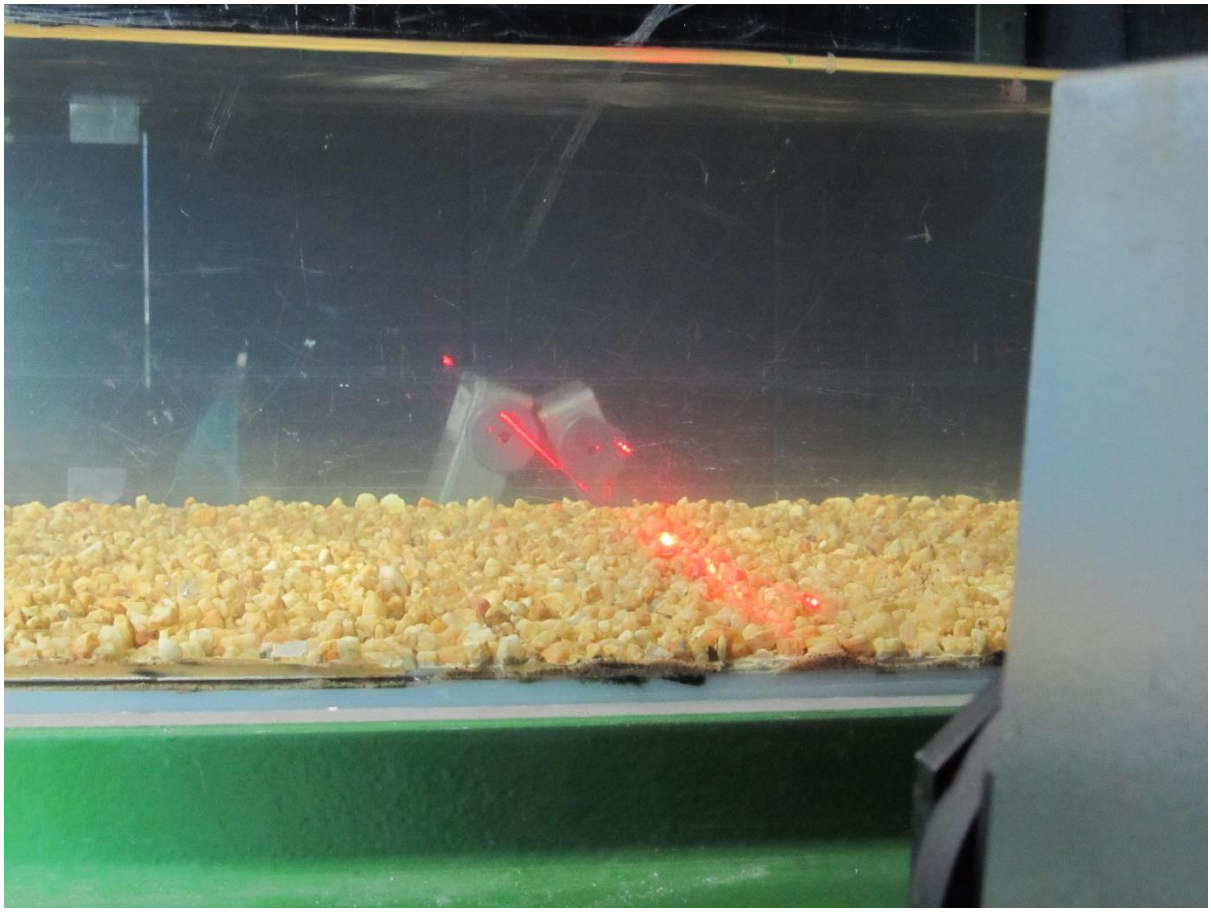

Image 2: The laser beams in the water with the detector on the other side of the flume.

4.3.4 Determining the locations of the measurements

The distance in x-direction from the step was measured with the help of a laser distance meter. (Image 3)
This distance meter was located at a fixed point, with a known distance downstream of the step. When the Laser Doppler meter was at the right location, the distance from the distance meter was measured and from that the distance from the step was also known.
Since the velocity measurements were always done before the water depth measurements, determining the location for the water depth measurements was just the opposite approach.

Image 3: The distance meter at its reference point

The exact location in the perpendicular direction is not determined, although it is assumed that the measurements are taken place in the middle of the flow. Since this research focusses on a 2-Dimensional situation, the effects of this are negligible.

4.3.5 Determining the height for the velocity measurements

The coordinates in vertical direction were measured with the help of a voltage meter.
A very small current was going into the system at the top of the structure and it went down until a "obstruction", which location depended on the height of the system. This means that the traveling length was dependent on the height of the structure and this influenced the electrical voltage in the system. A shorter distance led to a more negative voltage.

The relation between voltage and height was experientially determined as:
$\frac{dy}{dVolt} = -0.051$, which means that a decrease of 1.00 V on the voltage meter lower, is an increase of 5.1 cm of the measuring point.

It was assumed that the lowest possible measurement point above the step was at the step itself and with the average of the measured Volts on top of the step and the known step height the conversion from Volts to height could be done for all the measuring points, since it is a linear relationship.

Chapter 5

The results from experimental research

5.1 Data directly obtained from the experiments

Image 4 gives a view of the situation just after the step, which is located on the left. With the water flowing from left to right in this image, a water level increase on right side left is visible. The length of the glass window is 1.05 metres.
In this section only the results for situation 3, which has a water depth of 7 cm and Froude number of 0.75 on top of the step, with a “smooth” bed are given in order to illustrate the procedures that were followed for every situation.

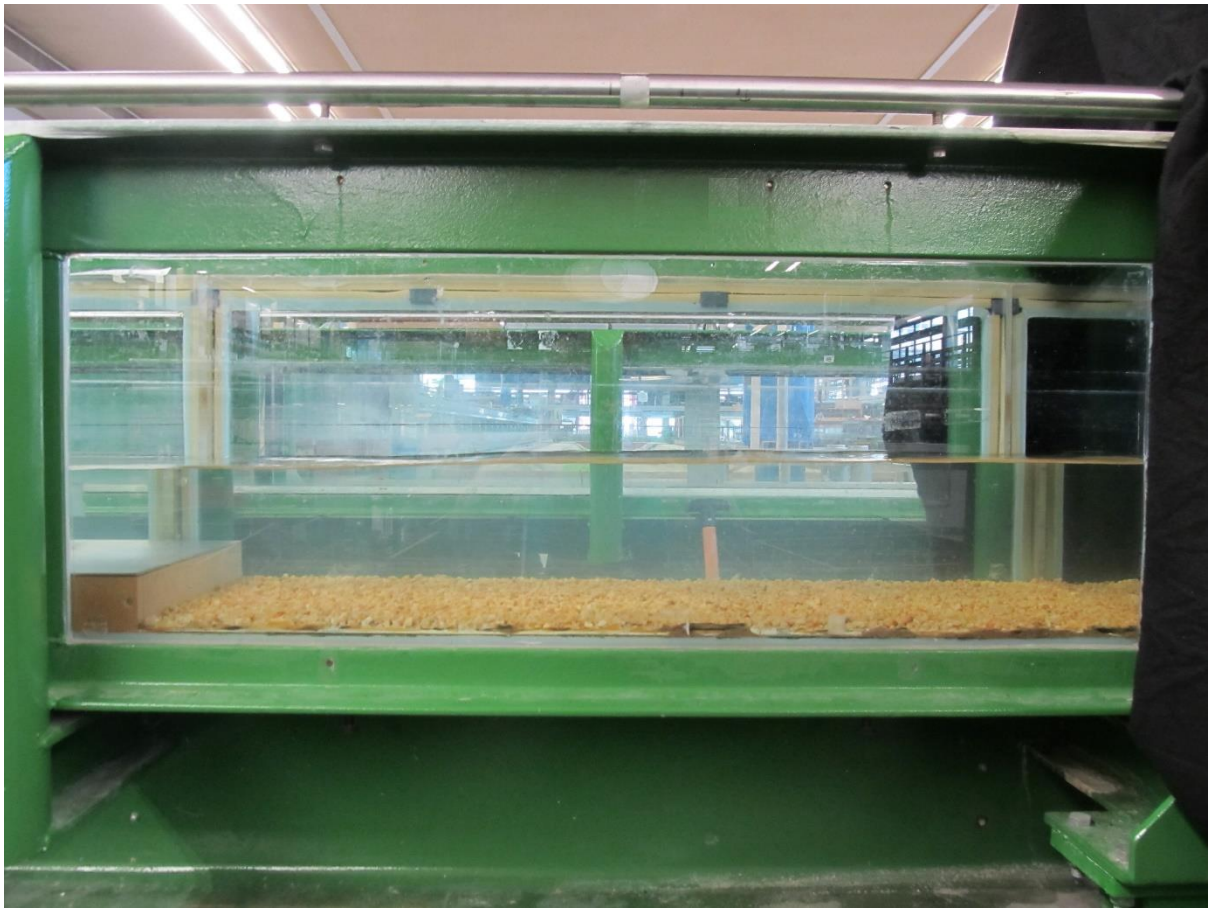

Image 4: The step and the situation in the first metre after the step.

5.1.1 Water depth

As described in Chapter 4 the water level measurements were done with a needle at every location. The water levels relative to the bed level are given in Figure 10. From this figure can be concluded that the water level grows rapidly in the first metre after the step and after that first metre the water level still rises slowly. This means that behind the reattachment point the water level still rises, with respect to the bed.

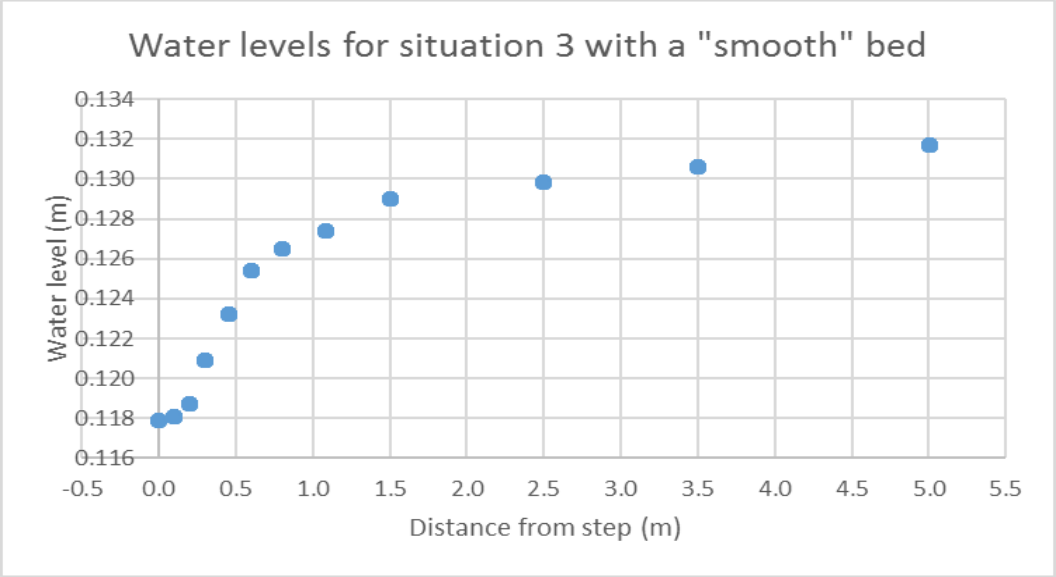

Figure 10: The water levels with respect to the bed for situation 3 with the "smooth" bed.

5.1.2 Flow velocity

The direct result of the LDA measurements at each location and height was a time-series of the electrical signal for both laser beams. Figure 11 gives this signal at the location x = 60.1 cm and y = 0.0537 m. From the graph is visible that signal A is almost always positive and that signal B is most of the time negative and that the absolute values of both signals are more or less identical. Only in the recirculation zone this pattern is different.

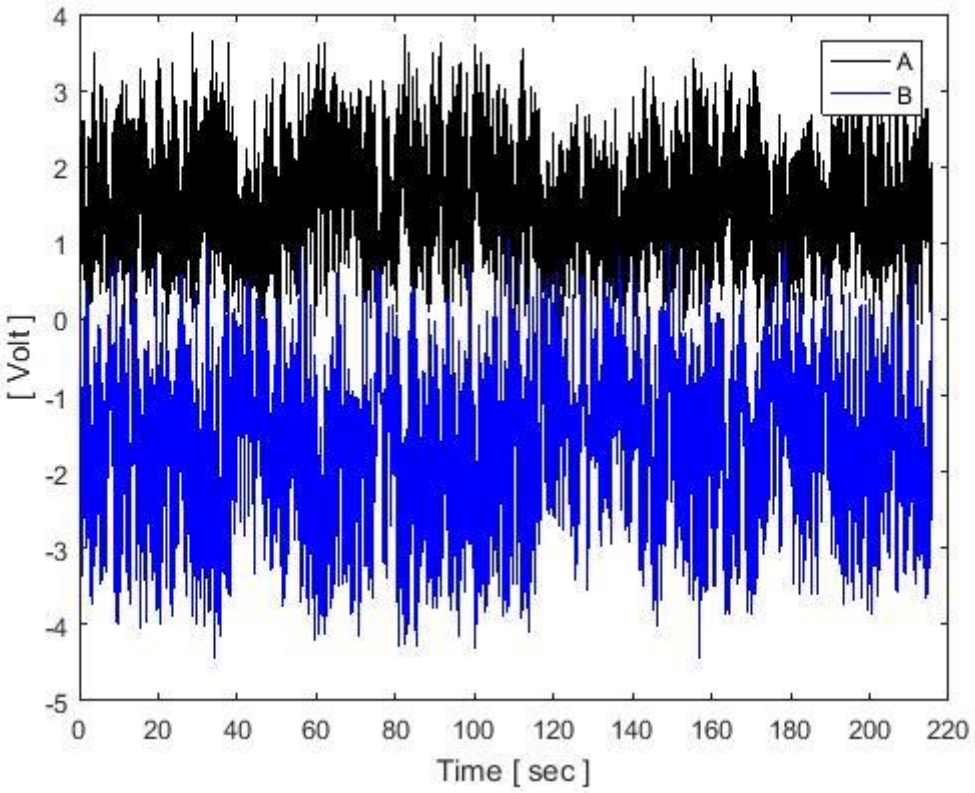

Figure 11: The electrical signal at x = 60.1 cm and y = 0.0537 for situation 3 with the "smooth" bed.

With the help of a MATLAB script these signals could be converted into a velocity time-series. From the user manual of the laser, De Vree (2016) came up the following formula for this specific laser:

$$u = 0.096 * (A - B)$$
$$v = 0.096 * (A + B) \quad (5.1)$$

In which u is the time-series for the velocity in stream wise direction and v is the velocity in the vertical direction.
In combination with the above stated findings about A and B, this means that, under most circumstances, u > 0 and v ≈ 0.

The horizontal and vertical velocities are shown in Figure 12. This figure confirms the expected result that u > 0 and v ≈ 0.

For one specific situation, the outcomes from these calculations have been compared with the expected results. Since the results were almost the same, it can be concluded that this formula is right.

With the same script, the averages and standard deviations are calculated as well, since these are the relevant parameters for further research. For the above described situation, this leads to the following results:

- $\bar{u} = 0.3064\ m/s$
- $u' = 0.1226\ m/s$
- $\bar{v} = -0.0202\ m/s$
- $v' = 0.0781\ m/s$

This approach was applied for every combination of situation and location.

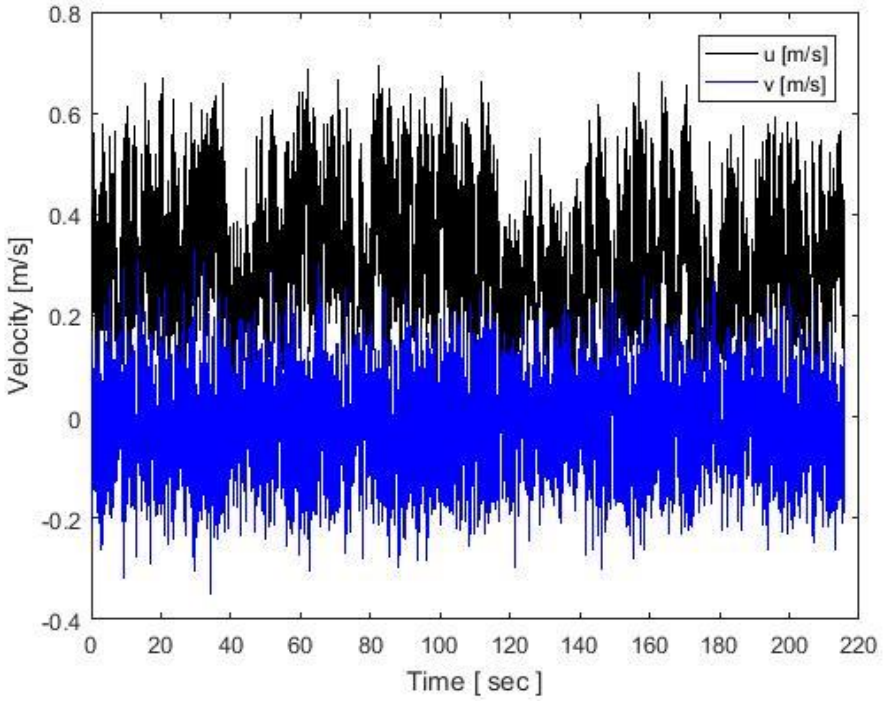

Figure 12: The horizontal and vertical velocities at x = 60.1 cm and y = 0.0537 m for situation 3 with the "smooth" bed.

From this the (horizontal) velocity profile at each location could be constructed. In Figure 13 the velocity profiles for three separate locations is visualized.

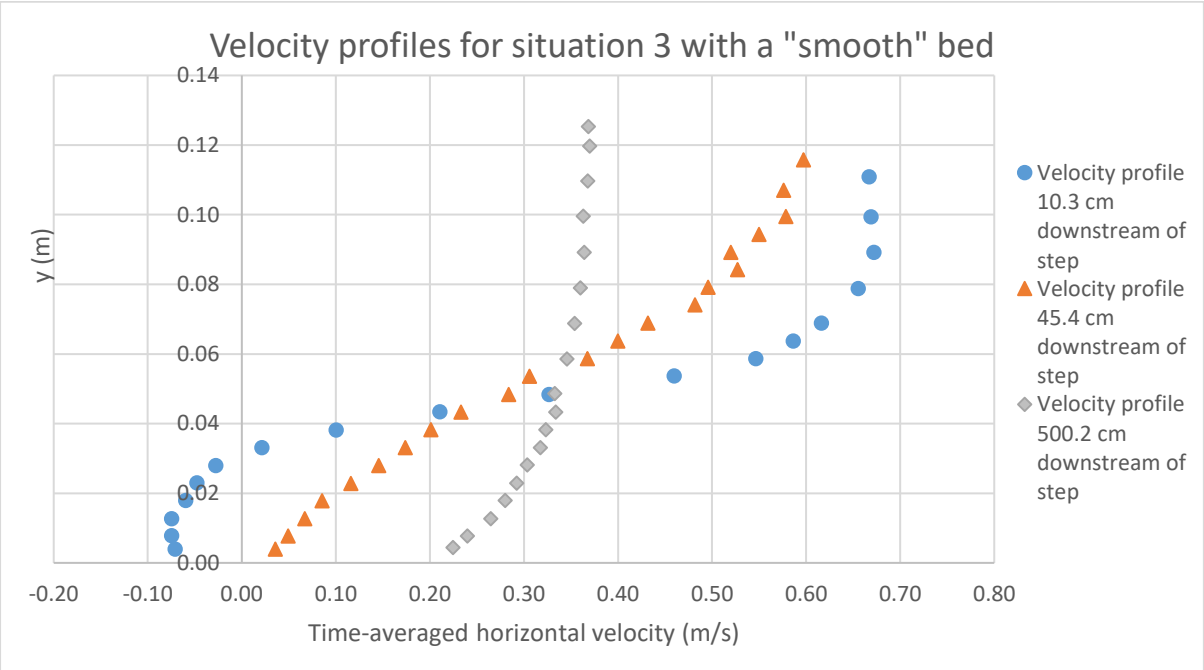

Figure 13: The horizontal velocities at certain locations for situation 3 with the "smooth" bed.

From this figure follows that the dispersion of the velocity over the depth decreases proportional with the distance from the step.
Close to the step, the velocity near the bottom is negative, which is an indication for the recirculation zone.
The other two profiles do not have negative velocities anywhere, indicating that at those locations the recirculation zone has disappeared.
The velocity 5 metres downstream of the step looks almost logarithmic, indicating that the velocity can be regarded as almost uniform at that location.

Because of limitations regarding the laser, the highest measurable point was in all cases approximately 1 cm below the water level. To compensate for this, an additional point was added near the water level, with a velocity that follows from the trendline of the velocity profile.
This approach was also used for the vertical velocities and the fluctuations in both directions.

In Figure 14 the velocity profile for the horizontal velocities for the first metre after the step is given. The velocity profiles for all situations are displayed in Appendix F. It can be noticed that the velocity on top of the step can be described with a logarithmic profile.
In Figure 15 the standard deviations for both the horizontal and vertical velocities in the first 1.5 m for the same situation are given. It can be noticed that in the recirculation zone the standard deviations are highest near the top of this zone.
The reason for this is that the production of turbulent energy is proportional with $\frac{d\bar{u}}{dy}$, which is highest near the top of the recirculation zone. (Bernard and Wallace)

It can also be noted that the standard deviations become smaller further downstream.

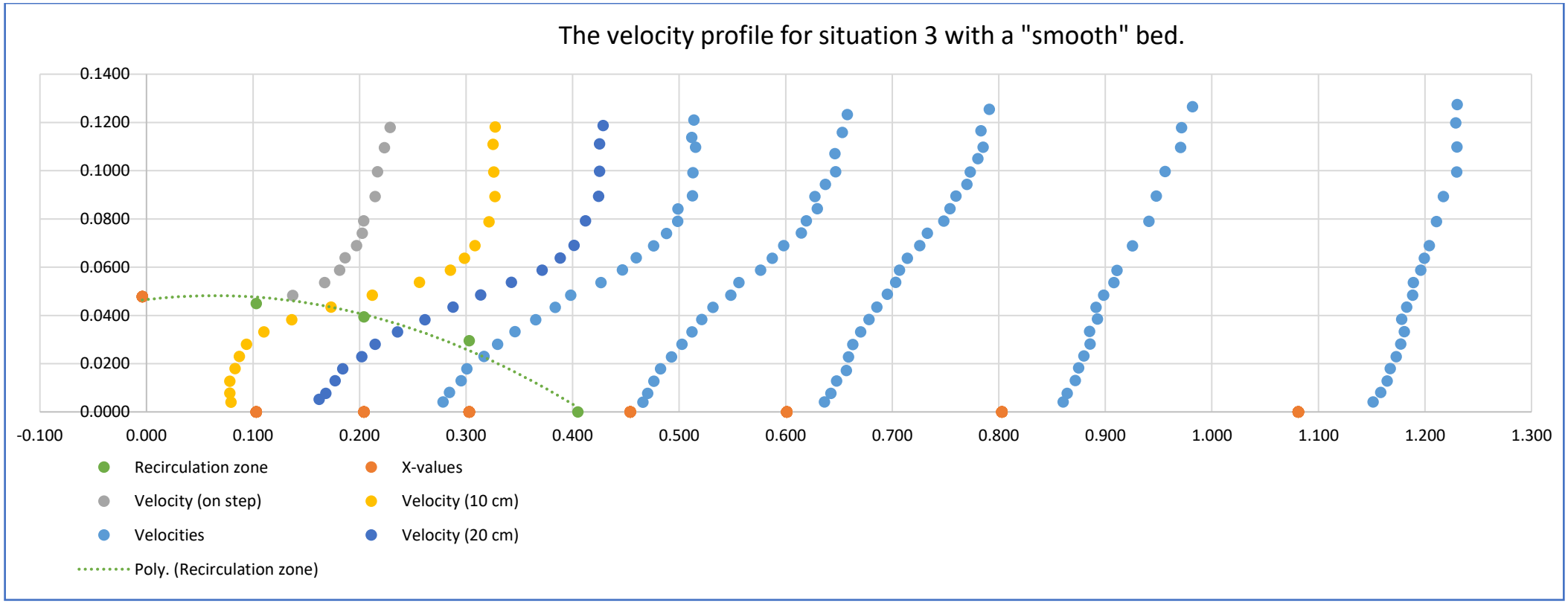

Figure 14: The velocity profile (for horizontal velocities) for the first metre of smooth situation 3.

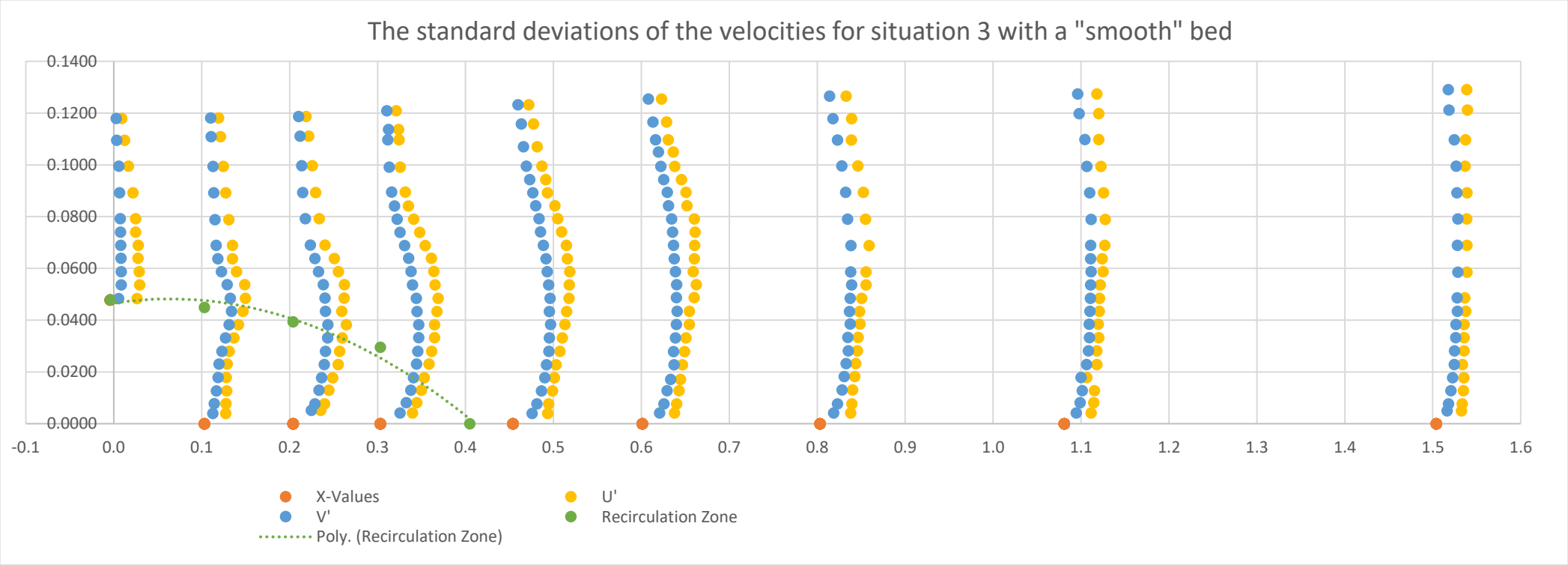

Figure 15: The standard deviations of both the horizontal and vertical velocities for the first 1.5 metres of smooth situation 3.

5.2 The shear velocity and the roughness

A uniform flow can be described with the formula $u(y) = \frac{u_*}{\kappa} \ln\left(\frac{y}{y_0}\right)$ (5.2).

For a hydraulically rough flow can be stated that $y_0 = \frac{k_s}{30}$ (Nikuradse, 1933).
When it is assumed that the flow is hydraulically rough, the Nikuradse roughness is two times the diameter of the stones and the flow is uniform at the last measurement location, the values of u_* can be calculated from the velocity profile for each situation. With these results, also the corresponding values of u^+ could be calculated (Appendix D). The results are given in Table 2.

situation	u_* **(m/s)**	y_0 **(m)**	u^+
1 Smooth	$9.5*10^{-3}$	$2.0*10^{-4}$	57
2 Smooth	0.018	$2.0*10^{-4}$	108
3 Smooth	0.026	$2.0*10^{-4}$	156
4 Smooth	0.012	$2.0*10^{-4}$	72
5 Smooth	0.024	$2.0*10^{-4}$	144
6 Smooth	0.034	$2.0*10^{-4}$	204
1 Rough	0.011	$6.67*10^{-4}$	220
2 Rough	0.023	$6.67*10^{-4}$	460
3 Rough	0.033	$6.67*10^{-4}$	660
4 Rough	0.015	$6.67*10^{-4}$	300
5 Rough	0.031	$6.67*10^{-4}$	620
6 Rough	0.044	$6.67*10^{-4}$	880

Table 2: The values of u_*, y_0 and k^+ for all situations.

Figure 16 shows the obtained logarithmic profile for situation 3 with a rough bed.

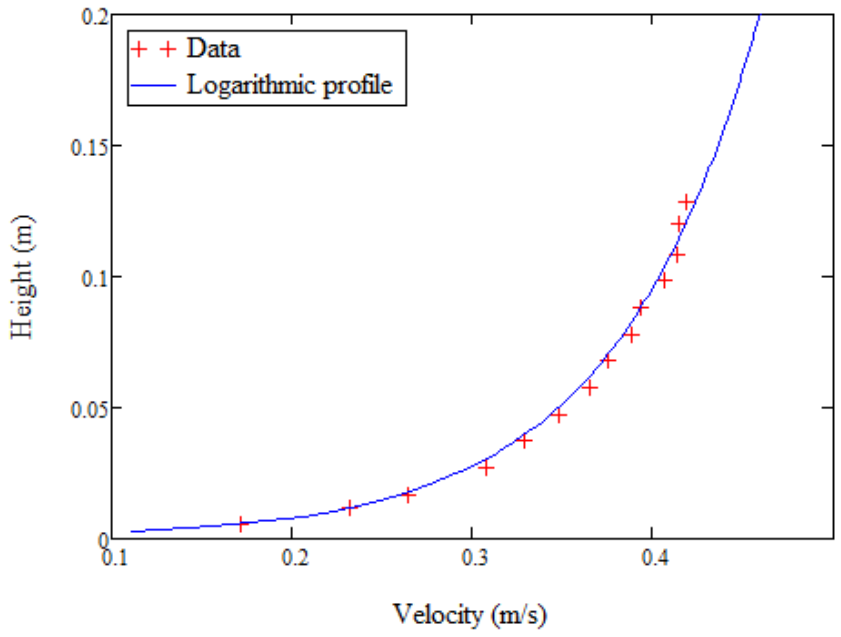

Figure 16: The logarithmic profile for situation 3 with a rough bed.

To check the validity of this method, for every situation the data was normalized by dividing the y-coordinates by the value of y_0 and taking the natural logarithm and dividing the velocities by the obtained values of u_*.
Figure 17 shows the results of this. The ideal line, which has a slope of κ (=0.41), is given as well, to check if the points are on this line.

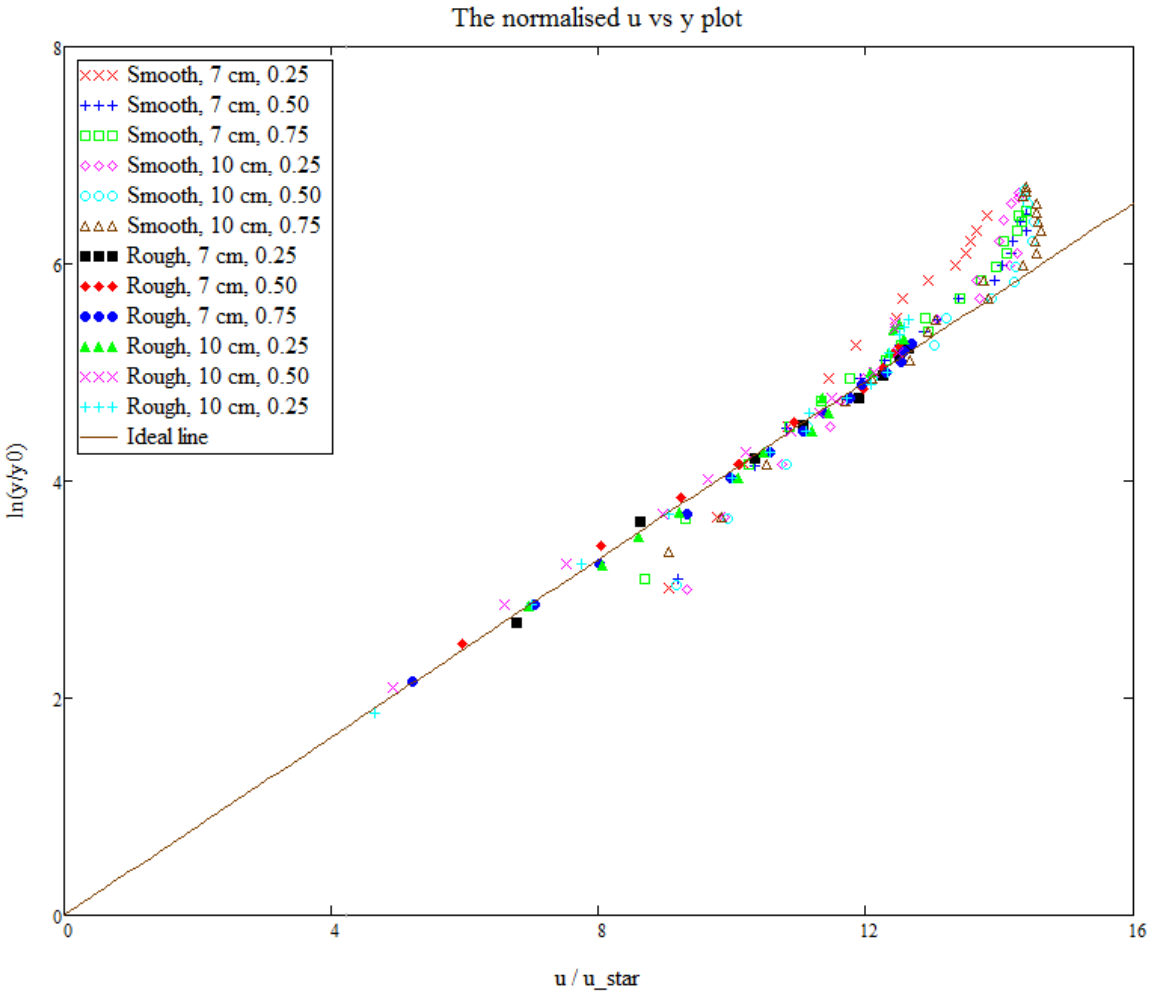

Figure 17: The normalised data for the last location of all situations.

From Figure 17 can be concluded that for the "rough" situations (with a diameter of about 1 cm) the measurement data follow the ideal line quite well.
For the "smooth" situations especially the measurement points higher in the water column do not lie exactly on this line. The explanation for this is that only the lowest 20% of the water column can be described by a logarithmic profile (Hofland, 2017).
The overall results are quite good, which means that it can be justified to use this approach in finding the values for y_0 and u_*.

Nikuradse (1933) stated that the flow can be regarded as hydraulically rough if $u^+>70$. From Table 2 follows that this is the case for all situations except smooth situation 1.

5.3 The reattachment points

The reattachment point marks the end of the recirculation zone and is defined as the point where the velocity just above the bed is zero.
In all situations, the reattachment point was located between 30 and 45 cm downstream of the step.

For the locations closest to the reattachment point, the velocities near the bed were plotted. Assuming a linear curve between these points, the location where the velocity is zero could be determined, as shown in Figure 18. The reattachment point was already included in Figure 14 as well.

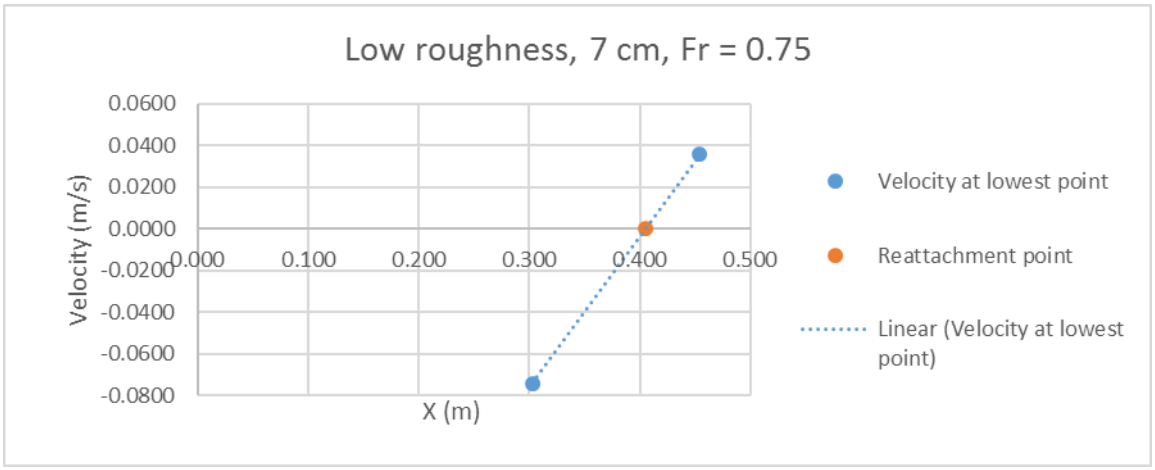

Figure 18: Determining the reattachment point.

In Figure 19 the reattachment point was divided by the step height and plotted versus the Froude number near the reattachment point. From this figure follows that the (relative) location of the reattachment point is in between 7 and 8.5 step heights. A reattachment length of 8 times the step height seems therefore advisable.
A slight dependency on the Froude seems visible, especially for the situations with a lower roughness of the bed.

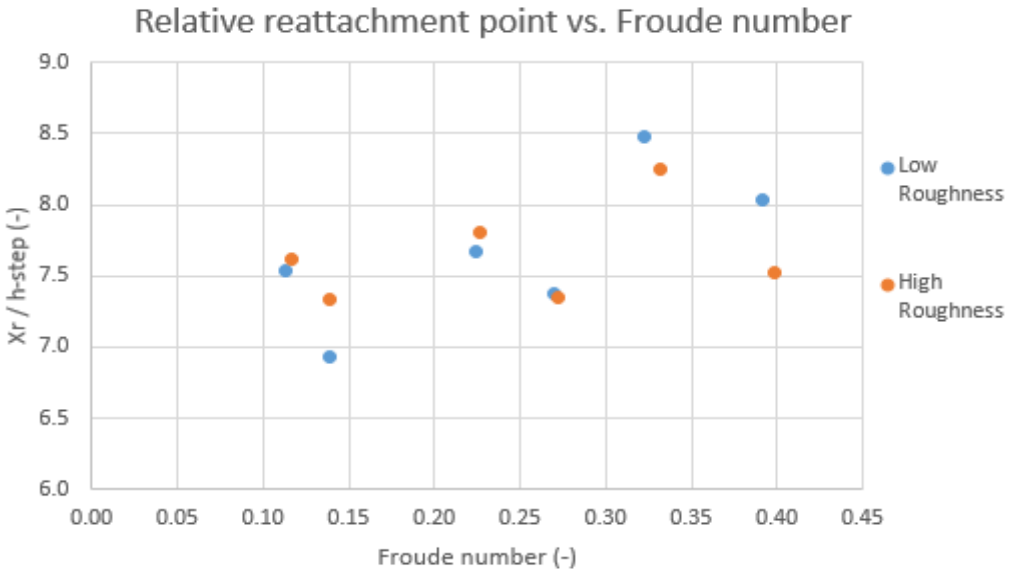

Figure 19: The relative reattachment points for all situations.

5.4 The depth-averaged velocity

With the velocities from the above paragraph the depth averaged velocity can be calculated, via:

$$\bar{\bar{u}} = \frac{1}{d} \int_{y_{bottom}}^{y_{top}} \bar{u}(y)\, dy \quad (5.3)$$

With y_{bottom} being the bottom of the water column at that specific location and y_{top} being the water level.

In the zone before the reattachment point, the recirculation zone is omitted from the calculations for the depth-averaged velocity. The height of the recirculation zone was determined as the point where the cumulative discharge (up from the bed) was zero.
Only the “mean flow”, which is the height above the recirculation zone, is used for the determination of the average velocity.
So only the (positive) discharge higher than that point is used to calculate the depth-averaged velocity.

To verify the correctness of these calculations, the depth-averaged velocity is multiplied with the water depth to get the discharge at each location. This discharge is then compared with the discharge measured with the Rehbock weir, which was the known discharge.

The discharge following from the LDA measurements is mostly higher than the discharge from the Rehbock weir. The reason for this is that the LDA measurements were done in the middle of the flume, where the sides of the flumes have the lowest influence. Near the sides of the flume, the velocity is a little lower, leading to a lower total discharge.

The differences between the two discharges are below 10% for all cases and even below 5% for more than 95% of the situations (Appendix G). The main reason for the differences is that the velocity is measured in the centre of the flow, where the highest velocities occur. The velocities near the walls are usually a little bit lower, because of the friction near the walls. This results in a little lower discharge.

From the depth-averaged velocities, which are shown in Figure 20, is visible that upstream of the reattachment point the velocity decreases rapidly in stream wise direction, while after the reattachment point the velocity remains almost constant. Since the loss in kinetic energy depends on the decay of velocity, it is expected that most of the head level loss will occur in the recirculation zone.

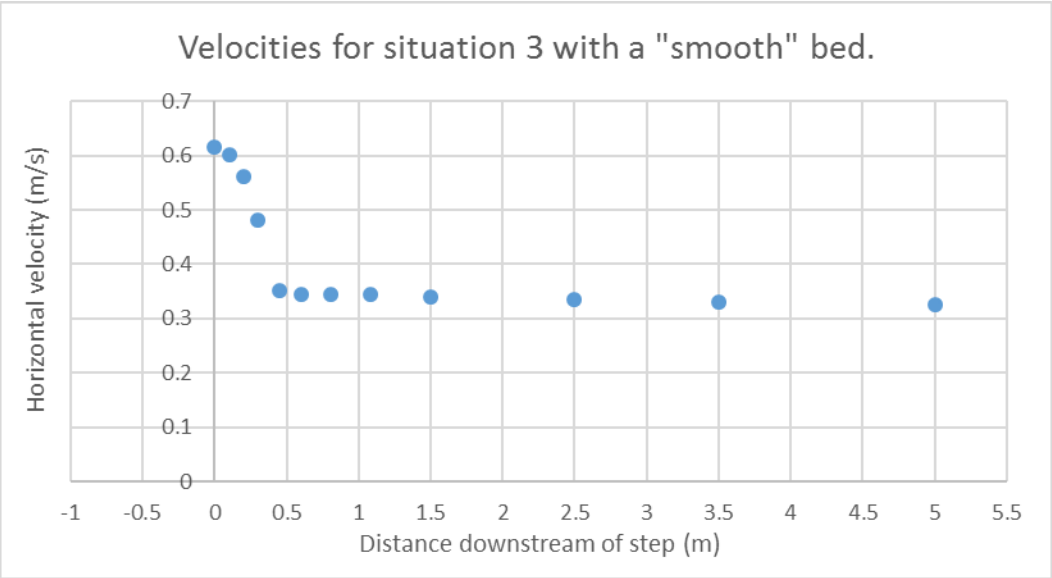

Figure 20: The depth-averaged horizontal velocities at various locations for situation 3 with a "smooth" bed.

5.5 Head level changes in streamwise direction

When both the water levels and velocities are known, in the case of uniform flow the head level can be calculated.

The flow in the experiments is however far from uniform, so the correction factor α, mentioned in Chapter 2, must be taken into account. The formula is:

$$\alpha = \frac{1}{d} \int_{y_{bottom}}^{y_{top}} \left(\frac{\bar{u}(y)}{\bar{\bar{u}}} \right)^3 dy \quad (5.4)$$

With $\bar{u}$ known at every height and $\bar{\bar{u}}$ known from the above equations, α can be calculated at every location in x-direction.

When the water level, the velocity and the correction factor are known, the head level can be calculated:

$$H(x) = y_b + h_b + \alpha \frac{\bar{\bar{u}}^2}{2g} \quad (5.5)$$

Until now, it was assumed that the bed level (and thus the flume) was horizontal and that z could be left out of the equation. However, this assumption let to increasing head levels far behind the reattachment point.
An extensive analysis (Appendix H) let to the conclusion that the bed was not horizontal, but had a tilt of $-1.3*10^{3}$.
This number was consequently added to the formula, so that the right head levels could be calculated via:

$$H(x) = \frac{dy_b}{dx}x + h_b + \alpha \frac{\bar{\bar{u}}^2}{2g} \quad (5.6)$$

in which $\frac{dy_b}{dx}$ = -1.3*10^3 and h_b is the water level relative to the bed.
This formula means that z=0 at x=0. This was choses out of simplicity and since in this research the head level change is more important than the actual head level, this does not influence any further results.

The calculated head levels for the same situation as above are given in Figure 21.

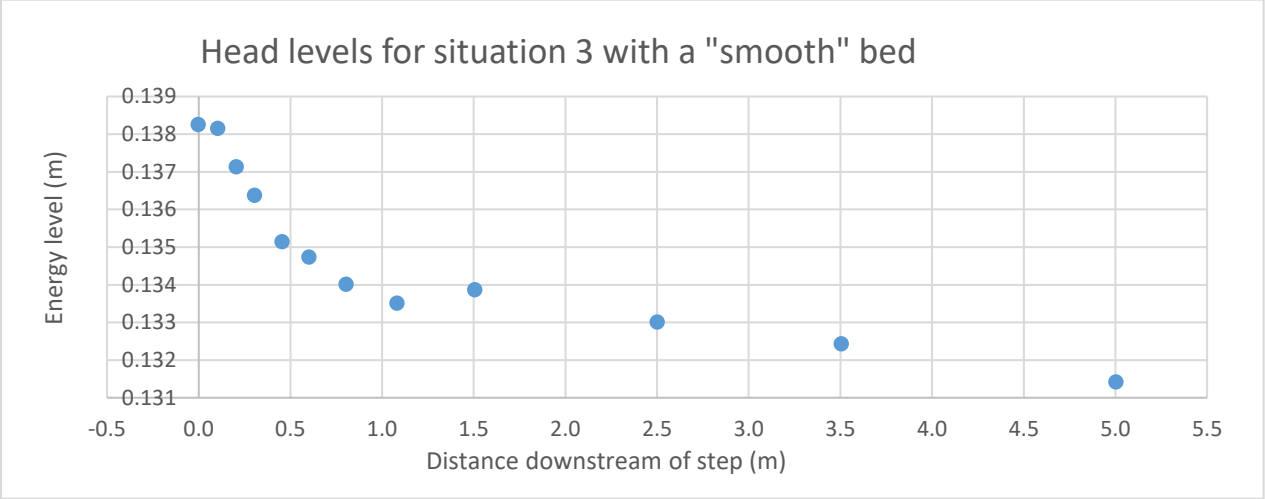

Figure 21: The head levels at various locations for situation 3 with a "smooth" bed.

5.6 Turbulent energy

From the standard deviations of the velocities in both x- and y-direction, an estimate of the turbulent energy level at every measuring point could be calculated with the formula:

$$k(y) = \frac{3}{4}u'^2 + \frac{3}{4}v'^2 \quad (5.7)$$

In this formula is included the assumption that $w' \approx \frac{1}{2}u'^2 + \frac{1}{2}v'^2$

At each location, the depth averaged turbulent energy level can then be calculated via:

$$\bar{k} = \frac{1}{d}\int_0^d k(y)\,dy \quad (5.8)$$

In Figure 22 the turbulent energy levels are given for situation 3 with a "smooth" bed. From this graph is visible that the turbulent energy increases behind the step up until the reattachment point. After that location, the turbulent energy decreases until an equilibrium amount of turbulence is reached. This pattern is visible for all situations and is in accordance with earlier experiments.

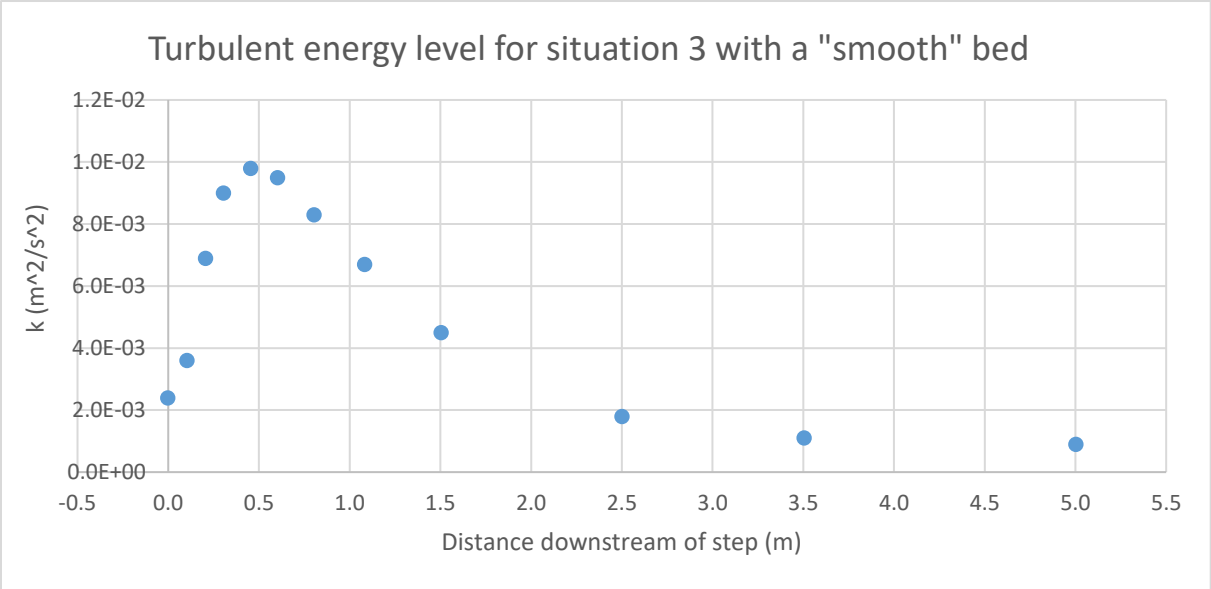

Figure 22: The turbulent energy levels at various locations for situation 3 with a "smooth" bed.

The mean flow energy levels and turbulent energy levels of all the experiments can be found in Appendix I and J respectively.

The combination of both mean flow energy and turbulent energy ($\widehat{H}$) is plotted in Figure 23. From this figure follows that the influence of turbulent energy is insignificant compared to the mean flow energy.

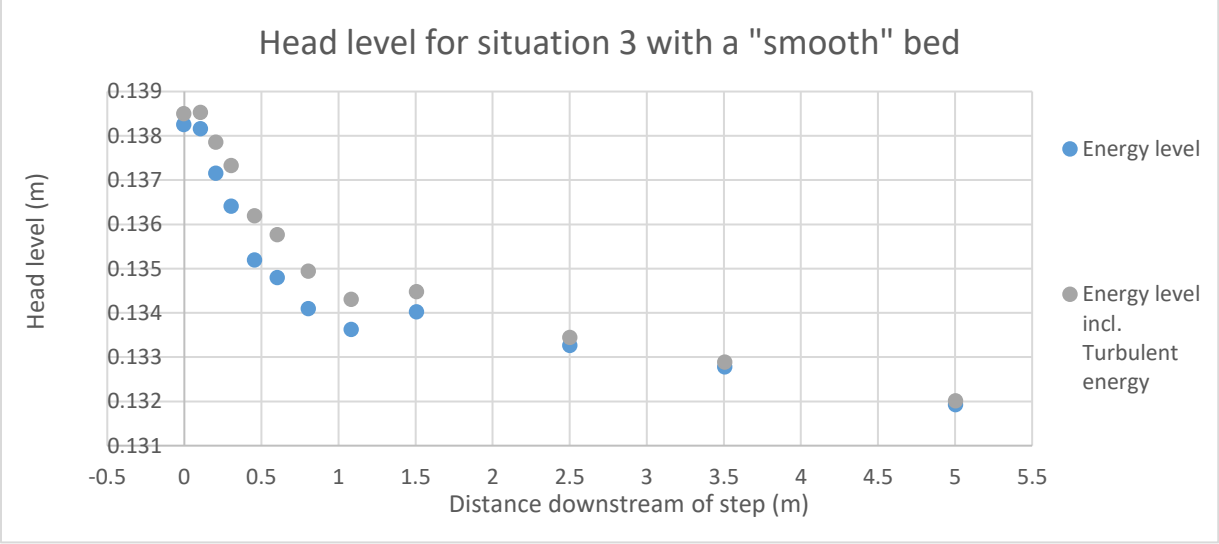

Figure 23: Both the mean flow energy and the combination of mean flow and turbulent energy levels at various locations for situation 3 with a "smooth" bed.

With both the calculated development of the energy head and the turbulent energy level, the method of Voortman can be improved, what will be done in the next chapter.

Chapter 6

Finding a solution to model the dissipation of turbulent energy

6.1 Introduction to the used approach

In Chapter 3 an analytical solution for Voortman's method was given. The formula for the dissipation of turbulent energy, after the reattachment point, would become:

$$k_{diss}(x) = (k_0 - k_{eq}) * \exp(-f\varphi(x - x_{reatt})) + k_{eq} \quad (6.1)$$

In this chapter, solutions for the different parameters will be proposed. These include the choice for the method, the initial turbulent energy, the equilibrium turbulent energy and the dissipation constant.

Figure 24 shows an example of a result from equation 6.1, in this case for situation 3 with a "smooth" bed. The used parameters will be treated below in this chapter.

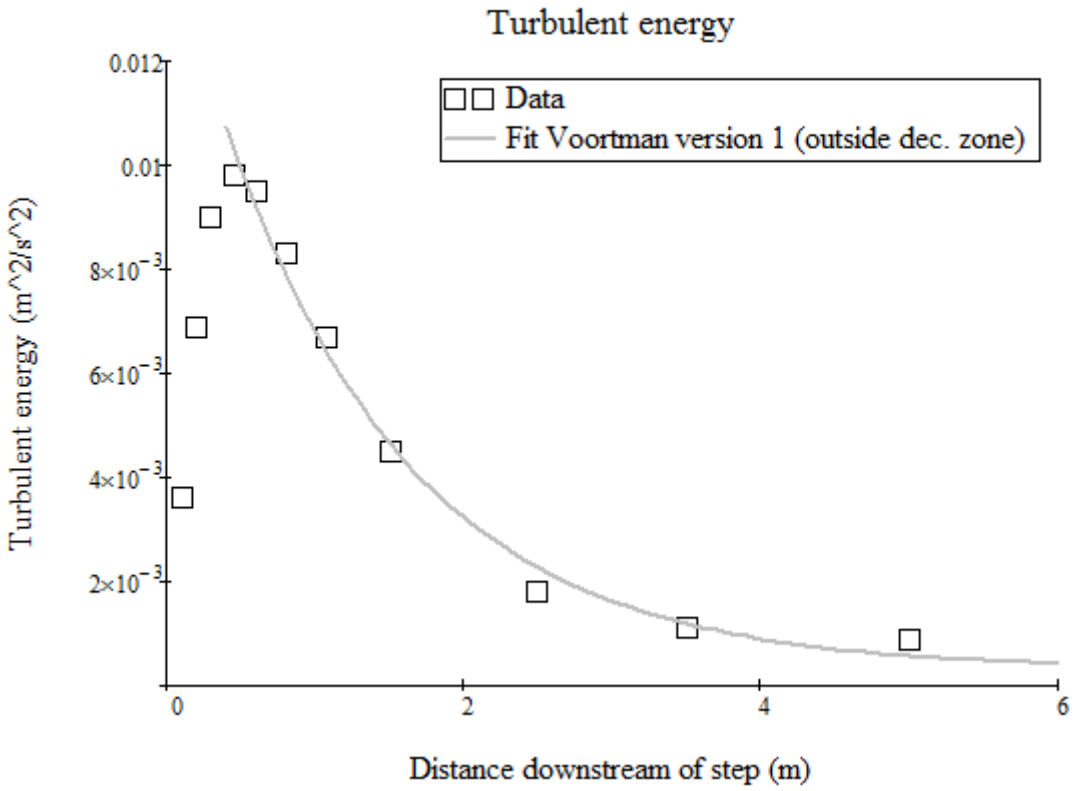

Figure 24: The exponential decay of turbulent energy for situation 3 with a "smooth" bed.

6.2 Determining which of Voortman's suggestions works best

Equation 6.1 contains a factor f, which influences the dissipation.
In Chapter 3.3, two alternatives for f were chosen:

1. $f = \frac{1}{R}$
2. $f = \frac{\sqrt{gd}}{q}$

The water depth occurring in both formulae was chosen to be the water depth at the last measurement point and the chosen discharge was the discharge according to the Rehbock weir.

For both alternatives, the values of ϕ were calculated for different scenarios. In Figures 25 resp. 26 the results of ϕ are plotted against the Froude numbers far downstream of the step. These figures show the results for a still unknown percentage, but exact amount of equilibrium turbulent energy does not influence the pattern shown.

An example of the used Mathcad script can be found in Appendix K.

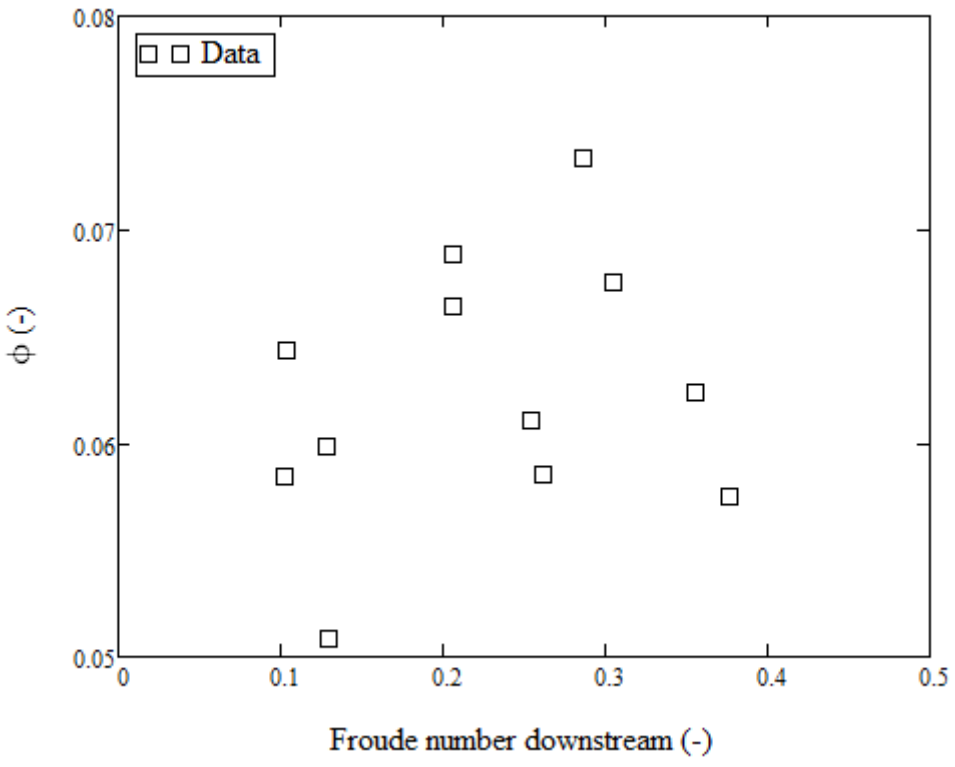

Figure 25: The values of φ plotted against the Froude number for $f = \frac{1}{R}$.

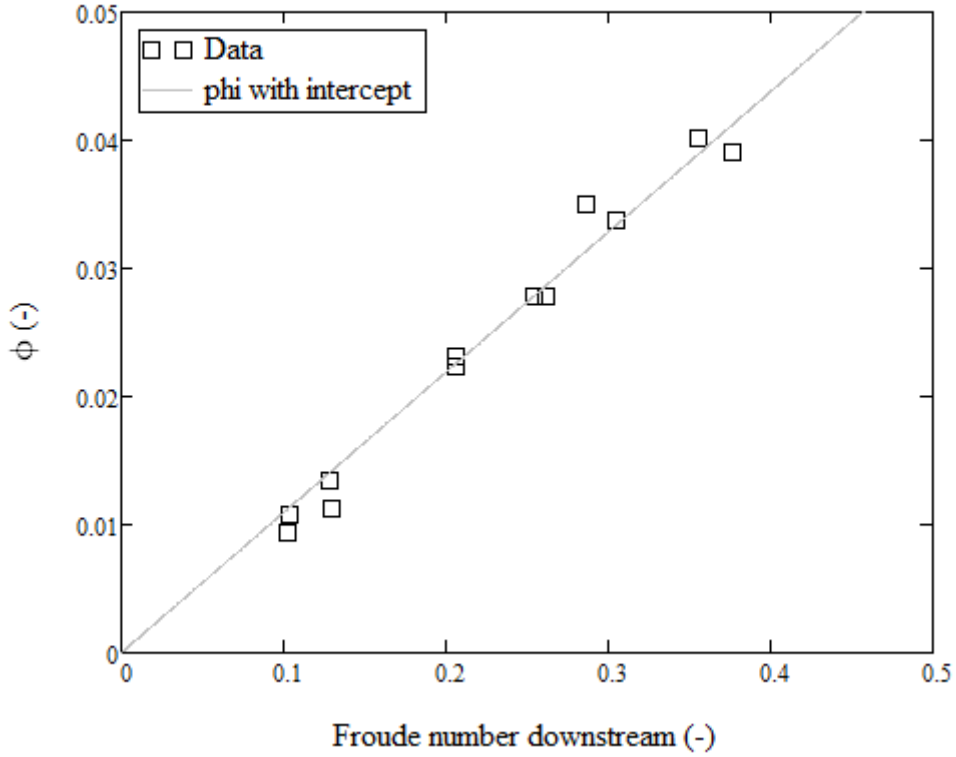

Figure 26: The values of φ plotted against the Froude number for $f = \frac{\sqrt{gd}}{q}$.

It can be noted from Figure 25 that for alternative 1 (with $f = \frac{1}{R}$) the obtained values of ϕ are more or less constant and no trend seems visible.

In Figure 26 an almost linear trend between the value of ϕ and the Froude number is visible.
This means that the value of φ can be described as $\varphi \approx constant * Fr = constant * \frac{u}{\sqrt{gd}} = constant * \frac{q/d}{\sqrt{gd}}$

The exponent in the exponential function consists of the multiplication of f and ϕ. For Voortman's second suggestion this becomes then:

$$f * \varphi \approx \frac{\sqrt{gd}}{q} * constant * \frac{\frac{q}{d}}{\sqrt{gd}} = constant * \frac{\sqrt{gd}}{\sqrt{gd}} * \frac{\frac{q}{d}}{q} = constant * \frac{1}{d}$$

This suggests that for this alternative the coefficient for dissipation is inversely proportional with the water depth. Since for the first alternative ($f = \frac{1}{R}$) the coefficient for dissipation ($f * \varphi = \frac{1}{R} * constant$) is inversely proportional with the water depth as well, this alternative seems the better option and will be further elaborated.
It was decided to continue with Voortman's initial idea and not to replace R with d, since the earlier is more generally applicable.

6.3 The maximum turbulent energy

Voortman's theory states that $\frac{d\bar{k}}{dx} = -g\frac{dH}{dx} - f\varphi\,\bar{k}$, which means that, if the dissipation term is neglected, the maximum turbulent energy k_0 can be calculated by adding $-g\Delta H$ to the turbulent energy on top of the step.

However, using this approach led to values of k_0 that were either much higher or much lower than the measured values of k. This could mean that between the end of the step and the reattachment point also dissipation of turbulent energy will take place and that the dissipation term should not be neglected. Further research on this subject is necessary.

Since this research focusses on the development of turbulent energy behind the reattachment point, the values for the maximum turbulent energy were obtained by a curve-fitting process, under the assumption that the maximum turbulent energy is present at the reattachment location. These values were almost identical as the maximum values from the data.

6.4 The equilibrium turbulent energy

The equilibrium turbulence could be calculated with the basic equation: setting $\frac{d\bar{k}}{dx} = 0$ leads to $-g\frac{dH}{dx} = f\varphi\,\bar{k}$, resulting in $k_{eq} = -\frac{g}{f\varphi}\frac{dH}{dx}$, for x >> x_{reatt}

If it is assumed that the head level can be described with a linear function ($H(x) = ax + b$), the change in energy head can be described as $\frac{dH}{dx} = a$.

Unfortunately, it was found that with using this equation the value for the equilibrium turbulent energy that was much higher than the turbulent energy calculated from the measurements.

This finding led to the conclusion that not all the dissipated mean flow energy was converted into turbulent energy. To include this effect, a factor p was introduced that stands for the conversion rate. The equilibrium turbulent energy is then defined as:

$k_{eq} = -p\frac{g}{f\varphi}\frac{dH}{dx}$, with $0 < p \leq 1$

As explained in previous chapters, it was assumed that almost all dissipated mean flow energy will be converted into turbulent energy. In this section will be checked what the exact conversion rate is. As explained above, this rate determined the equilibrium turbulent energy.

If the value of p is too large, the calculated equilibrium turbulent energy will be too high, as can be seen in Figure 27, where $p = 0.8$.

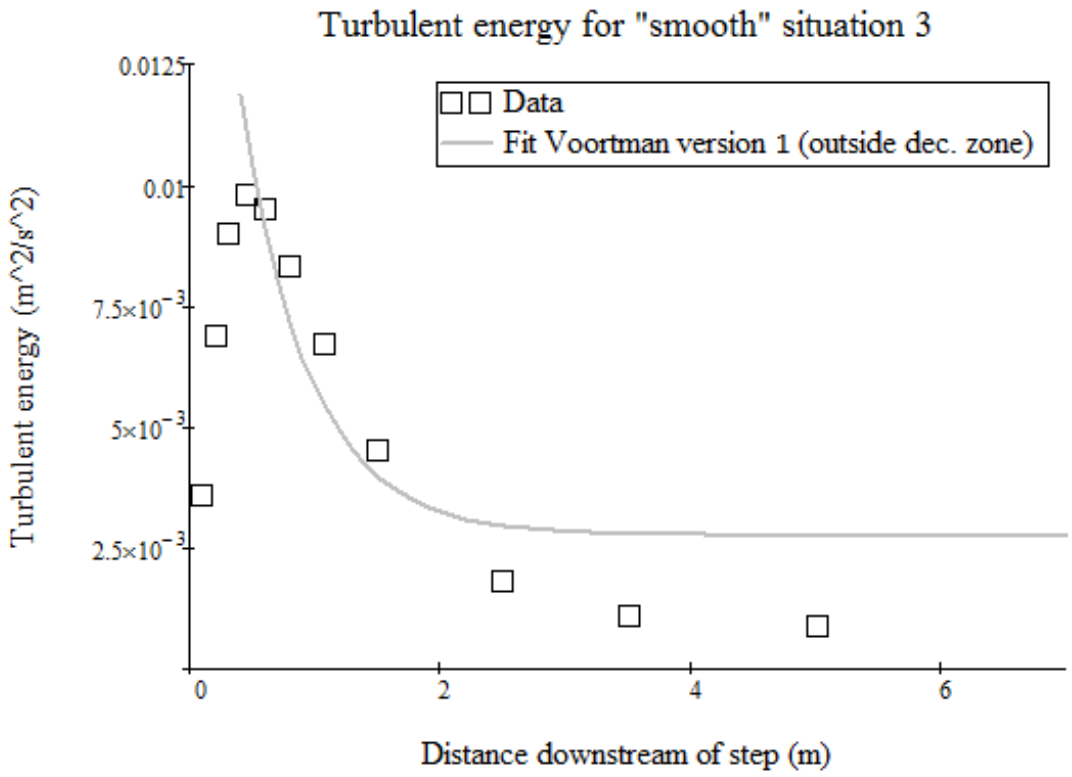

Figure 27: A typical result of the turbulent energy when the value of p is too large.

In order to find the best value for p, both the parameters coefficient of variation and sum of the squared errors were introduced.

$$CoV = \frac{\sigma}{\mu} \quad (6.2)$$

$$SSE = \sum_{m=reatt\ point}^{end} (k_{data_m} - k_{calculated_m})^2 \quad (6.3)$$

The SSE's for all experiments were added together, to come up with the total SSE for each value of p.

For a few educated guesses for p the corresponding values of φ were calculated, leading to the coefficient of variation for φ. The value for p that leaded tot the lowest CoV for φ was chosen as the best one, since in that cases the values of φ were closest together. If more values had the same CoV, the one with the lowest total SSE was chosen for the remainder of this analysis.

The results of this analysis are given in Table 3. From this table follows that $p = 0.125$ gives the best results, since it has a CoV of 0.135.

p	CoV	Total SSE
0.05	**0.171**	**3.82E-06**
0.075	**0.15**	**3.77E-06**
0.1	**0.139**	**4.15E-06**
0.125	**0.135**	**4.88E-06**
0.13	**0.135**	**5.06E-06**
0.135	**0.135**	**5.26E-06**
0.14	**0.135**	**5.47E-06**
0.15	**0.136**	**5.92E-06**
0.175	**0.139**	**7.21E-06**
0.2	**0.144**	**8.72E-06**

Table 3: The CoV and total SSE for different values of p.

This value seems quite low, since it means that most dissipated mean flow energy will not be transferred into turbulent energy.

An alternative solution is using the equilibrium turbulence that was mentioned in Hoffmans (1993):

$$k_{eq} = 1.44\, {u_*}^2 \quad (6.4)$$

This approach is directly applicable with the calculated values for u_* calculated in Chapter 5.

The results for the equilibrium turbulent energy following from both approaches is given in Table 4.

Experiment	Voortman (p=0.125)	Literature (k_{eq}=1.44*u_*^2)
1 Smooth	$1.492*10^{-4}$	$1.3*10^{-4}$
2 Smooth	$4.071*10^{-4}$	$4.718*10^{-4}$
3 Smooth	$8.54*10^{-4}$	$9.585*10^{-4}$
4 Smooth	$2.608*10^{-4}$	$2.143*10^{-4}$
5 Smooth	$5.78*10^{-4}$	$8.294*10^{-4}$
6 Smooth	$1.627*10^{-3}$	$1.694*10^{-3}$
1 Rough	$2.263*10^{-4}$	$1.839*10^{-4}$
2 Rough	$8.126*10^{-4}$	$7.552*10^{-4}$
3 Rough	$1.354*10^{-3}$	$1.568*10^{-3}$
4 Rough	$3.546*10^{-4}$	$3.371*10^{-4}$
5 Rough	$1.158*10^{-3}$	$1.357*10^{-3}$
6 Rough	$2.029*10^{-3}$	$2.788*10^{-3}$

Table 4: The results for k_{eq} (in m^2/s^2) following from the two discussed approaches.

It can be noted in Table 4 that in most cases the values do not differ much, although in some cases the values are significantly higher or lower.
Because the value of p still seems very small and the second approach is based on literature regarding this subject, it was decided to use that approach for the remaining calculations.

6.5 Calculating the best value for the dissipation coefficient

With all the other variables known, the dissipation coefficient ϕ can be calculated.
First, the best fit for ϕ for each situation was obtained. From this, both the average value and standard deviation were taken. These were 0.062 and 0.0058 respectively, which leads to a coefficient of variation of 0.093.

Since this CoV was rather small, it was decided to check if all the situations could be described with the average value for ϕ. The results are given in Appendix L and three typical results will be shown below in Figures 28, 29 and 30.

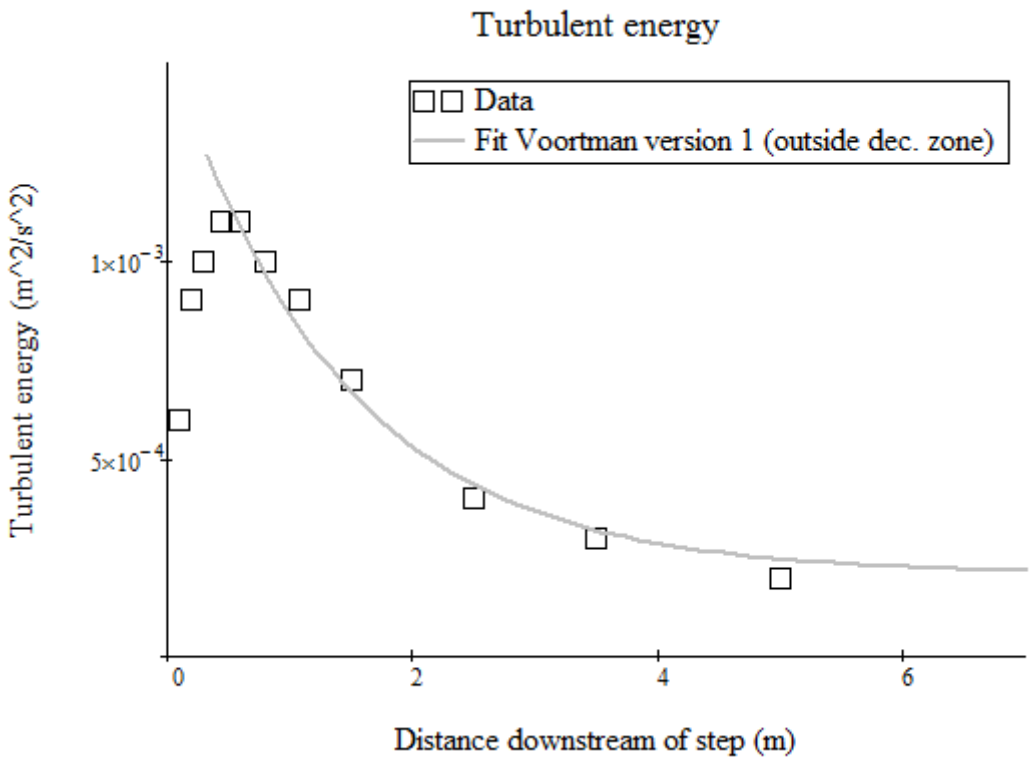

Figure 28: The curve fitted results with $k_{eq} = 1.44\ u_*{}^2$ for situation 4 with a "smooth" bed.

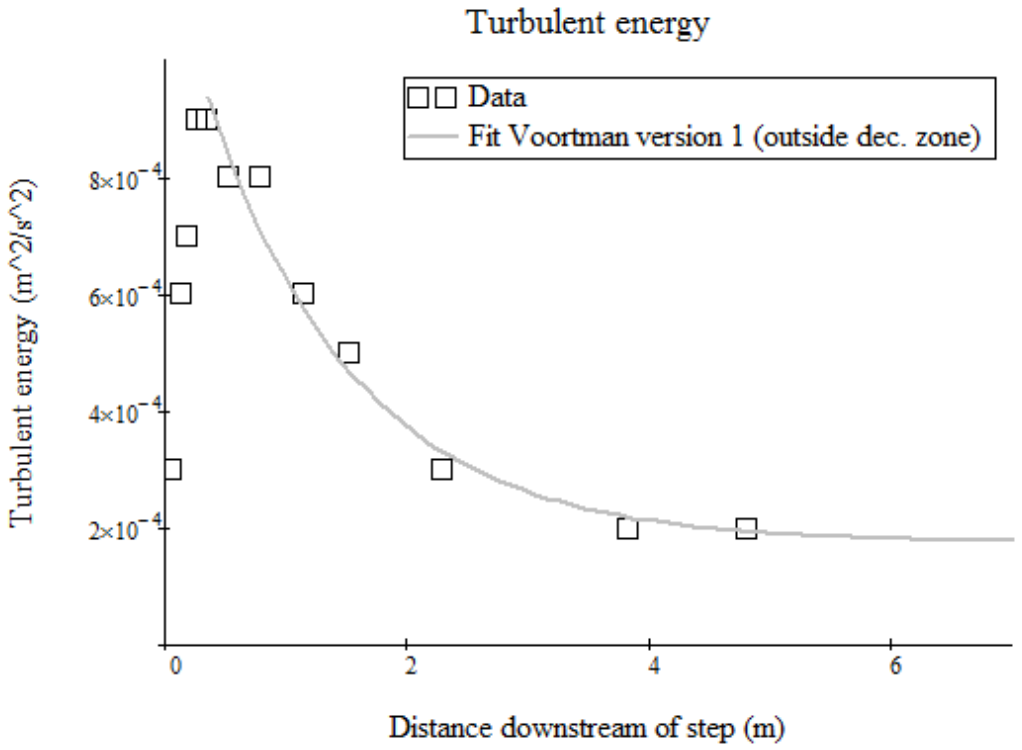

Figure 29: The curve fitted results with $k_{eq} = 1.44\ {u_*}^2$ for situation 1 with a "rough" bed.

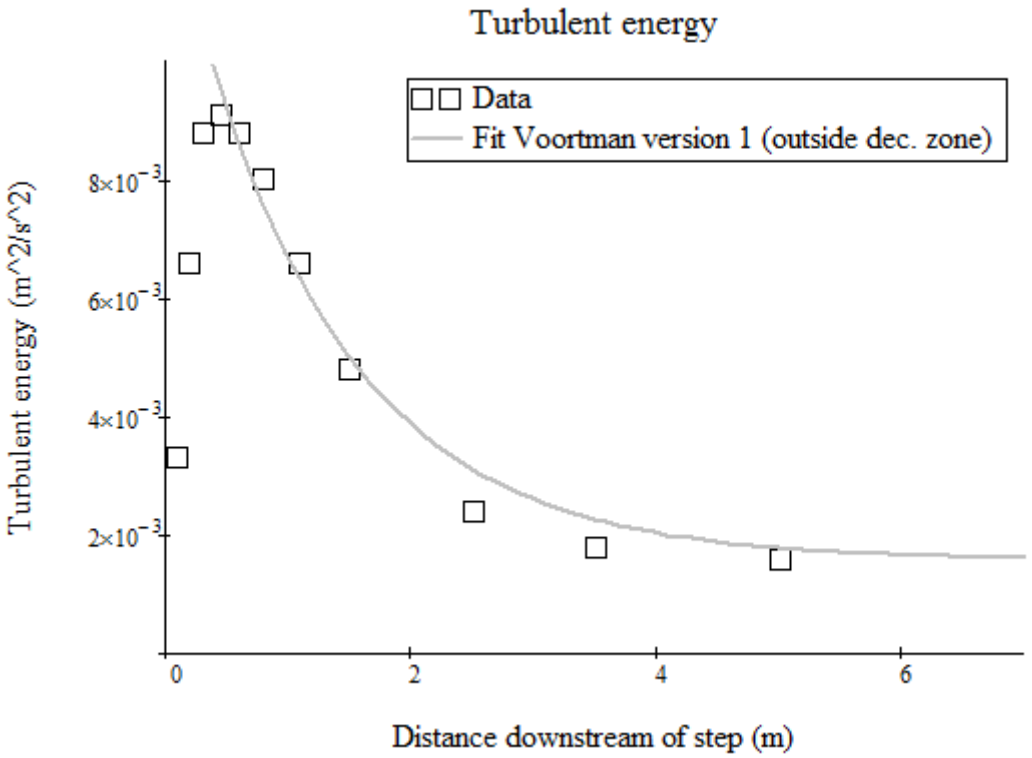

Figure 30: The curve fitted results with $k_{eq} = 1.44\ {u_*}^2$ for situation 3 with a "rough" bed.

In Figure 31, all the calculated and measured values of k were plotted in one graph. In an ideal scenario, the values would be the same and they would lie on the black line.
This is not the case, but the values do not differ that much.

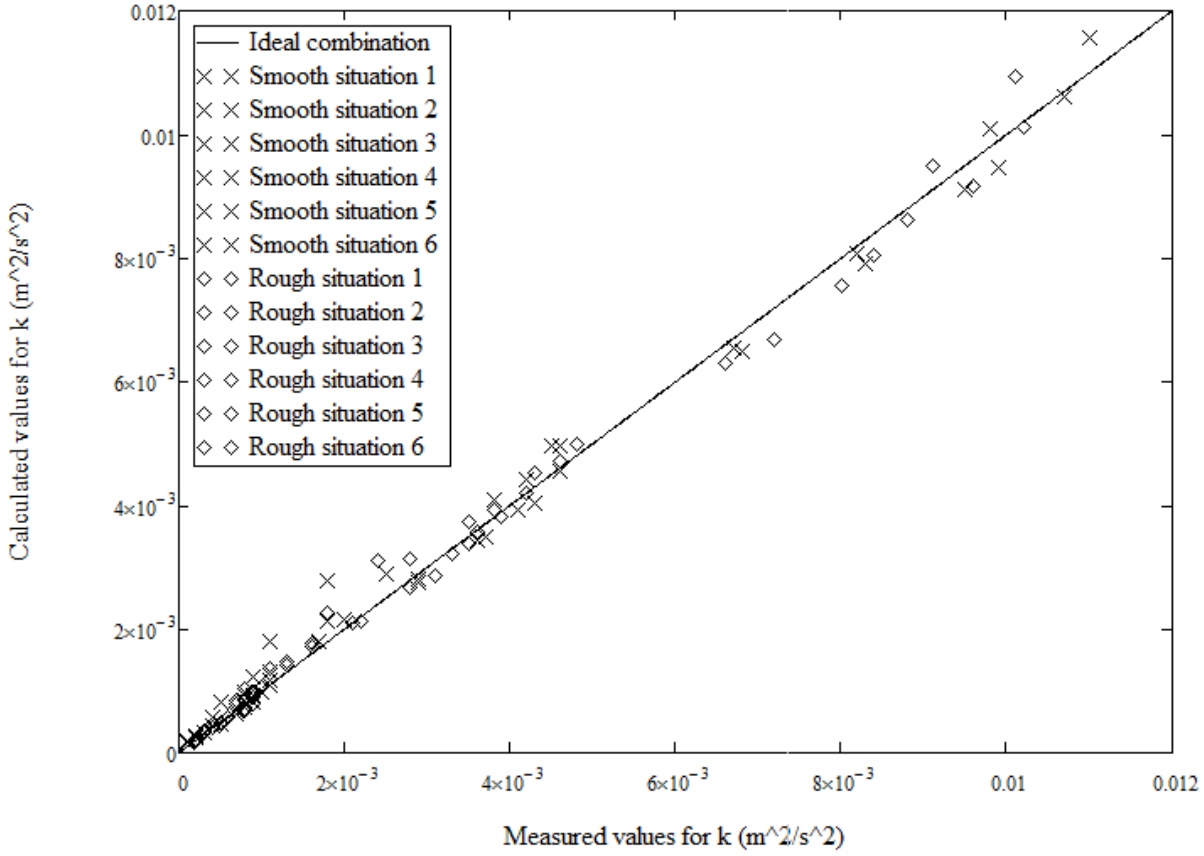

Figure 31: All the measured and calculated values of k.

This means that for most situations the fitting process works quite well. For only a few situations the calculated formula gives too high values, but that is mainly the result of a higher calculated amount of equilibrium turbulent energy.

Although it is not the preferred approach, the suggestion that the amount of equilibrium turbulent energy can be described with $k_{eq} = -0.125 \frac{R}{\varphi} \frac{dH}{dx}$ was also taken into account for all the sitautions. Using the same approach as above, leads to a mean value of φ is 0.064. Again, the total SSE is calculated and this time the value of φ with the lowest total SSE is used as the best option. The results are given in Table 5.

phi	sum SSE
0.06	**3.18E-05**
0.062	**3.11E-05**
0.063	**3.10E-05**
0.064	**3.10E-05**
0.065	**3.12E-05**
0.07	**3.38E-05**

Table 5: The total SSE for different values of φ with $p = 0.125$.

The conclusion from this analysis is that the combination of $p = 0.125$ and $\varphi = 0.064$ indeed gives the smallest SSE. One typical result with these values are shown in Figures 32. Further research is however necessary to improve this approach.

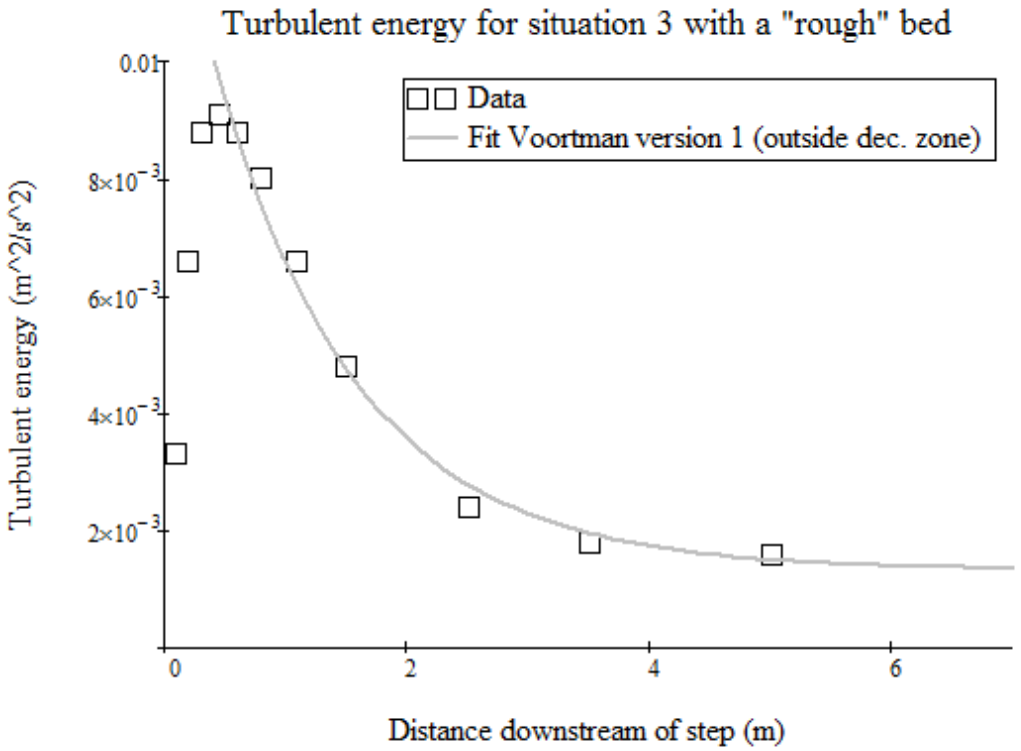

Figure 32: The curve fitted results for $p = 0.125$ and $\varphi = 0.064$ *for situation 3 with a "rough" bed.*

6.6 Calculating the relative turbulence

Until this point, the turbulent kinetic energy has been used, since energy is a preserved quantity. However, in the current formulae for stone stability the relative turbulence is mostly used, which means that this value should be calculated as well.

Hoffmans (1993) stated that for a uniform flow the relative turbulence can be calculated via:

$$r = \frac{\sqrt{k}}{\bar{\bar{u}}} \quad (6.5)$$

The relative turbulence at each location can therefore be calculated by using this formula for the calculated values for the turbulent energy at each location. Since it is expected that the depth-averaged velocity does not change much, the value for $\bar{\bar{u}}$ at the last measurement location was chosen. This might lead to a small overestimation.

In Figure 33, the calculated values are compared with the measured values for the relative turbulence (squares in Figure 33). For both results equation 6.5 was used.
Since this formula is only valid for a uniform flow, also the values for the relative turbulence directly obtained from the data will be shown (crosses in Figure 33). These data are obtained via:

$$r = \frac{u'}{\bar{\bar{u}}} \quad (6.6)$$

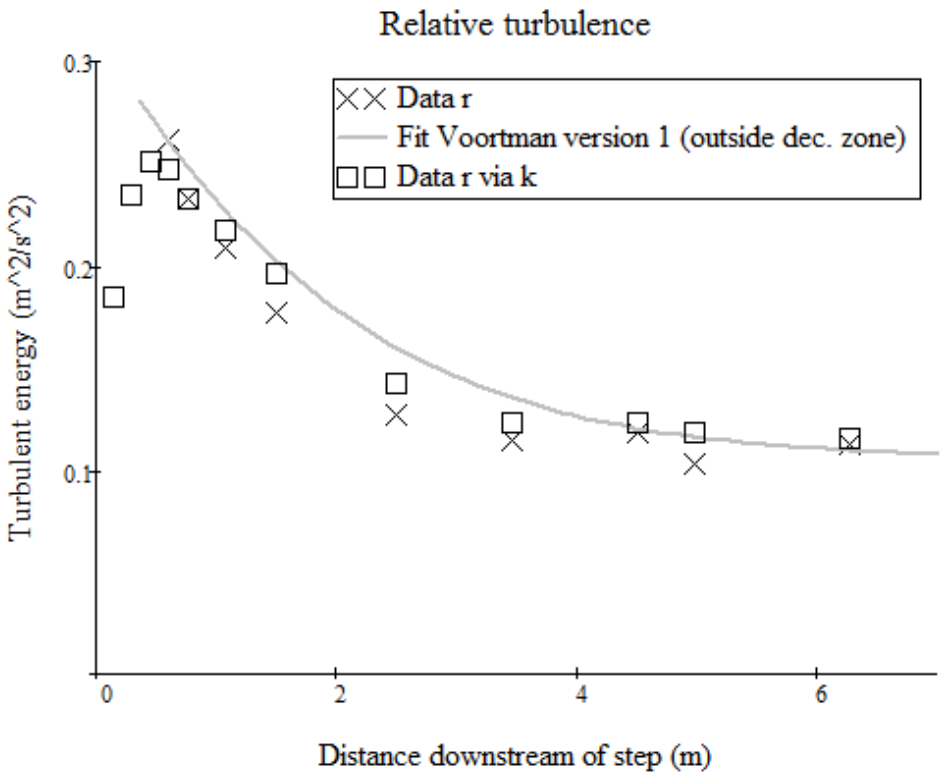

Figure 33: The relative turbulence of situation 2 with a rough bed.

From Figure 33 follows that the above-mentioned relation between the turbulent energy and relative turbulence in uniform flows works also pretty well in non-uniform flow.
Figure 33 also shows that the relative turbulence can be quite well predicted with the combination of Voortman's method and this relation.

6.7 Comparison with the method of Hoffmans

As explained in Chapter 2, Hoffmans formulated a method that is based on e.g. the step height and a certain relaxation length (Schiereck, 2001):

$$r_0(x) = \sqrt{0.5\, k_0 \left(1 - \frac{h_{step}}{d}\right)^{-2} \left(\frac{x}{\lambda} + 1\right)^{-1.08} + 1.45 \frac{g}{C^2}}$$

In this formula, the term $\frac{g}{C^2}$ is replaced by $\frac{{u_*}^2}{\overline{u}^2}$ with u_* following from section 5.2.

The calculated values from Hoffmans' formula will be compared with both the results from Voortman's formula, the measured data following from $r = \frac{\sqrt{k}}{\overline{u}}$ and the real measured values for the relative turbulence.

An example of the used Mathcad script can be found in Appendix M.

Two typical results will be shown in Figures 34 and 35, while the others can be found in Appendix N.

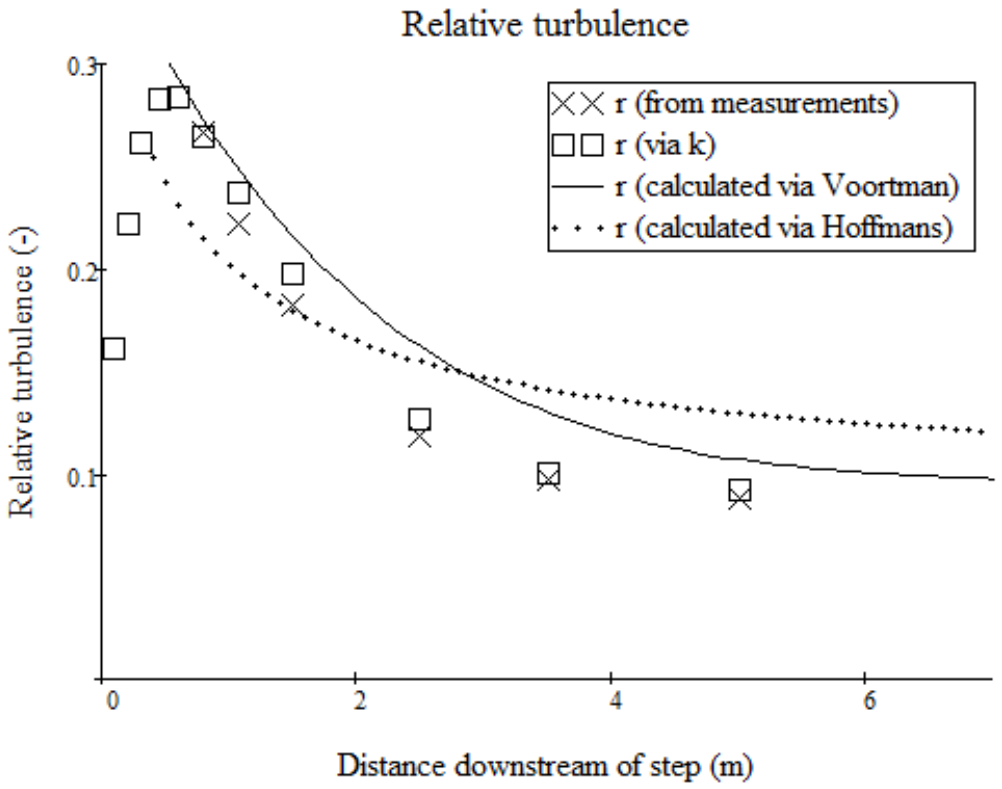

Figure 34: The results of both methods for situation 3 with a "smooth" bed.

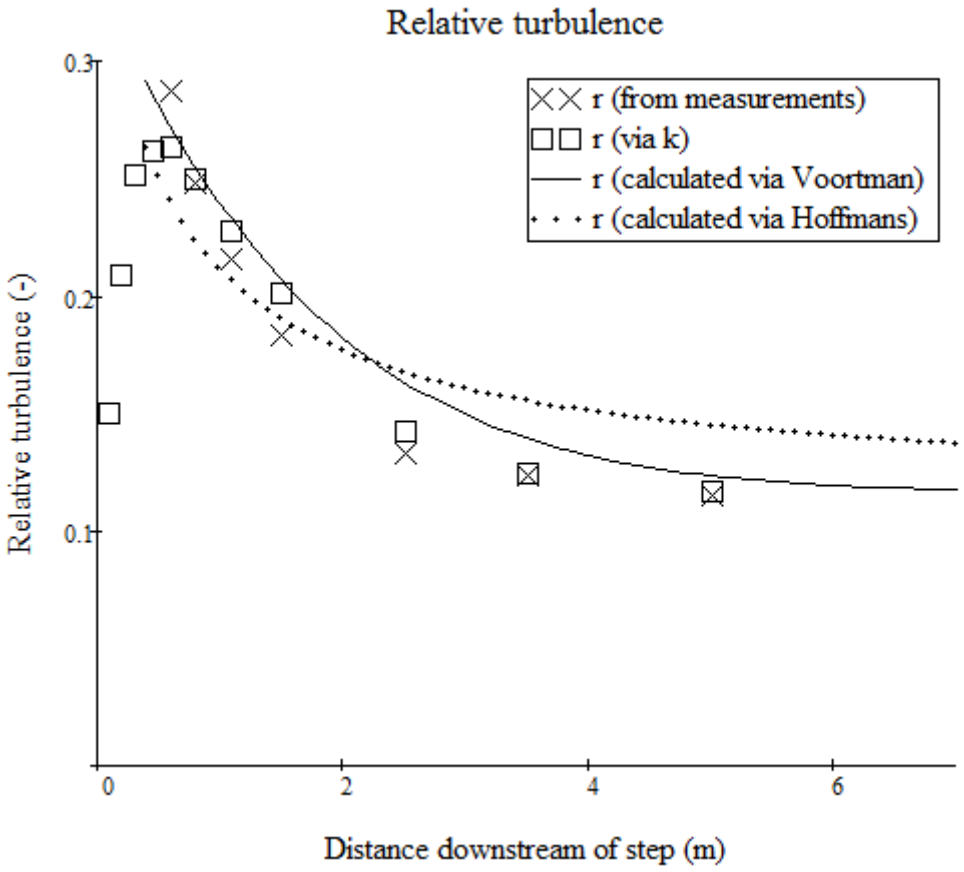

Figure 35: The results of both methods for situation 3 with a "rough" bed.

From the results follows that Hoffmans' formula gives a pretty accurate prediction of the amount of relative turbulence near the reattachment point, but a too high amount of relative turbulence further downstream. This is especially the case for the "rough" situations.
In some situations, however, the calculated relative turbulence near the reattachment point is too low, which might lead to failure of a bed protection, due to the higher loads.
Voortman's method gives a too high amount of relative turbulence far downstream as well, but it is always lower than according to Hoffmans' method and more in accordance with the measurement data.
The amount of equilibrium turbulent energy is equal for both situations, so the difference is mainly because Voortman's method follows an exponential function, while Hoffmans' formula is a power function.
Another advantage of Voortman's method over Hoffmans' formula is that in the latter one of the terms is a relaxation length of which it is uncertain to what extent it is applicable for the situations as described in this research. In Voortman's method a relaxation length does not have to be known beforehand.

Chapter 7

Conclusion and recommendations

7.1 Conclusions

In this research, twelve new experiments were performed in order to make a better description of the development of the turbulent energy downstream of a structure. The practical application was being able to design better bed protections.

Voortman's method (2013) is a differential equation based on a single decay factor for the equations for the turbulent kinetic energy:

$$\frac{d\bar{k}}{dx} = -g\frac{dH}{dx} - \varphi f\bar{k} \quad (7.1)$$

An analytical solution for the dissipation would than become an exponential function:

$$k_{diss}(x) = (k_0 - k_{eq}) * \exp(-f\varphi(x - x_{reatt})) + k_{eq} \quad (7.2)$$

From the calculations in Chapter 6 follows that it is possible to predict the dissipation of excess turbulence with this solution.
For the different parameters in the formula, the following recommendations were given:

- $f = \frac{1}{R}$
- $k_{eq} = 1.44\, {u_*}^2$
- $\varphi = 0.062$

For the maximum turbulent energy, no single solution was found, which means that further research on this aspect might be necessary. However, it is assumed that it can be calculated from the decay of mean flow energy.

Since in the current formulae for bed protections the relative turbulence is the most used parameter, the found result was converted to r as well. This was done via the formula $r = \frac{\sqrt{k}}{\bar{u}}$, which turned out to give satisfactory results in non-uniform flow as well.
From this analysis followed that Voortman's method can also be used to predict the relative turbulence.
If, in the future, k would become the governing parameter in the formulae for stone stability, the results would be even more universally applicable.

In comparison with Hoffmans' formula, the formula based on Voortman's method gives results that better fit the experimental data for all twelve flow situations. Especially the decay at longer distances is better predicted.
The faster decay can be explained by the fact that Voortman's method is based on an exponential decay, while Hoffman's formula is based on a power function. The equilibrium relative turbulence is almost identical for both methods.

7.2 Recommendations for further research

Experimental research

A general recommendation for doing experimental research is that a good measurement plan should be made and checked by others. It is also advised to check if all the preparations are done and to check afterwards if all the experiments had been done as they were intended to be.

It has to be kept in mind that doing experiments will always take longer than expected, even if already some extra time is reserved.

Horizontal flume

Although the results were quite satisfying and the problems could be solved, a new research in a truly horizontal flume could prove the validity of this method even more.

Measurements in a longer and wider flume

The experiments were performed in a flume with a width of 40 cm, which is small compared to most natural flows. Since the goal of this research was to look at a 2-Dimensional method, the effects of the width are not included, but they are indeed present, for example in the velocity distribution over the width. Doing experiments in a wider flume could reduce this effect.

Although it was initially the idea to do measurements up until the location was uniform, this was not completely possible, because the flow was influenced by the weir at the end of the flow.
Although in this report the flow at the last measurement locations is assumed to be uniform and the velocity profiles also looked like those of uniform flow, they were probably not. The result of this is that some assumptions regarding uniform flow were not completely true. The errors made with this are expected to be small, but further research on this topic might be necessary. It is therefore advisable to do future experiments in a longer flume, so that the uniform flow state could be reached and more information about this state could be obtained.

Energy levels

In hydraulic energy, the amount of energy is usually described in terms of energy level with the unit metre. It might be useful to escribe all terms as energy (J), because that has a more fundamental physical background. This might provide better results.

The generation of turbulence

The focus of this research was to come up with a description of the dissipation of the added turbulence. The generation of turbulence was not included, except for determining the equilibrium turbulence. Hoeve (2015) did an analysis about the generation of turbulence, but the link between his and this research is not yet discovered.

Conversion from mean flow energy to turbulence

Voortman initially assumed that the conversion from mean flow energy to turbulent energy was close to 100%. From the data, it turned out that this conversion was only 12.5%, which seems very low.
In this thesis, the energy loss is only used to calculate the equilibrium turbulent energy. The turbulent energy is constant if the flow is uniform and the energy loss is constant in space as well.

The problem might be caused by the fact that the energy loss is described as a linear function in this thesis. In reality, the energy loss becomes smaller more downstream and looks more like an exponential function.

The recommendation is therefore to use another approach in describing the mean energy flow loss, so that a higher percentage of the mean energy flow loss will be converted into turbulent energy. This could also give a better understanding of the maximum turbulent energy.

Turbulent stresses

Describing the turbulent stresses was not part of this thesis. However, it might be useful to use the obtained data to calculate the corresponding stresses $\overline{\acute{u}\acute{v}}$ and describe their influence on stone stability.

Other situations

Until this thesis, Voortman's method has only be validated for use in a Backward Facing Step Flow. The aim of the method is that it can be used in any situation, so in a subsequent research the method can be updated for use in other situations. It might be necessary to perform new experiments for these situations.
A recommendation is that these experiments are done in wider flumes, so that the side effects are as low as possible.

Practical applications

The ultimate target of this method is that it can be used in the designing process of a bed protection. For this reason, it is useful to do experiments in which the required stone diameter is calculated via this method so that can be checked if this method works for practical applications.

Bibliography

Battjes, J. A. & Labeur, R. J. (2009), *Vloeistofmechanica 2: Collegehandleiding CT2140*, Delft: Delft University of Technology

Bernard, P.S. & Wallace, J. M. (2002), *Turbulent Flow. Analysis, Measurement and Prediction*, Hoboken (New Jersey); John Wiley & Sons Inc.

Cruise, J.F., Sherif, M.M., Singh, V.P. (2007), *Elementary Hydraulics,* page 127 – 129

George, W. K. (2013), *Lectures in Turbulence for the 21st Century*. Göteborg: Chalmers University of Technology.

Greenblatt, D., & Wygnanski, I. J. (2000). *The control of flow separation by periodic excitation.* Progress in Aerospace Sciences, 36(7), 487-545

Hinze, J. O. (1975), *Turbulence* (Second edition), McGraw-Hill series in mechanical engineering

Hoeve, J. B. (2015), *Rapid assessment tool for turbulence in backward facing step flow*, Amersfoort / Enschede: graduation project at Arcadis

Hoffmans, G.J.CM. (1992), *Two-dimensional mathematical modelling of local-scour holes.* Doctoral thesis, Faculty of Civil Engineering, Hydraulic and Geotechnical Engineering Division, Delft: Delft University of Technology

Hoffmans, G. J. C. M. (1993), *A study concerning the influence of the relative turbulence intensity on local-scour holes*. Delft: Rijkswaterstaat, DWW.

Hofland, B. (2005), *Rock and roll: Turbulence-induced damage to granular bed protections*, Delft: Delft University of Technology.

Hofland, B. (2017), Internal correspondance during graduation. (M. Koote, Interviewer)

Izbash, S. V.. (1935). *Construction of by dumping of Stone in running Water.* Moscow-Leningrad.

Mierlo, M.C.L.M. van, and De Ruiter, J.C.C. (1988), *Turbulence measurements above dunes.* Report No. Q789, Vol.1 and 2, Delft Hydraulics, Delft.

MIT (2016), Turbulence. lecture notes**:** http://www.mit.edu/course/1/1.061/www/dream/SEVEN/SEVENTHEORY.PDF , Retrieved 13th November 2016

MIT (2006), Open Channel flow. lecture notes**:** https://ocw.mit.edu/courses/earth-atmospheric-and-planetary-sciences/12-090-introduction-to-fluid-motions-sediment-transport-and-current-generated-sedimentary-structures-fall-2006/course-textbook/ch5.pdf , Retrieved 13th November 2016

Nakagawa, H., & Nezu, I. (1987), *Experimental investigation on turbulent structure of backward facing step flow in an open channel.* Journal of Hydraulic Research, 25(1), 67-88.

Nikuradse, J. (1933), *Laws for flows in rough pipes.* NACA Tech. Memo. 1292.

PBL (2007), http://www.pbl.nl/dossiers/klimaatverandering/content/correctie-formulering-over-overstromomgsrisico [sic], Retrieved 21st February 2017

Richardson, L. F. (1922), *Weather Prediction by Numerical Process*, Cambridge University Press

Rijn, L. C. van (1990), *Principles of fluid flow and surface waves in rivers, estuaries, seas and oceans*, Amsterdam: Aqua Publications

Rock Manual (2007), *The Rock Manual (Vol. 683),* Construction Industry Research, Information Association, Civieltechnisch Centrum Uitvoering Research en Regelgeving (Netherlands), & Centre d'études maritimes et fluviales (France). (2007). London: Ciria, pages 550 - 551 & 648 – 652

Reynolds, O. (1883), *An experimental investigation of the circumstances which determine whether the motion of water shall be direct or sinuous, and the law of resistance in parallel channels.* Trans. Roy. Soc. Lond. 174: 935–982.

Schiereck, G. J. (2001), *Introduction to bed, bank and shore protection*. Delft: CRC Press, page 22 – 74

Schlichting, H. (1949), *Lecture series "Boundary Layer Theory" Part II – Turbulent Flows*, NASA, https://ntrs.nasa.gov/archive/nasa/casi.ntrs.nasa.gov/20050040758.pdf, page 31 – 33, Retrieved 12th April 2016

Shields, A. (1936), *Application of similarity principles and turbulence research to bed-load movement.* Soil Conservation Service.

Stowa (1994), *Handboek debietmeten in open waterlopen*, http://www.stowa.nl/Upload/publicaties2/mID_4924_cID_3914_93216555_1994-13_handboek-debietmeten-open-waterlopen.pdf, Retrieved 14th July 2016

Tennekes, H., & Lumley, J. L. (1972), *A first course in turbulence.* Cambridge: MIT press.

CIE 5312 (2016), *lecture notes „Turbulence in hydraulics / CT 5312"*, written by W.S.J. Uijttewaal, Delft: Delft University of Technology, retrieved in 2016.

Voortman, H. G. (2013, 2016), *Semi-analytic model for turbulence in open channel flow*. Amersfoort: Arcadis (internal document)

Voortman, H. (2016/2017), Internal correspondance during graduation at Arcadis. (M. Koote, Interviewer)

Vree, S. de. (2016), Internal correspondance during graduation at Laboratory for Fluid Dynamics, TU Delft. (M. Koote, Interviewer)

Appendix A:
Comparison of the formulae of Pilarczyk and Escarmeia & May

Example in which the formulae of Pliarczyk and Escarmeia & May are compared

$\rho_w := 1000 \cdot \frac{kg}{m^3}$ $\rho_s := 2650 \cdot \frac{kg}{m^3}$

$\Delta := \frac{\rho_s - \rho_w}{\rho_w}$

$g = 9.807 \frac{m}{s^2}$

$u := 1 \cdot \frac{m}{s}$

$u_b := 0.75 \cdot u$

$r := 0.6$

Pilarczyk:

$\phi_{sc} := 1$

$\psi_{cr} := 0.035$

$k_h := 1$

$k_{sl} := 1$

$k_t := \frac{1 + 3 \cdot r}{1.3} = 2.154$

$D := \frac{\phi_{sc}}{\Delta} \cdot \frac{0.035}{\psi_{cr}} \cdot k_h \cdot k_{sl}^{-1} \cdot k_t^2 \cdot \frac{u^2}{2 \cdot g} = 0.143\,m$

Escarameia and May:

$c_T := 12.3 \cdot r - 0.20$

$D_{n50} := c_T \cdot \frac{u_b^2}{2 \cdot g \cdot \Delta} = 0.125\,m$

Appendix B: Current methods of turbulence modelling

The full differential equation for the transport of a fluid is called the Navier-Stokes equation. It also includes turbulence, but it can still not be completely solved.
For this reason different models are used to get a better insight into the nature and effects of turbulence. (CIE 5312, 2016).

Two types of models are available: theoretical and physical models. The aim of theoretical models is to find a good approximation of the turbulence equations, by simplifying them and compute the answers numerically. Physical models are used to see and measure what the effects of turbulence are.
When a design has to be made, it is common to use both types of modelling: first the (desired) outcome is computed and then with the help of physical model will be checked if the outcome is the same as what was expected.

The most used theoretical method for solving the turbulence equations is using the in Chapter 3 mentioned Reynolds stresses. As said before the amount of turbulence can be calculated if the turbulent viscosity is known and for that the mixing length has to be computed.

The κ-ε model provides a way to compute the mixing length by computing the dissipation of the turbulent energy first. This gives a relatively easy and complete model to compute the turbulence. The disadvantage of this model is there is no such thing as conservation of dissipation and that is why the physical relevance of this method is not quite obvious and it is not universally applicable.
(CIE 5312, 2016).

Another widely used method for computational modelling is the Large Eddy Simulation. This method is based on the fact that turbulence becomes more isotropic in the smaller scales. It is assumed that the smaller scales are only responsible for the withdrawal of turbulence and when this effect is added as an extra term to the larger scales, the smaller scales can be filtered out of the model, so that smaller grid sizes can be used to get a good image of the large-scale turbulence.
The disadvantage of this model is that in some cases the dissipation of energy is not modelled well enough, which affects the levels of turbulent kinetic energy.

Appendix C: Physical modelling and scaling laws

Physical models are used when reality has to be simulated on a smaller scale, for instance to understand the physical processes or to check whether a solution is possible.

To make sure that the real-life processes are well implemented in the model, the scaling laws are have to be obeyed.

The scaling generally starts with the length scale, because this is based on the physical limitations of the model. From the length scaling it is possible to determine the other scaling factors.

Two different options are normally used for this, either the Reynolds number or the Froude number must be the same in the model and for real situations to keep at least a part of the flow characteristics the same. Unfortunately, it is impossible to satisfy both dimensionless numbers as will follow from their equations.

Reynolds: $Re = \frac{u*d}{\nu}$

Froude: $Fr = \frac{u}{\sqrt{g*d}}$

During these experiments, the Froude numbers on top of the weir will have certain predefined values to see the effect of the Froude number on the formation and decay of turbulence. All other parameters will be defined based on the Froude numbers. There are several reasons to do so.

The first reason is that it is important that the Froude number determines whether the fluid is subcritical (Fr < 1) or super-critical (Fr >1). Subcritical flow means a relatively large water depth and a small velocity while super-critical means the opposite. This means that to make a correct model of the real-life situation the characteristics of the flow in the model need to be the same as in real-life, or in other words, you will get different results when the flow in the model is supercritical flow while the flow in reality is subcritical.

The second reason is that the exact value of the Reynolds number is not of importance as long as the flow is completely turbulent, which is according to Van Rijn (1990) the case if Re > 10000. This means in practice that with a water depth of 0.1 m the velocity should be 0.1 m/s.

The third reason is that in the Reynolds equation d and u are inversely proportional. This means that to keep Re constant, a smaller d results in a larger u, which can cause the flow to transform from subcritical to super-critical.

Based on this, the scaling factors can be determined.
The scaling factors are given the letter n with a subscript corresponding to their meaning. “L” stands for length (or depth), “u” stands for velocity and “t” means time.

For example: $u_{real} = n_u * u_{model}$ and $d_{real} = n_L * d_{model}$

This leads to: $Fr_{model} = \frac{u_{model}}{\sqrt{g*d_{model}}}$ and $Fr_{real} = \frac{u_{real}}{\sqrt{g*d_{real}}}$

The latter one can be rewritten as $Fr_{real} = \frac{n_u*u_{model}}{\sqrt{g*n_L*d_{model}}} = \frac{n_u}{\sqrt{n_L}} * \frac{u_{model}}{\sqrt{g*d_{model}}}$

Giving the demand that $Fr_{real} = Fr_{model}$ this means that $\frac{n_u}{\sqrt{n_L}} = 1$ or $n_u = {n_L}^{1/2}$

Since $q = h * u$, it can also be concluded that $n_q = n_u * n_L = {n_L}^{3/2}$.

That means that if the scaling factor for the length is known, also the scaling factors for the other dimensions can be determined. This conclusion can be important for later use of the obtained results.

Appendix D: Roughness of the bed

To make sure that the resistance coefficient is independent of the Reynold's number, the flow must be hydraulically rough. This is the case when the equivalent sand roughness height is much larger than the thickness of the viscous sublayer. (Nikuradse, 1933).

The roughness can be checked with the formula:

$$u^+ = \frac{u_* * k_s}{\nu}$$ (Nikuradse, 1933)

The flow is hydraulically rough when $u^+ > 70$. (Nikuradse, 1933).

According to the diagram of Nikuradse, this is generally the case when Re > 10000. Since this is the same number as Van Rijn recommends maintaining for doing model tests, the experiments will be done with a Reynold's number larger than 10000. This is the case for all the examples above.

The bottom roughness will consist of metal plates with little rocks glued on them. Each of the 6 experiments mentioned in Chapter4 will be performed twice, with different bottom roughness, so in total 12 different experiments will be done.

For the first set of experiments stones with a diameter of 3 mm are used. Assuming that $k_s = 2*d_{n50}$ (Schiereck, 2001), the equivalent sand roughness will be 6 mm.

The second half of the experiment will be executed with stones with a diameter of 1 cm, which means that the equivalent sand roughness will be 2 cm.

According to Schiereck (2001): $u_* = \sqrt{c_f} * u$ and $c_f = \left(\frac{\kappa}{\ln\left(\frac{12*R}{k_s}\right)}\right)^2$

With these formulae can be calculated that in case 1 the value of k_s^+ is 60, which is just a little under 70. This means that the flow in this situation is expected to not be completely hydraulically rough. On the other hand, the flow is almost hydraulically rough, so it is assumed that the errors made by this are very small.
Since case 1 has the lowest shear velocity and the flow is expected to be almost hydraulically rough even in this case, it can be assumed that the flow is expected to be hydraulically rough in all cases.

Appendix E: Rehbock weir

For the determination of the discharge in the flume, the height of the water above the Rehbock weir, situated in the return flume, was measured. This return flume was located directly under the normal flume and has a width of 0.45 m.

A Rehbock weir is a horizontal sharp crested weir whose crest is slanted at the downstream side. An important aspect of this type of weir is that the space just behind the weir (and under the flowing water) is aerated, to prevent that the discharge relationship is disrupted due to under pressure. (Stowa)
Image E1 shows a picture of the used Rehbock weir.

Image E1: The Rehbock weir in the return flow. On the right is the red device visible that measures the water depth on top of the weir.

In the return flume, a floating device measures the water depth on top of the Rehbock weir.

Two different formulas to calculate the discharge with the help of the Rehbock weir are known, both giving a slightly different answer:

1) $Q = C_e * \frac{2}{3} * \sqrt{2 * g} * B * h_e^{\frac{3}{2}}$, with $h_e = h_k + 0.0012$ and $C_e = 0.602 + 0.083 * \frac{h_k}{a}$ (Stowa)

2) $Q = m' * \frac{2}{3} * h_e * \sqrt{g * \frac{2}{3} * h_e} * B$, with $h_e = h_k + 0.0011$ and $m' = 1.045 + 0.141 * \frac{h_e}{a}$ (Battjes & Labeur)

The height of the weir , which is “a” in the formula, was 25 cm above the canal bed upstream of the weir.

With the help of the formula the discharge was checked and with this discharge and the height above the weir the Froude number was calculated.

This was once done for all three formulae to see if they gave the same results. It turned out that with the same value for h_k the difference in Froude number was in the order of 0.0005, which is even smaller than 0.001 which was the order of difference for using a slightly different value for h_k.

In this report, the formula by Stowa (1994) is used, because this was recommended by De Vree (2016) as it was already used in earlier experiments.

Since it took on average three days to measure one flow situation and the pump was switched off at the end of each day, at the beginning of every day (within one flow scenario) the water depth over the Rehbock weir had to be checked again.
The maximum difference on top of the Rehbock weir for one flow situation was 0.2 mm. In terms of discharge this error could be up to 0.5%.

Appendix F: Velocity profiles

In this Appendix the velocity profiles for all twelve experiments will be shown.

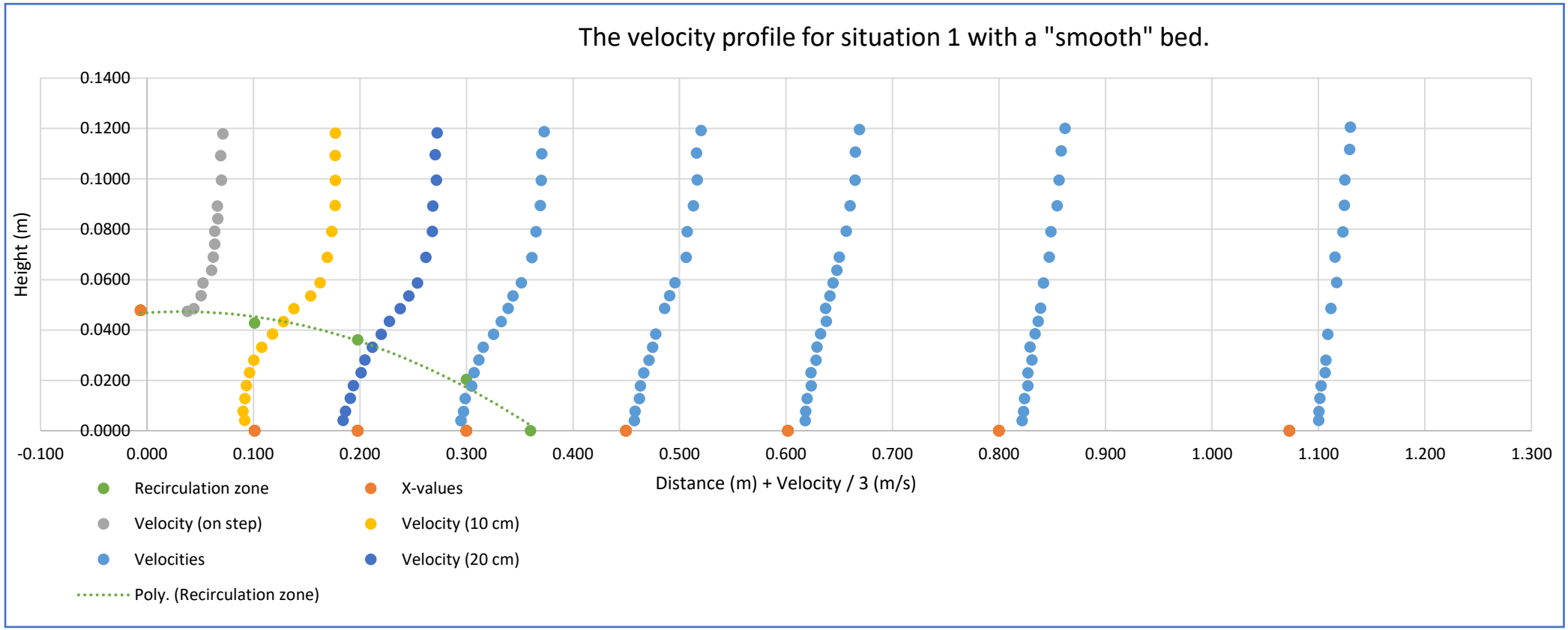

Figure F1: The velocity profile (for horizontal velocities) for the first metre of smooth situation 1.

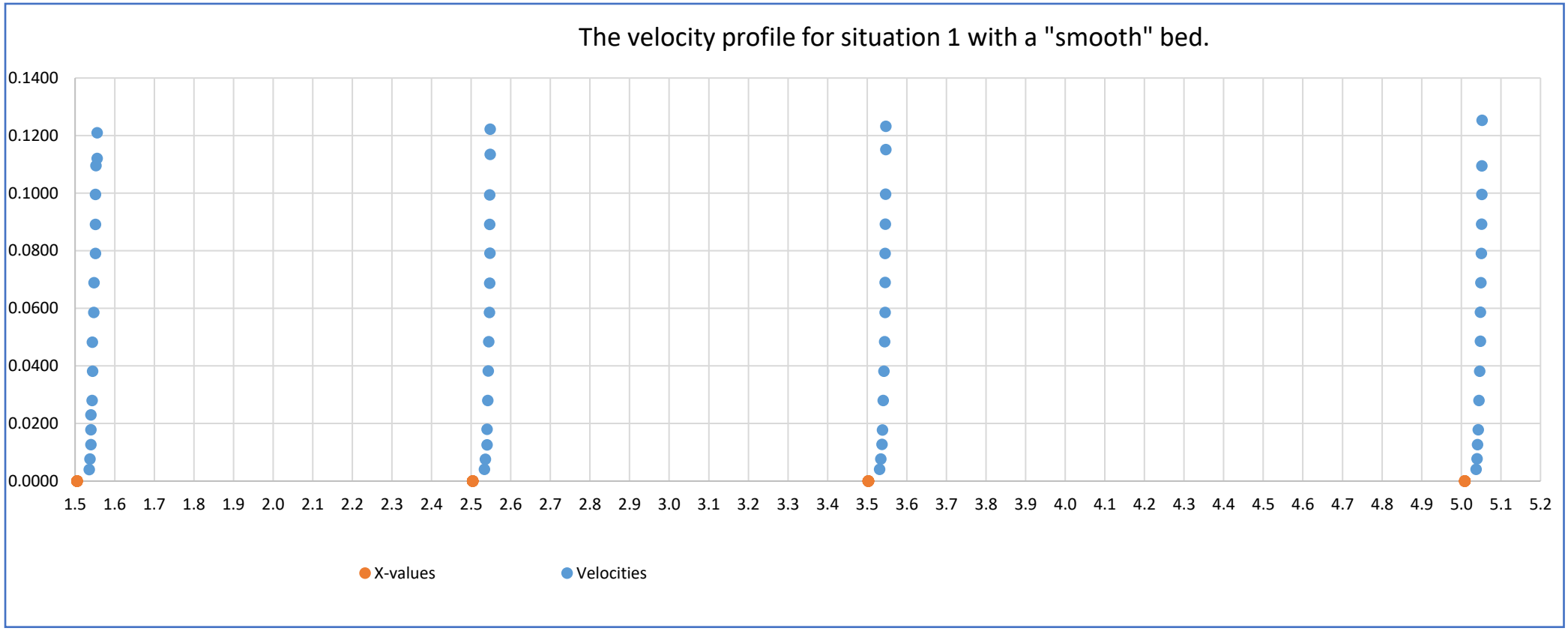

Figure F2: The velocity profile (for horizontal velocities) for the last four metres of smooth situation 1.

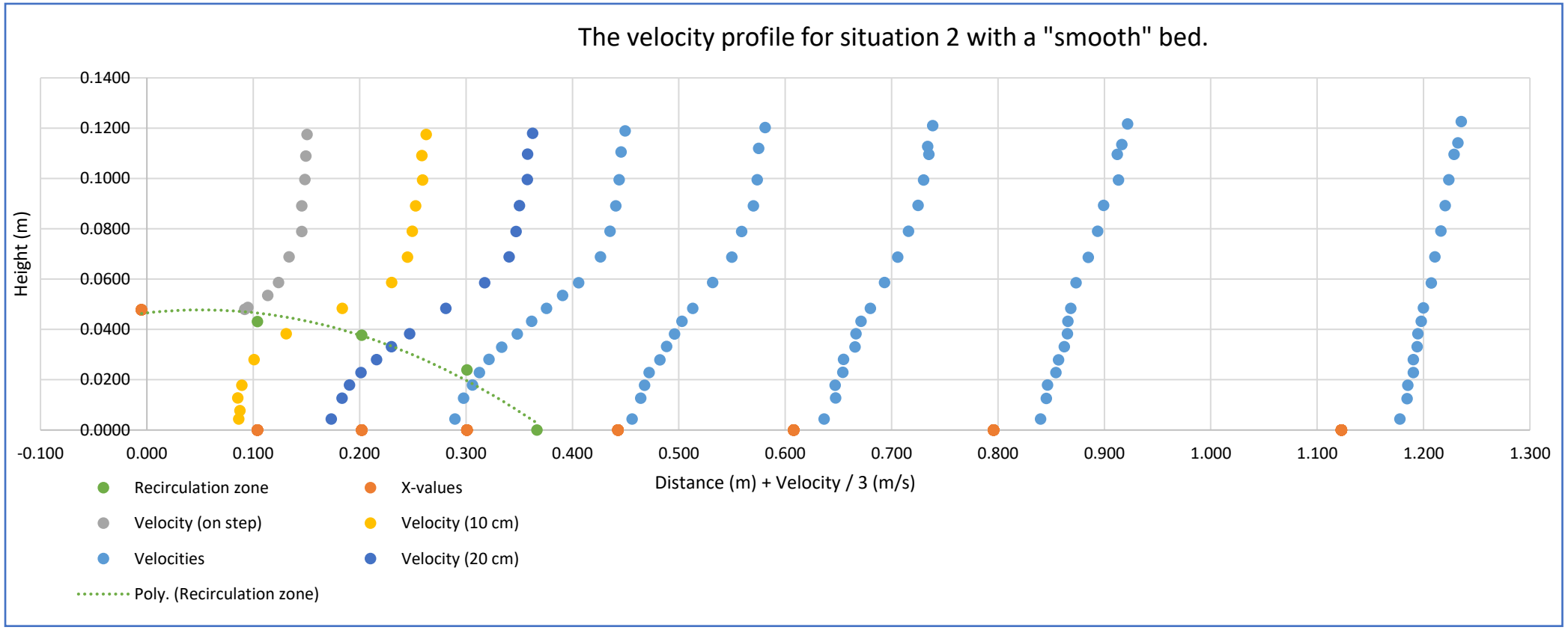

Figure F3: The velocity profile (for horizontal velocities) for the first metre of smooth situation 2.

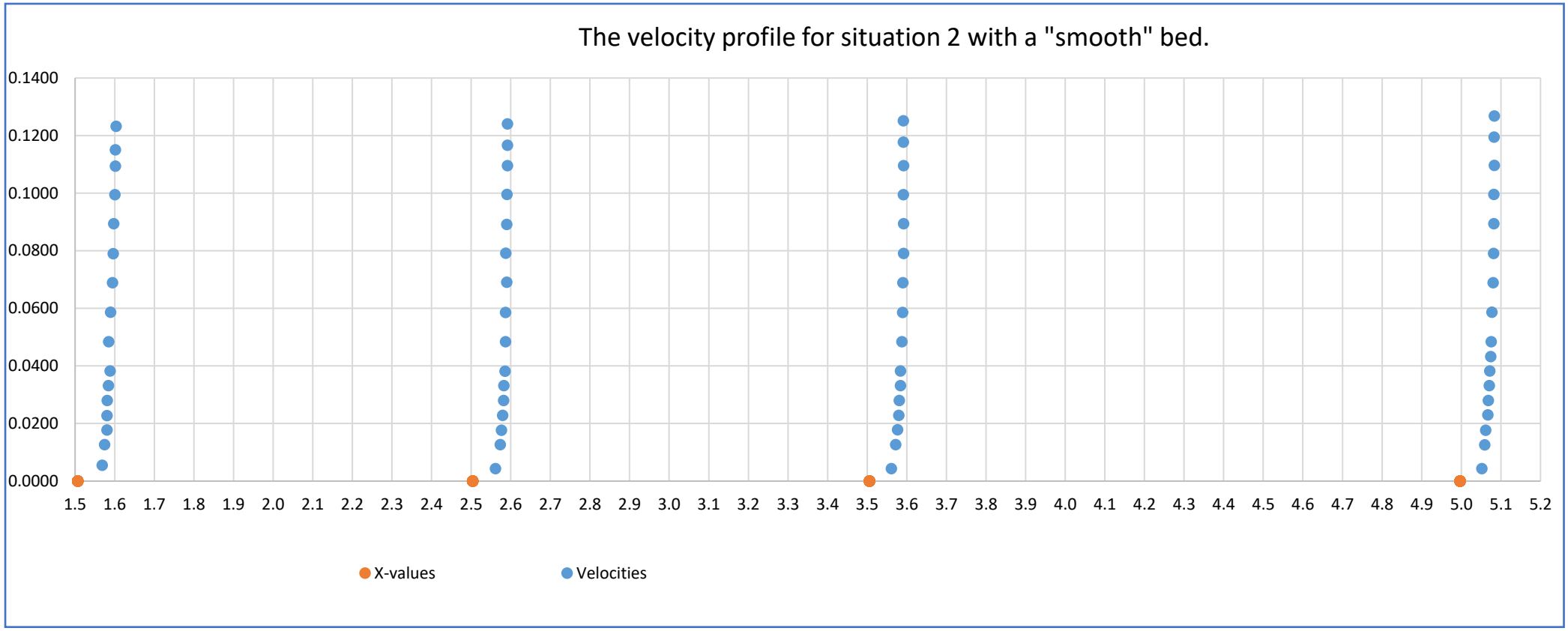

Figure F4: The velocity profile (for horizontal velocities) for the last four metres of smooth situation 2.

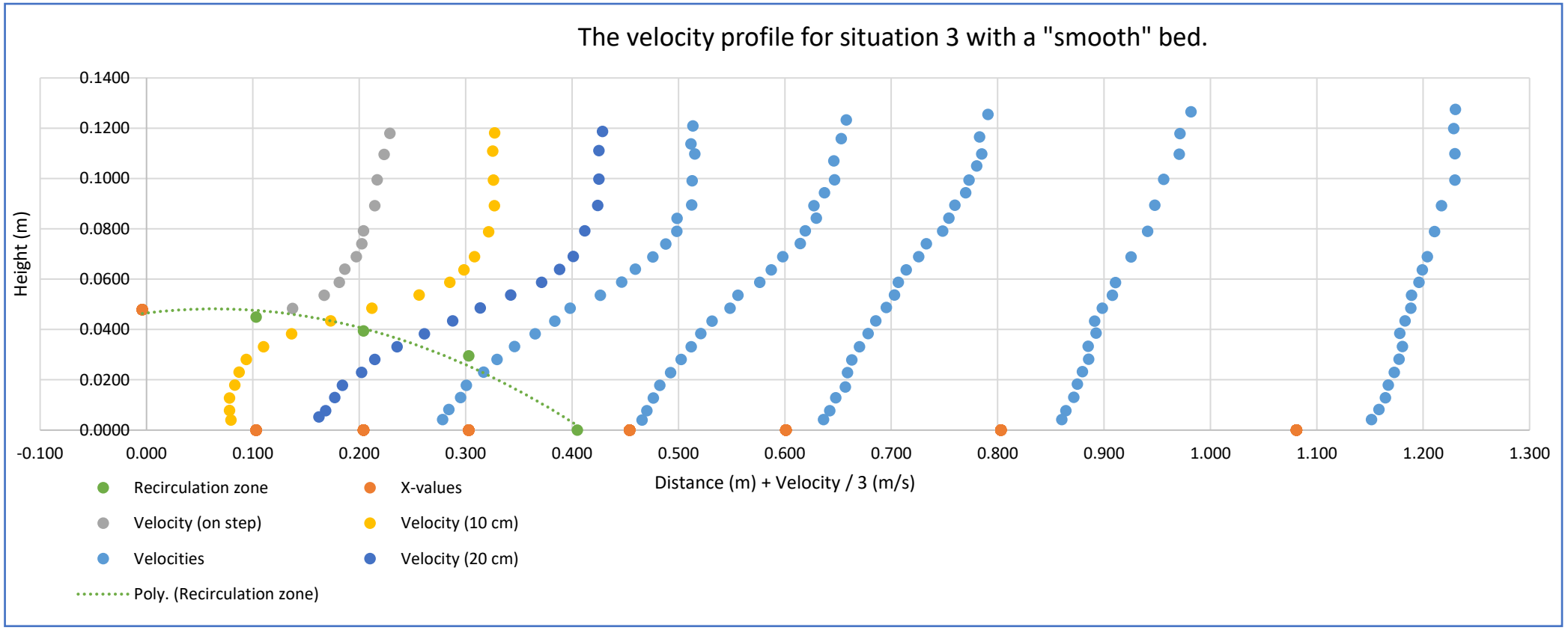

Figure F5: The velocity profile (for horizontal velocities) for the first metre of smooth situation 3.

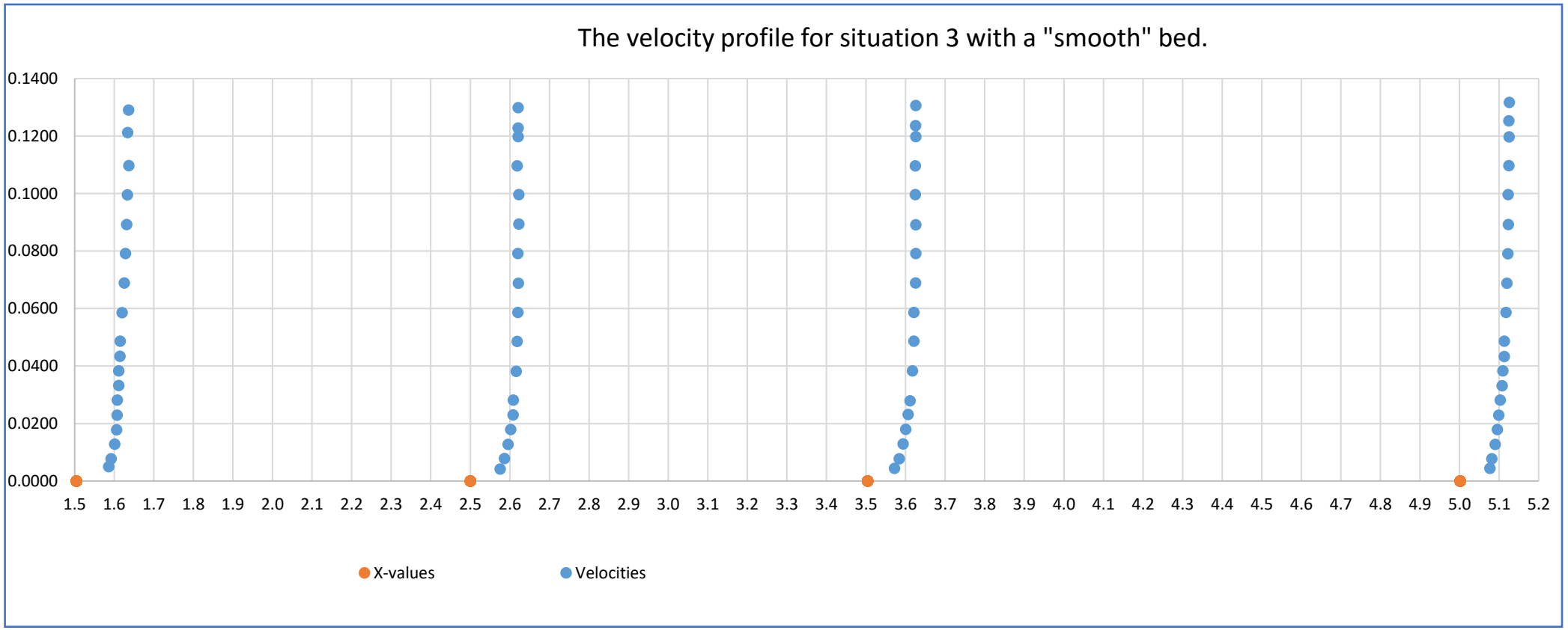

Figure F6: The velocity profile (for horizontal velocities) for the last four metres of smooth situation 3.

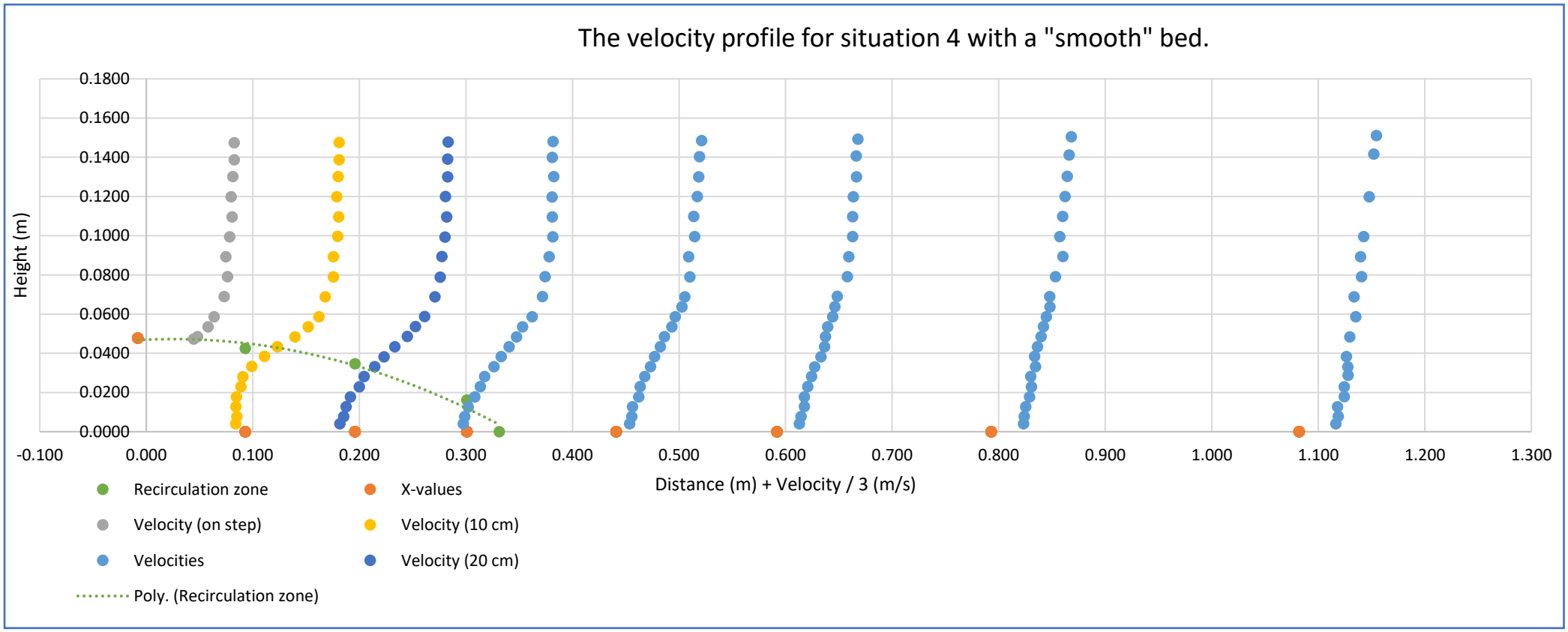

Figure F7: The velocity profile (for horizontal velocities) for the first metre of smooth situation 4.

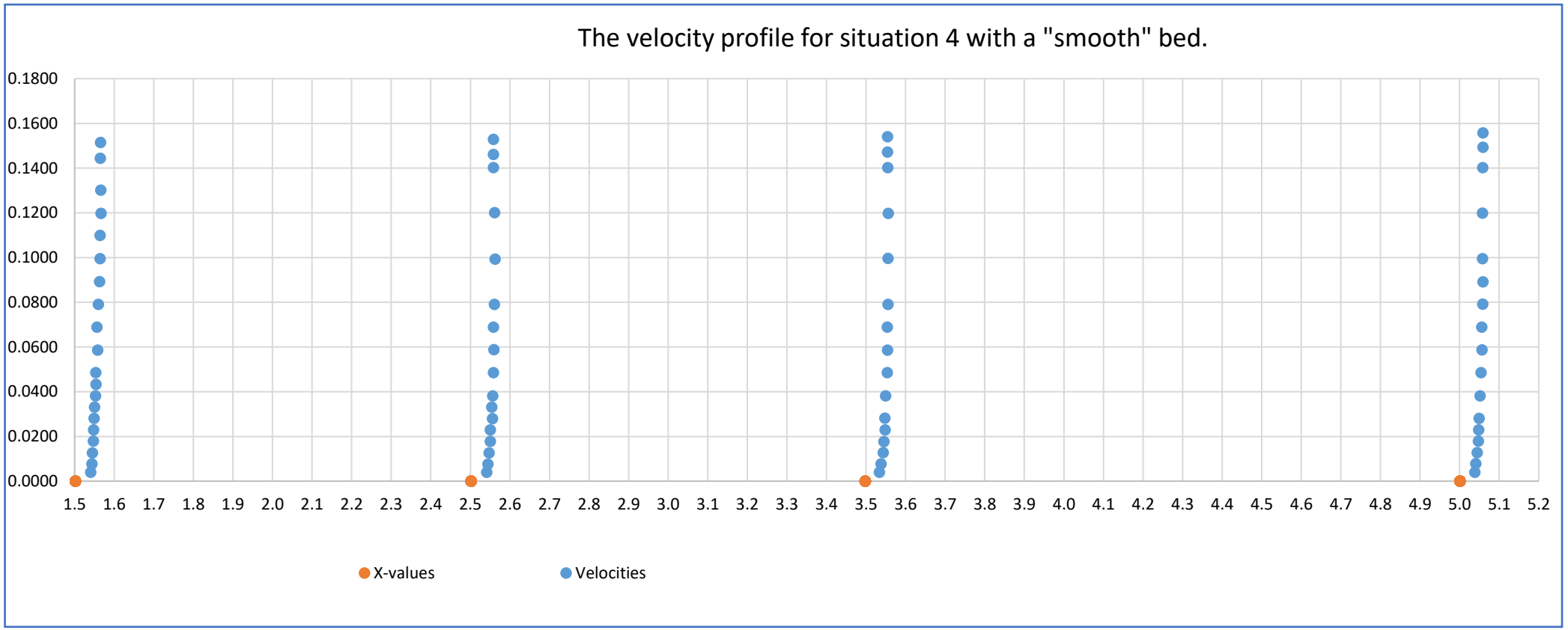

Figure F8: The velocity profile (for horizontal velocities) for the last four metres of smooth situation 4.

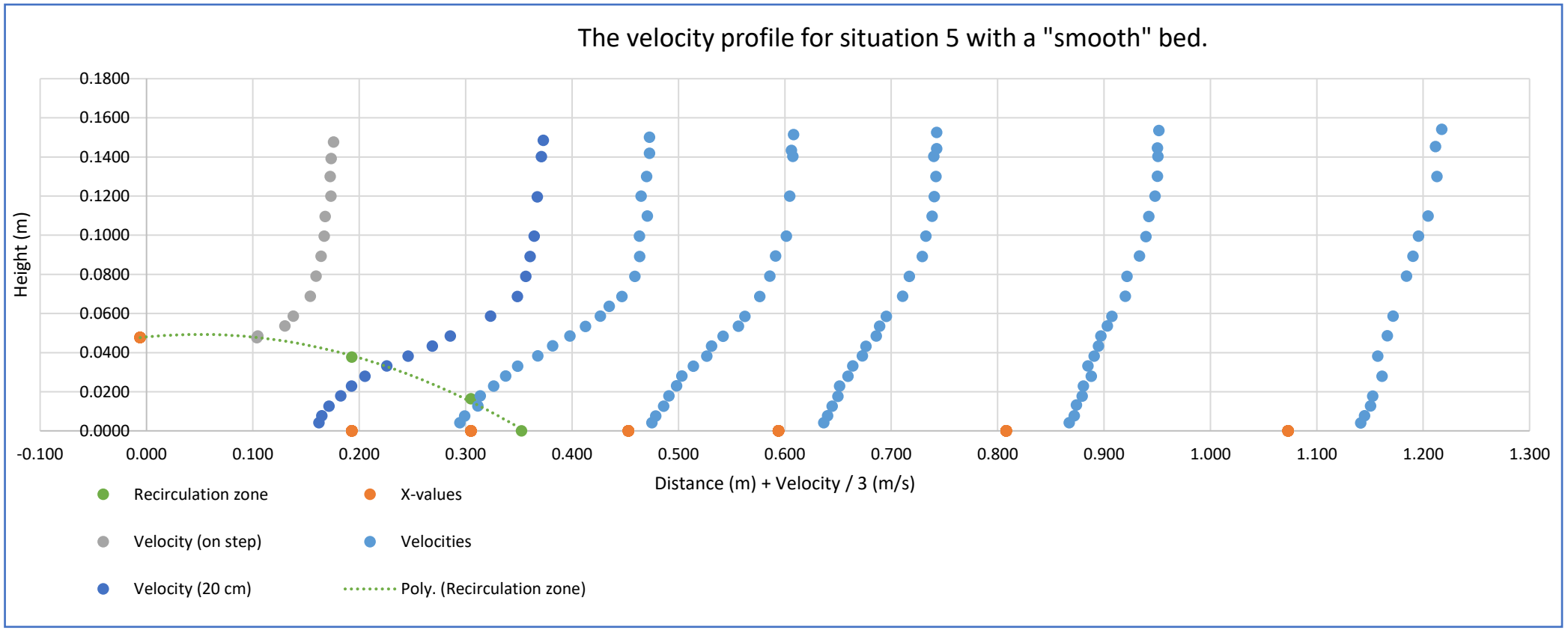

Figure F9: The velocity profile (for horizontal velocities) for the first metre of smooth situation 5.

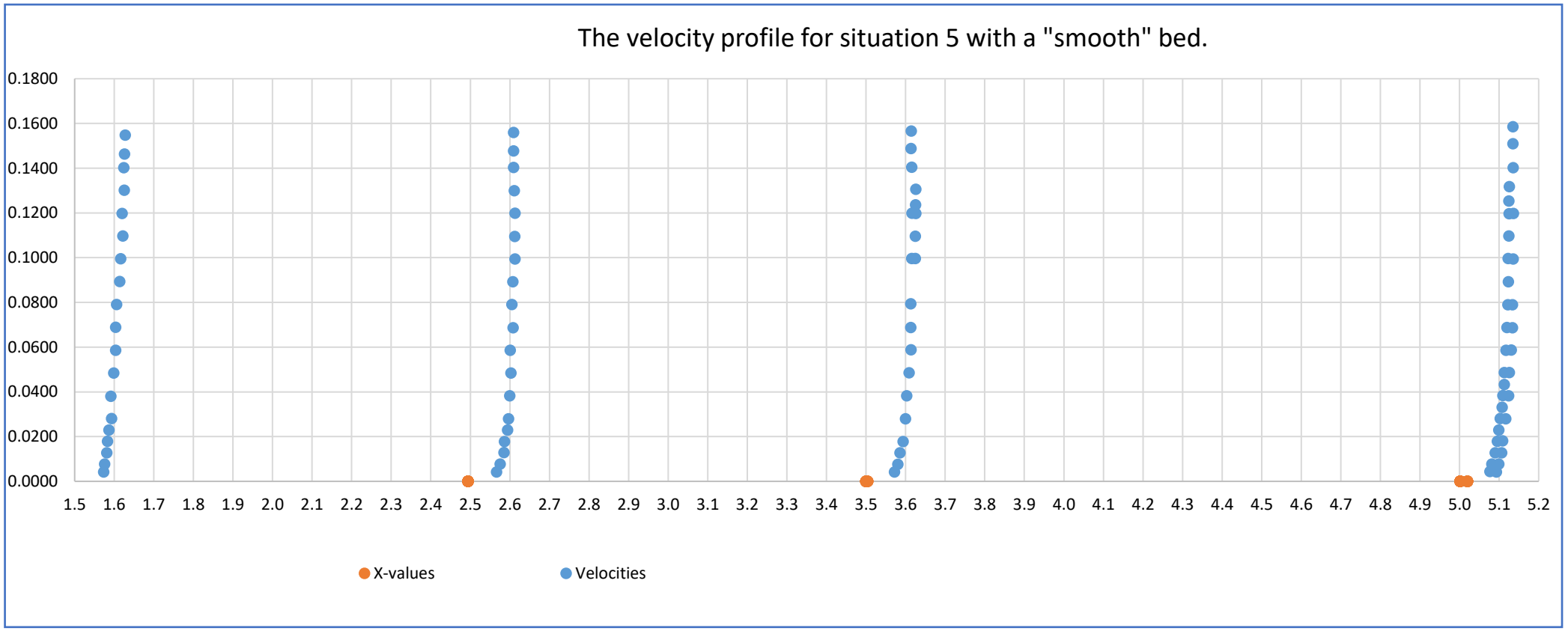

Figure F10: The velocity profile (for horizontal velocities) for the last four metres of smooth situation 5.

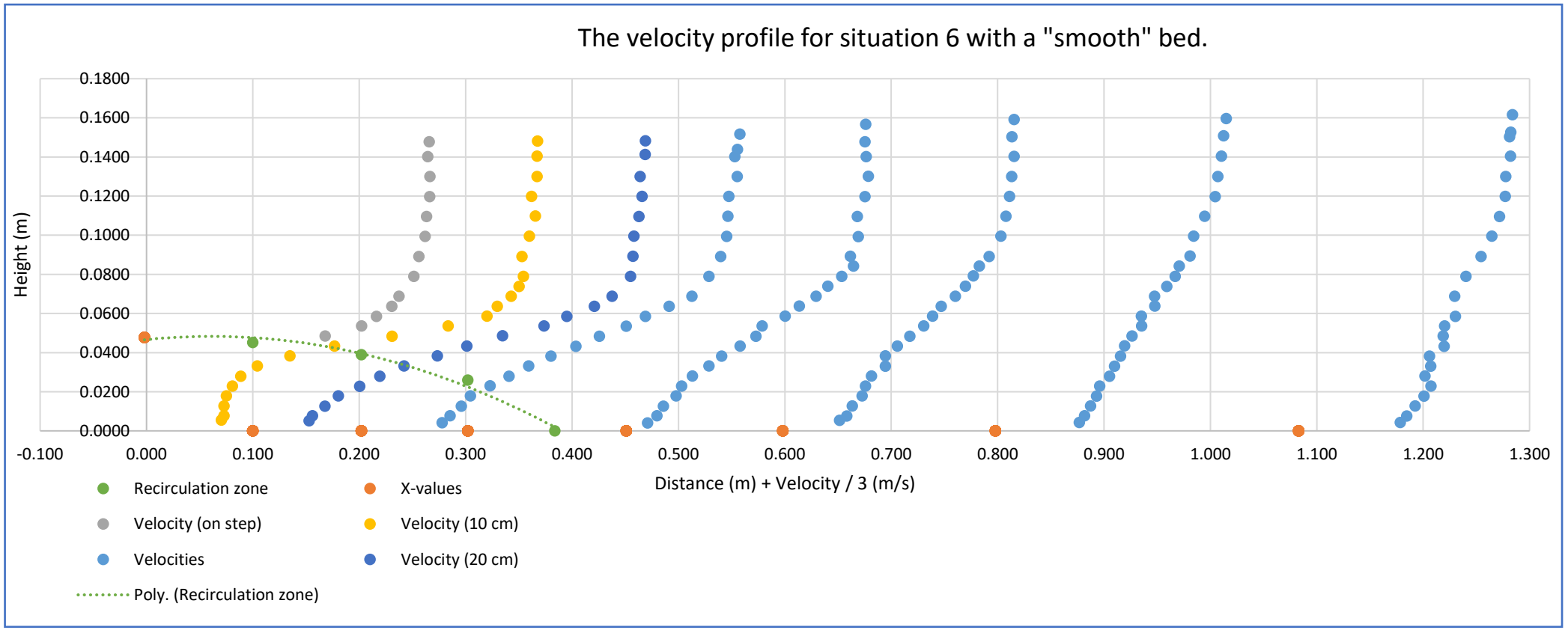

Figure F11: The velocity profile (for horizontal velocities) for the first metre of smooth situation 6.

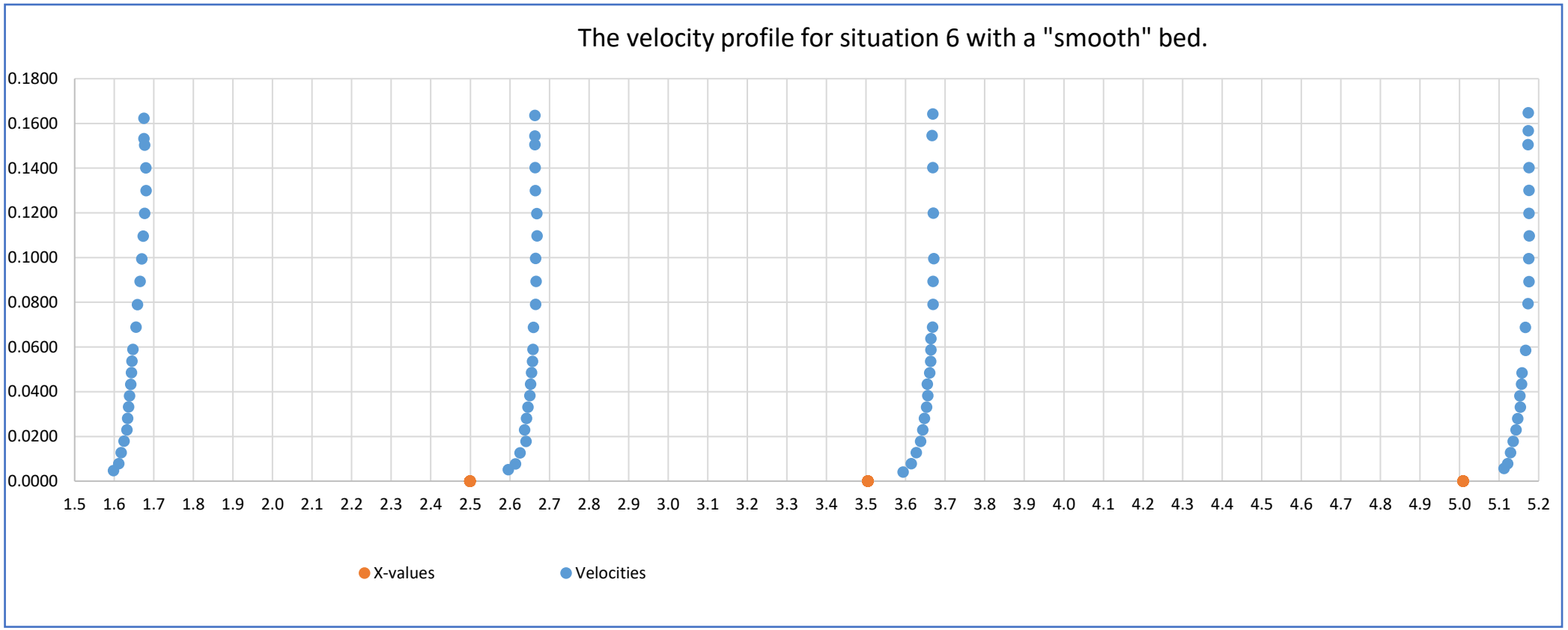

Figure F12: The velocity profile (for horizontal velocities) for the last four metres of smooth situation 6.

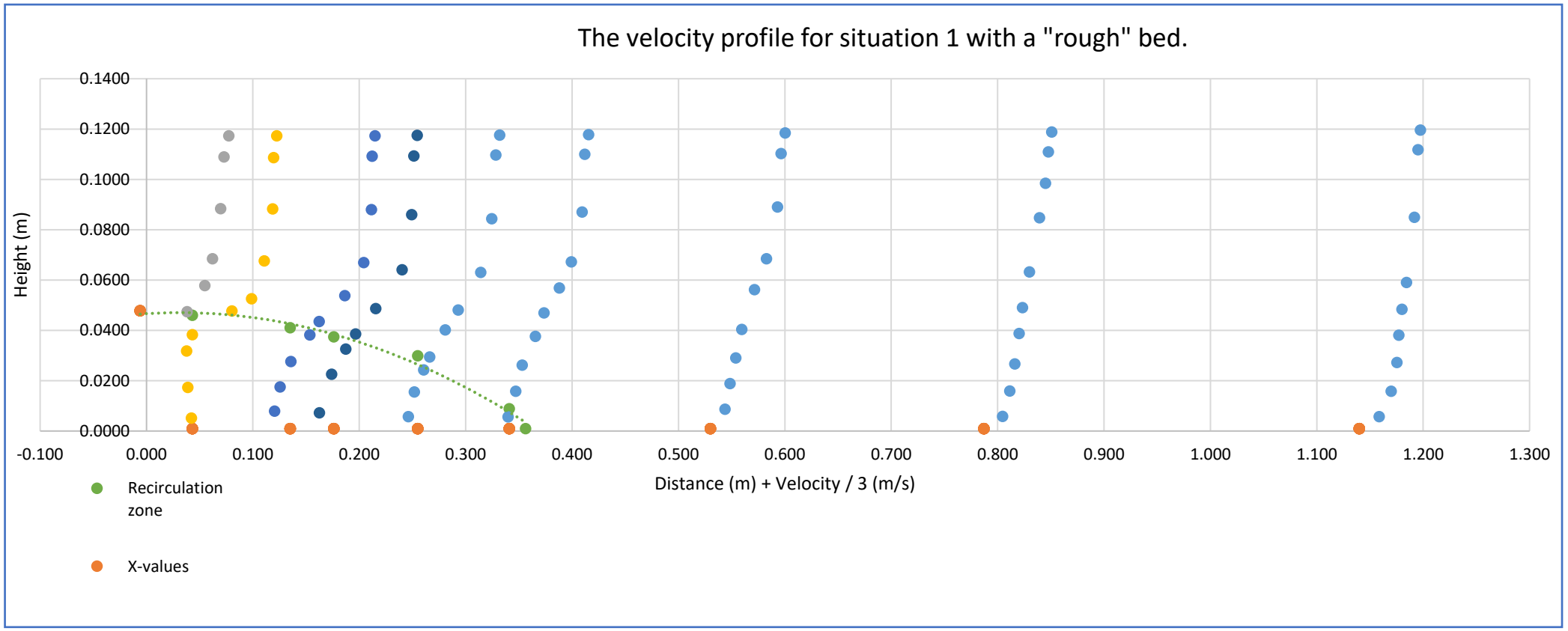

Figure F13: The velocity profile (for horizontal velocities) for the first metre of rough situation 1.

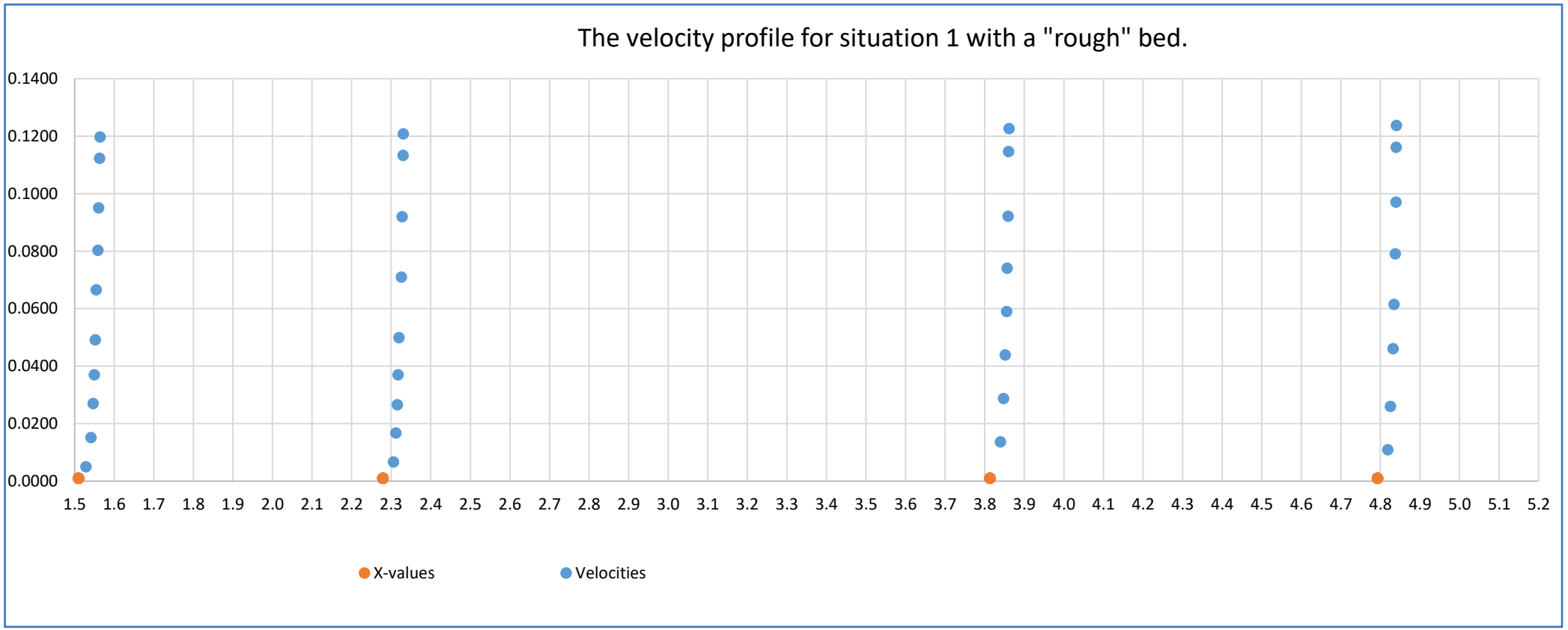

Figure F14: The velocity profile (for horizontal velocities) for the last four metres of rough situation 1.

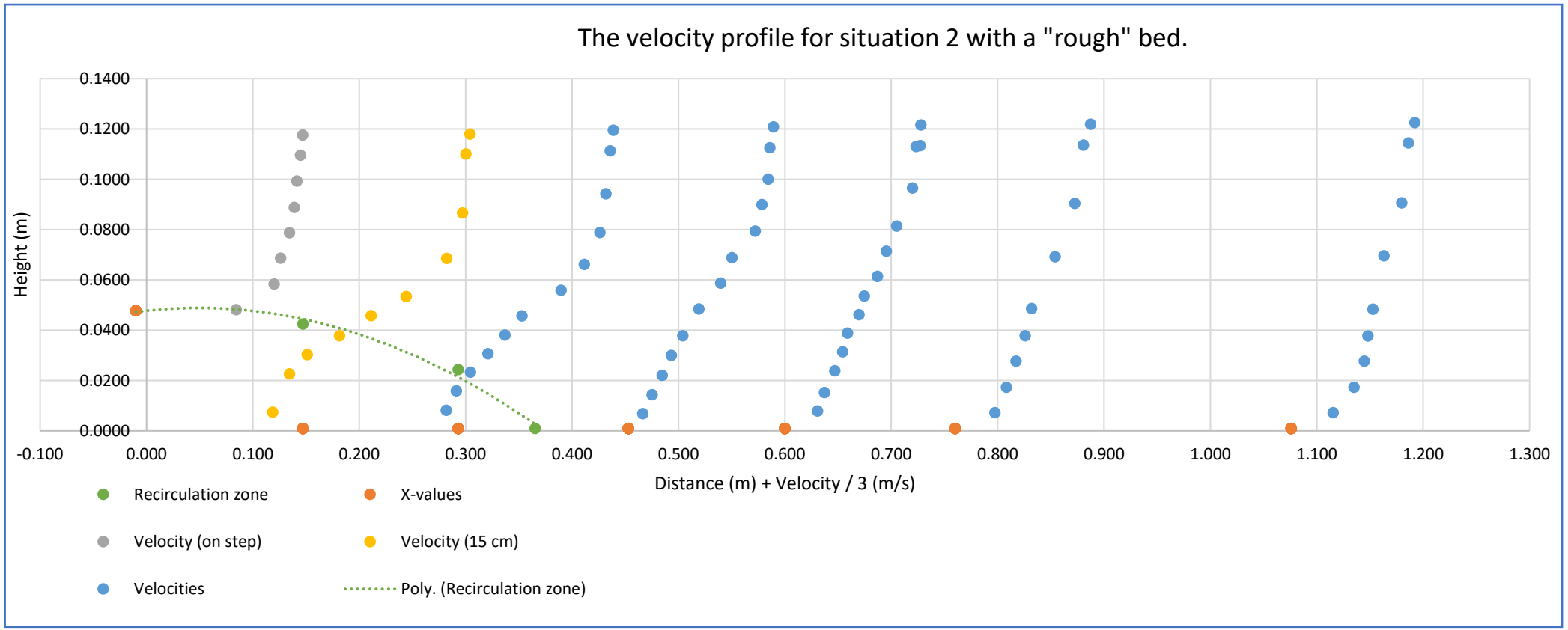

Figure F15: The velocity profile (for horizontal velocities) for the first metre of rough situation 2.

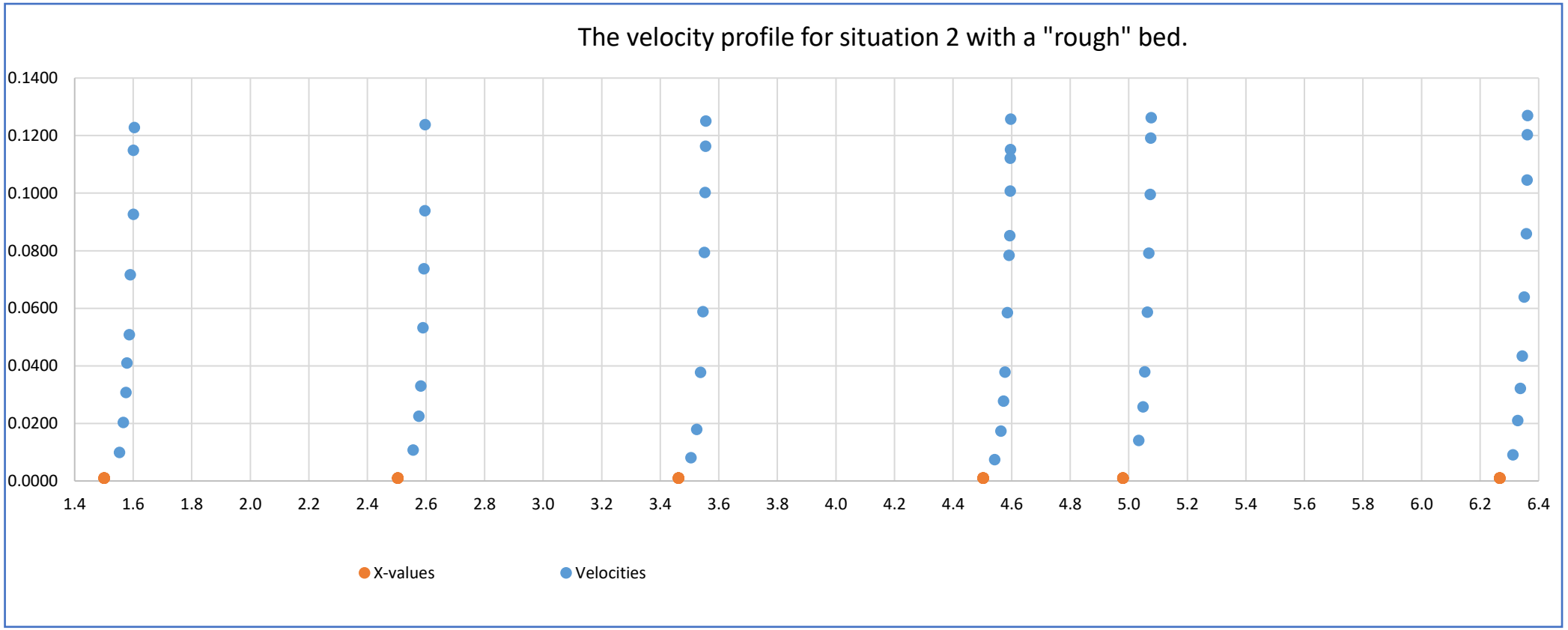

Figure F16: The velocity profile (for horizontal velocities) for the last five metres of smooth situation 2.

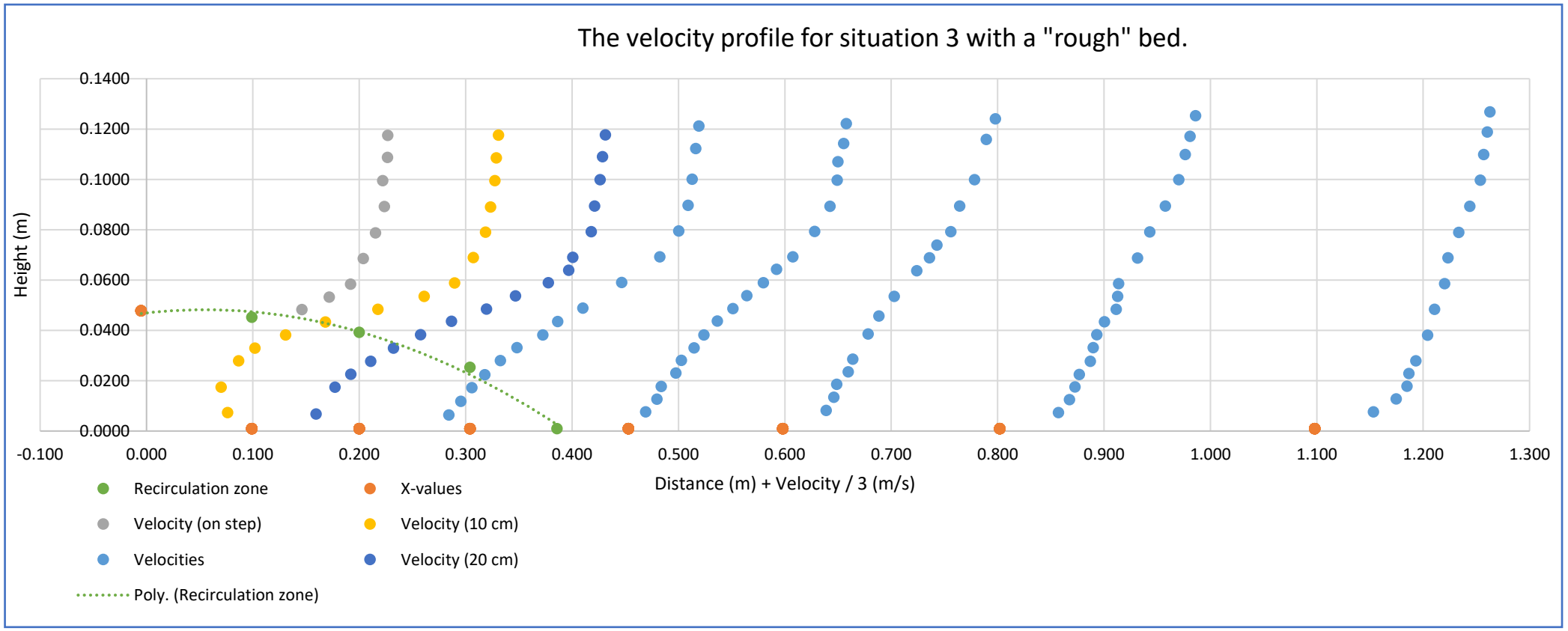

Figure F17: The velocity profile (for horizontal velocities) for the first metre of rough situation 3.

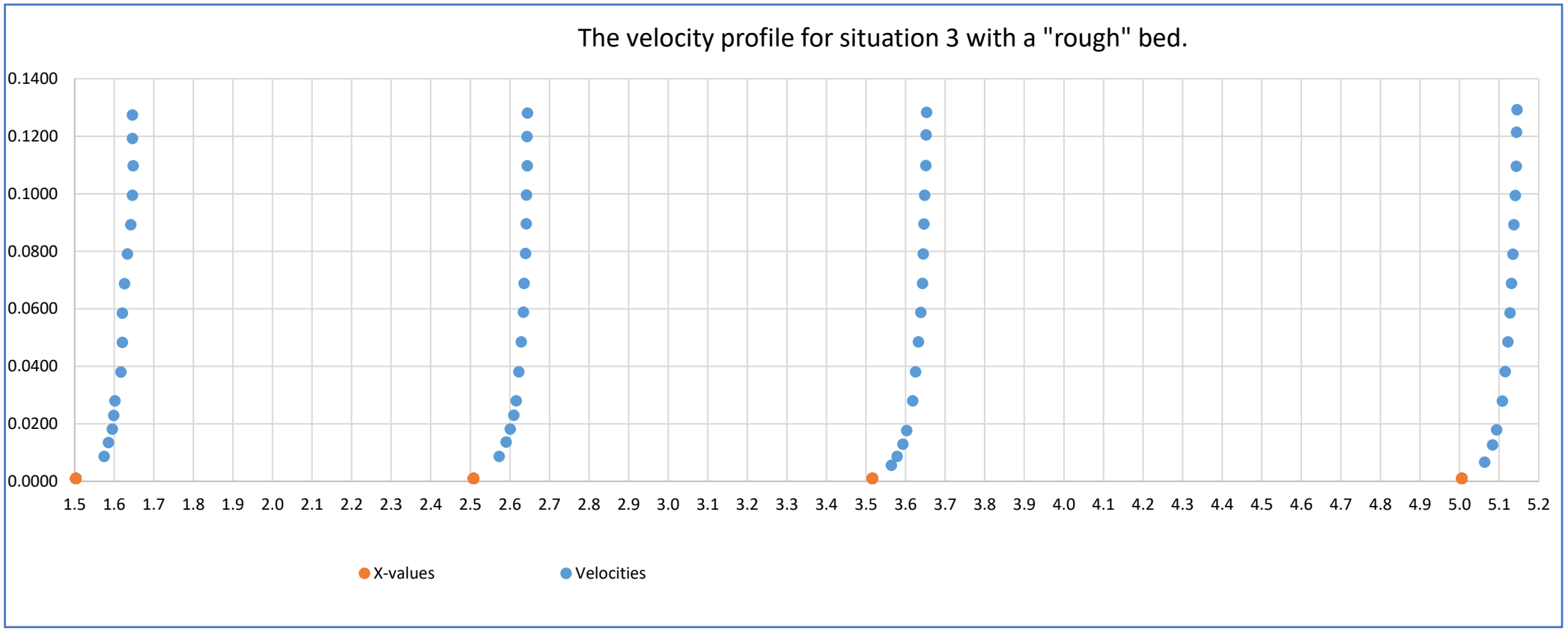

Figure F18: The velocity profile (for horizontal velocities) for the last four metres of rough situation 3.

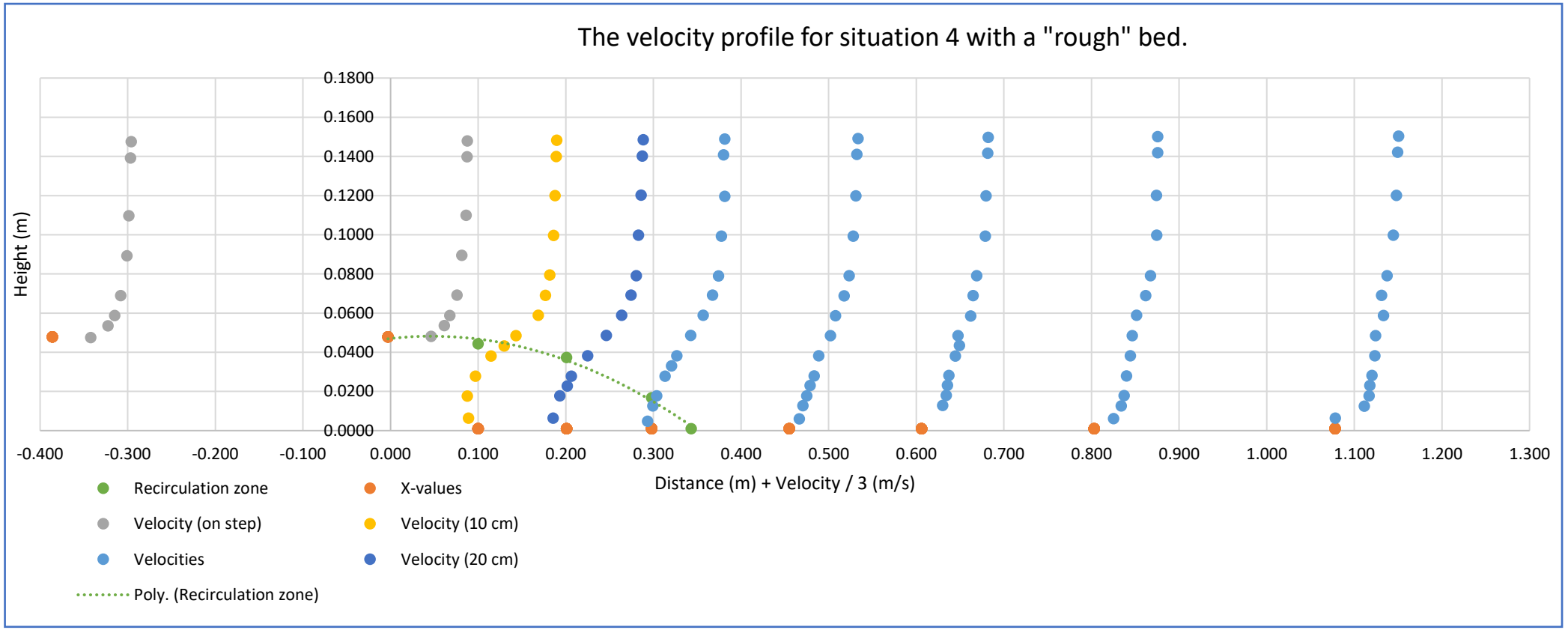

Figure F19: The velocity profile (for horizontal velocities) for the first metre of rough situation 4.

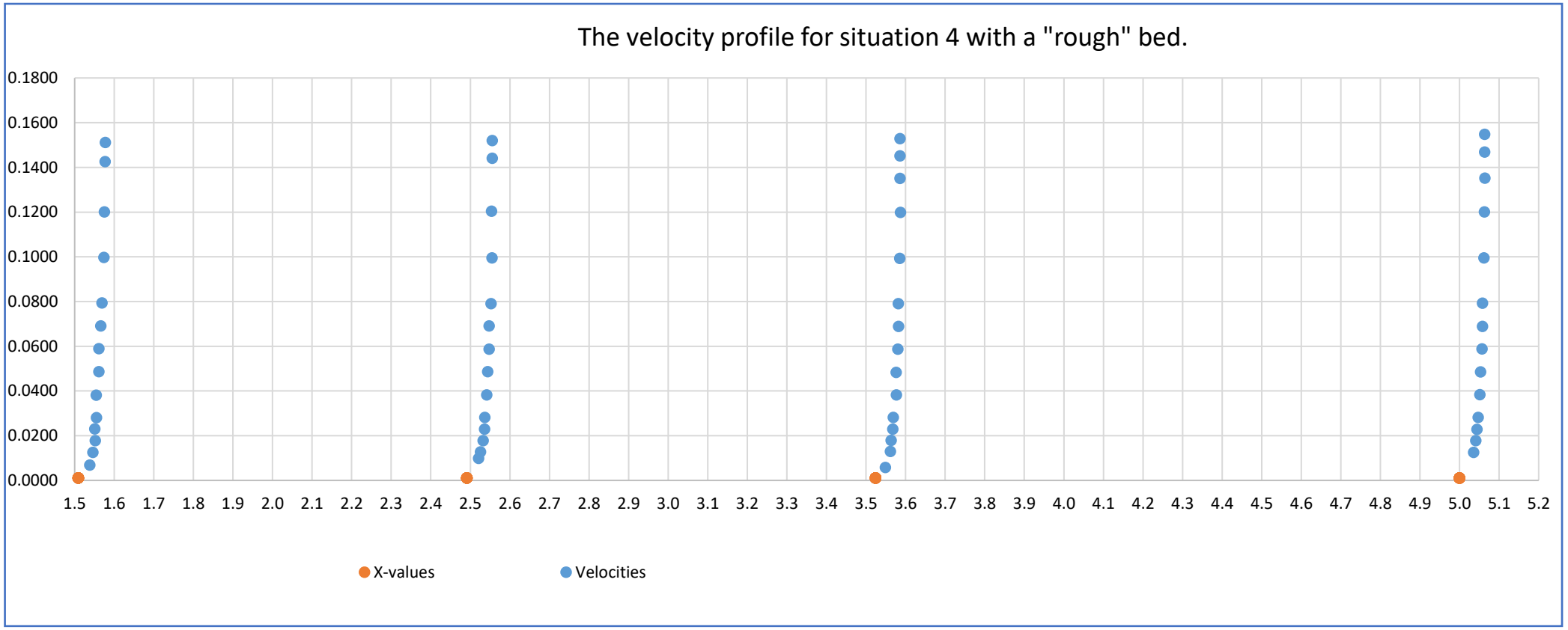

Figure F20: The velocity profile (for horizontal velocities) for the last four metres of rough situation 4.

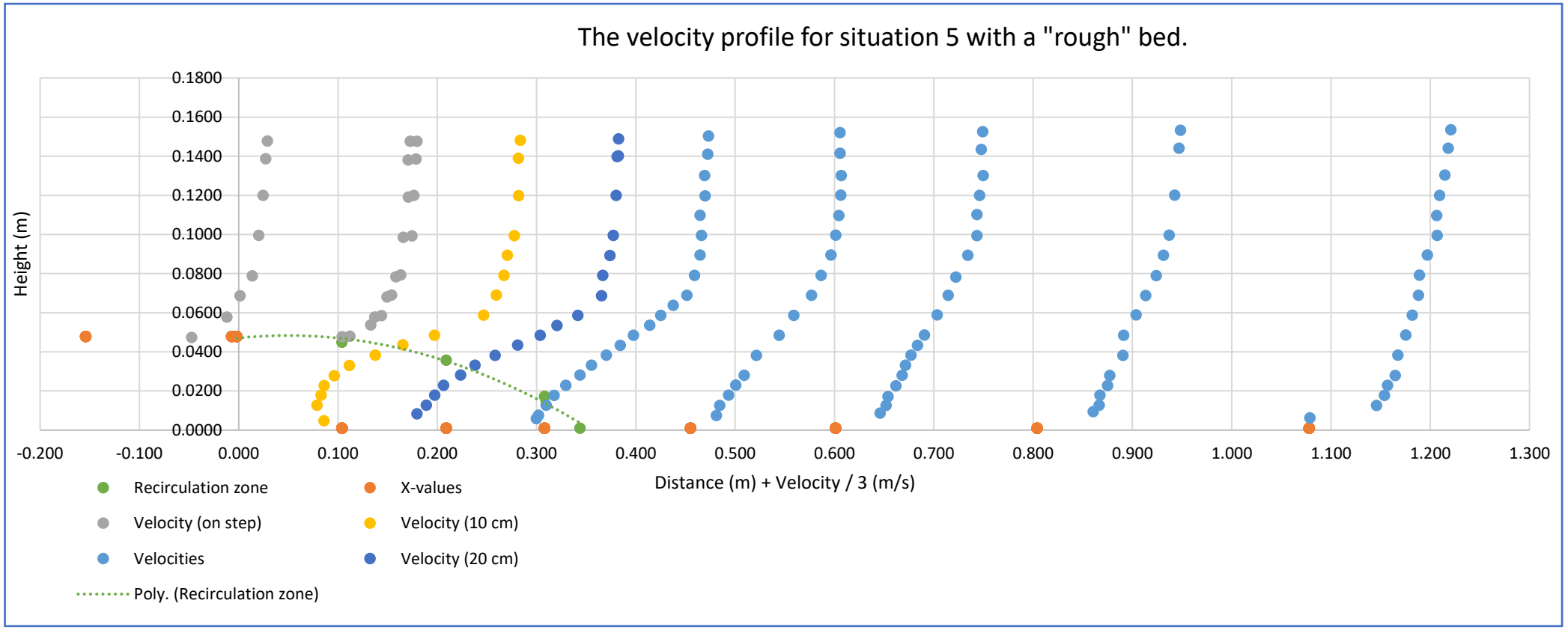

Figure F21: The velocity profile (for horizontal velocities) for the first metre of rough situation 5.

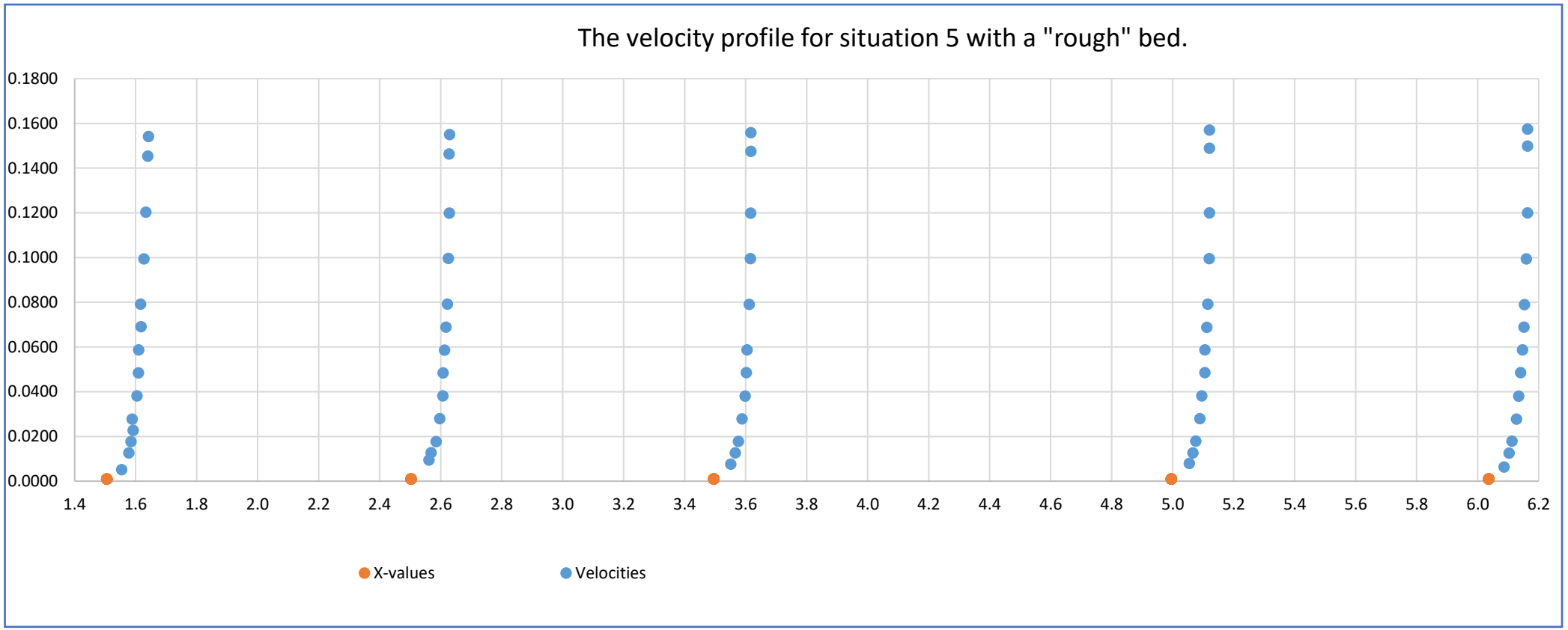

Figure F22: The velocity profile (for horizontal velocities) for the last five metres of rough situation 5.

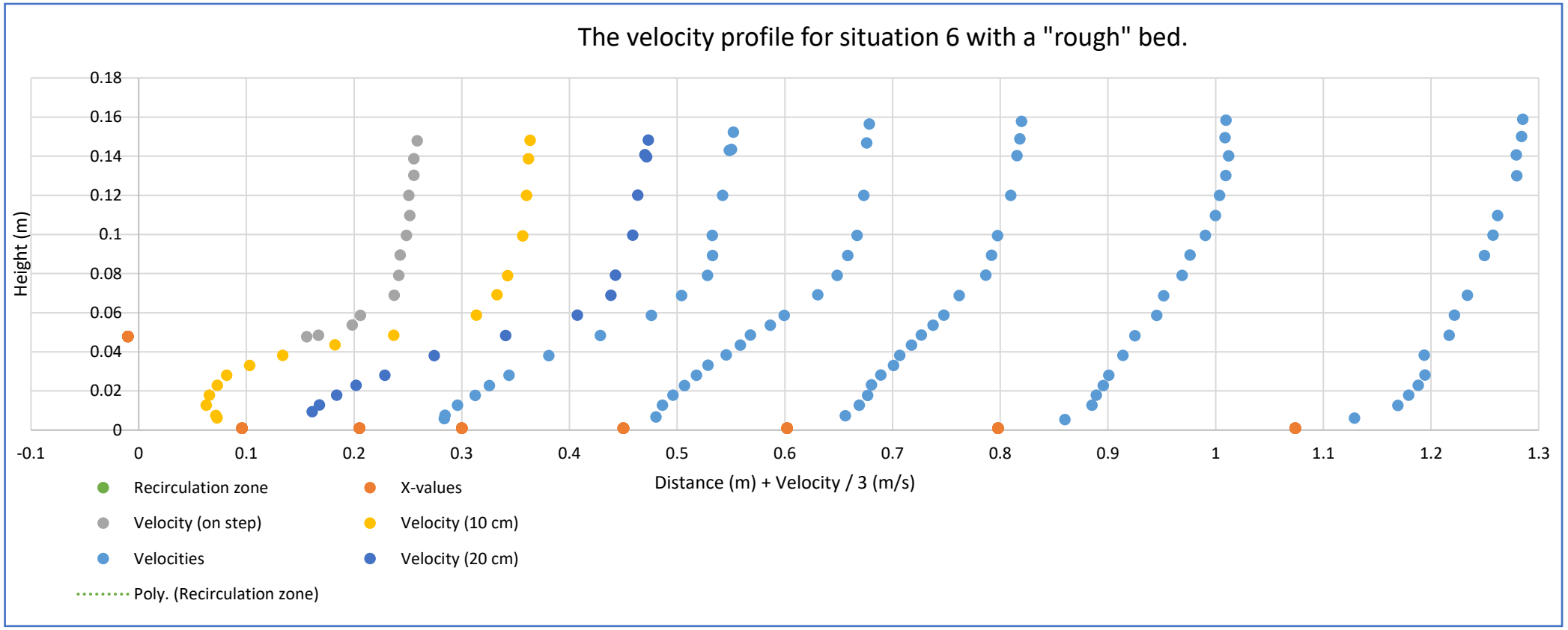

Figure F23: The velocity profile (for horizontal velocities) for the first metre of rough situation 6.

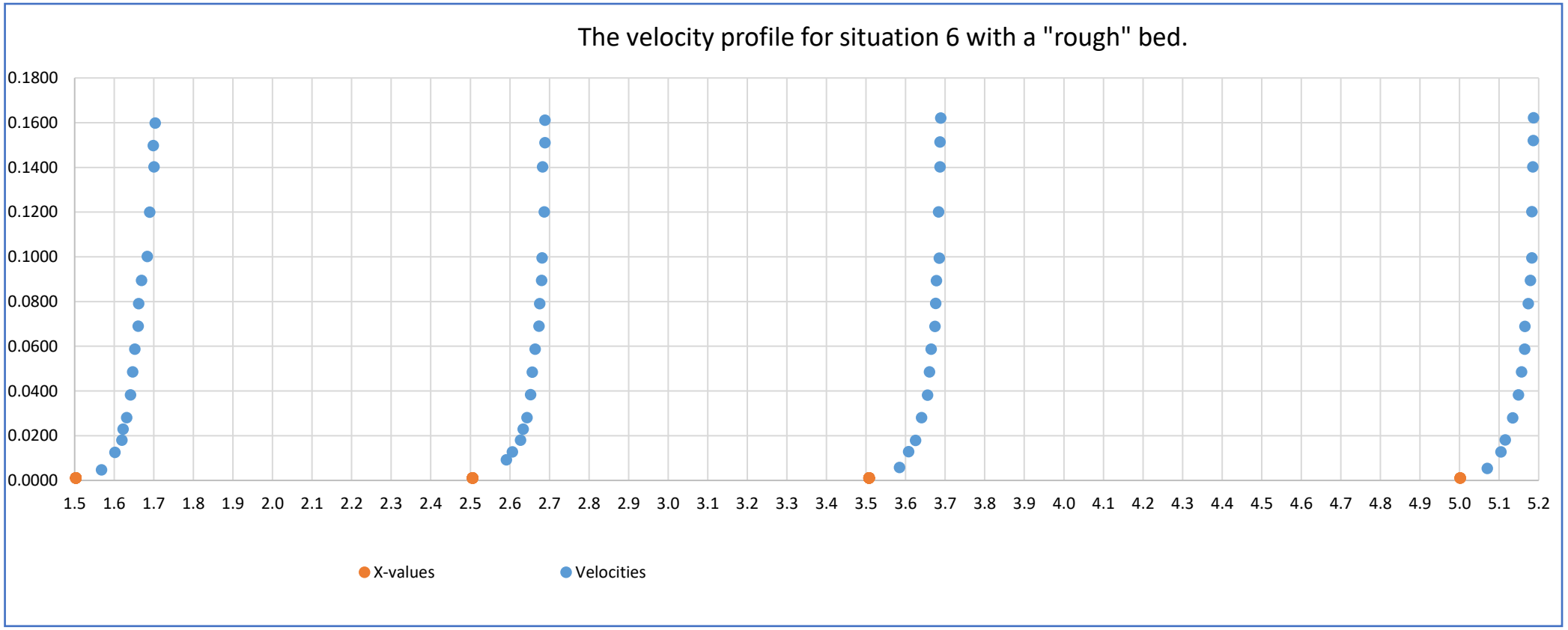

Figure F24: The velocity profile (for horizontal velocities) for the last four metres of rough situation 6.

Appendix G: Calculated discharges versus set discharges

In this Appendix, the discharges calculated from the measurement data will be compared with the discharges that were measured from the Rehbock weir. From this the accuracy of the measurements can be shown.

Bed type	Water depth on step (m)	Froude number on step (-)	x m	q calculated m^2/s	q Rehbock m^2/s	Difference %	Within "10%"	Within "5%"	Within "1%"
Smooth	0.07	0.25	-0.006	0.0146	0.0145	0.8240	Yes	Yes	Yes
Smooth	0.07	0.25	0.101	0.0151	0.0145	4.2769	Yes	Yes	No
Smooth	0.07	0.25	0.198	0.0149	0.0145	2.8958	Yes	Yes	No
Smooth	0.07	0.25	0.300	0.0151	0.0145	4.2769	Yes	Yes	No
Smooth	0.07	0.25	0.450	0.0151	0.0145	4.2769	Yes	Yes	No
Smooth	0.07	0.25	0.602	0.0150	0.0145	3.5863	Yes	Yes	No
Smooth	0.07	0.25	0.800	0.0149	0.0145	2.8958	Yes	Yes	No
Smooth	0.07	0.25	1.073	0.0150	0.0145	3.5863	Yes	Yes	No
Smooth	0.07	0.25	1.505	0.0148	0.0145	2.2052	Yes	Yes	No
Smooth	0.07	0.25	2.504	0.0146	0.0145	0.8240	Yes	Yes	Yes
Smooth	0.07	0.25	3.503	0.0146	0.0145	0.8240	Yes	Yes	Yes
Smooth	0.07	0.25	5.009	0.0144	0.0145	-0.5571	Yes	Yes	Yes
Smooth	0.07	0.50	-0.005	0.0298	0.0291	2.3613	Yes	Yes	No
Smooth	0.07	0.50	0.104	0.0303	0.0291	4.0788	Yes	Yes	No
Smooth	0.07	0.50	0.202	0.0311	0.0291	6.8267	Yes	No	No
Smooth	0.07	0.50	0.301	0.0304	0.0291	4.4223	Yes	Yes	No
Smooth	0.07	0.50	0.443	0.0298	0.0291	2.3613	Yes	Yes	No
Smooth	0.07	0.50	0.608	0.0302	0.0291	3.7353	Yes	Yes	No
Smooth	0.07	0.50	0.796	0.0300	0.0291	3.0483	Yes	Yes	No

Smooth	0.07	0.50	1.123	0.0302	0.0291	3.7353	Yes	Yes	No
Smooth	0.07	0.50	1.507	0.0298	0.0291	2.3613	Yes	Yes	No
Smooth	0.07	0.50	2.504	0.0295	0.0291	1.3308	Yes	Yes	No
Smooth	0.07	0.50	3.506	0.0293	0.0291	0.6438	Yes	Yes	Yes
Smooth	0.07	0.50	4.997	0.0291	0.0291	-0.0432	Yes	Yes	Yes
Smooth	0.07	0.75	-0.004	0.0431	0.0433	-0.5712	Yes	Yes	Yes
Smooth	0.07	0.75	0.103	0.0441	0.0433	1.7358	Yes	Yes	No
Smooth	0.07	0.75	0.204	0.0445	0.0433	2.6585	Yes	Yes	No
Smooth	0.07	0.75	0.303	0.0439	0.0433	1.2744	Yes	Yes	No
Smooth	0.07	0.75	0.454	0.0432	0.0433	-0.3405	Yes	Yes	Yes
Smooth	0.07	0.75	0.601	0.0431	0.0433	-0.5712	Yes	Yes	Yes
Smooth	0.07	0.75	0.803	0.0435	0.0433	0.3516	Yes	Yes	Yes
Smooth	0.07	0.75	1.081	0.0440	0.0433	1.5051	Yes	Yes	No
Smooth	0.07	0.75	1.504	0.0437	0.0433	0.8130	Yes	Yes	Yes
Smooth	0.07	0.75	2.500	0.0435	0.0433	0.3516	Yes	Yes	Yes
Smooth	0.07	0.75	3.504	0.0432	0.0433	-0.3405	Yes	Yes	Yes
Smooth	0.07	0.75	5.002	0.0429	0.0433	-1.0325	Yes	Yes	No
Smooth	0.10	0.25	-0.008	0.0250	0.0248	0.9515	Yes	Yes	Yes
Smooth	0.10	0.25	0.093	0.0248	0.0248	0.1439	Yes	Yes	Yes
Smooth	0.10	0.25	0.196	0.0251	0.0248	1.3553	Yes	Yes	No
Smooth	0.10	0.25	0.301	0.0247	0.0248	-0.2599	Yes	Yes	Yes
Smooth	0.10	0.25	0.441	0.0246	0.0248	-0.6637	Yes	Yes	Yes
Smooth	0.10	0.25	0.592	0.0244	0.0248	-1.4713	Yes	Yes	No
Smooth	0.10	0.25	0.793	0.0247	0.0248	-0.2599	Yes	Yes	Yes
Smooth	0.10	0.25	1.082	0.0245	0.0248	-1.0675	Yes	Yes	No
Smooth	0.10	0.25	1.502	0.0249	0.0248	0.5477	Yes	Yes	Yes
Smooth	0.10	0.25	2.502	0.0249	0.0248	0.5477	Yes	Yes	Yes

Smooth	0.10	0.25	3.498	0.0246	0.0248	-0.6637	Yes	Yes	Yes
Smooth	0.10	0.25	5.001	0.0247	0.0248	-0.2599	Yes	Yes	Yes
Smooth	0.10	0.50	-0.006	0.0500	0.0495	1.1021	Yes	Yes	No
Smooth	0.10	0.50	0.193	0.0511	0.0495	3.3264	Yes	Yes	No
Smooth	0.10	0.50	0.305	0.0509	0.0495	2.9220	Yes	Yes	No
Smooth	0.10	0.50	0.453	0.0498	0.0495	0.6977	Yes	Yes	Yes
Smooth	0.10	0.50	0.594	0.0499	0.0495	0.8999	Yes	Yes	Yes
Smooth	0.10	0.50	0.808	0.0498	0.0495	0.6977	Yes	Yes	Yes
Smooth	0.10	0.50	1.073	0.0499	0.0495	0.8999	Yes	Yes	Yes
Smooth	0.10	0.50	1.496	0.0502	0.0495	1.5065	Yes	Yes	No
Smooth	0.10	0.50	2.494	0.0500	0.0495	1.1021	Yes	Yes	No
Smooth	0.10	0.50	3.500	0.0499	0.0495	0.8999	Yes	Yes	Yes
Smooth	0.10	0.50	5.020	0.0503	0.0495	1.7087	Yes	Yes	No
Smooth	0.10	0.75	-0.002	0.0752	0.0744	1.1117	Yes	Yes	No
Smooth	0.10	0.75	0.100	0.0756	0.0744	1.6495	Yes	Yes	No
Smooth	0.10	0.75	0.202	0.0763	0.0744	2.5907	Yes	Yes	No
Smooth	0.10	0.75	0.302	0.0756	0.0744	1.6495	Yes	Yes	No
Smooth	0.10	0.75	0.451	0.0748	0.0744	0.5738	Yes	Yes	Yes
Smooth	0.10	0.75	0.598	0.0749	0.0744	0.7083	Yes	Yes	Yes
Smooth	0.10	0.75	0.798	0.0756	0.0744	1.6495	Yes	Yes	No
Smooth	0.10	0.75	1.083	0.0760	0.0744	2.1873	Yes	Yes	No
Smooth	0.10	0.75	1.497	0.0757	0.0744	1.7840	Yes	Yes	No
Smooth	0.10	0.75	2.499	0.0751	0.0744	0.9772	Yes	Yes	Yes
Smooth	0.10	0.75	3.505	0.0750	0.0744	0.8428	Yes	Yes	Yes
Smooth	0.10	0.75	5.009	0.0744	0.0744	0.0360	Yes	Yes	Yes
Rough	0.07	0.25	-0.006	0.0148	0.0145	1.7889	Yes	Yes	No
Rough	0.07	0.25	0.043	0.0148	0.0145	1.7889	Yes	Yes	No

Rough	0.07	0.25	0.135	0.0152	0.0145	4.5400	Yes	Yes	No
Rough	0.07	0.25	0.176	0.0150	0.0145	3.1645	Yes	Yes	No
Rough	0.07	0.25	0.255	0.0149	0.0145	2.4767	Yes	Yes	No
Rough	0.07	0.25	0.341	0.0149	0.0145	2.4767	Yes	Yes	No
Rough	0.07	0.25	0.530	0.0149	0.0145	2.4767	Yes	Yes	No
Rough	0.07	0.25	0.787	0.0145	0.0145	-0.2743	Yes	Yes	Yes
Rough	0.07	0.25	1.140	0.0149	0.0145	2.4767	Yes	Yes	No
Rough	0.07	0.25	1.510	0.0149	0.0145	2.4767	Yes	Yes	No
Rough	0.07	0.25	2.279	0.0148	0.0145	1.7889	Yes	Yes	No
Rough	0.07	0.25	3.813	0.0136	0.0145	-6.4642	Yes	No	No
Rough	0.07	0.25	4.793	0.0138	0.0145	-5.0887	Yes	No	No
Rough	0.07	0.50	-0.010	0.0294	0.0291	0.9873	Yes	Yes	Yes
Rough	0.07	0.50	0.147	0.0298	0.0291	2.3613	Yes	Yes	No
Rough	0.07	0.50	0.293	0.0299	0.0291	2.7048	Yes	Yes	No
Rough	0.07	0.50	0.453	0.0294	0.0291	0.9873	Yes	Yes	Yes
Rough	0.07	0.50	0.600	0.0293	0.0291	0.6438	Yes	Yes	Yes
Rough	0.07	0.50	0.760	0.0299	0.0291	2.7048	Yes	Yes	No
Rough	0.07	0.50	1.076	0.0296	0.0291	1.6743	Yes	Yes	No
Rough	0.07	0.50	1.501	0.0292	0.0291	0.3003	Yes	Yes	Yes
Rough	0.07	0.50	2.504	0.0287	0.0291	-1.4171	Yes	Yes	No
Rough	0.07	0.50	3.462	0.0285	0.0291	-2.1041	Yes	Yes	No
Rough	0.07	0.50	4.503	0.0287	0.0291	-1.4171	Yes	Yes	No
Rough	0.07	0.50	4.980	0.0281	0.0291	-3.4781	Yes	Yes	No
Rough	0.07	0.50	6.267	0.0288	0.0291	-1.0736	Yes	Yes	No
Rough	0.07	0.75	-0.005	0.0446	0.0436	2.2684	Yes	Yes	No
Rough	0.07	0.75	0.099	0.0447	0.0436	2.4977	Yes	Yes	No
Rough	0.07	0.75	0.200	0.0454	0.0436	4.1028	Yes	Yes	No

Rough	0.07	0.75	0.304	0.0449	0.0436	2.9563	Yes	Yes	No
Rough	0.07	0.75	0.453	0.0442	0.0436	1.3512	Yes	Yes	No
Rough	0.07	0.75	0.598	0.0438	0.0436	0.4340	Yes	Yes	Yes
Rough	0.07	0.75	0.802	0.0445	0.0436	2.0391	Yes	Yes	No
Rough	0.07	0.75	1.098	0.0449	0.0436	2.9563	Yes	Yes	No
Rough	0.07	0.75	1.503	0.0436	0.0436	-0.0246	Yes	Yes	Yes
Rough	0.07	0.75	2.508	0.0437	0.0436	0.2047	Yes	Yes	Yes
Rough	0.07	0.75	3.516	0.0433	0.0436	-0.7126	Yes	Yes	Yes
Rough	0.07	0.75	5.006	0.0438	0.0436	0.4340	Yes	Yes	Yes
Rough	0.10	0.25	-0.386	0.0246	0.0248	-0.9500	Yes	Yes	Yes
Rough	0.10	0.25	-0.003	0.0249	0.0248	0.2579	Yes	Yes	Yes
Rough	0.10	0.25	0.100	0.0248	0.0248	-0.1447	Yes	Yes	Yes
Rough	0.10	0.25	0.201	0.0246	0.0248	-0.9500	Yes	Yes	Yes
Rough	0.10	0.25	0.298	0.0249	0.0248	0.2579	Yes	Yes	Yes
Rough	0.10	0.25	0.455	0.0244	0.0248	-1.7553	Yes	Yes	No
Rough	0.10	0.25	0.606	0.0241	0.0248	-2.9632	Yes	Yes	No
Rough	0.10	0.25	0.803	0.0246	0.0248	-0.9500	Yes	Yes	Yes
Rough	0.10	0.25	1.078	0.0243	0.0248	-2.1579	Yes	Yes	No
Rough	0.10	0.25	1.509	0.0246	0.0248	-0.9500	Yes	Yes	Yes
Rough	0.10	0.25	2.491	0.0243	0.0248	-2.1579	Yes	Yes	No
Rough	0.10	0.25	3.524	0.0245	0.0248	-1.3527	Yes	Yes	No
Rough	0.10	0.25	5.000	0.0244	0.0248	-1.7553	Yes	Yes	No
Rough	0.10	0.50	-0.154	0.0501	0.0495	1.3043	Yes	Yes	No
Rough	0.10	0.50	-0.007	0.0497	0.0495	0.4955	Yes	Yes	Yes
Rough	0.10	0.50	-0.002	0.0500	0.0495	1.1021	Yes	Yes	No
Rough	0.10	0.50	0.104	0.0500	0.0495	1.1021	Yes	Yes	No
Rough	0.10	0.50	0.209	0.0506	0.0495	2.3153	Yes	Yes	No

Rough	0.10	0.50	0.308	0.0503	0.0495	1.7087	Yes	Yes	No
Rough	0.10	0.50	0.455	0.0491	0.0495	-0.7177	Yes	Yes	Yes
Rough	0.10	0.50	0.601	0.0491	0.0495	-0.7177	Yes	Yes	Yes
Rough	0.10	0.50	0.804	0.0486	0.0495	-1.7287	Yes	Yes	No
Rough	0.10	0.50	1.078	0.0487	0.0495	-1.5265	Yes	Yes	No
Rough	0.10	0.50	1.505	0.0495	0.0495	0.0911	Yes	Yes	Yes
Rough	0.10	0.50	2.503	0.0492	0.0495	-0.5155	Yes	Yes	Yes
Rough	0.10	0.50	3.495	0.0492	0.0495	-0.5155	Yes	Yes	Yes
Rough	0.10	0.50	4.996	0.0502	0.0495	1.5065	Yes	Yes	No
Rough	0.10	0.50	6.036	0.0507	0.0495	2.5175	Yes	Yes	No
Rough	0.10	0.75	-0.010	0.0750	0.0744	0.8428	Yes	Yes	Yes
Rough	0.10	0.75	0.096	0.0751	0.0744	0.9772	Yes	Yes	Yes
Rough	0.10	0.75	0.205	0.0759	0.0744	2.0529	Yes	Yes	No
Rough	0.10	0.75	0.300	0.0756	0.0744	1.6495	Yes	Yes	No
Rough	0.10	0.75	0.450	0.0746	0.0744	0.3049	Yes	Yes	Yes
Rough	0.10	0.75	0.602	0.0733	0.0744	-1.4430	Yes	Yes	No
Rough	0.10	0.75	0.798	0.0746	0.0744	0.3049	Yes	Yes	Yes
Rough	0.10	0.75	1.074	0.0748	0.0744	0.5738	Yes	Yes	Yes
Rough	0.10	0.75	1.503	0.0746	0.0744	0.3049	Yes	Yes	Yes
Rough	0.10	0.75	2.506	0.0741	0.0744	-0.3674	Yes	Yes	Yes
Rough	0.10	0.75	3.508	0.0749	0.0744	0.7083	Yes	Yes	Yes
Rough	0.10	0.75	5.002	0.0763	0.0744	2.5907	Yes	Yes	No

Table G1: The measured discharges.

Appendix H: Explanation about tilted flume

Introduction:

In Figure H1 the velocity profile for situation 3 with a rough bed is given in the first metre behind the step. It can be noticed that the velocity on top of the step can be described with a logarithmic profile. This is not the case for the other situations. Figure H2 gives for the same situation the velocity profile for the other locations. Further downstream the velocity profile looks almost logarithmic again.

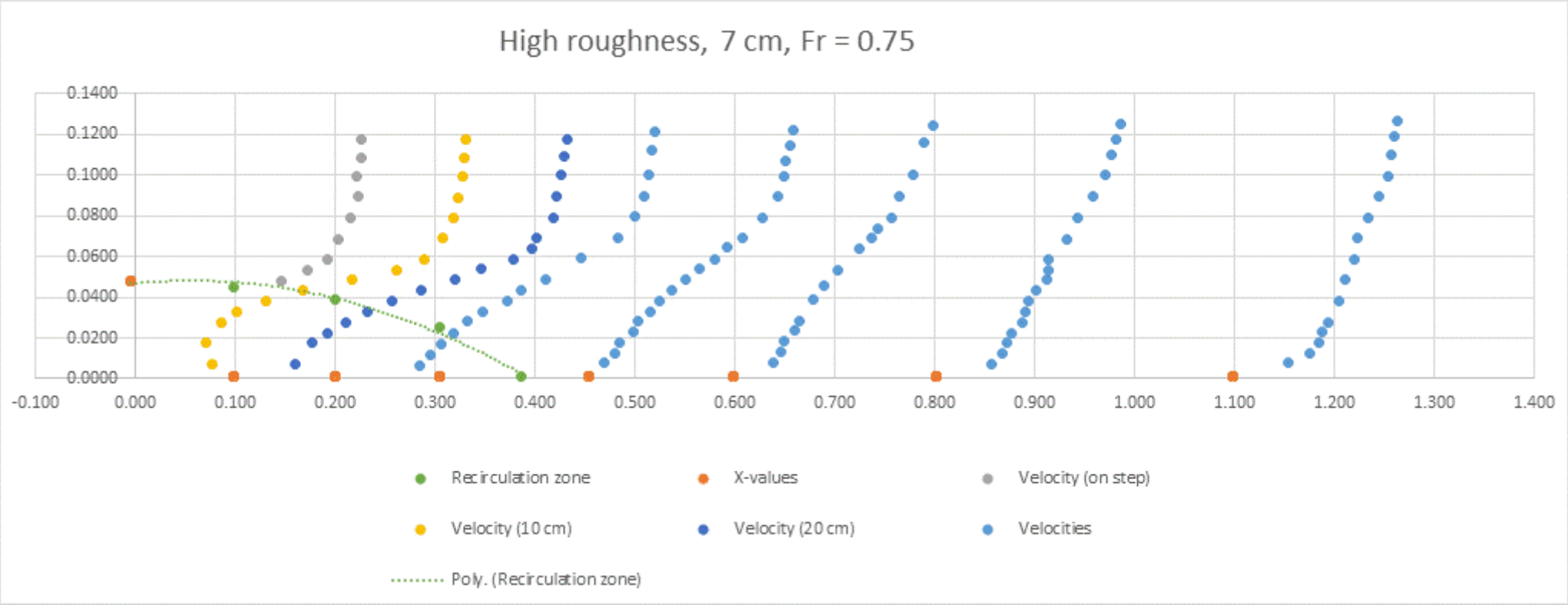

Figure H1: The velocity profile for the first metre of situation 3 with a rough bed.

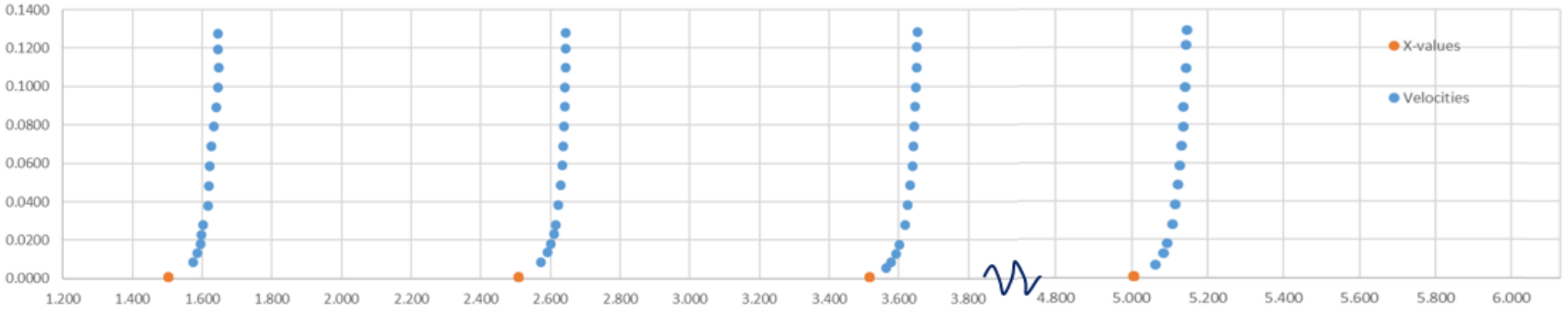

Figure H2: The velocity profile for the last 4 metres of situation 3 with a rough bed.

As explained in Chapters 2 and 5, the head levels can be calculated with the formula

$H = y_b + h_b + \alpha \frac{U^2}{2g}$, in which:

H = head level with respect to the bed

h_b = the water level with respect to the bed

y_b = the height of the bed (which is 0 in case of a horizontal bed)

α = a correction factor for the kinetic energy, determined from the measurements

U = the depth and temporal averaged velocity.

In Figure H3 the calculated head levels for situation 3 with a rough bed are given.

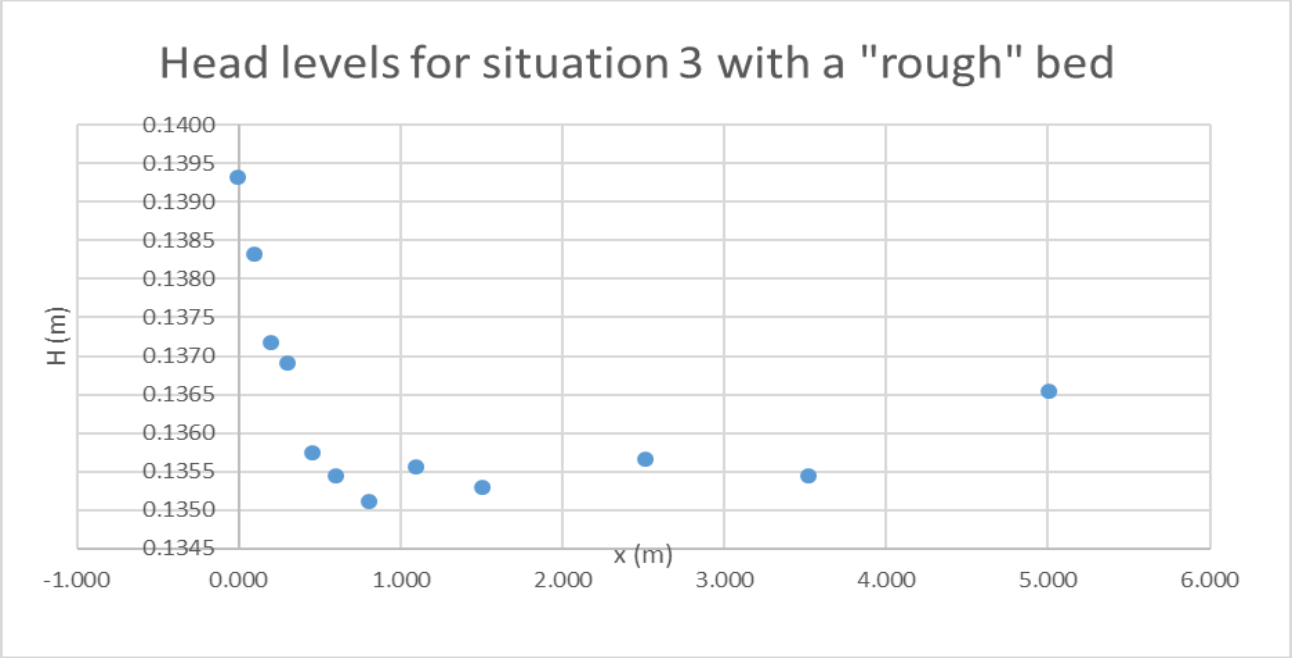

Figure H3: The head levels for situation 3 with a rough bed.

Problem definition:

As can be seen from Figure H3 the head levels increase further downstream of the step. This is however physically impossible, since energy can only be transformed instead of created or destroyed. In the flume, no energy is added to the flow, which means that the total energy cannot grow. A small decrease of the energy head is expected, since the bottom friction transforms a small part of the flow energy into heat.

This above mentioned unexpected result is the strongest for the situations with the lowest Froude-numbers. This can be explained by the fact that in those situations the flow velocity is lowest and also the related bed friction is lower.
For situations with a higher Froude number a decrease in head level is visible in the first metre behind the step, followed by an increase in head level.

Hypothesis:

The reason for the increase in head level with respect to the bed is that the increase of water depth is not compensated by a decrease in velocity head, even when the decreasing value of α is taken into account. Since the total energy level cannot increase, the conclusion can be drawn that the bed is not a good reference level for the head level.
Since any horizontal level could be a good reference level for the energy head, this means that the bed, and thus the flume, is not horizontal, but tilted in streamwise direction (meaning that $\frac{dy_b}{dx} < 0$).

Approach for proving this hypothesis to be true:

In all twelve situations two locations were chosen:

Location 1: Located at ± 45 cm downstream from the step (just behind the reattachment point)
Location 2: Located at 5 à 6 metres downstream from the step (the last measurement location)

At both locations, the discharge is equal and the water depth is known. As a first approach, the velocity is calculated as $u = \frac{q}{d}$ The head level is then calculated as $H = y_b + d + \alpha \frac{q^2}{2g\,d^2}$, with y_b=0 at both locations.

With the help of the formulae of Nikuradse and Colebrook the roughness coefficient c_f and the expected decrease of the head level can be calculated. The formulae below are taken from Battjes & Labeur (2009):

$$\boxed{\frac{1}{\sqrt{c_f}} = \frac{1}{\kappa} \ln \frac{12R}{k + \delta/3,5}.}$$

$$i_w = c_f \frac{U^2}{gd},$$ Hierin is $\delta = 11,6\nu/u_\star$ en $u_\star = \sqrt{c_f}U$

The total energy loss due to friction can then be calculated by multiplying i_w with the length between the two locations. The expected value of H_2 is then the value of H_1 minus the absolute value of this energy loss.
The difference between the expected and the measured value of H_2 is then the expected lowering of the bed, called dz. By dividing dz over this distance the bed gradient $\frac{dz}{dx}$ can be calculated.

$$dz = H_{2,measurement} - H_{2,expected} = H_{2,measurement} - H_1 - \Delta H$$

For the calculations of both H_1 and $H_{2,measurement}$ the measured values of α were used. Simplifying the calculation by using α=1, would lead to an underestimation of the value of H_1 and therefore an overestimation of dz.

Results:

For each of the twelve experiments de head level at the first location was calculated with the data from the measurements.
At the second location the head level was calculated in three different ways:

- Directly following from the measurements (hence the head level with respect to the bed)
- Friction is absent and therefore the head level is equal to that at the first location
- The head level decreases as a result of the expected friction

These scenarios are shown in Figure H4.

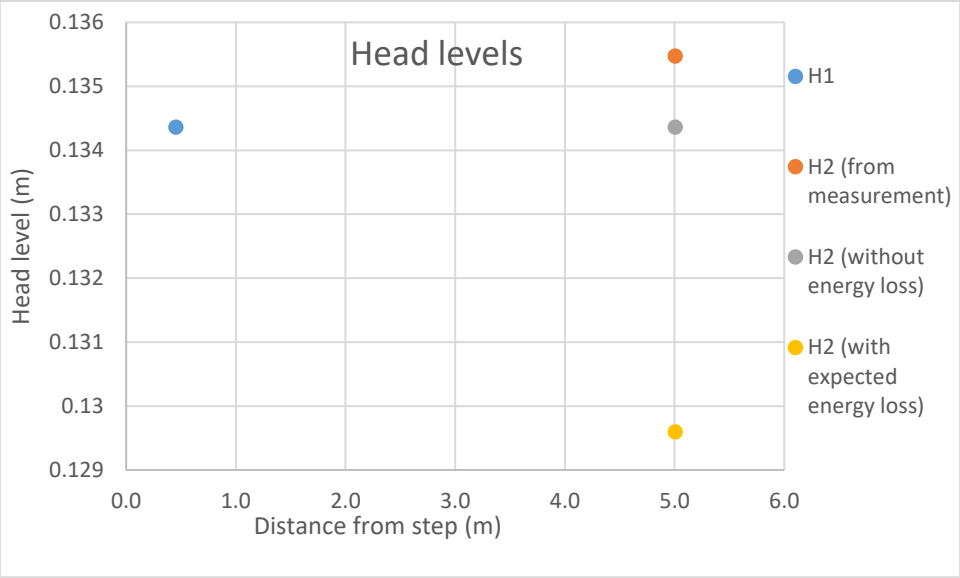

Figure H4: The head levels at two locations for situation 3 with a rough bed.

The case without energy loss will not be further elaborated, since a higher Froude number leads to more friction and a higher (expected) energy loss, which means that $\frac{dy_b}{dx}$ would be different between the experiments. It is however expected that $\frac{dy_b}{dx}$ should be the same in every situation, since the flume was not adjusted during or between experiments.

For all the situations with a rough bed, the expected head loss, the corresponding head level and the lowering of the bed are given in Table H1.

Water depth on step (cm)	Froude number on step	Change in water depth	H_1	H_2 (measured)	ΔH (because of friction)	H_2 (expected) (=H_1+ ΔH)	dy_b	dx	dy_b/dx
(cm)	(-)	(m)	(m)	(m)	(m)	(m)	(m)	(m)	(-)
7	0.25	0.005	0.1188	0.1237	-0.0006	0.1182	-0.0055	4.263	$-1.3*10^{-3}$
7	0.50	0.006	0.1256	0.1295	-0.0029	0.1227	-0.0068	5.814	$-1.2*10^{-3}$
7	0.75	0.007	0.1344	0.1355	-0.0048	0.1296	-0.0059	4.553	$-1.3*10^{-3}$
10	0.25	0.006	0.1503	0.1555	-0.0009	0.1495	-0.0060	4.545	$-1.3*10^{-3}$
10	0.50	0.006	0.1596	0.1626	-0.0039	0.1557	-0.0069	5.581	$-1.2*10^{-3}$
10	0.75	0.006	0.1741	0.1738	-0.0065	0.1676	-0.0062	4.552	$-1.4*10^{-3}$

Table H1: The expected head loss, head levels and bed gradient for all situations with a rough bed.

In Table H2 the same results are given for the situations with a smoother bed.

Water depth on step (cm)	Froude number on step	Change in water depth	H_1	H_2 (measured)	ΔH (because of friction)	H_2 (expected) (=H_1+ ΔH)	dy_b	dx	dy_b/dx
(cm)	(-)	(m)	(m)	(m)	(m)	(m)	(m)	(m)	(-)
7	0.25	0.006	0.1206	0.1261	-0.0003	0.1202	-0.0058	4.559	$-1.3*10^{-3}$
7	0.50	0.006	0.1259	0.1299	-0.0013	0.1246	-0.0053	4.554	$-1.2*10^{-3}$
7	0.75	0.009	0.1358	0.1381	-0.0025	0.1333	-0.0047	4.548	$-1.0*10^{-3}$
10	0.25	0.007	0.1507	0.1572	-0.0005	0.1502	-0.0071	4.560	$-1.5*10^{-3}$
10	0.50	0.007	0.1598	0.1640	-0.0018	0.1580	-0.0060	4.567	$-1.3*10^{-3}$
10	0.75	0.008	0.1752	0.1766	-0.0036	0.1716	-0.0050	4.558	$-1.1*10^{-3}$

Table H2: The expected head loss, head levels and bed gradient for all situations with a smooth bed.

From both table follows that the expected bed gradient is around $-1.3 * 10^{-3}$ for all situations. This means that the lowering of the bed is 1.3 mm per metre.
Tables H1 and H2 therefore support the expectation that $\frac{dy_b}{dx}$ is almost the same for all experiments.

Conclusion:

From the above analysis follows that it is very likely that the flume was indeed non-horizontal.

This means that the formula for the head level can be rewritten as $H(x) = \frac{dy_b}{dx} x + h_b + \alpha \frac{\overline{u}^2}{2g}$, in which $\frac{dy_b}{dx}$ = $-1.3*10^3$ and h is relative to the bed. Is this formula is used that y_b=0 at x=0, which is only used as a reference point. In Figure H5 the head levels with and without this extra term $\frac{dy_b}{dx}$ are shown to illustrate the effect of adding this correction factor for the sloping bed.

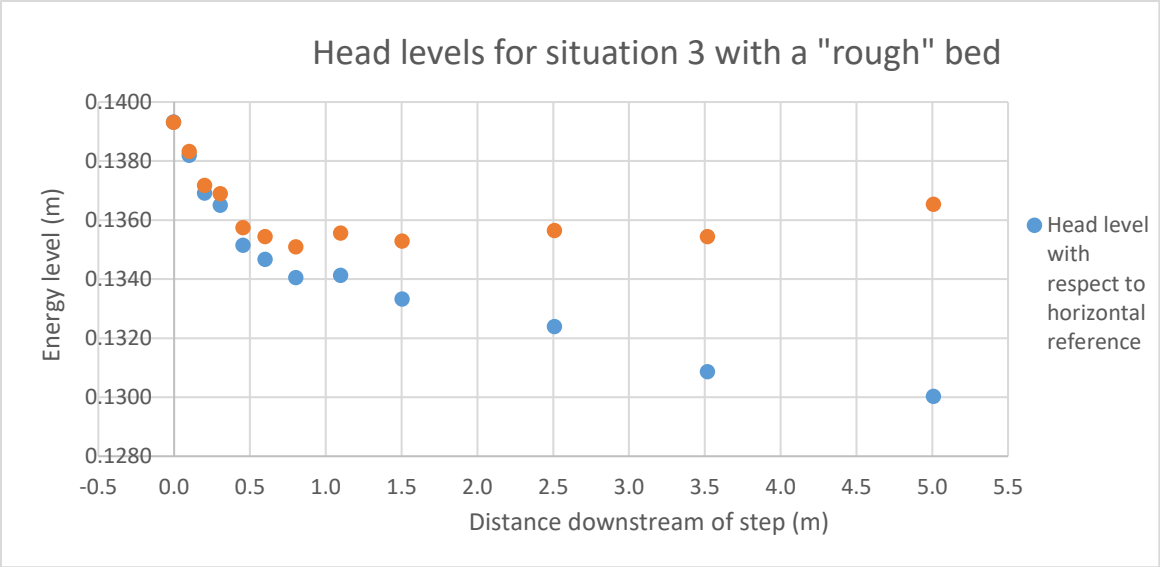

Figure H5: The head levels for situation 3 with a rough bed.

Appendix I: Head levels

In this Appendix, the calculated head levels will be shown.

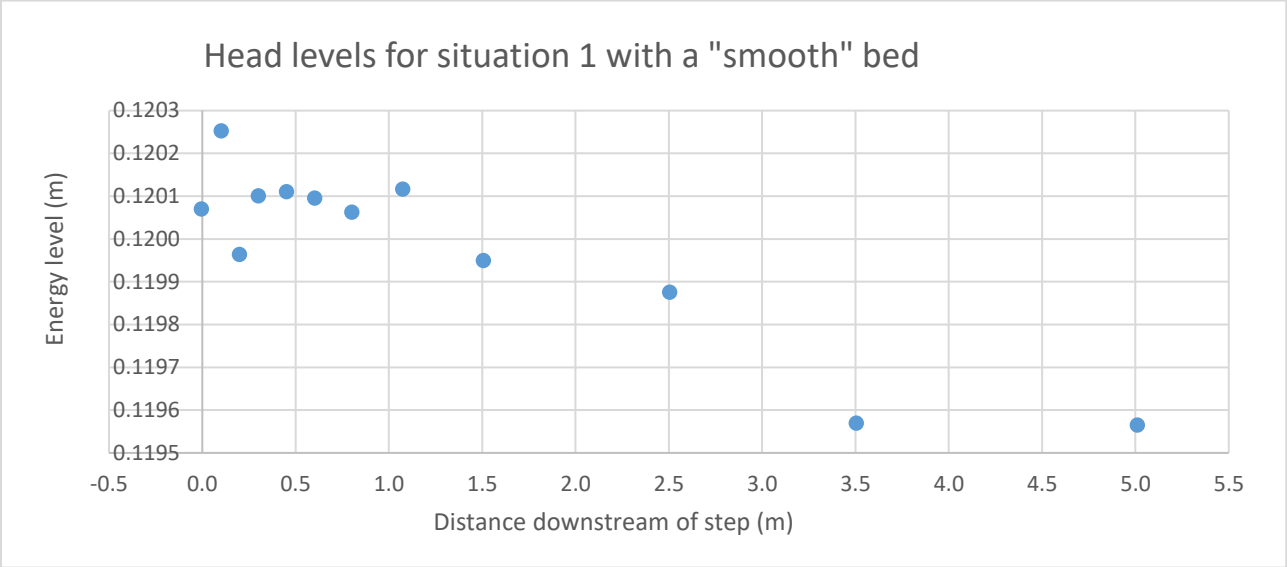

Figure I1: The head levels for situation 1 with a smooth bed.

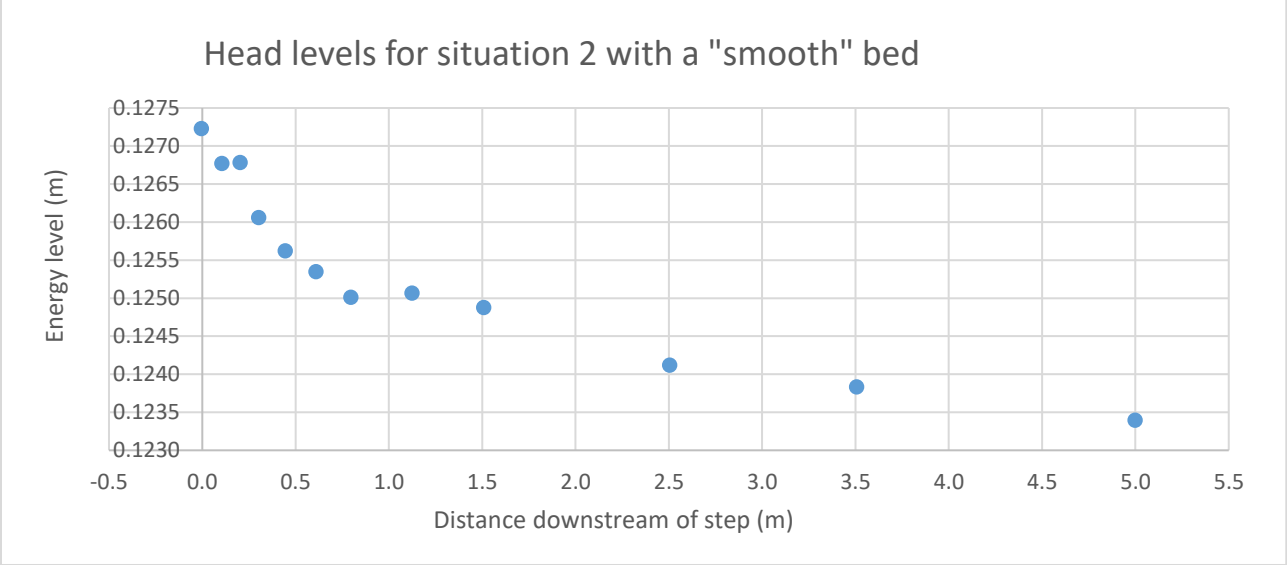

Figure I2: The head levels for situation 2 with a smooth bed.

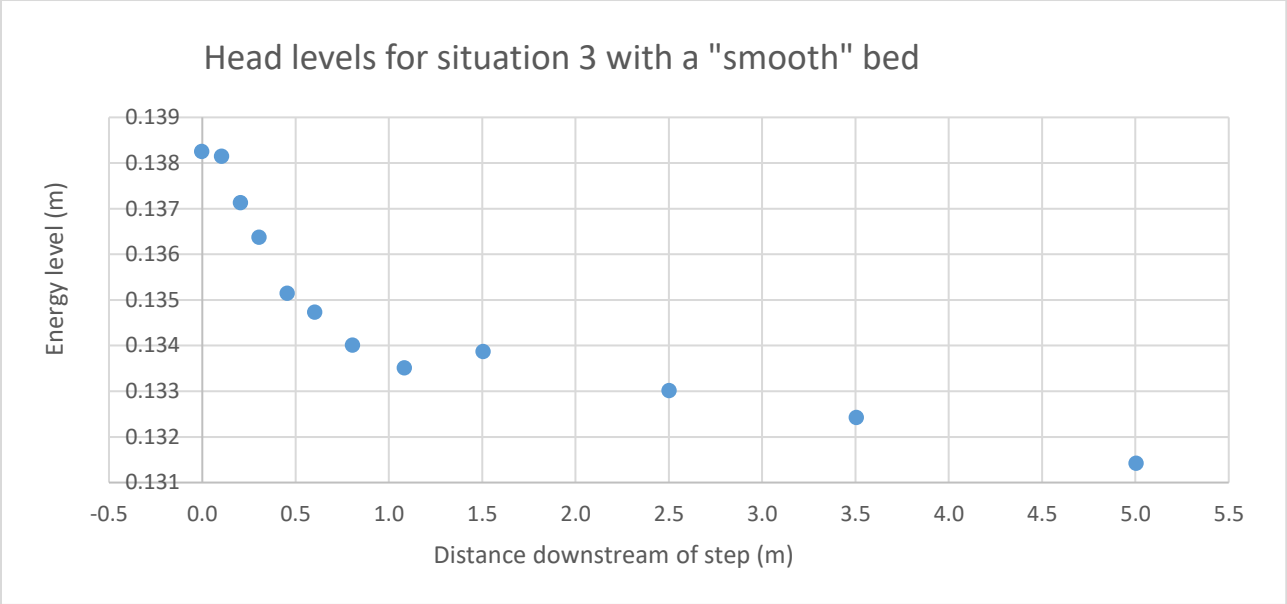

Figure I3: The head levels for situation 3 with a smooth bed.

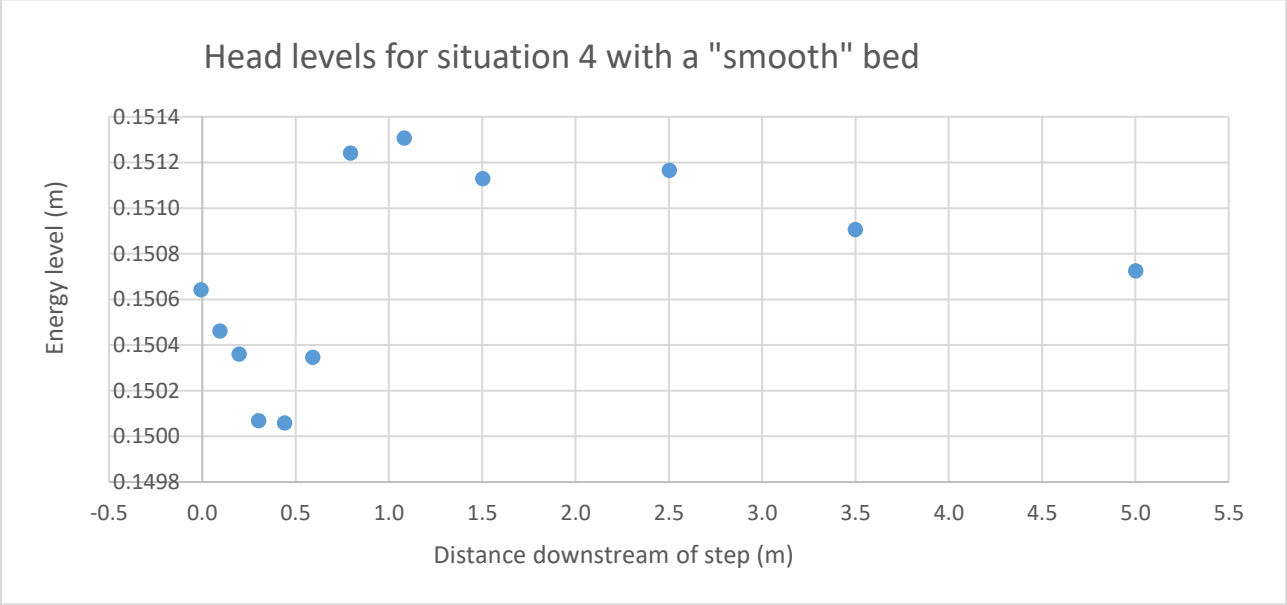

Figure I4: The head levels for situation 4 with a smooth bed.

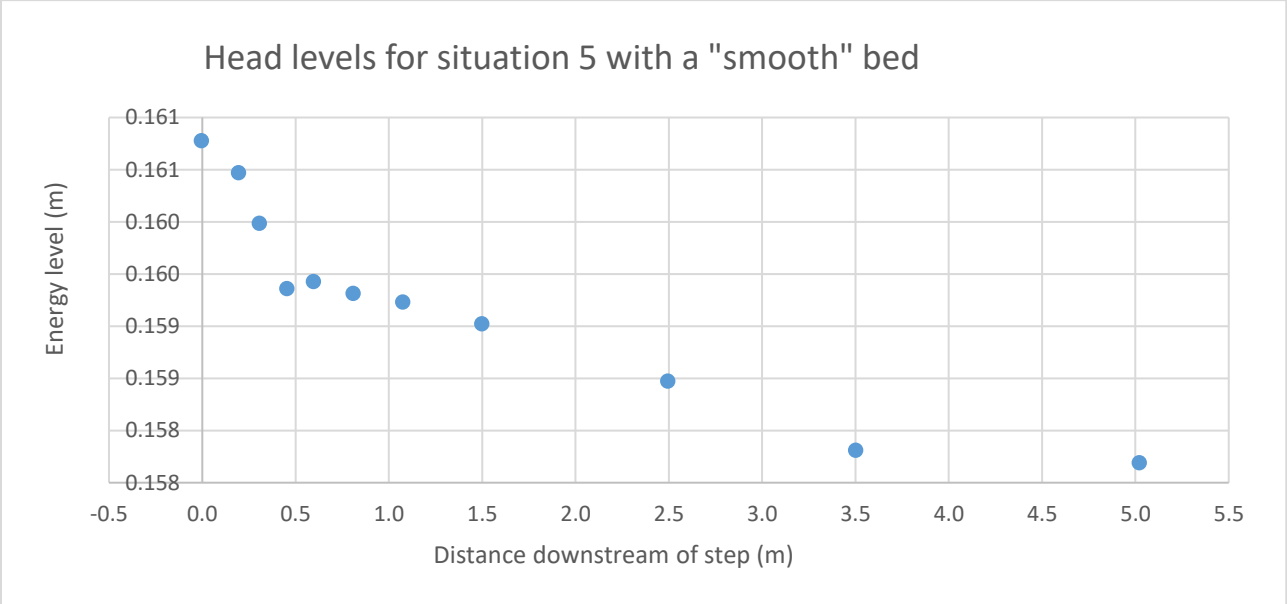

Figure I5: The head levels for situation 5 with a smooth bed.

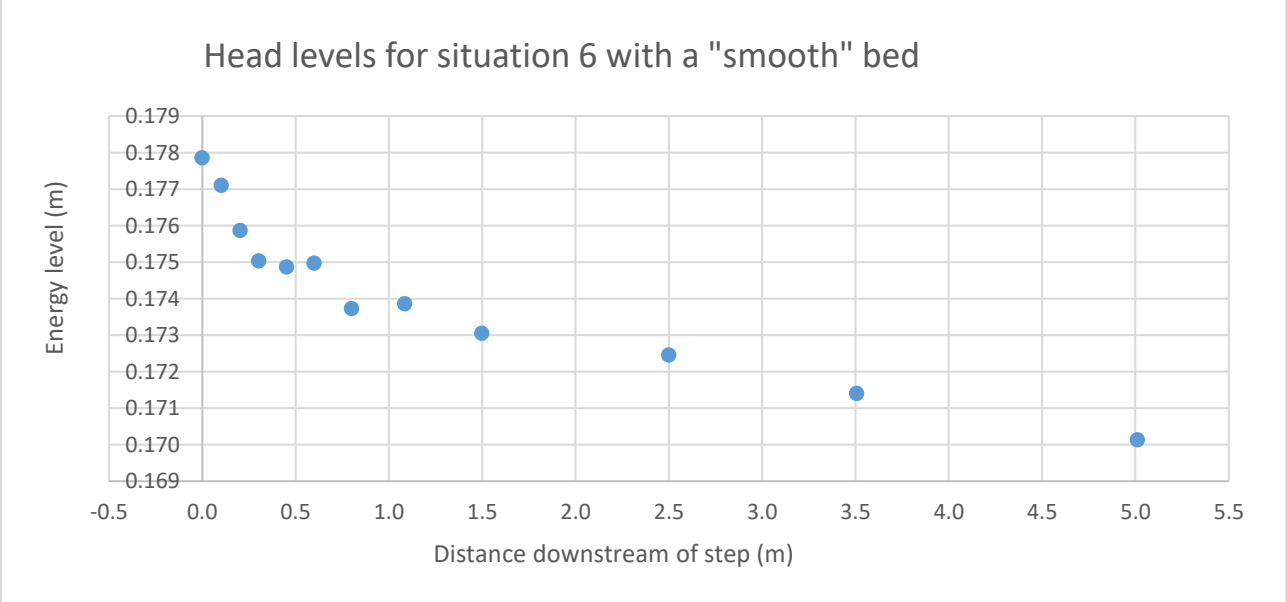

Figure I6: The head levels for situation 6 with a smooth bed.

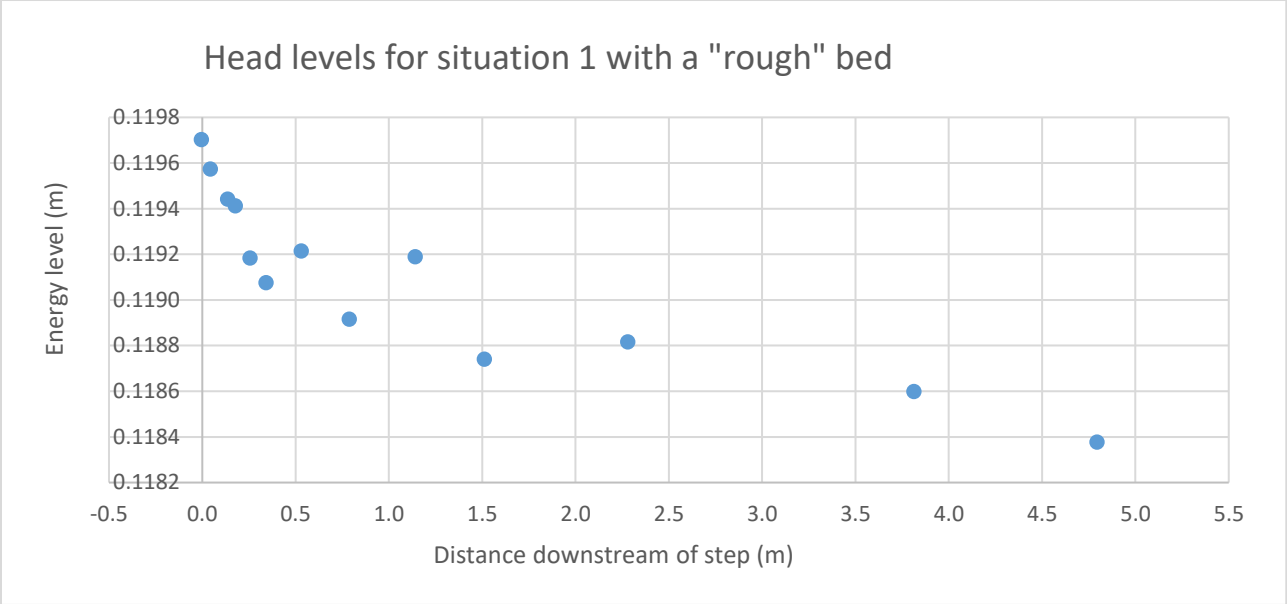

Figure I7: The head levels for situation 1 with a rough bed.

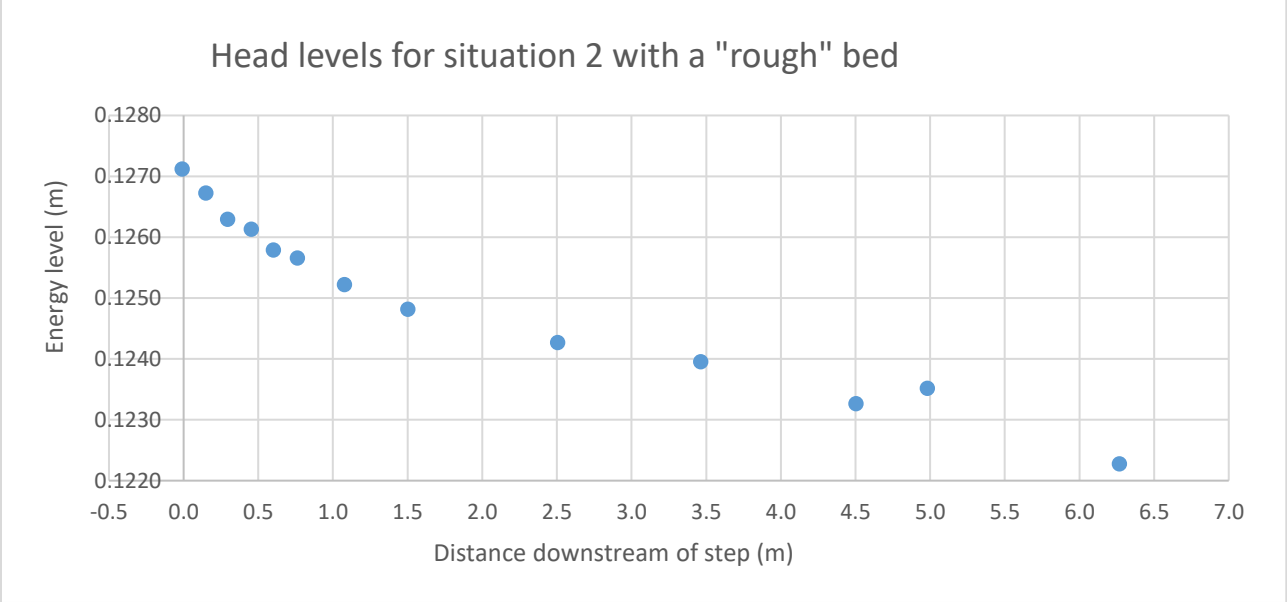

Figure I8: The head levels for situation 2 with a rough bed.

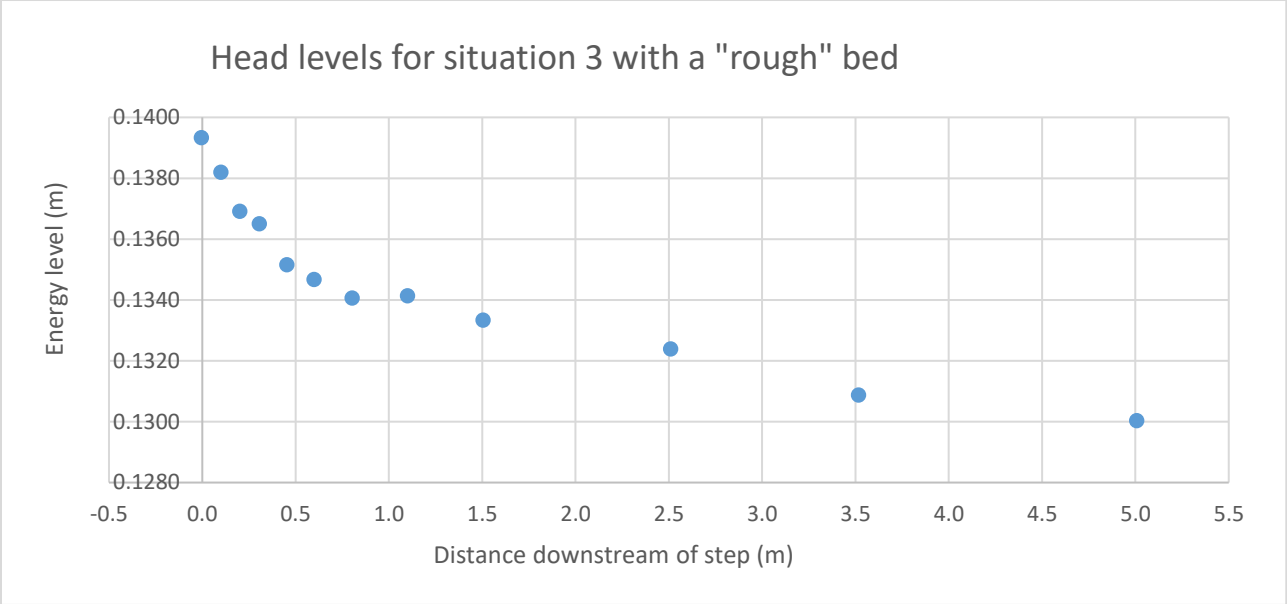

Figure I9: The head levels for situation 3 with a rough bed.

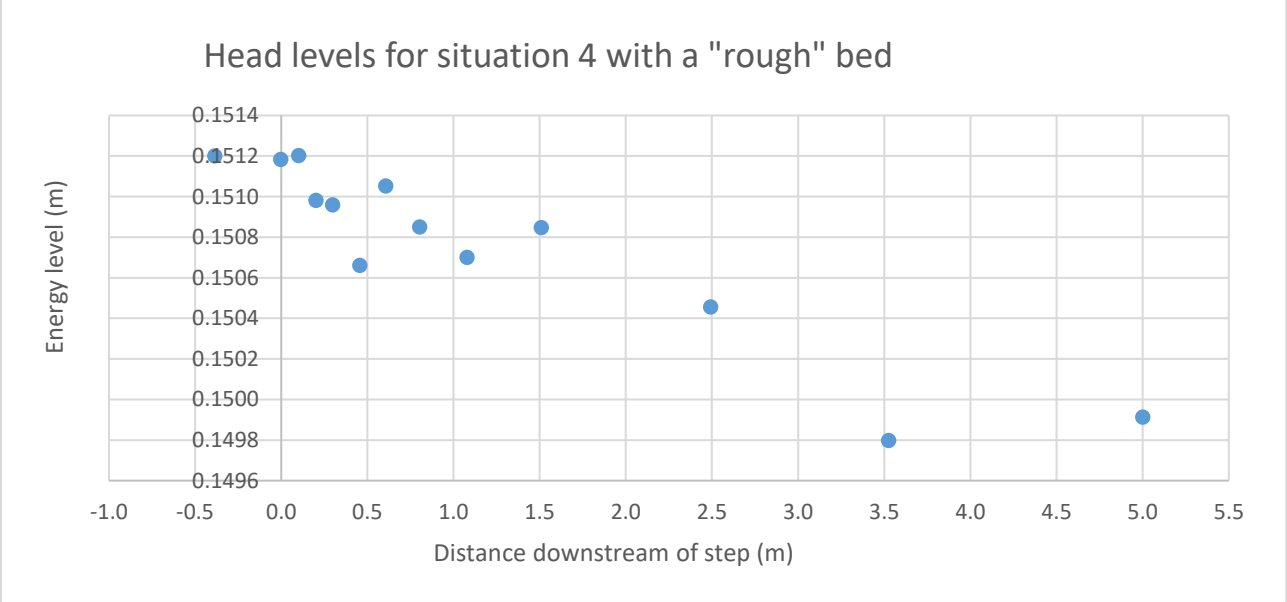

Figure I10: The head levels for situation 4 with a rough bed.

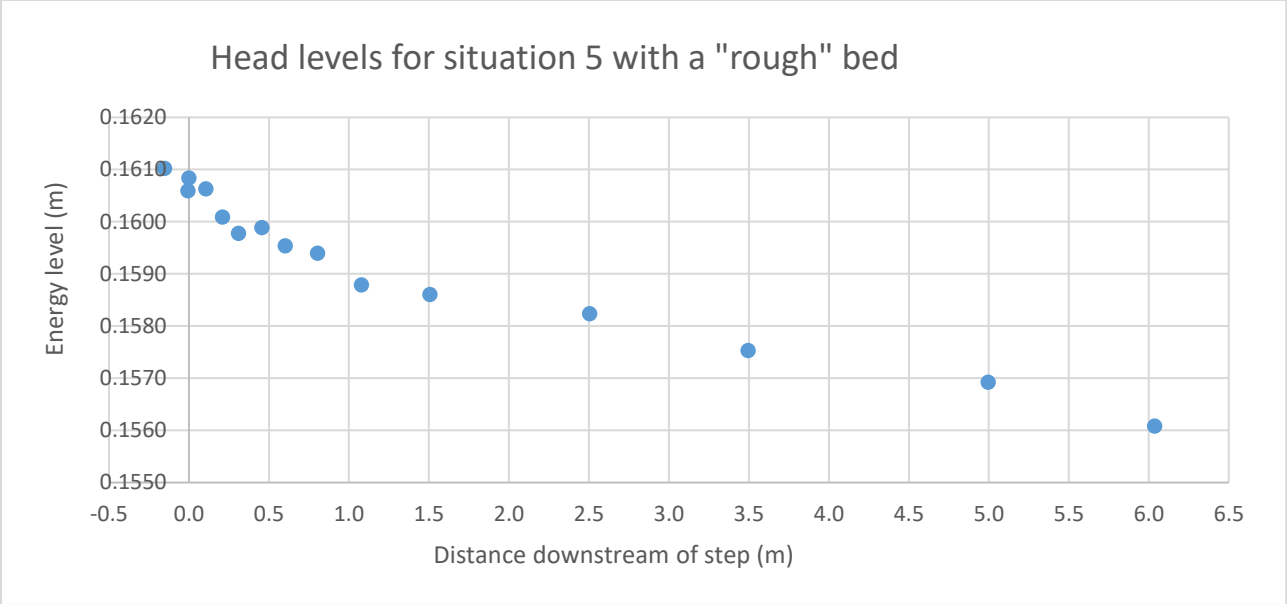

Figure I11: The head levels for situation 5 with a rough bed.

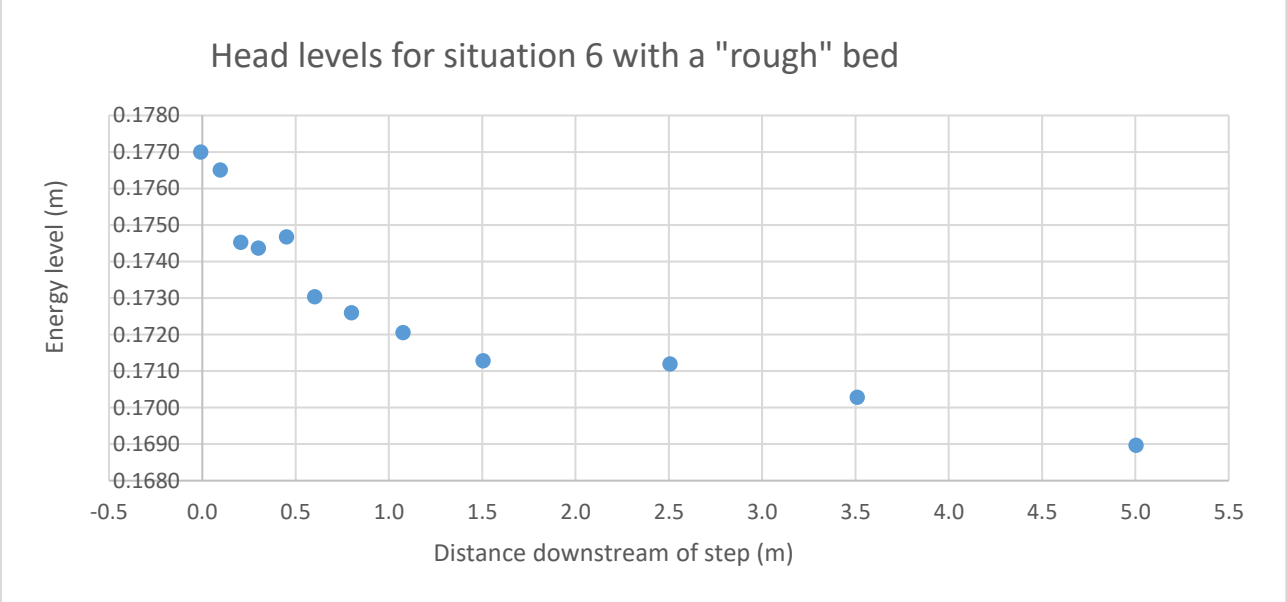

Figure I12: The head levels for situation 6 with a rough bed.

Appendix J: Turbulent energy levels

In this Appendix, the calculated turbulent energy levels will be shown.

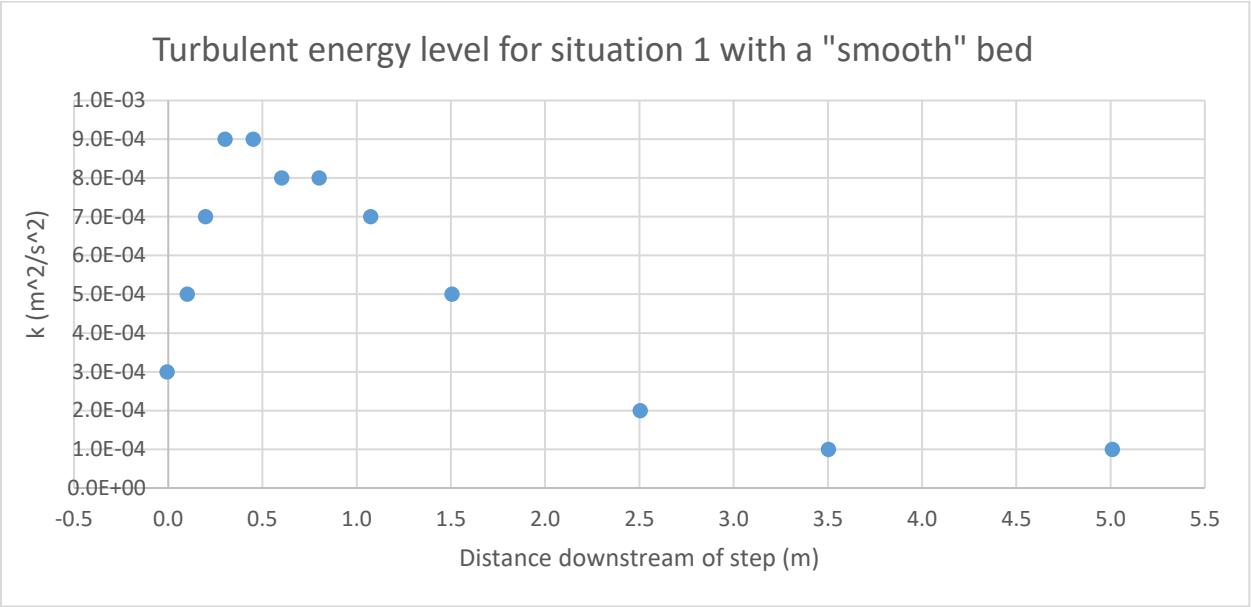

Figure J1: The turbulent energy levels for situation 1 with a smooth bed.

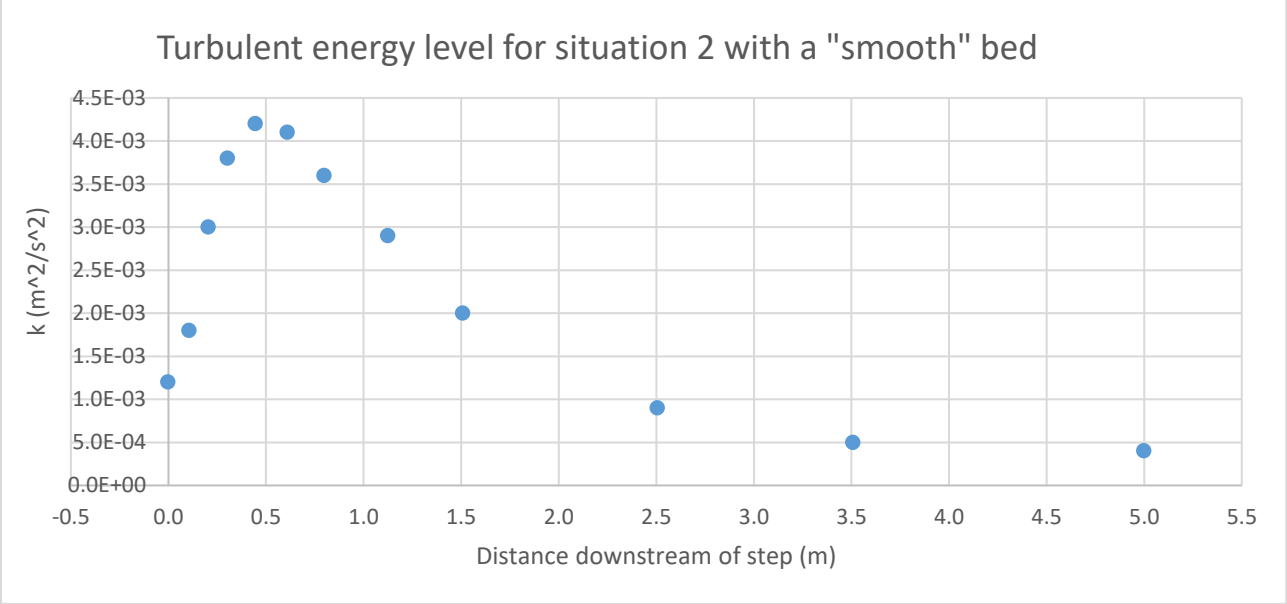

Figure J2: The turbulent energy levels for situation 2 with a smooth bed.

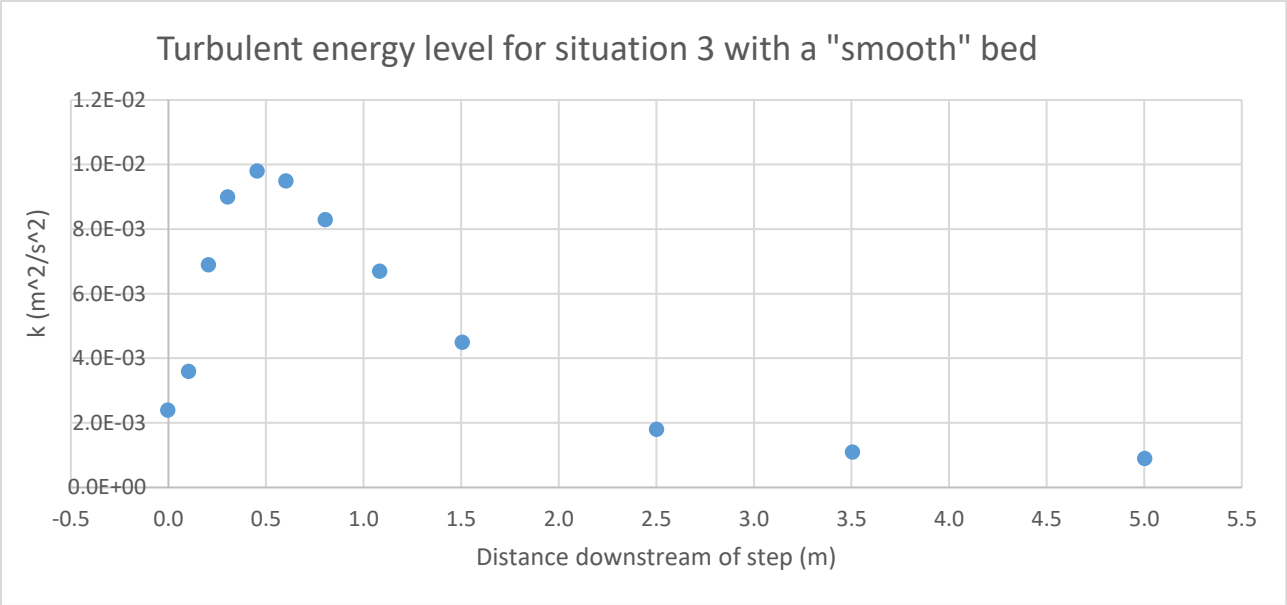

Figure J3: The turbulent energy levels for situation 3 with a smooth bed.

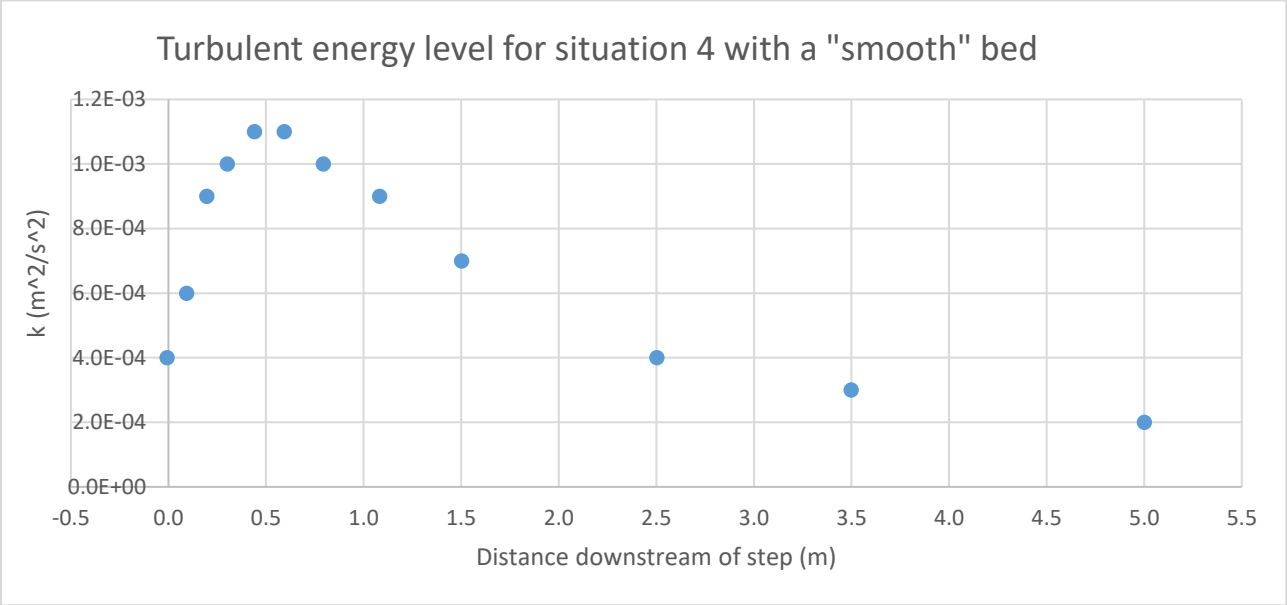

Figure J4: The turbulent energy levels for situation 4 with a smooth bed.

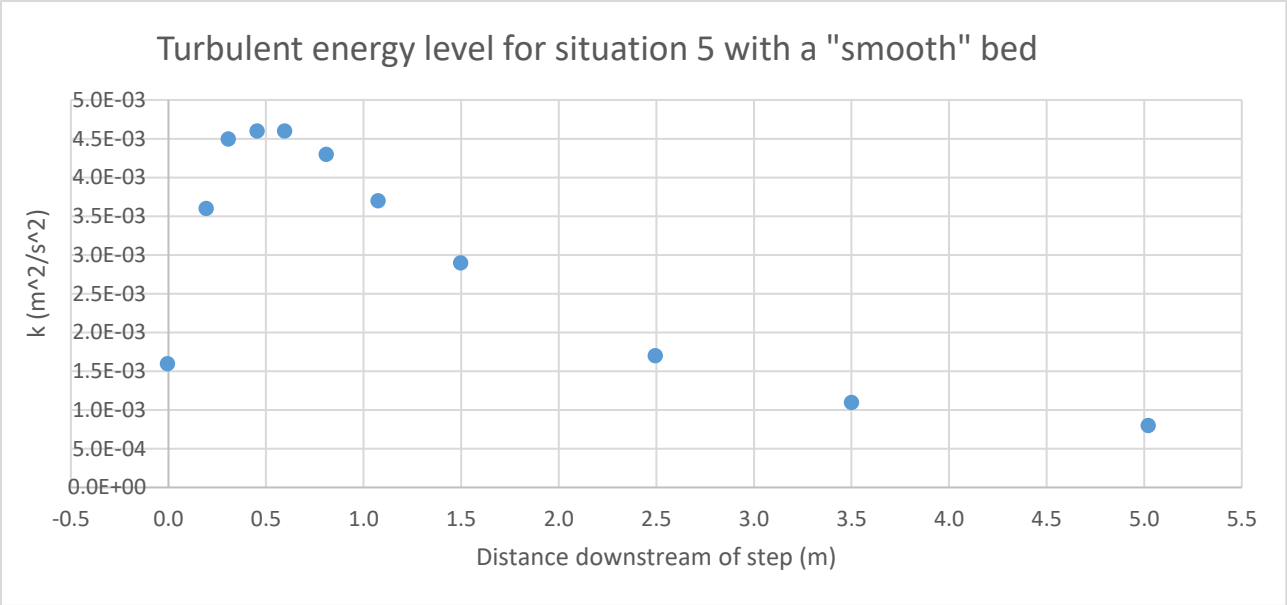

Figure J5: The turbulent energy levels for situation 5 with a smooth bed.

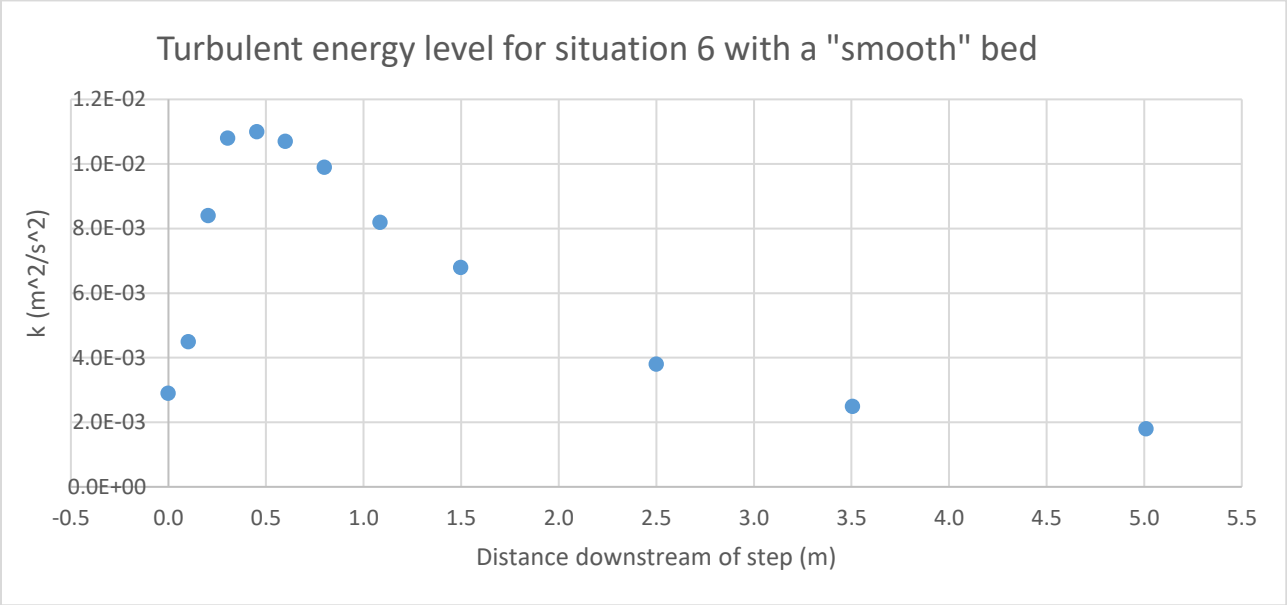

Figure J6: The turbulent energy levels for situation 6 with a smooth bed.

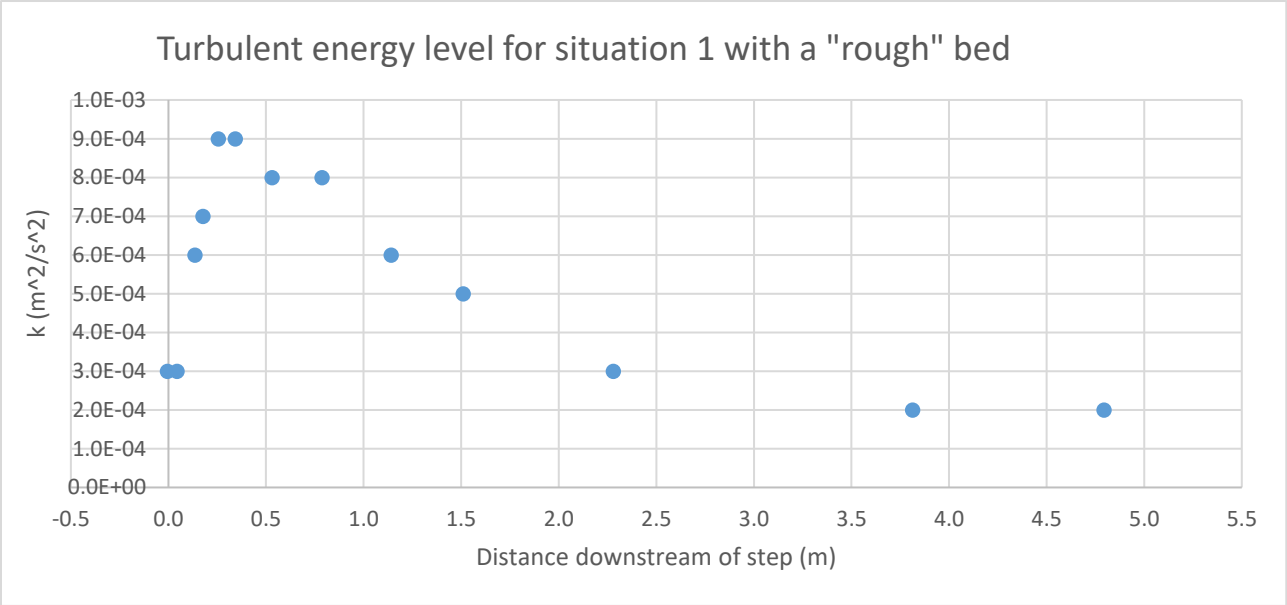

Figure J7: The turbulent energy levels for situation 1 with a rough bed.

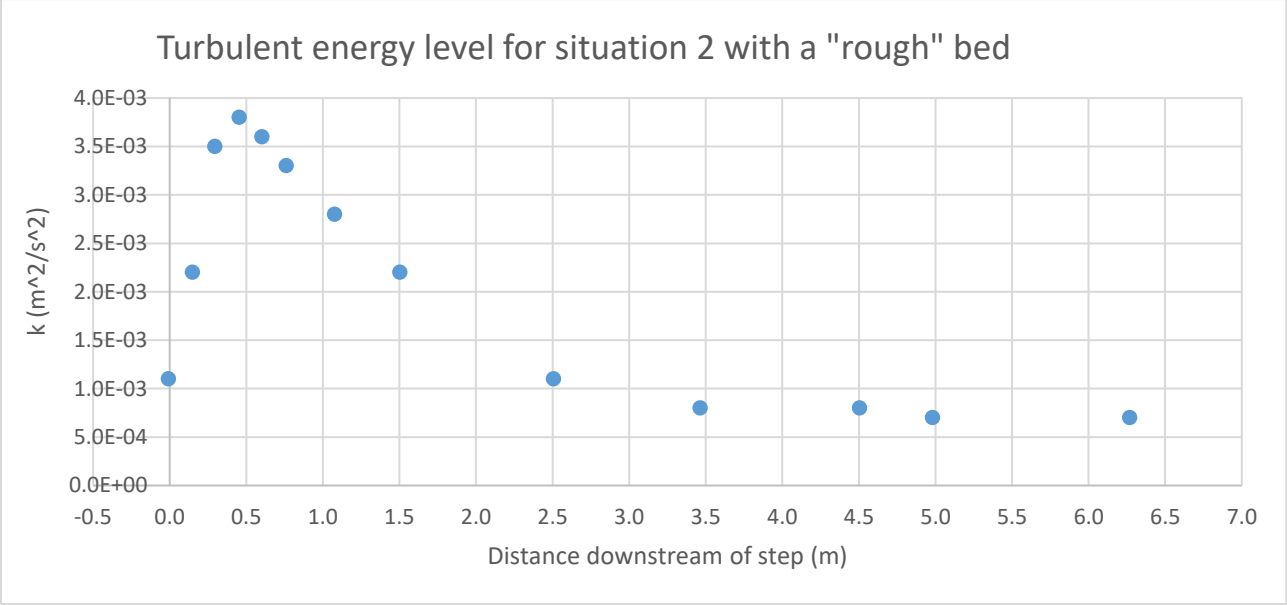

Figure J8: The turbulent energy levels for situation 2 with a rough bed.

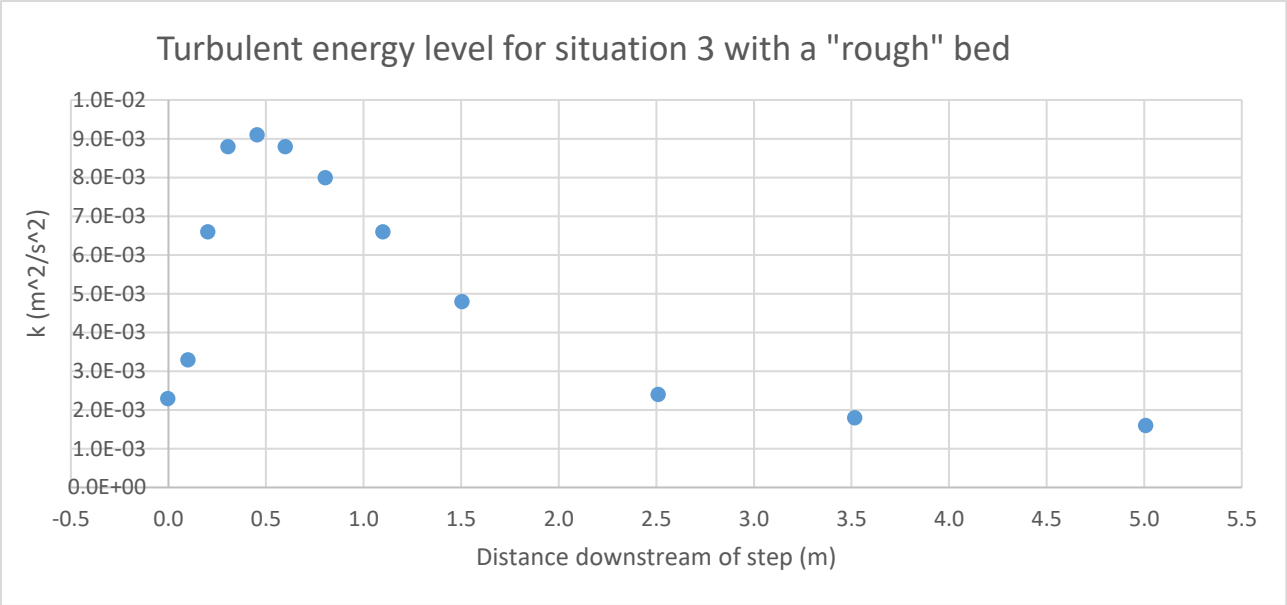

Figure J9: The turbulent energy levels for situation 3 with a rough bed.

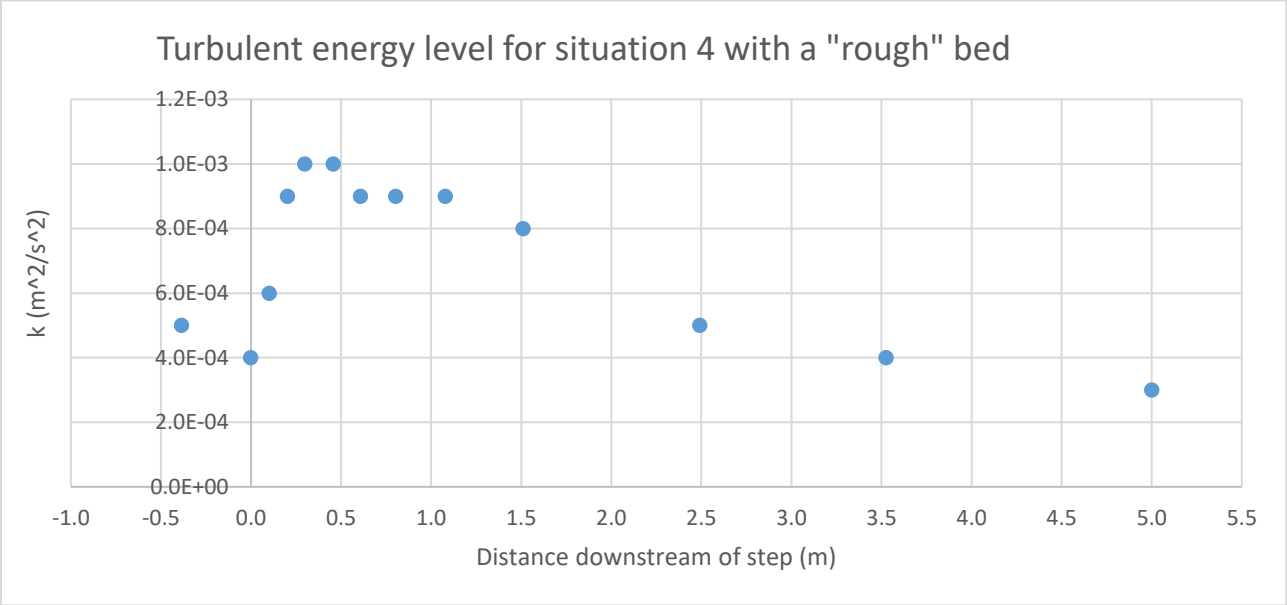

Figure J10: The turbulent energy levels for situation 4 with a rough bed.

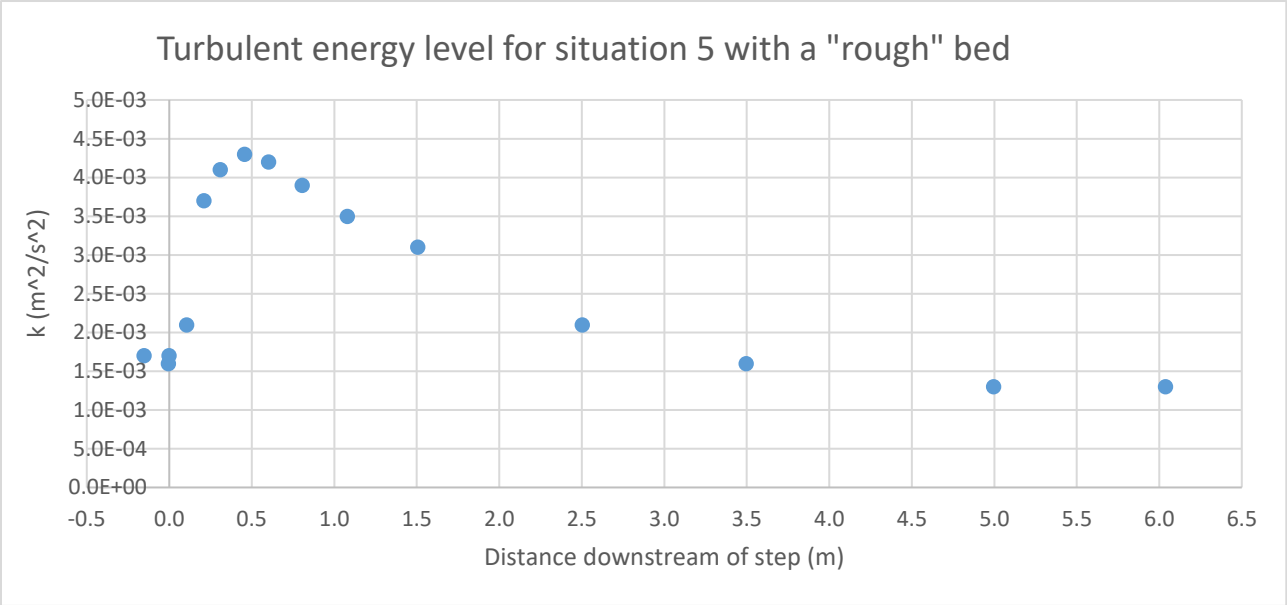

Figure J11: The turbulent energy levels for situation 5 with a rough bed.

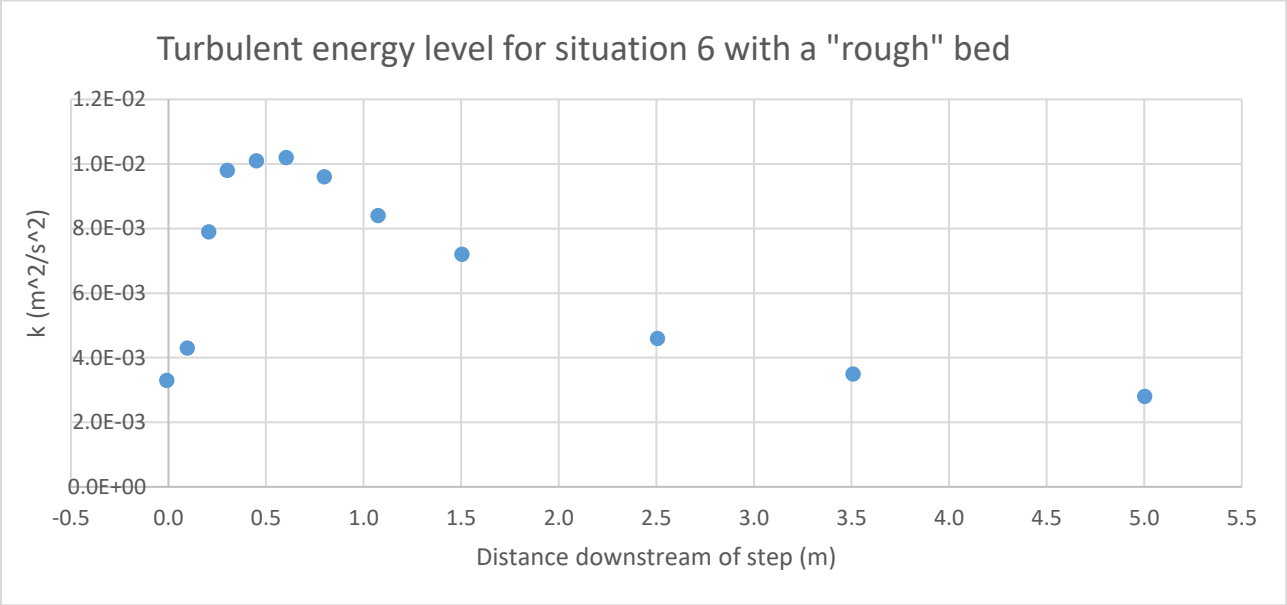

Figure J12: The turbulent energy levels for situation 6 with a rough bed.

Appendix K: Mathcad script for Voortman's method

In this Appendix, the Mathcad script used for Voortman's method will be shown. Since the script is identical for all twelve situations, only the script for situation 1 with a "smooth" bed will be shown.

Project:	**Graduation of Melvin Koote / The Arcadis Turbulence Method**		
Subject:	**The dissipation of turbulent energy via method Voortman 1**		
	Door:	Datum:	Paraaf:
Opgesteld:	**M. Koote**	**18th August 2017**	_____
Gecontroleerd:			_____
Vrijgegeven:		_____	
Versie:	**2.0**		
Status:	**Concept-intern**		

Definitions

ORIGIN := 1

x = distance downstream of step (m) x_{reatt} = reattachment point (m)

k = turbulent kinetic energy (m^2/s^2)

k_0 = turbulent kinetic energy at the reattachment point (m^2/s^2)

k_{eq} = equilibrium turbulent kinetic energy in uniform flow (m^2/s^2)

ϕ = constant value (-)

R = hydraulic radius (m)

SSE = sum of the squared errors

Description of worksheet

In this worksheet a formula for the turbulent energy as function of the distance from the step will be created based on experimental results.
This formula is exponential and depends on a certain maximum turbulence that occurs at the reattachment point, an equilibrium turbulence and a constant.
It is assumed that after the reattachment point the generation of turbulent energy can be neglected.
The hydraulic radius is assumed to be constant.

General start values

Data :=

[redacted]

Data =

	1	2	3	4	5	6
1	"S1"	1	0.07	0.25	$-6 \cdot 10^{-3}$	0.07
2	"S1"	1	0.07	0.25	0.101	0.118
3	"S1"	1	0.07	0.25	0.198	0.118
4	"S1"	1	0.07	0.25	0.3	0.119
5	"S1"	1	0.07	0.25	0.45	0.119
6	"S1"	1	0.07	0.25	0.602	0.12
7	"S1"	1	0.07	0.25	0.8	0.12
8	"S1"	1	0.07	0.25	1.073	0.121
9	"S1"	1	0.07	0.25	1.505	0.121
10	"S1"	1	0.07	0.25	2.504	0.122
11	"S1"	1	0.07	0.25	3.503	0.123
12	"S1"	1	0.07	0.25	5.009	0.125
13	"S2"	1	0.07	0.5	$-5 \cdot 10^{-3}$	0.07
14	"S2"	1	0.07	0.5	0.104	0.118
15	"S2"	1	0.07	0.5	0.202	0.118
16	"S2"	1	0.07	0.5	0.301	0.119
17	"S2"	1	0.07	0.5	0.443	0.12
18	"S2"	1	0.07	0.5	0.608	0.121
19	"S2"	1	0.07	0.5	0.796	0.122
20	"S2"	1	0.07	0.5	1.123	0.123
21	"S2"	1	0.07	0.5	1.507	0.123
22	"S2"	1	0.07	0.5	2.504	0.124
23	"S2"	1	0.07	0.5	3.506	0.125
24	"S2"	1	0.07	0.5	4.997	0.127
25	"S3"	1	0.07	0.75	$-4 \cdot 10^{-3}$	0.07
26	"S3"	1	0.07	0.75	0.103	...

$Code := Data^{\langle 1 \rangle}$

$Ruwh := Data^{\langle 2 \rangle}$

$d_{step} := Data^{\langle 3 \rangle} \cdot m$

$Fr_{step} := Data^{\langle 4 \rangle}$

$x_{loc} := Data^{\langle 5 \rangle} \cdot m$

$d_{loc} := Data^{\langle 6 \rangle} \cdot m$

$B := 0.4 \cdot m$

$h_{loc} := Data^{\langle 8 \rangle} \cdot m$

$H_{loc} := Data^{\langle 9 \rangle} \cdot m$

$q := Data^{\langle 10 \rangle} \cdot \frac{m^2}{s}$

$k_{loc} := Data^{\langle 11 \rangle} \cdot \frac{m^2}{s^2}$

$x_{reatt} := Data^{\langle 12 \rangle} \cdot m$

$$row_{start} := \begin{pmatrix} 1 \\ 13 \\ 25 \\ 37 \\ 49 \\ 60 \\ 72 \\ 85 \\ 98 \\ 110 \\ 123 \\ 138 \end{pmatrix}$$

$$row_{end} := \begin{pmatrix} row_{start_2} - 1 \\ row_{start_3} - 1 \\ row_{start_4} - 1 \\ row_{start_5} - 1 \\ row_{start_6} - 1 \\ row_{start_7} - 1 \\ row_{start_8} - 1 \\ row_{start_9} - 1 \\ row_{start_{10}} - 1 \\ row_{start_{11}} - 1 \\ row_{start_{12}} - 1 \\ 149 \end{pmatrix}$$

$$row_{last3} := \begin{pmatrix} row_{start_2} - 3 \\ row_{start_3} - 3 \\ row_{start_4} - 3 \\ row_{start_5} - 3 \\ row_{start_6} - 3 \\ row_{start_7} - 3 \\ row_{start_8} - 3 \\ row_{start_9} - 3 \\ row_{start_{10}} - 3 \\ row_{start_{11}} - 3 \\ row_{start_{12}} - 3 \\ 147 \end{pmatrix}$$

$$row_{diss} := \begin{pmatrix} row_{start_1} - 1 + 5 \\ row_{start_2} - 1 + 5 \\ row_{start_3} - 1 + 5 \\ row_{start_4} - 1 + 5 \\ row_{start_5} - 1 + 4 \\ row_{start_6} - 1 + 5 \\ row_{start_7} - 1 + 6 \\ row_{start_8} - 1 + 4 \\ row_{start_9} - 1 + 5 \\ row_{start_{10}} - 1 + 6 \\ row_{start_{11}} - 1 + 7 \\ row_{start_{12}} - 1 + 5 \end{pmatrix}$$

Dataset:

$n := 1$

Input values

$x_{loc.n} := submatrix\left(x_{loc}, row_{start_n}, row_{end_n}, 1, 1\right)$

$x_{loc.dl} := x_{loc.n} \cdot \frac{1}{m}$

$x_{reatt.n} := submatrix\left(x_{reatt}, row_{start_n}, row_{start_n}, 1, 1\right)$

$x_{last3.n} := submatrix\left(x_{loc}, row_{last3_n}, row_{end_n}, 1, 1\right)$

$x_{diss.n} := submatrix\left(x_{loc}, row_{diss_n}, row_{end_n}, 1, 1\right)$

$x_{diss.dl} := x_{diss.n} \cdot \frac{1}{m}$ $x_{reatt.dl} := x_{reatt.n} \cdot \frac{1}{m}$ $x_{last3.dl} := x_{last3.n} \cdot \frac{1}{m}$

$d_{loc.n} := submatrix\left(d_{loc}, row_{start_n}, row_{end_n}, 1, 1\right)$

$h_{loc.n} := submatrix\left(h_{loc}, row_{start_n}, row_{end_n}, 1, 1\right)$

$H_{loc.n} := submatrix\left(H_{loc}, row_{start_n}, row_{end_n}, 1, 1\right)$

$H_{diss.n} := submatrix\left(H_{loc}, row_{diss_n}, row_{end_n}, 1, 1\right)$

$H_{last3.n} := submatrix\left(H_{loc}, row_{last3_n}, row_{end_n}, 1, 1\right)$

$q_n := submatrix\left(q, row_{start_n}, row_{end_n}, 1, 1\right)$

$k_{loc.n} := submatrix\left(k_{loc}, row_{start_n}, row_{end_n}, 1, 1\right)$

$k_{diss.n} := submatrix\left(k_{loc}, row_{diss_n}, row_{end_n}, 1, 1\right)$

$H_{loc.dl} := H_{loc.n} \cdot \frac{1}{m}$ $H_{diss.dl} := H_{diss.n} \cdot \frac{1}{m}$

$k_{loc.dl} := k_{loc.n} \cdot \frac{s^2}{m^2}$ $k_{diss.dl} := k_{diss.n} \cdot \frac{s^2}{m^2}$

$reatt := row_{diss_n} - row_{start_n} + 1 = 5$ $end := row_{end_n} - row_{start_n} + 1 = 12$

$d_{end} := d_{loc.n_{end}} = 0.125\,m$ $q_{end} := q_{n_{end}} = 0.014 \frac{m^2}{s}$

$R := \frac{B \cdot d_{end}}{B + 2 \cdot d_{end}} = 0.077\,m$ $f := \frac{1}{R} = 12.98 \frac{1}{m}$ $Fr_1 := \frac{q_{end}}{\sqrt{g \cdot d_{end}^{\,3}}} = 0.104$

$$u_{star} := 9.5 \times 10^{-3} \cdot \frac{m}{s}$$

$$k_{eq} := 1.44 \cdot u_{star}^{2} = 1.3 \times 10^{-4} \frac{m^2}{s^2}$$

$$k_{eq.dl} := k_{eq} \cdot \frac{s^2}{m^2}$$

Formulae

After the reattachment point, the amount of turbulent energy can be described with:

$$k\left(x, k_0, \phi\right) := \left(k_0 - k_{eq}\right) \cdot \exp\left[-f \cdot \phi \cdot \left(x - x_{reatt.n_1}\right)\right] + k_{eq}$$

Results

In order to calculate the unknown variables, the formula must be made dimensionless

$$f_{dl} := f \cdot m = 12.98 \qquad g_{dl} := g \cdot \frac{s^2}{m}$$

$$k_{dl}\left(x_{dl}, k_{0.dl}, \phi\right) := \left(k_{0.dl} - k_{eq.dl}\right) \cdot \exp\left[-f_{dl} \cdot \phi \cdot \left(x_{dl} - x_{reatt.dl_1}\right)\right] + k_{eq.dl}$$

$$k_{0\_guess} := 0.01 \cdot \frac{m^2}{s^2} \qquad \phi_{guess} := 0.01$$

$$guess := \begin{pmatrix} k_{0\_guess} \cdot \frac{s^2}{m^2} \\ \phi_{guess} \end{pmatrix}$$

$$\begin{pmatrix} k_{0.dl} \\ \phi \end{pmatrix} := genfit\left(x_{diss.dl}, k_{diss.dl}, guess, k_{dl}\right) = \begin{pmatrix} 1.009 \times 10^{-3} \\ 0.064 \end{pmatrix}$$

$$x := x_{reatt.n_1}, x_{reatt.n_1} + 0.1 \cdot m .. x_{reatt.n_1} + 7 \cdot m$$

$$k_0 := k_{0.dl} \cdot \frac{m^2}{s^2}$$

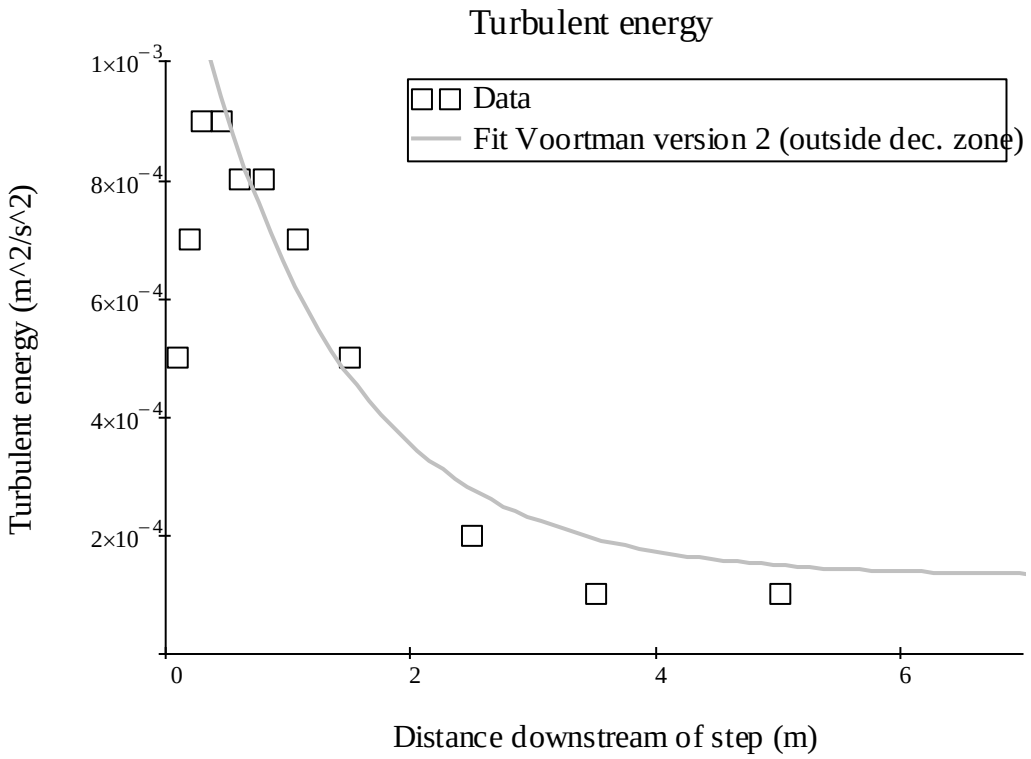

$$dk := k_0 - k_{eq} = 8.791 \times 10^{-4} \frac{m^2}{s^2}$$

$$k_{half} := k_0 - 0.5 \cdot dk = 5.695 \times 10^{-4} \frac{m^2}{s^2}$$

The distance after which half of the excess turbulence is dissipated, can be calculated with:

$$x_{guess} := 1.0 \cdot m$$

$$x_{half} := root\left(k\left(x_{guess}, k_0, \phi\right) - k_{half}, x_{guess}\right) = 1.19\,m$$

$$\phi_1 := \phi$$

$$k_1 := k_{eq}$$

$$error := \left(k_{loc.n} - k\left(x_{loc.n}, k_0, \phi\right)\right)^2$$

$$SSE_1 := \sum_{m=reatt}^{end} error_m = 3.342 \times 10^{-8} \frac{m^4}{s^4}$$

$$\frac{x_{diss.n}}{d_{end}} = \begin{pmatrix} 3.591 \\ 4.804 \\ 6.384 \\ 8.562 \\ 12.01 \\ 19.982 \\ 27.954 \\ 39.971 \end{pmatrix}$$

$$k_{m1} := \frac{(k_{diss.n} - k_{eq})}{(k_0 - k_{eq})} = \begin{pmatrix} 0.876 \\ 0.762 \\ 0.762 \\ 0.648 \\ 0.421 \\ 0.08 \\ -0.034 \\ -0.034 \end{pmatrix}$$

$$k(x) := k(x, k_0, \phi)$$

$$k_{c1}(x) := \frac{(k(x) - k_{eq})}{(k_0 - k_{eq})}$$

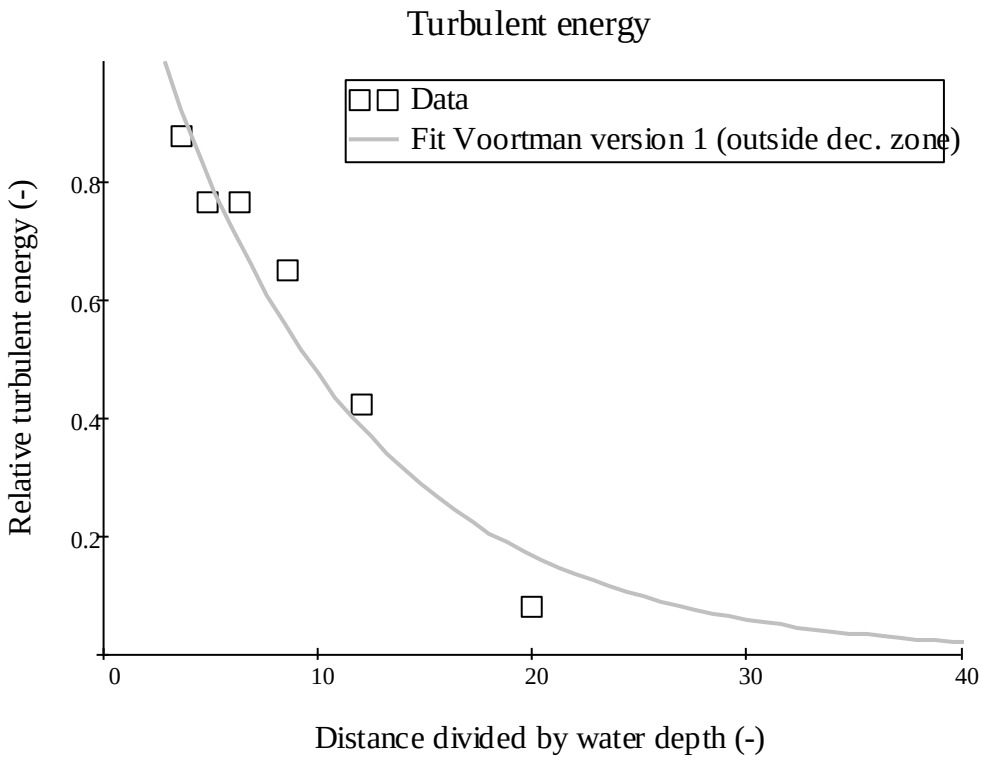

Appendix L: The results from Voortman's method

In this Appendix, the resulting graphs from Voortman's first method with $p = 0.125$ and $\varphi = 0.064$ will be shown.

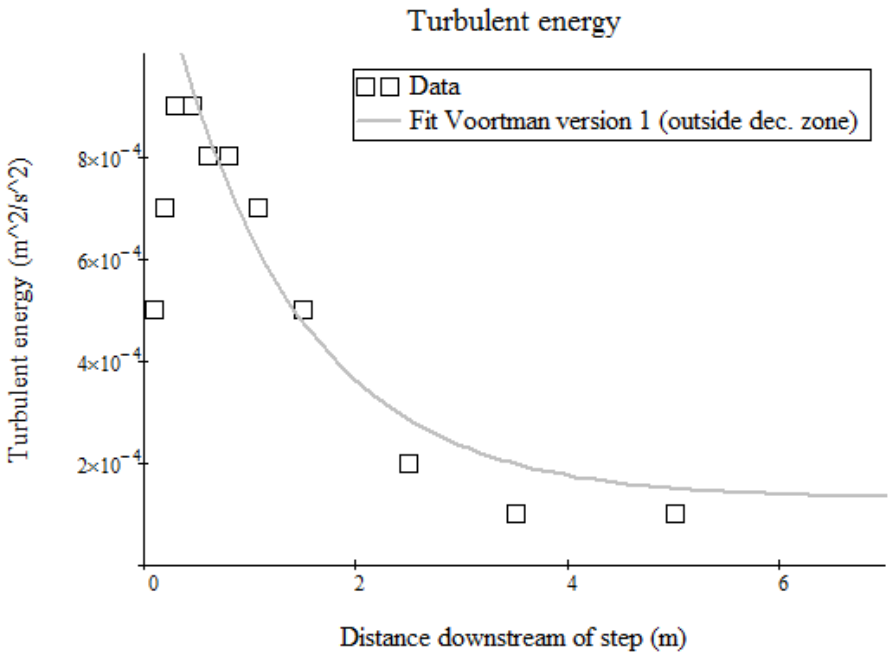

Figure L1: The turbulent energy levels for situation 1 with a smooth bed.

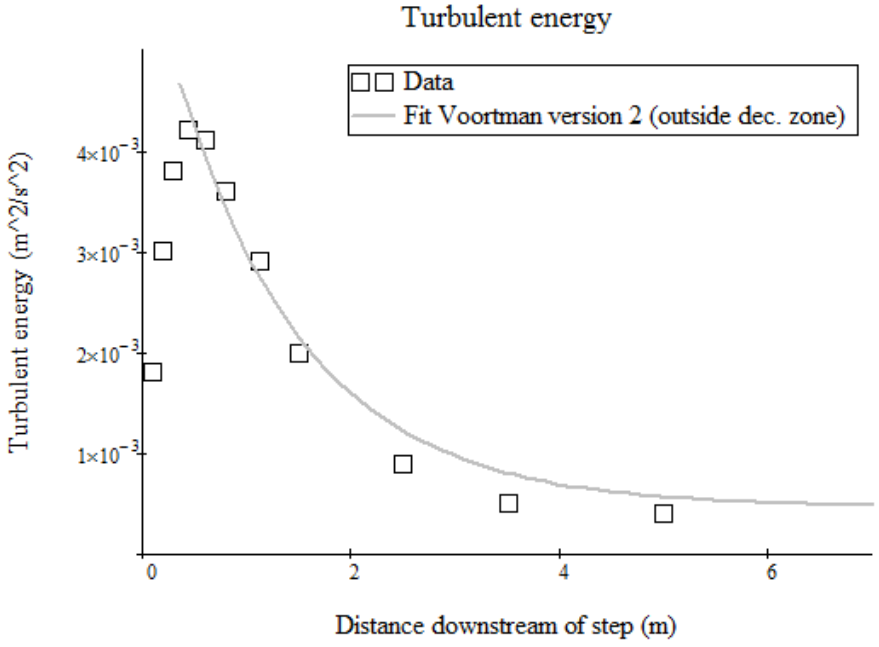

Figure L2: The turbulent energy levels for situation 2 with a smooth bed.

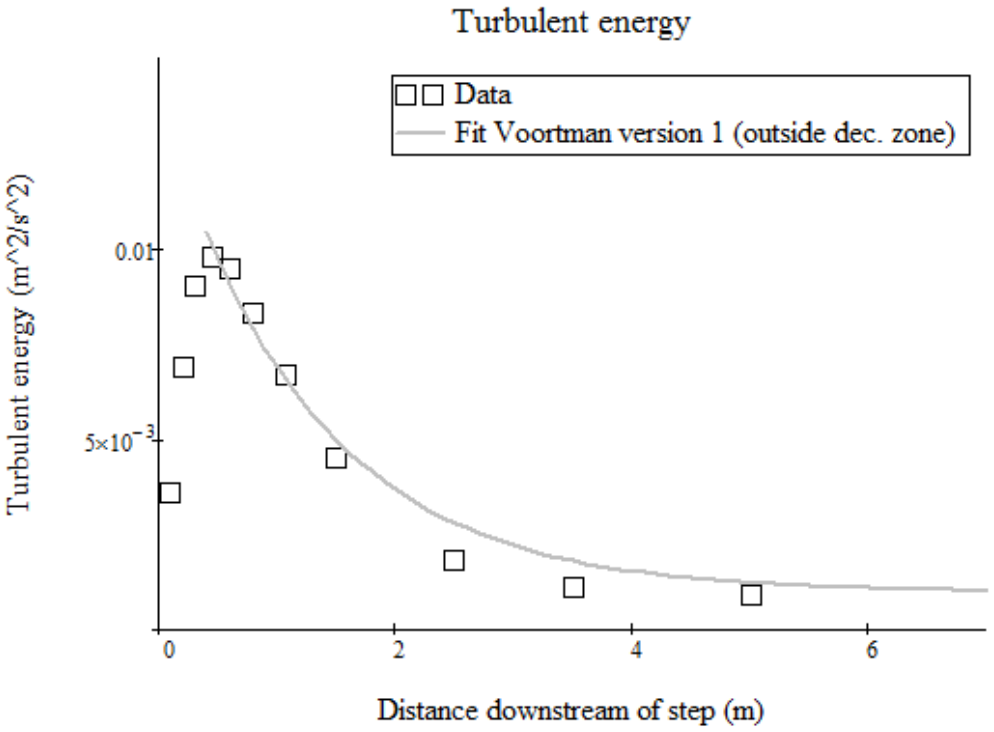

Figure L3: The turbulent energy levels for situation 3 with a smooth bed.

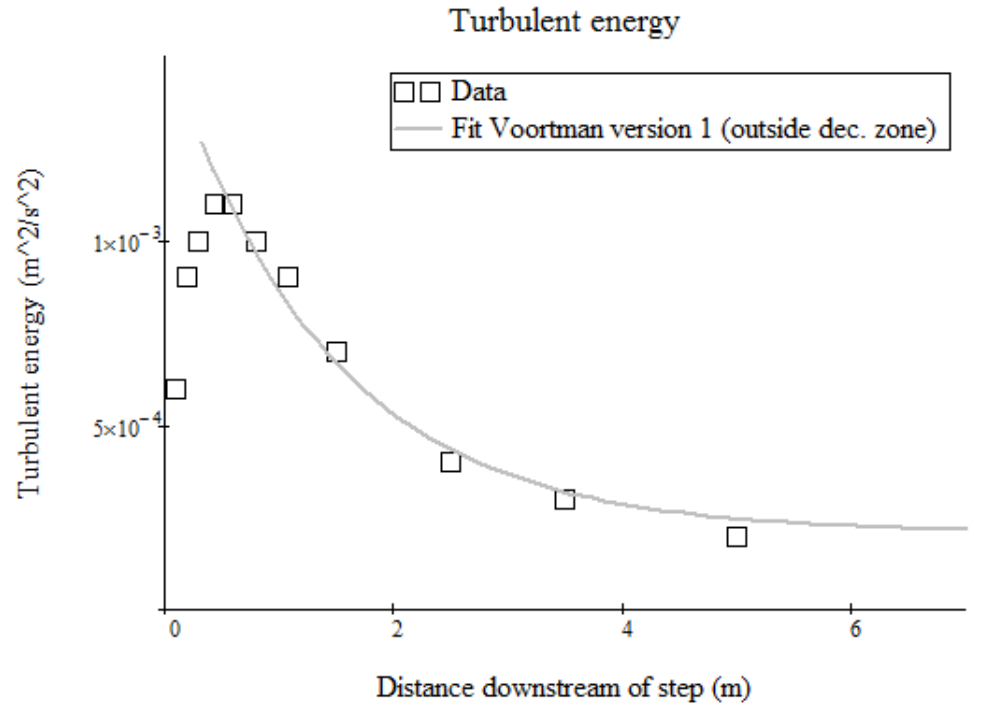

Figure L4: The turbulent energy levels for situation 4 with a smooth bed.

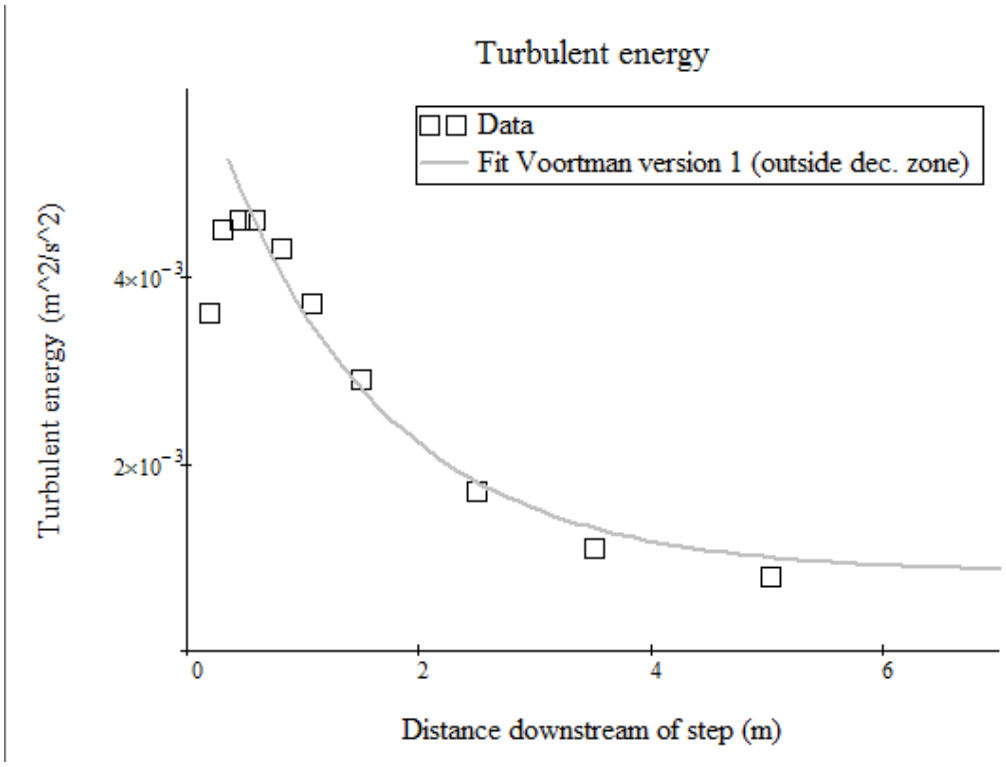

Figure L5: The turbulent energy levels for situation 5 with a smooth bed.

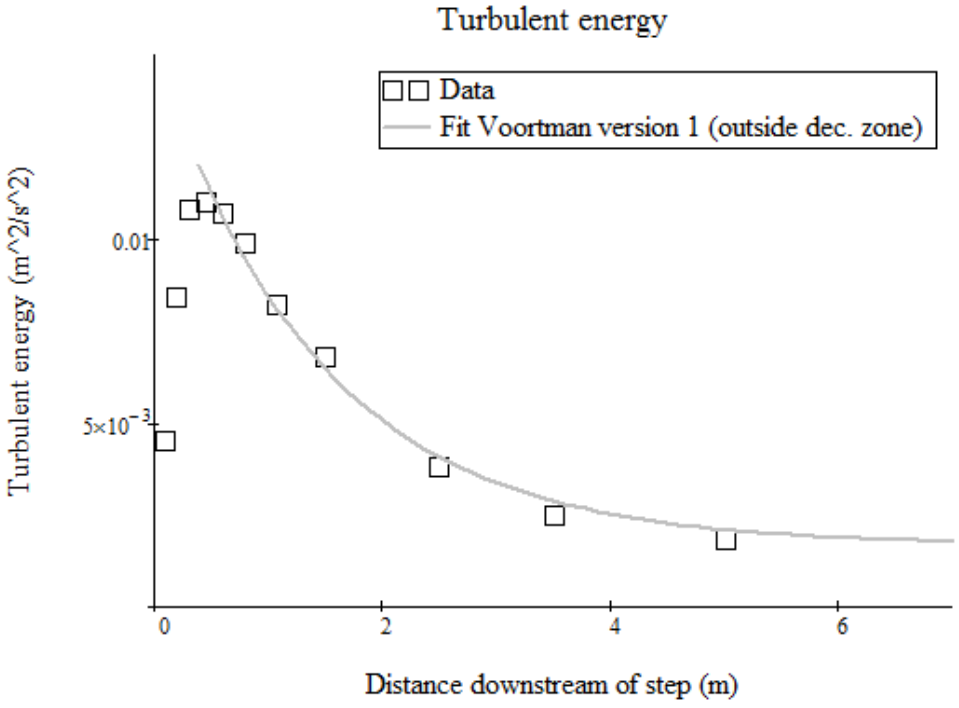

Figure L6: The turbulent energy levels for situation 6 with a smooth bed.

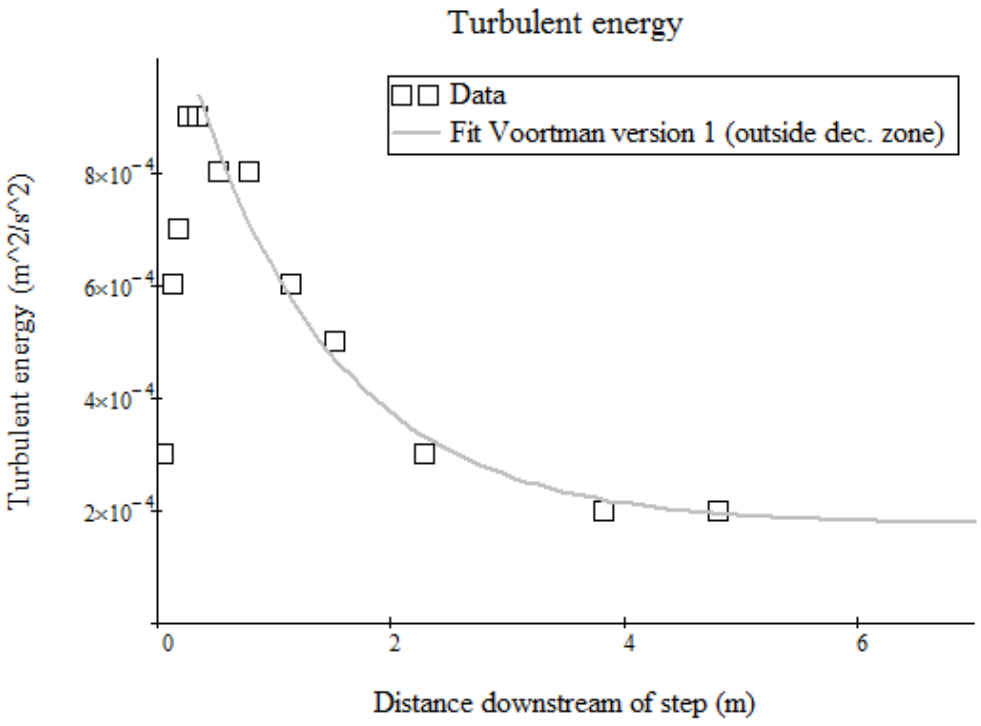

Figure L7: The turbulent energy levels for situation 1 with a rough bed.

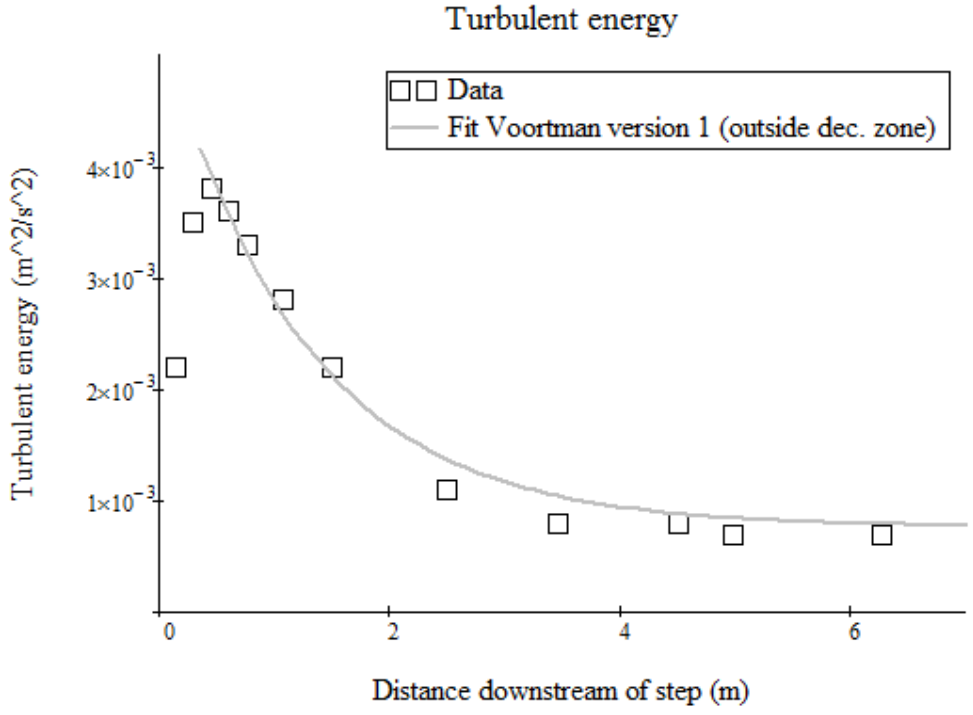

Figure L8: The turbulent energy levels for situation 2 with a rough bed.

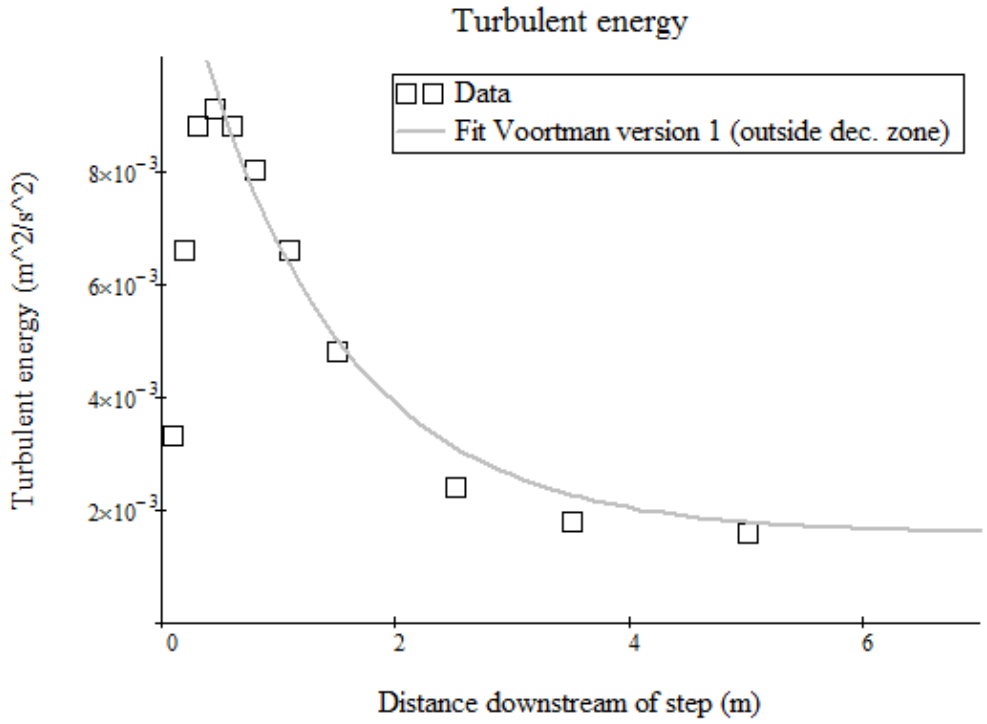

Figure L9: The turbulent energy levels for situation 3 with a rough bed.

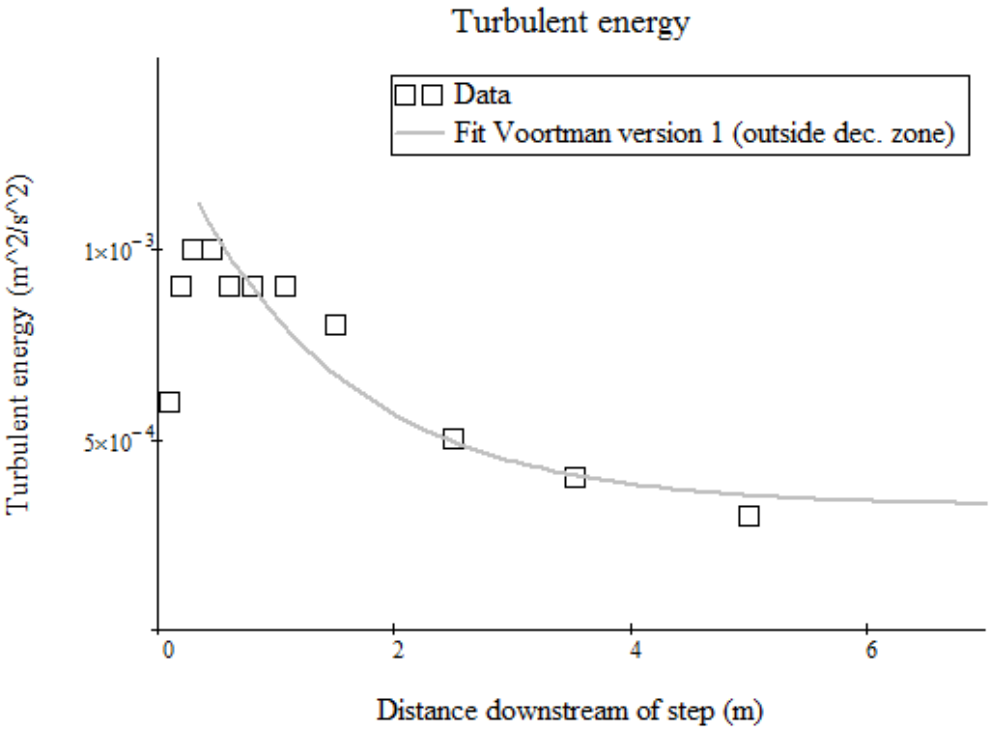

Figure L10: The turbulent energy levels for situation 4 with a rough bed.

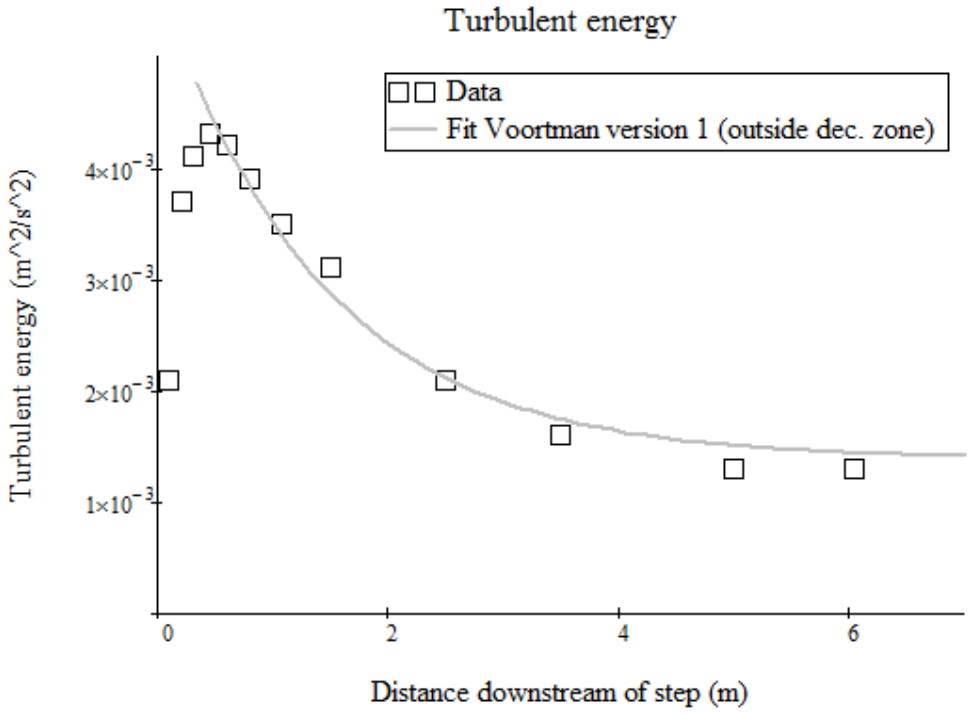

Figure L11: The turbulent energy levels for situation 5 with a rough bed.

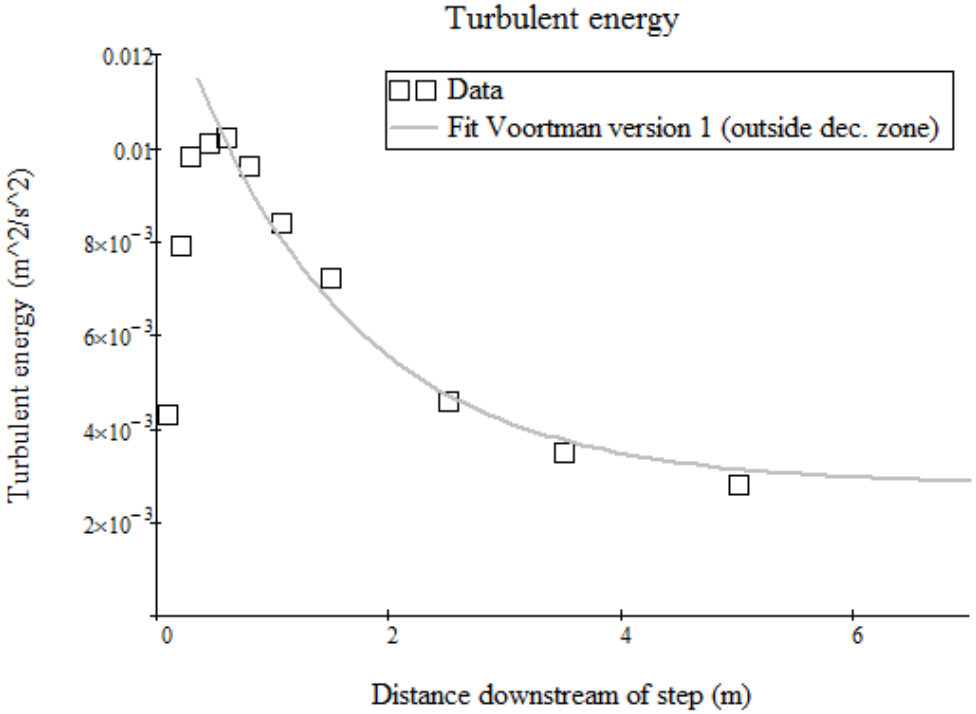

Figure L12: The turbulent energy levels for situation 6 with a rough bed.

Appendix M: Mathcad script for voortman's and Hoffman's formula

In this Appendix, the Mathcad script used for the combination of Voortman's and Hoffmans' formula will be shown. Since the script is identical for all twelve situations, only the script for situation 1 with a "smooth" bed will be shown.

Project:	**Graduation of Melvin Koote / The Arcadis Turbulence Method**		
Subject:	**The dissipation of turbulent energy via method Voortman 1**		
	Door:	Datum:	Paraaf:
Opgesteld:	**M. Koote**	**18th August 2017**	_____
Gecontroleerd:			_____
Vrijgegeven:		_____	
Versie:	**2.0**		
Status:	**Concept-intern**		

Definitions

ORIGIN := 1

x = distance downstream of step (m) x_{reatt} = reattachment point (m)

k = turbulent kinetic energy (m^2/s^2)

k_0 = turbulent kinetic energy at the reattachment point (m^2/s^2)

k_{eq} = equilibrium turbulent kinetic energy in uniform flow (m^2/s^2)

ϕ = constant value (-)

R = hydraulic radius (m)

SSE = sum of the squared errors

Description of worksheet

In this worksheet a formula for the turbulent energy as function of the distance from the step will be created based on experimental results.
This formula is exponential and depends on a certain maximum turbulence that occurs at the reattachment point, an equilibrium turbulence and a constant.
It is assumed that after the reattachment point the generation of turbulent energy can be neglected.
The hydraulic radius is assumed to be constant.

General start values

Data :=

[redacted]

Data =

	1	2	3	4	5	6
1	"S1"	1	0.07	0.25	$-6 \cdot 10^{-3}$	0.07
2	"S1"	1	0.07	0.25	0.101	0.118
3	"S1"	1	0.07	0.25	0.198	0.118
4	"S1"	1	0.07	0.25	0.3	0.119
5	"S1"	1	0.07	0.25	0.45	0.119
6	"S1"	1	0.07	0.25	0.602	0.12
7	"S1"	1	0.07	0.25	0.8	0.12
8	"S1"	1	0.07	0.25	1.073	0.121
9	"S1"	1	0.07	0.25	1.505	0.121
10	"S1"	1	0.07	0.25	2.504	0.122
11	"S1"	1	0.07	0.25	3.503	0.123
12	"S1"	1	0.07	0.25	5.009	0.125
13	"S2"	1	0.07	0.5	$-5 \cdot 10^{-3}$	0.07
14	"S2"	1	0.07	0.5	0.104	0.118
15	"S2"	1	0.07	0.5	0.202	0.118
16	"S2"	1	0.07	0.5	0.301	0.119
17	"S2"	1	0.07	0.5	0.443	0.12
18	"S2"	1	0.07	0.5	0.608	0.121
19	"S2"	1	0.07	0.5	0.796	0.122
20	"S2"	1	0.07	0.5	1.123	0.123
21	"S2"	1	0.07	0.5	1.507	0.123
22	"S2"	1	0.07	0.5	2.504	0.124
23	"S2"	1	0.07	0.5	3.506	0.125
24	"S2"	1	0.07	0.5	4.997	0.127
25	"S3"	1	0.07	0.75	$-4 \cdot 10^{-3}$	0.07
26	"S3"	1	0.07	0.75	0.103	...

$Code := Data^{\langle 1 \rangle}$

$Ruwh := Data^{\langle 2 \rangle}$

$d_{step} := Data^{\langle 3 \rangle} \cdot m$

$Fr_{step} := Data^{\langle 4 \rangle}$

$x_{loc} := Data^{\langle 5 \rangle} \cdot m$

$d_{loc} := Data^{\langle 6 \rangle} \cdot m$

$h_{loc} := Data^{\langle 8 \rangle} \cdot m$

$H_{loc} := Data^{\langle 9 \rangle} \cdot m$

$q := Data^{\langle 10 \rangle} \cdot \frac{m^2}{s}$

$k_{loc} := Data^{\langle 11 \rangle} \cdot \frac{m^2}{s^2}$

$x_{reatt} := Data^{\langle 12 \rangle} \cdot m$

$r_{loc} := Data^{\langle 13 \rangle}$

$B := 0.4 \cdot m$

$D_1 := 4.78 \cdot cm$

$D_2 := 4.68 \cdot cm$

$k_{0H} := 0.045$

$$row_{start} := \begin{pmatrix} 1 \\ 13 \\ 25 \\ 37 \\ 49 \\ 60 \\ 72 \\ 85 \\ 98 \\ 110 \\ 123 \\ 138 \end{pmatrix}$$

$$row_{end} := \begin{pmatrix} row_{start_2} - 1 \\ row_{start_3} - 1 \\ row_{start_4} - 1 \\ row_{start_5} - 1 \\ row_{start_6} - 1 \\ row_{start_7} - 1 \\ row_{start_8} - 1 \\ row_{start_9} - 1 \\ row_{start_{10}} - 1 \\ row_{start_{11}} - 1 \\ row_{start_{12}} - 1 \\ 149 \end{pmatrix}$$

$$row_{last3} := \begin{pmatrix} row_{start_2} - 3 \\ row_{start_3} - 3 \\ row_{start_4} - 3 \\ row_{start_5} - 3 \\ row_{start_6} - 3 \\ row_{start_7} - 3 \\ row_{start_8} - 3 \\ row_{start_9} - 3 \\ row_{start_{10}} - 3 \\ row_{start_{11}} - 3 \\ row_{start_{12}} - 3 \\ 147 \end{pmatrix}$$

$$row_{diss} := \begin{pmatrix} row_{start_1} - 1 + 5 \\ row_{start_2} - 1 + 5 \\ row_{start_3} - 1 + 5 \\ row_{start_4} - 1 + 5 \\ row_{start_5} - 1 + 4 \\ row_{start_6} - 1 + 5 \\ row_{start_7} - 1 + 6 \\ row_{start_8} - 1 + 4 \\ row_{start_9} - 1 + 5 \\ row_{start_{10}} - 1 + 6 \\ row_{start_{11}} - 1 + 7 \\ row_{start_{12}} - 1 + 5 \end{pmatrix}$$

Dataset:

$n := 1$

Input values

$x_{loc.n} := submatrix\left(x_{loc}, row_{start_n}, row_{end_n}, 1, 1\right)$

$x_{loc.dl} := x_{loc.n} \cdot \frac{1}{m}$

$x_{reatt.n} := submatrix\left(x_{reatt}, row_{start_n}, row_{start_n}, 1, 1\right)$

$x_{last3.n} := submatrix\left(x_{loc}, row_{last3_n}, row_{end_n}, 1, 1\right)$

$x_{diss.n} := submatrix\left(x_{loc}, row_{diss_n}, row_{end_n}, 1, 1\right)$

$x_{diss.dl} := x_{diss.n} \cdot \frac{1}{m}$ $\quad x_{reatt.dl} := x_{reatt.n} \cdot \frac{1}{m}$ $\quad x_{last3.dl} := x_{last3.n} \cdot \frac{1}{m}$

$d_{loc.n} := submatrix\left(d_{loc}, row_{start_n}, row_{end_n}, 1, 1\right)$

$h_{loc.n} := submatrix\left(h_{loc}, row_{start_n}, row_{end_n}, 1, 1\right)$

$H_{loc.n} := submatrix\left(H_{loc}, row_{start_n}, row_{end_n}, 1, 1\right)$

$H_{diss.n} := submatrix\left(H_{loc}, row_{diss_n}, row_{end_n}, 1, 1\right)$

$H_{last3.n} := submatrix\left(H_{loc}, row_{last3_n}, row_{end_n}, 1, 1\right)$

$q_n := submatrix\left(q, row_{start_n}, row_{end_n}, 1, 1\right)$

$k_{loc.n} := submatrix\left(k_{loc}, row_{start_n}, row_{end_n}, 1, 1\right)$

$k_{diss.n} := submatrix\left(k_{loc}, row_{diss_n}, row_{end_n}, 1, 1\right)$

$H_{loc.dl} := H_{loc.n} \cdot \frac{1}{m}$ $\quad H_{diss.dl} := H_{diss.n} \cdot \frac{1}{m}$

$k_{loc.dl} := k_{loc.n} \cdot \frac{s^2}{m^2}$ $\quad k_{diss.dl} := k_{diss.n} \cdot \frac{s^2}{m^2}$

$reatt := row_{diss_n} - row_{start_n} + 1 = 5$ $\quad end := row_{end_n} - row_{start_n} + 1 = 12$

$d_{end} := d_{loc.n_{end}} = 0.125\,m$ $\quad q_{end} := q_{n_{end}} = 0.014 \frac{m^2}{s}$

$R := \frac{B \cdot d_{end}}{B + 2 \cdot d_{end}} = 0.077\,m$ $\quad f := \frac{1}{R} = 12.98 \frac{1}{m}$ $\quad Fr_1 := \frac{q_{end}}{\sqrt{g \cdot d_{end}^{\,3}}} = 0.104$

$$u_{star} := 9.5 \times 10^{-3} \cdot \frac{m}{s}$$

$$k_{eq} := 1.44 \cdot u_{star}^{2} = 1.3 \times 10^{-4} \frac{m^2}{s^2}$$

$$k_{eq.dl} := k_{eq} \cdot \frac{s^2}{m^2}$$

$$u_{end} := \frac{q_{end}}{d_{end}} \qquad u_n := \frac{q_n}{d_{loc.n}}$$

$$r_n := \frac{\sqrt{k_{loc.n}}}{u_n} \qquad r_{loc.n} := \text{submatrix}\left(r_{loc}, row_{start_n}, row_{end_n}, 1, 1\right)$$

$$D := D_1 \qquad \lambda := 6.67 \cdot d_{end}$$

Formulae

After the reattachment point, the amount of turbulent energy can be described with:

$$k\left(x, k_0, \phi\right) := \left(k_0 - k_{eq}\right) \cdot \exp\left[-f \cdot \phi \cdot \left(x - x_{reatt.n_1}\right)\right] + k_{eq}$$

$$r_H(x) := \sqrt{0.5 \cdot k_{0H} \cdot \left(1 - \frac{D}{d_{end}}\right)^{-2} \cdot \left[\frac{\left(x - x_{reatt.n_1}\right)}{\lambda} + 1\right]^{-1.08} + 1.45 \cdot \left(\frac{u_{star}}{u_{end}}\right)^2}$$

Results

In order to calculate the unknown variables, the formula must be made dimensionless

$$f_{dl} := f \cdot m = 12.98 \qquad g_{dl} := g \cdot \frac{s^2}{m}$$

$$k_{dl}\left(x_{dl}, k_{0.dl}, \phi\right) := \left(k_{0.dl} - k_{eq.dl}\right) \cdot \exp\left[-f_{dl} \cdot \phi \cdot \left(x_{dl} - x_{reatt.dl_1}\right)\right] + k_{eq.dl}$$

$$k_{0\_guess} := 0.01 \cdot \frac{m^2}{s^2} \qquad \phi_{guess} := 0.01$$

$$guess := \begin{pmatrix} k_{0\_guess} \cdot \frac{s^2}{m^2} \\ \phi_{guess} \end{pmatrix}$$

$$\begin{pmatrix} k_{0.dl} \\ \phi \end{pmatrix} := genfit\left(x_{diss.dl}, k_{diss.dl}, guess, k_{dl}\right) = \begin{pmatrix} 1.009 \times 10^{-3} \\ 0.064 \end{pmatrix}$$

$$x := x_{reatt.n_1}, x_{reatt.n_1} + 0.1 \cdot m .. x_{reatt.n_1} + 7 \cdot m$$

$$k_0 := k_{0.dl} \cdot \frac{m^2}{s^2}$$

$$k(x) := k\left(x, k_0, \phi\right)$$

$$r_V(x) := \frac{\sqrt{k(x)}}{u_{end}}$$

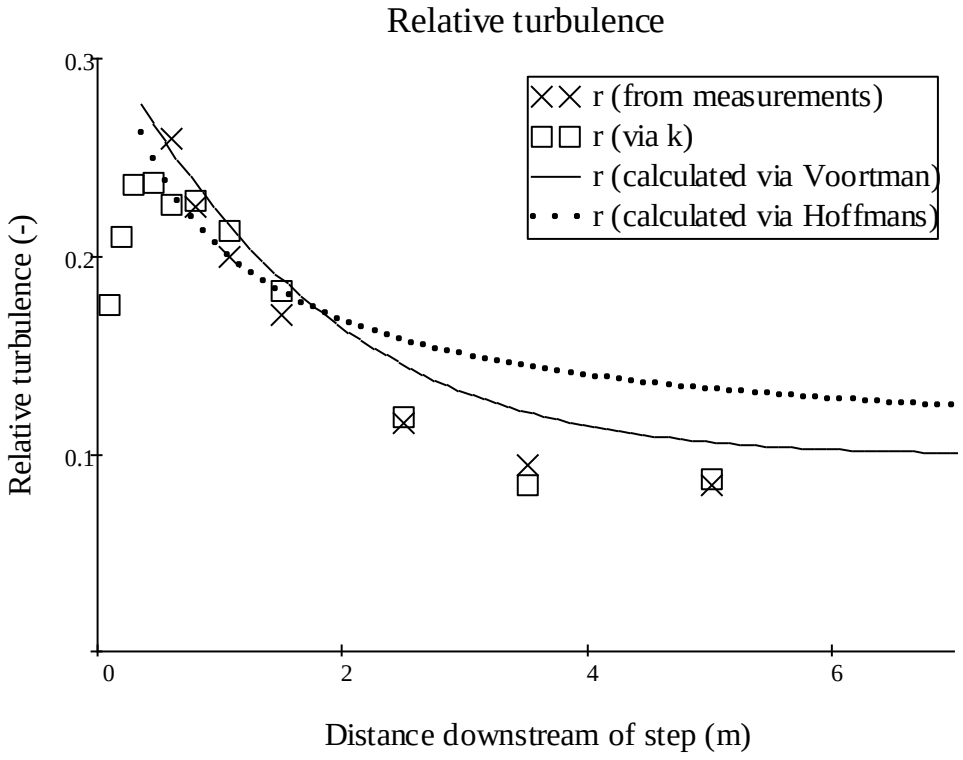

$$dk := k_0 - k_{eq} = 8.791 \times 10^{-4} \frac{m^2}{s^2}$$

$$k_{half} := k_0 - 0.5 \cdot dk = 5.695 \times 10^{-4} \frac{m^2}{s^2}$$

The distance after which half of the excess turbulence is dissipated, can be calculated with:

$$x_{guess} := 1.0 \cdot m$$

$$x_{half} := root\left(k\left(x_{guess}\right) - k_{half}, x_{guess}\right) = 1.19\,m$$

$$\phi_1 := \phi$$

$$k_1 := k_{eq}$$

$$error := \left(r_{loc.n} - r_V\left(x_{loc.n}\right)\right)^2$$

$$SSE_1 := \sum_{m=reatt}^{end} error_m = 6.366 \times 10^{-3}$$

Appendix N: The results from both Voortman's and Hoffmans' formula

In this Appendix, the calculated decay of turbulence following from Hoffmans' formula will be shown.

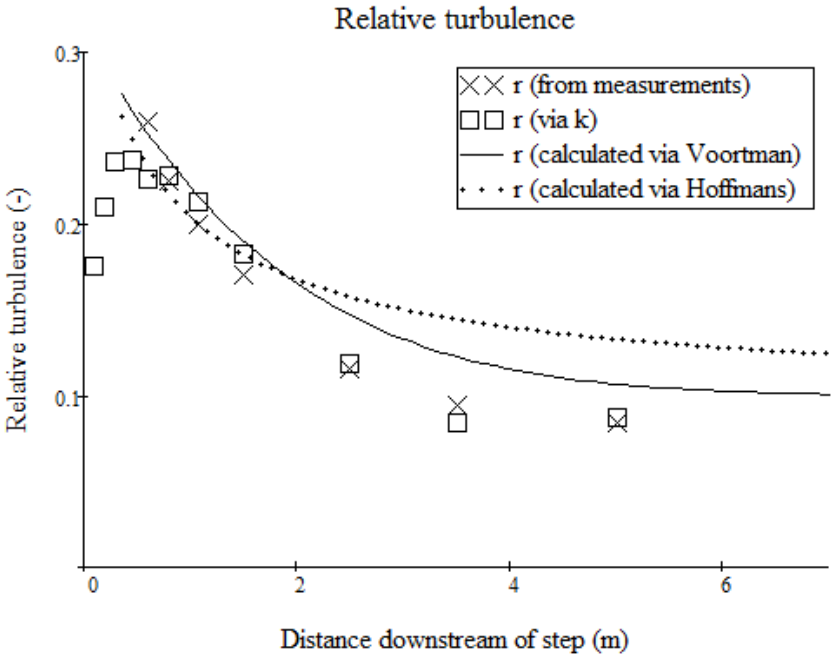

Figure N1: The relative turbulence for situation 1 with a smooth bed.

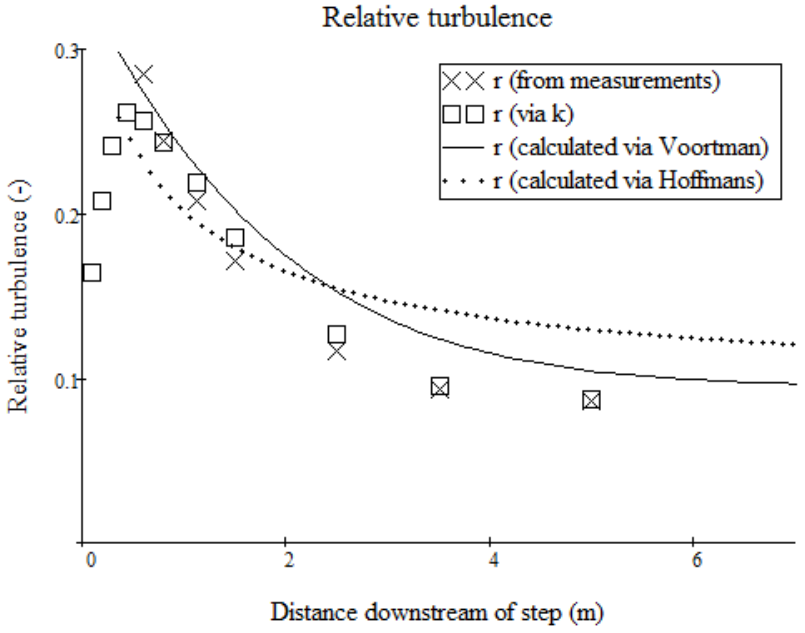

Figure N2: The relative turbulence for situation 2 with a smooth bed.

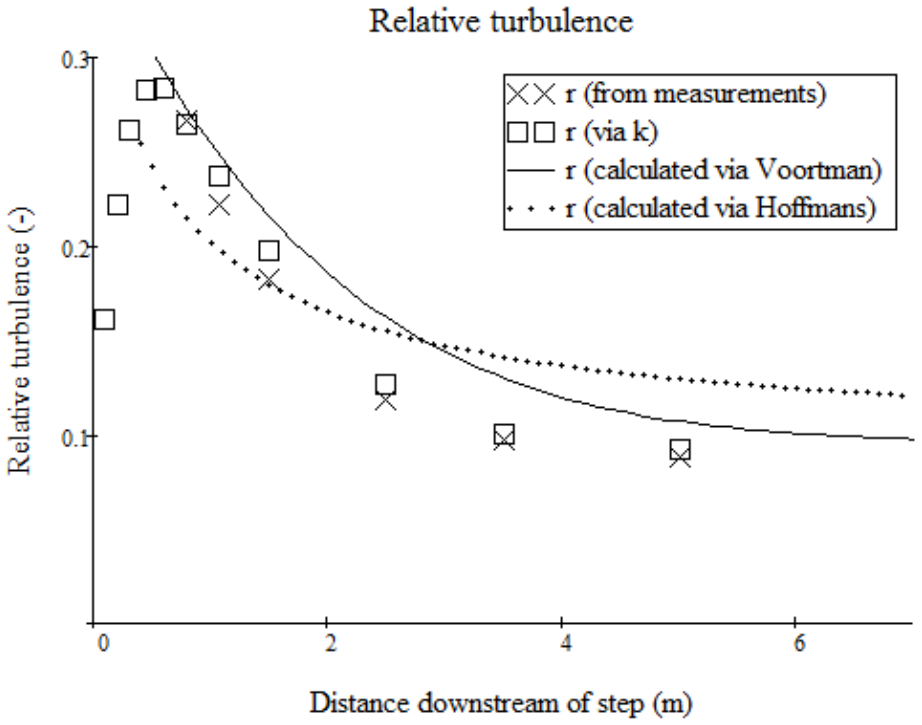

Figure N3: The relative turbulence for situation 3 with a smooth bed.

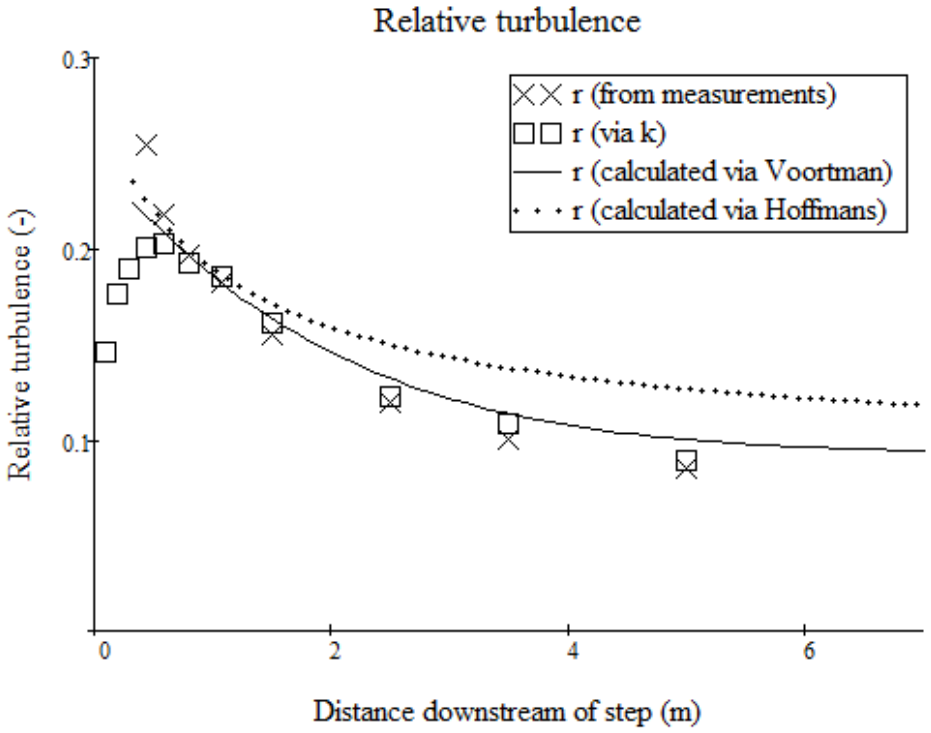

Figure N4: The relative turbulence for situation 4 with a smooth bed.

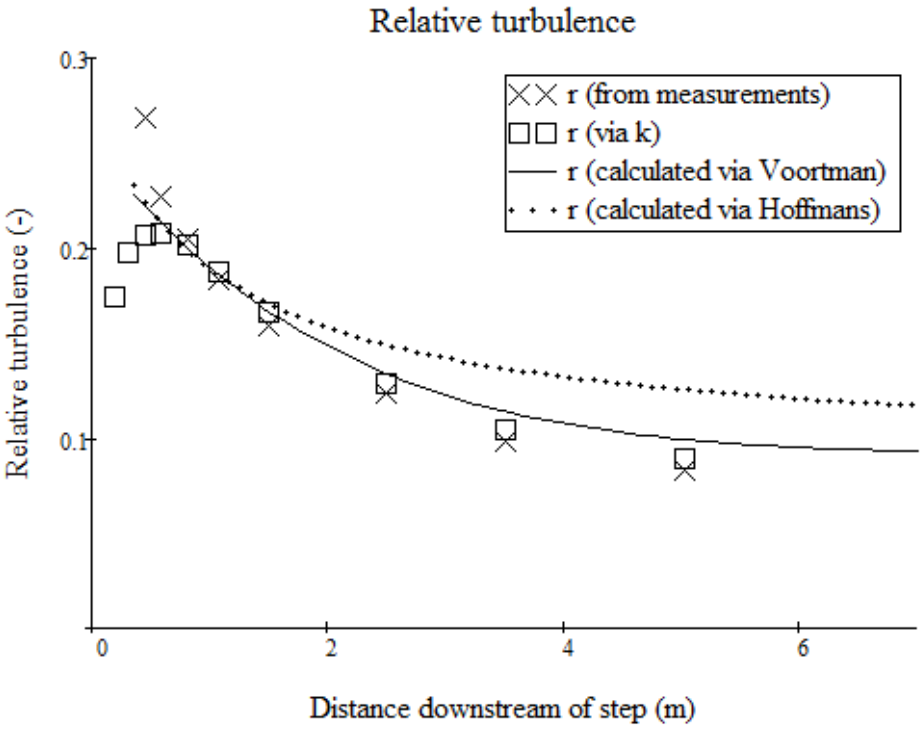

Figure N5: The relative turbulence for situation 5 with a smooth bed.

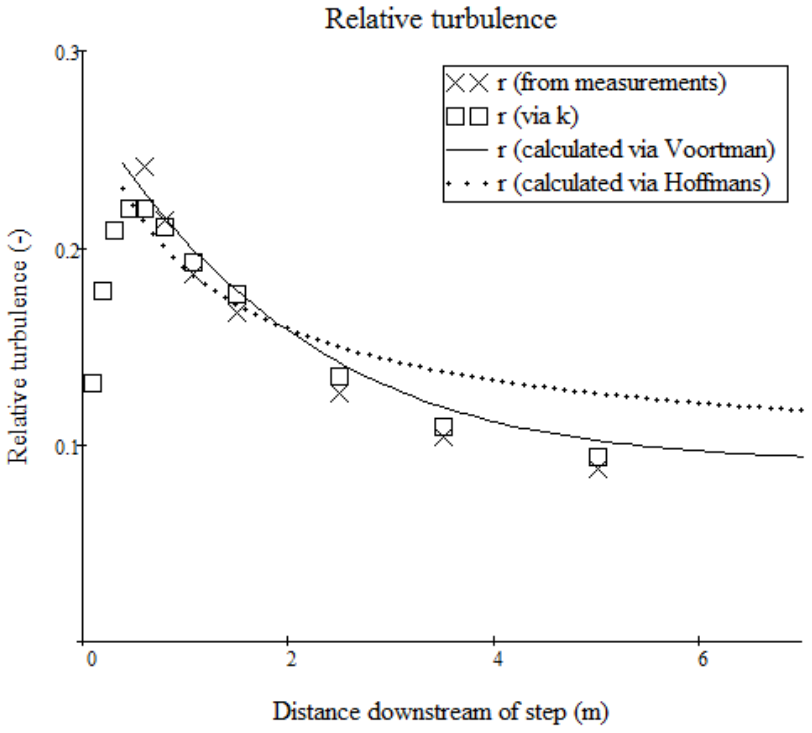

Figure N6: The relative turbulence for situation 6 with a smooth bed.

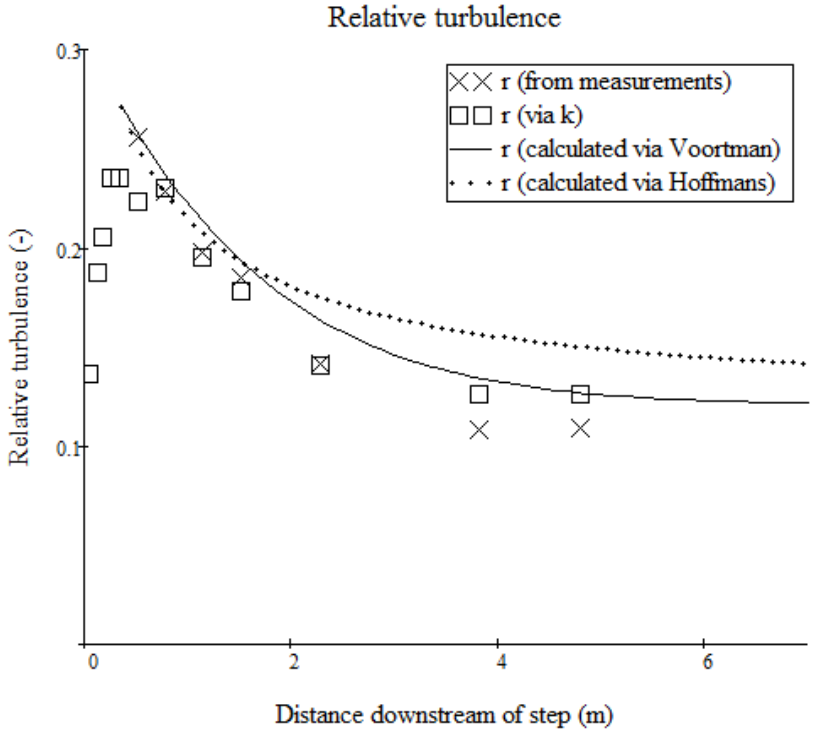

Figure N7: The relative turbulence for situation 1 with a rough bed.

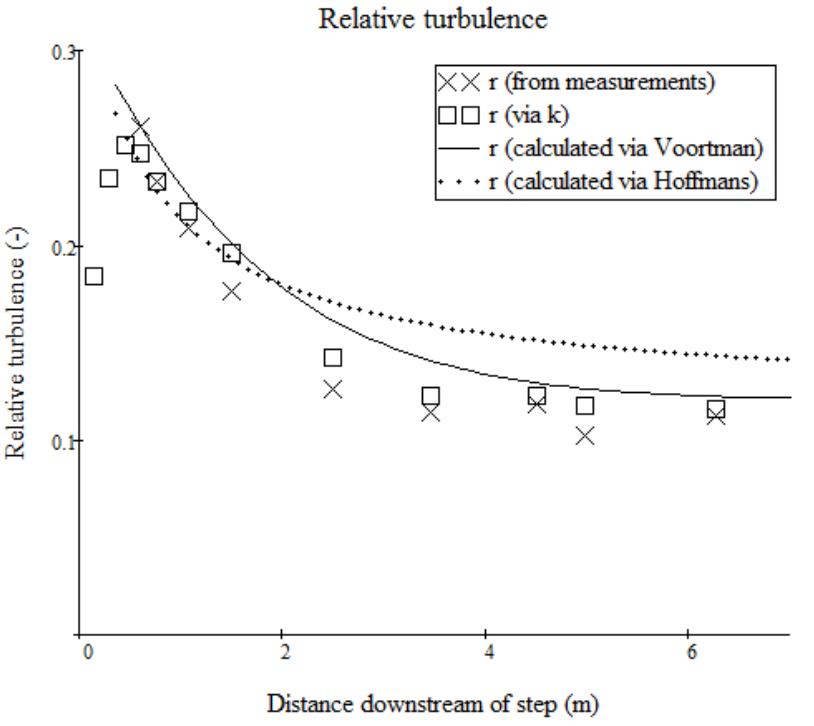

Figure N8: The relative turbulence for situation 2 with a rough bed.

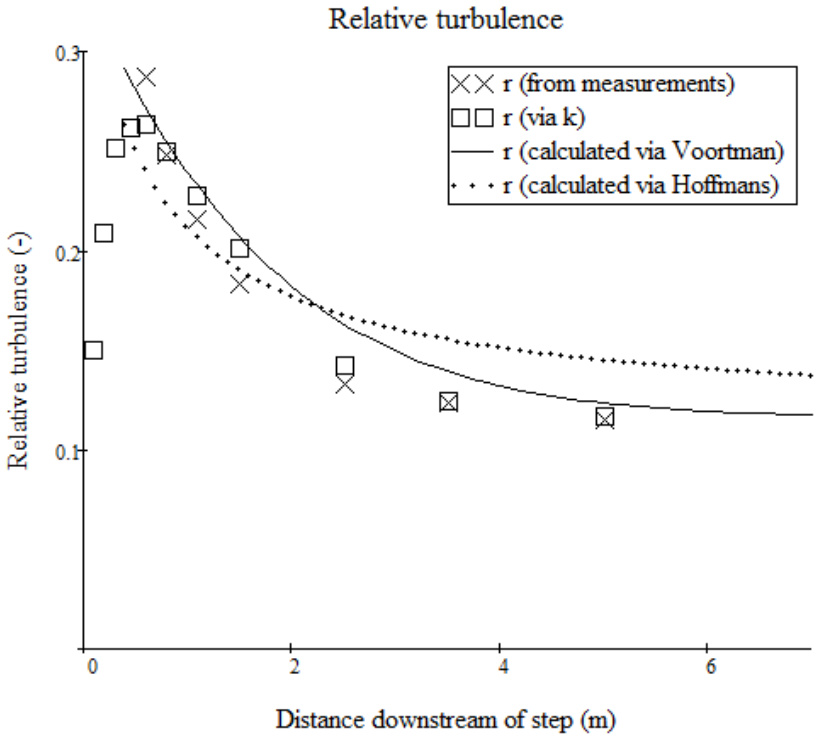

Figure N9: The relative turbulence for situation 3 with a rough bed.

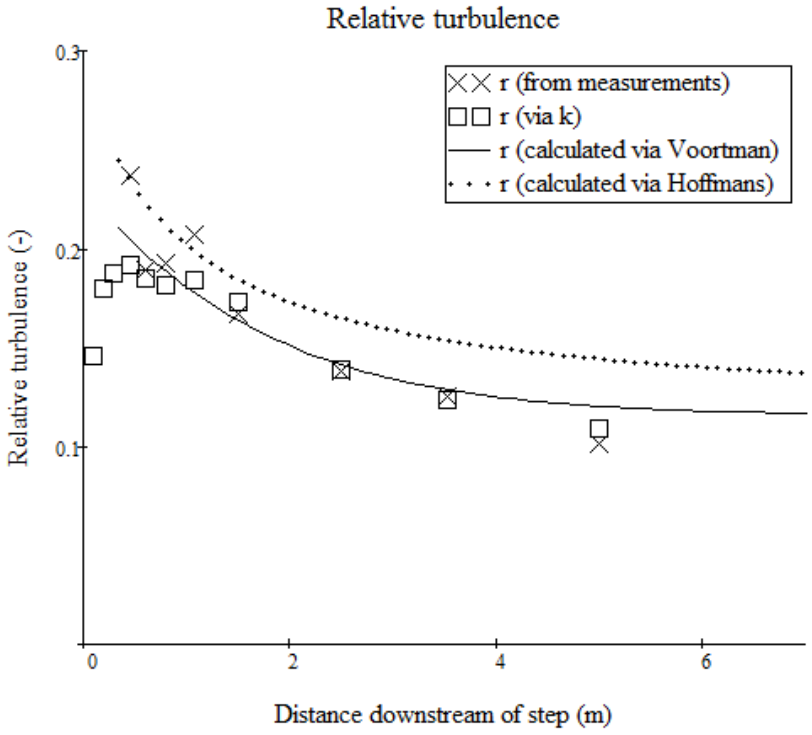

Figure N10: The relative turbulence for situation 4 with a rough bed.

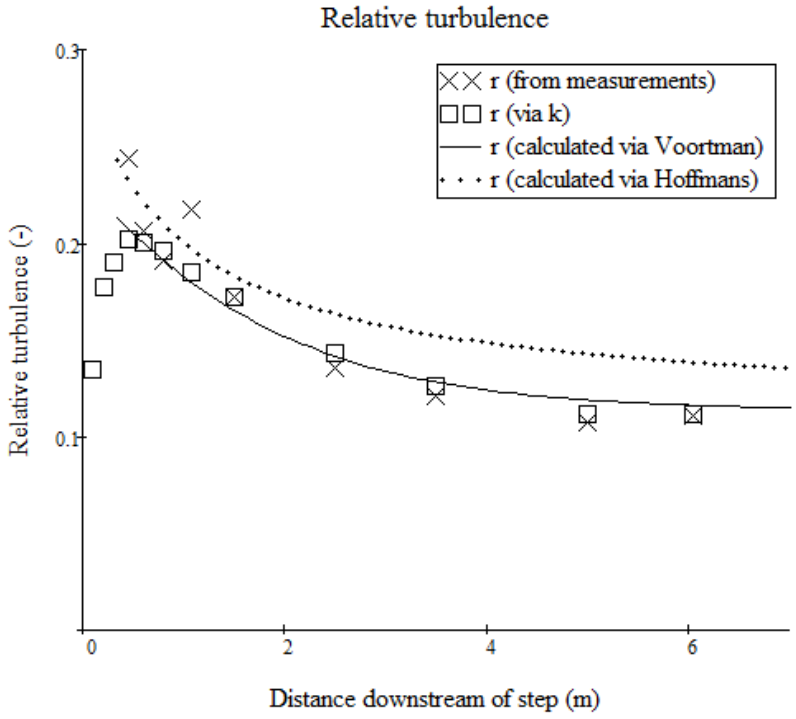

Figure N11: The relative turbulence for situation 5 with a rough bed.

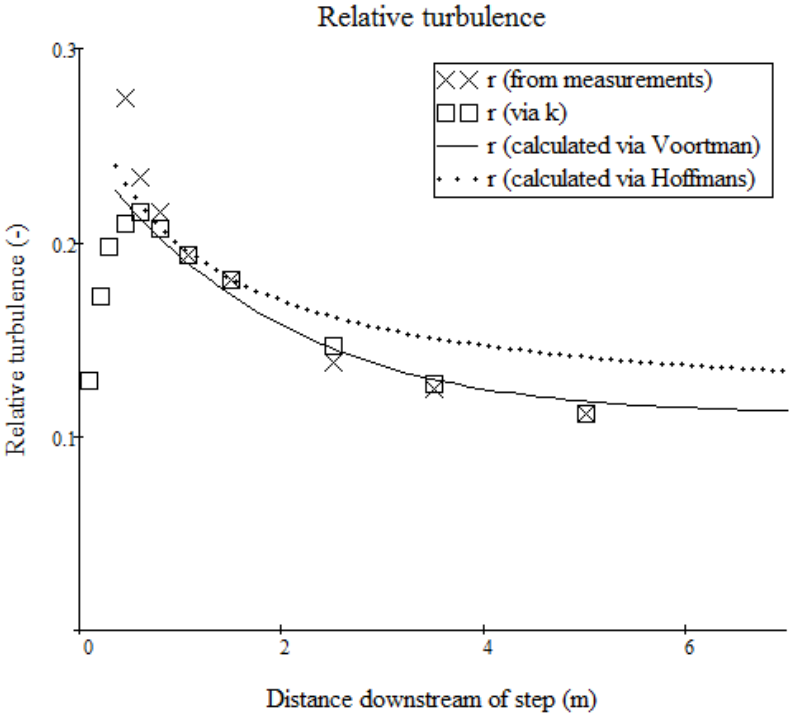

Figure N12: The relative turbulence for situation 6 with a rough bed.